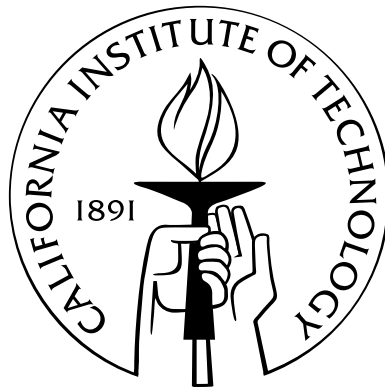


# Novel Methods for Force-Detected Nuclear Magnetic Resonance

Thesis by  
Mark C. Butler

In Partial Fulfillment of the Requirements  
for the Degree of  
Doctor of Philosophy



California Institute of Technology  
Pasadena, California

2008  
(Defended December 11, 2007)

© 2008

Mark C. Butler

All Rights Reserved

To my mom

# Acknowledgements

I would like to begin by thanking my advisor, Dan Weitekamp. Because of his deep scientific understanding and limitless creativity, I often found our discussions to be intellectually thrilling experiences. Dan consistently opened my eyes to new ways of looking at problems that I thought I already understood, and his first comments in response to my work would often give me startling moments of clarity. I eventually became used to the fact that for hours or days after a conversation with him I would find it very difficult to put down the work and return to the world of ordinary living because the questions that he brought up were so compelling to me. I would like to thank Dan for creating an environment in which I was free to grow intellectually, and also for encouraging me to stay focused on productive research. I enjoyed my research, and I thank Dan for the opportunity to work on these problems.

I would also like to thank several members of Dan's research group for their guidance and collaboration on a variety of projects. Gary Leskowitz and Lou Madsen graduated from the group around the time that I joined, but they remained available to me as mentors throughout my time in the group. They consistently helped me with experimental work in force-detected NMR. Gary, in particular, spent many hours helping me in the lab, giving me encouragement, and teaching me about experimental work. I regularly felt that I would have been lost without access to Valerie Norton's expertise with computers; on many occasions her ability to solve computer problems and use computers in clever ways saved me many hours of work. Choonsup Lee was endlessly patient in teaching me the basics of microfabrication and collaborating with me on the problem of fabricating a microresonator. Pratip Bhattacharya transformed my experience at Caltech. His positive energy, good-natured optimism,

practical wisdom, relentless encouragement, and his forceful generosity at restaurants are unique in my experience.

I thank my mom for her gentle confidence in me and the goals I was pursuing at every stage of my life, even when those goals were difficult to understand. My dad challenged me intellectually when I was a very young child; I have vivid memories of early conversations with him as some of the most intellectually intense experiences of my life. Together my parents introduced me to the world as a place that I could explore and understand. My dad was also very supportive throughout my time at Caltech, and I am grateful to him for proofreading this thesis.

During six years of marriage to my wife, Kendra, I have often felt that her commitment to my goals was even greater than my own. At times when those goals have seemed out of reach to me, she has been unstoppable in her confidence, her willingness to do whatever would support me and further my goals, and in her resourceful ability to find ways for us to function well in day-to-day life.

# Abstract

This thesis is concerned with the problem of extending methods for force-detected nuclear magnetic resonance (NMR) to the nanoscale regime. A magnetic mechanical resonator can be used both as a sensitive detector of spins and a means of inducing spin relaxation between detected transients. At the mK temperatures achievable in a dilution refrigerator, spin-lattice interactions are "frozen out," and resonator-induced relaxation can replace spin-lattice relaxation in returning the spins to equilibrium between detected transients. We analyze resonator-induced spin relaxation and the sensitivity of schemes which use a nanoscale mechanical resonator to detect spins.

Relaxation equations are derived from first principles, and a physical interpretation of the processes contributing to resonator-induced relaxation is given. The intrinsically quantum mechanical nature of the relaxation is highlighted by comparing the quantum mechanical relaxation equations with analogous equations derived using a semiclassical model in which all spin components have a definite value simultaneously. In the case where the spins all experience the same field, the semiclassical spins cannot become polarized as a result of their interaction with the resonator, and a quantum mechanical model is necessary even for a qualitative description of the polarization process.

Resonator-induced relaxation of spin systems is complicated by the fact that an indirect spin-spin interaction is present when all spins are coupled to the same resonator, since the resonator's field at a given spin is determined by the interactions which have occurred between the resonator and the other spins of the system. This indirect interaction can prevent the spins from relaxing to a thermal state characterized by a spin temperature. We present a physical interpretation of the mechanism

by which an indirect spin-spin torque develops during resonator-induced relaxation, and we estimate the magnitude of this torque and the time  $T_{\text{corr}}$  required for it to induce strong spin-spin correlations. A perturbation in the spin Hamiltonian which periodically reverses the direction of the indirect torques within a time period shorter than  $T_{\text{corr}}$  will prevent the development of resonator-induced correlations and allow the spins to relax to a thermal state.

The mechanisms by which the spin Hamiltonian  $H_s$  modifies resonator-induced relaxation are characterized. In the case where the eigenstates of  $H_s$  are weakly perturbed from product states, the system will relax exponentially to thermal equilibrium with the resonator, provided that resonator-induced couplings between populations and certain zero-quantum coherences are suppressed by terms in  $H_s$  which shift the frequencies of these coherences sufficiently far from zero. Analysis of longitudinal relaxation in example systems containing three dipole-dipole coupled spins shows that the relaxation occurs in two stages governed by different physical processes, and the three-spin systems do not relax to a thermal state. For substantially larger dipole-dipole coupled system (e.g.,  $N = 50$ ), we propose the hypotheses that the secular dipolar Hamiltonian will quickly equalize the population of states which lie in the same eigenspace of  $I_z$ . Simulations of the longitudinal relaxation predicted by this hypothesis suggest that a single resonator could efficiently relax dipole-dipole coupled systems to a thermal state.

Arguments based on general properties of the master equation suggest that the transverse relaxation induced by the mechanical resonator could occur on a shorter time scale than that of the longitudinal relaxation. We derive conditions which guarantee that the time constant for transverse relaxation will be  $2/R_h$ , where  $1/R_h$  is the time constant for resonator-induced longitudinal relaxation of a single-spin sample to thermal equilibrium. Under these conditions, transverse relaxation can be interpreted as the "lifetime broadening" associated with the shortened lifetime of energy eigenstates due to coupling with the resonator. For a two-spin system, however, we show analytically that "turning on" the dipolar coupling can accelerate resonator-induced transverse relaxation, and we give an interpretation of the mechanism by which this

occurs. Simulations of four-spin systems also show that the presence of dipolar couplings can substantially accelerate resonator-induced transverse relaxation, and that this accelerated relaxation can be distinguished from so-called radiation damping. In addition, we find that spin-locking limits the rate of resonator-induced transverse relaxation. In the case where the spin-locking field is large enough to average the dipolar Hamiltonian and the superoperator responsible for resonator-induced relaxation, we have  $T_{1\rho} = 2/R_h$ .

We propose a general definition of signal-to-noise ratio (SNR) which can be used to compare the sensitivity of methods that measure the amplitude of a signal with the sensitivity of methods that yield a continuous record of a signal. This definition is used to compare the sensitivity of three schemes for detecting the NMR signal of a sample consisting of a few spins: spin-locked detection of a transverse dipole, detection of a freely-precessing dipole, and detection of a correlated product  $\langle I_x(t_1) I_x(0) \rangle$ . The dependence of SNR and acquisition time on resonator parameters is analyzed. We find that when the time constant for decay of the signal during the detection period is  $2/R_h$ , with instrument noise substantially larger than spin noise, the only resonator parameter which appears in the SNR expressions is  $\omega_h/T_h$ , where  $\omega_h$  is the mechanical frequency and  $T_h$  is the temperature. This result suggests, in particular, that SNR for spin-locked detection will be insensitive to details of resonator design.

A torsional mechanical resonator design is presented. We discuss the advantages of using soft magnetic material and eliminating relative motion between the sample and the resonator, as well as the validity of the models used to characterize the resonator. The possibility of using non-metallic magnetic material as the source of the resonator's magnetic field is introduced. A numerical example is presented for which the calculated time constant for the longitudinal relaxation of a single-spin sample is  $1/R_h = 0.77$  s. Simulations of detected NMR spectra for two-spin samples suggest the possibility of chemical studies in which force-detected NMR spectroscopy is used with single-spin sensitivity.

The final chapter studies the possibility of using hyperpolarized spins to cool a single mechanical mode. Numerical examples suggest that cooling would be negligible

for resonators of size scale  $\sim 10 \mu\text{m}$  or larger. In the regime characterized by these examples, substantial cooling requires sufficiently strong spin-resonator coupling that neither a mechanical mode nor a spin mode can be distinguished in the spin-resonator system; instead, the modes of the system include equal contributions from the spins and the mechanical resonator. The spin-resonator correlations responsible for cooling make a significant contribution to the symmetric correlation function of the resonator coordinate, with the result that the noisy "thermal torque" acting on the resonator is increased rather than diminished by the presence of the hyperpolarized spins.

# Contents

<b>Acknowledgements</b>	<b>iv</b>
<b>Abstract</b>	<b>vi</b>
<b>1 Introduction</b>	<b>1</b>
<b>2 Description of the nanoscale spin-resonator system</b>	<b>7</b>
1 Average Hamiltonian . . . . .	7
2 Equations of motion for spin operators . . . . .	11
2.1 Reduced master equation for the spins . . . . .	11
2.2 Full master equation for the spin-resonator system . . . . .	16
3 Spontaneous and stimulated transitions . . . . .	18
4 Physical interpretation of the cooling process . . . . .	21
5 Semiclassical model . . . . .	24
6 Polarization of spins using an inductive resonator . . . . .	29
6.1 Rate constant for longitudinal relaxation . . . . .	29
6.2 Comparison of mechanical and inductive resonators . . . . .	31
<b>3 Resonator-induced spin relaxation</b>	<b>34</b>
1 Trapping of the spin system due to angular momentum conservation . . . . .	34
2 Indirect spin-spin interaction . . . . .	37
3 Modification of the relaxation processes by the spin Hamiltonian . . . . .	40
4 Longitudinal relaxation . . . . .	47
4.1 Noninteracting spins . . . . .	47

4.1.1	Two spins . . . . .	47
4.1.2	$N$ spins . . . . .	50
4.2	Dipole-dipole coupled spins . . . . .	54
4.2.1	Two spins . . . . .	54
4.2.2	Three spins . . . . .	56
4.2.3	$N$ spins . . . . .	58
5	Transverse relaxation of freely-precessing spins . . . . .	60
6	Transverse relaxation during spin-locking . . . . .	66
<b>4</b>	<b>Sensitivity of spin detection by a nanoscale resonator</b>	<b>69</b>
1	Definition of signal-to-noise ratio for measurement of an amplitude . . . . .	69
2	Generalization to measurement of a continuous signal . . . . .	74
3	Comparison with a standard definition . . . . .	77
4	Signal-to-noise ratio for amplitude detection . . . . .	82
4.1	Definition of the signal . . . . .	82
4.2	Definition of the noise . . . . .	85
4.3	Spectral density of the instrument noise . . . . .	86
4.4	Spectral density of the spin noise . . . . .	90
4.5	SNR formula for amplitude detection . . . . .	91
5	Signal-to-noise ratio for detection of a continuous signal . . . . .	94
6	Comparison of detection sensitivities . . . . .	96
6.1	Dependence of sensitivity on the energy in the signal . . . . .	96
6.2	Effect of resonator-induced transverse relaxation . . . . .	98
7	Dependence of signal-to-noise ratio and acquisition time on resonator parameters . . . . .	101
8	Signal-to-noise ratio for a product of correlated measurements . . . . .	104
8.1	Definition of the signal and the noise . . . . .	104
8.2	SNR formula . . . . .	107
8.3	Comparison of the first-order and second-order methods . . . . .	113

<b>5</b>	<b>Resonator design</b>	<b>116</b>
1	Description of the resonator and the detection scheme . . . . .	116
2	Selection of the resonator design . . . . .	119
3	Condition for resonance between the spins and the resonator . . . . .	121
4	Model of the resonator's magnetization . . . . .	124
4.1	Uniform magnetization . . . . .	124
4.2	Magnetization constant in the lab frame . . . . .	126
5	Strength of the spin-resonator coupling . . . . .	129
5.1	Effect of soft magnetic material on the coupling strength . . . . .	129
5.2	Upper bound on the torque between the spins and the resonator	133
6	Optimization of example resonators . . . . .	135
7	Use of non-metallic magnetic material . . . . .	140
<b>6</b>	<b>Simulations of spectra and spin relaxation</b>	<b>143</b>
1	Simulations of two-spin spectra . . . . .	143
1.1	Noninteracting spins . . . . .	144
1.2	Vinyl bromide . . . . .	147
2	Simulations of spin relaxation . . . . .	148
2.1	Relaxation of noninteracting spins . . . . .	150
2.2	Relaxation of dipole-dipole coupled spins . . . . .	155
<b>7</b>	<b>Cooling a single mode with hyperpolarized spins?</b>	<b>166</b>
1	Hyperpolarized spins as a cold bath . . . . .	166
2	Model of the spin-resonator system . . . . .	170
3	Steady-state number of quanta in the resonator . . . . .	174
4	Numerical example of cooling . . . . .	178
5	Modes of the spin-resonator system . . . . .	181
6	Response of the system to a torque acting on the resonator . . . . .	188
7	The cooled mode as a sensitive detector? . . . . .	193

<b>A</b>	<b>Derivation of the spin-relaxation equations from the full master equation</b>	<b>198</b>
<b>B</b>	<b>Relative magnitudes of the rate constants for lifetime and secular broadening</b>	<b>202</b>
<b>C</b>	<b>Longitudinal relaxation when the resonator's field is inhomogeneous</b>	<b>205</b>
<b>D</b>	<b>Derivation of the semiclassical equation for longitudinal relaxation</b>	<b>209</b>
<b>E</b>	<b>Longitudinal relaxation due to coupling between product-state populations</b>	<b>215</b>
<b>F</b>	<b>Transverse relaxation due to coupling between product-state coherences</b>	<b>218</b>
<b>G</b>	<b>Comparison between the use of an optimal filter and least-squares fitting</b>	<b>223</b>
<b>H</b>	<b>Spectral density in signal-to-noise ratio estimates</b>	<b>226</b>
<b>I</b>	<b>Statistics of a classical resonator</b>	<b>229</b>
	1 Correlation function of the oscillator's coordinate . . . . .	229
	2 Spectral density of the thermal torque . . . . .	232
<b>J</b>	<b>Contribution of the induced electric field to the resonator's kinetic energy</b>	<b>235</b>
<b>K</b>	<b>General formula for the magnetic spring constant</b>	<b>238</b>
<b>L</b>	<b>Spring constant and moment of inertia of a torsion beam</b>	<b>246</b>
<b>M</b>	<b>Eddy-current heating of metallic cylinders</b>	<b>250</b>
<b>N</b>	<b>Correlation function of the mechanical coordinate during cooling by hyperpolarized spins</b>	<b>257</b>



# List of Figures

1.1	Schematic representation of the energy flow during resonator-induced spin polarization. . . . .	3
5.1	Torsional resonator for force-detected NMR spectroscopy. . . . .	117
5.2	Torsional resonator for force-detected NMR imaging. . . . .	119
5.3	Comparison of magnetization orientation for hard and soft magnetic materials . . . . .	130
5.4	Comparison of the transverse field for hard and soft magnetic materials	131
6.1	Detection of two noninteracting spins without spin-locking. . . . .	145
6.2	Spin-locked detection of two noninteracting spins. . . . .	146
6.3	Two structures for dibromoethylene adsorbed on a silicon surface. . . .	148
6.4	Spin-locked detection of adsorbed vinyl bromide. . . . .	149
6.5	Longitudinal relaxation of noninteracting systems having $N = 36$ and $N = 144$ . . . . .	151
6.6	Transverse and longitudinal relaxation of four noninteracting spins which experience the same field and are initially aligned along the $x$ -axis. . .	153
6.7	Transverse and longitudinal relaxation of four noninteracting spins which have chemical shift offsets and are initially aligned along the $x$ -axis. . .	153
6.8	Longitudinal relaxation of four noninteracting spins which experience the same field and are initially disordered. . . . .	154
6.9	Longitudinal relaxation of four noninteracting spins which have chemical shift offsets and are initially disordered. . . . .	154

6.10	Longitudinal relaxation of four dipole-dipole coupled spins from an initially disordered state. . . . .	156
6.11	Transverse relaxation of four dipole-dipole coupled spins which are initially aligned with the $x$ -axis. . . . .	159
6.12	Longitudinal relaxation of four-spin systems when all spins are initially aligned along the $x$ -axis. . . . .	160
6.13	Accelerated transverse relaxation distinguished from radiation damping.	161
6.14	Resonator-induced relaxation of a spin-locked sample of four dipole-dipole coupled spins. . . . .	162
6.15	Longitudinal relaxation of 50 spins in the regime where dipolar interactions efficiently redistribute population within each eigenspace of $I_z$ during the relaxation. . . . .	164
6.16	Longitudinal relaxation of 150 spins in the regime where dipolar interactions efficiently redistribute population within each eigenspace of $I_z$ during the relaxation. . . . .	165

# List of Tables

3.1	Mixing of angular momentum systems. . . . .	58
5.1	Selected parameters for a resonator optimized with a separation of 50 nm between magnetic cylinders. . . . .	137
5.2	Selected parameters for a resonator optimized with a separation of 25 nm between magnetic cylinders. . . . .	137
5.3	Parameters for the optimized example resonator. . . . .	139
5.4	Sensitivity of the optimized example resonator. . . . .	139
7.1	Resonators cooled by hyperpolarized spins . . . . .	179
7.2	Scaled-up spin-resonator systems . . . . .	180
7.3	Dependence of rate constants on size . . . . .	181

# Chapter 1

## Introduction

This thesis is concerned with the problem of extending methods for force-detected nuclear magnetic resonance (NMR) methods to the nanoscale regime. Two fundamental problems must be solved for this goal to be achieved. First, a sensitive detector of NMR signals is needed. In an NMR experiment, the signal consists of a collection of precessing nuclear magnetic dipoles. Because nuclear dipole magnetic moments are extremely weak, their interaction with a detector in general has a weak effect on the detector, and a detector with optimal coupling to the spins is needed in order to obtain a signal which is not negligible compared to the detector's thermal noise.

A second problem which must be solved is that fluctuations in the sample dipole become more pronounced in comparison with those of the mean dipole as the sample is scaled down. In a system of  $10^5$  room-temperature hydrogen nuclei placed in a 25 T static field, for example, the uncertainty  $\Delta\mu$  is 37 times larger than  $\langle\mu\rangle$ . The response of a detector which has been designed to interact strongly with the nuclear dipole moment of this sample will be determined by the instantaneous state of the spins, which may be visualized as having an instantaneous dipole moment that fluctuates randomly around a mean value  $\langle\mu\rangle$  that is much smaller than the instantaneous moment. For NMR experiments which obtain microscopic information about a sample by measuring  $\langle\mu\rangle$ , even a noiseless detector would be unable to extract microscopic information in an efficient way by detecting a signal in which the dipole fluctuations are many times larger than  $\langle\mu\rangle$ .

Both the thermal noise in the detector and the spin fluctuations decrease with

temperature. At the mK temperatures achievable with a dilution refrigerator, for instance, the fluctuations in the dipole moment of a single-proton sample are smaller than the mean dipole  $\langle\mu\rangle$  if the proton is exposed to an applied field of a few tesla. However, detection of NMR signals in general depends on the acquisition of many transients, with the spin sample relaxing to a state near thermal equilibrium between transients. At mK temperatures, the spin-lattice interactions which restore the spins to thermal equilibrium between transients become "frozen out," and the time constant  $T_1$  for relaxation to equilibrium increases by orders of magnitude over the room temperature value of  $T_1$ . Slow relaxation of the spins to thermal equilibrium translates to a pathologically long delay between transients, which makes acquisition of many transients impractical.

The results in this thesis suggest that a low-temperature mechanical resonator can be used both to induce longitudinal relaxation between transients and to detect the spectrum of samples consisting of a few nuclear spins. The use of a magnetic mechanical resonator as a sensitive detector of magnetic resonance has already been demonstrated in the applications of force microscopy [1] and NMR spectroscopy [2]. In particular, detection of a single electron spin by magnetic resonance force microscopy has been reported [3]. The additional role of a mechanical resonator as a replacement for spin-lattice interactions is portrayed schematically in figure 1.1. Because of the weak coupling between the spins and the cold bath, direct transfer of energy from the spins to the bath is inefficient. However, the magnetic mechanical resonator is coupled strongly both to the spins and to the cold bath, and energy transferred from the spins to the resonator is quickly dissipated into the bath, rather than being cycled back to the spins.

This thesis analyzes resonator-induced spin relaxation and the sensitivity of schemes which use a nanoscale resonator to detect nuclear spins. Chapter 2 derives relaxation equations from first principles and gives a physical interpretation of the processes contributing to relaxation. The intrinsically quantum mechanical nature of the relaxation is highlighted by comparing the quantum mechanical relaxation equations with analogous equations derived using a semiclassical model in which all spin compo-

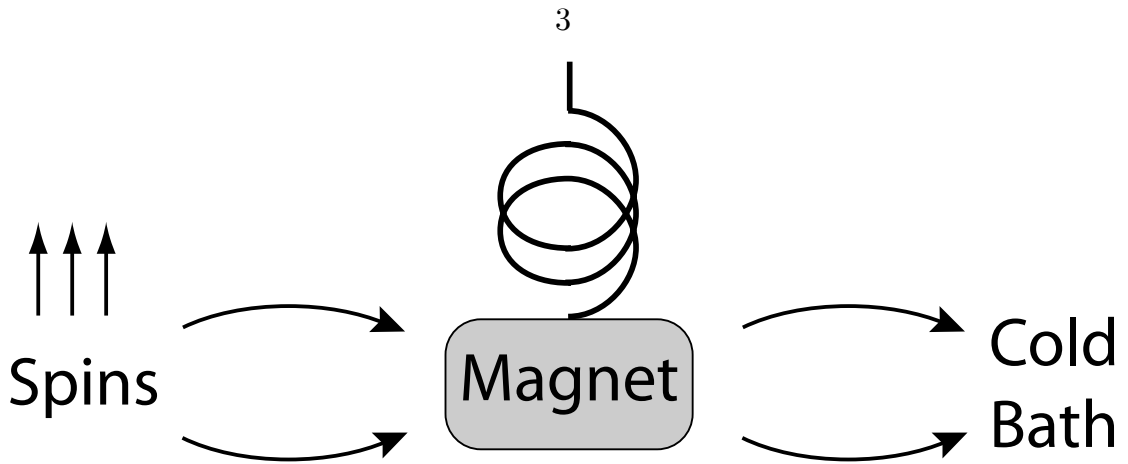


Figure 1.1: Schematic representation of the energy flow during resonator-induced spin polarization.

nents have a definite value simultaneously. In the case where the spins all experience the same field, the semiclassical spins cannot become polarized as a result of their interaction with the resonator, and a quantum mechanical model is necessary even for a qualitative description of the polarization process.

Chapter 3 analyzes resonator-induced relaxation. When multiple spins interact with the same resonator, the spins will not in general relax to a thermal state characterized by a spin temperature. Even in the case where spins are not directly coupled to each other, an indirect spin-spin interaction is present when all spins are coupled to the same resonator, since the resonator's field at a given spin is determined by the interactions which have occurred between the resonator and the other spins. We present a physical interpretation of the mechanism by which an indirect spin-spin torque develops during resonator-induced relaxation, and we estimate the magnitude of this torque and the time  $T_{\text{corr}}$  required for it to induce strong spin-spin correlations. A perturbation in the spin Hamiltonian which periodically reverses the direction of the indirect torques within a period  $T_{\text{corr}}$  will prevent the development of resonator-induced correlations and allow the spins to relax to a thermal state.

The longitudinal and transverse relaxation associated with different forms of the spin Hamiltonian  $H_s$  is characterized, and the mechanisms by which  $H_s$  modifies the relaxation are given a physical interpretation. In the case where the eigenstates of

$H_s$  are weakly perturbed from product states, the system will relax exponentially to thermal equilibrium with the resonator, provided that resonator-induced couplings between populations and zero-quantum "flip-flop" coherences are suppressed by terms in  $H_s$  which shift the frequencies of these coherences sufficiently far from zero. Analysis of longitudinal relaxation in example systems of three dipole-dipole coupled spins shows that the relaxation occurs in two stages governed by different physical processes and that the three-spin systems do not relax to a thermal state. For substantially larger dipole-dipole coupled system (e.g.,  $N = 50$ ), we propose the hypotheses that the secular dipolar Hamiltonian  $H_D$  will quickly equalize the population of states which lie in the same eigenspace of  $I_z$ . Chapter 6 presents simulations of the longitudinal relaxation predicted by this hypothesis, and these simulations suggests that a single resonator could efficiently relax dipole-dipole coupled systems to a thermal state.

The analysis in chapter 3 suggests that the transverse relaxation induced by the mechanical resonator could occur on a shorter time scale than the longitudinal relaxation. We derive conditions which guarantee that the time constant for transverse relaxation will be  $2/R_h$ , where  $1/R_h$  is the time constant for resonator-induced longitudinal relaxation of a single-spin sample to thermal equilibrium. Under these conditions, transverse relaxation can be interpreted as "lifetime broadening" associated with the shortened lifetime of energy eigenstates due to coupling with the resonator. For a two-spin system, however, we show analytically that "turning on" the dipolar coupling can accelerate resonator-induced transverse relaxation, and we give an interpretation of the mechanism by which this occurs. Chapter 6 presents simulations of four-spin systems which show that perturbations in the spin Hamiltonian can substantially accelerate resonator-induced transverse relaxation, and that this accelerated relaxation can be distinguished from so-called radiation damping. Analysis in chapter 3, as well as a simulation presented in chapter 6, show that spin-locking limits the rate of resonator-induced transverse relaxation. In the case where spin-locking field is large enough to average the terms of the dipolar Hamiltonian as

well as the superoperator responsible for resonator-induced relaxation, we find that

$$T_{1\rho} = 2/R_h. \quad (1.1)$$

The sensitivity of signal detection by the mechanical resonator is analyzed in chapter 4. Since the term "signal-to-noise ratio" is attached to a variety of different measures of sensitivity, we begin by defining the measures which we will use. We propose a general definition of signal-to-noise ratio (SNR) which can be used to compare the sensitivity of methods which measure the amplitude of a signal with the sensitivity of methods which yield a continuous record of a signal. This definition is used to compare the sensitivity of three schemes for detecting the NMR signal of a sample consisting of a few spins: spin-locked detection of a transverse dipole, detection of a freely-precessing dipole, and detection of a correlated product  $\langle I_x(t_1) I_x(0) \rangle$ . The dependence of SNR and acquisition time on resonator parameters is analyzed. We find that when the time constant for decay of the signal is  $2/R_h$ , with instrument noise substantially larger than spin noise, the only resonator parameter which appears in the SNR expression for spin-locked detection is  $\omega_h/T_h$ , where  $\omega_h$  is the mechanical frequency and  $T_h$  is the temperature. This result suggests that SNR for spin-locked detection will be insensitive to details of resonator design.

A torsional mechanical resonator design is presented in chapter 5. We discuss the advantages of using soft magnetic material and eliminating relative motion between the sample and the resonator, as well as the validity of the models used to characterize the resonator. The possibility of using non-metallic magnetic material as the source of the resonator's magnetic field is introduced. A numerical example is presented for which the calculated time constant for longitudinal relaxation of a single-spin sample is

$$1/R_h = 0.77 \text{ s}.$$

In chapter 6, resonator-induced spin relaxation is simulated for various sample sizes and spin Hamiltonians, and the simulations are interpreted using the results obtained in chapter 3. In addition, we present simulations of NMR spectra for

samples containing two spins, with instrument noise and spin fluctuations included in the simulations. These simulations suggest the possibility of chemical studies in which force-detected NMR spectroscopy is used with single-spin sensitivity.

The final chapter studies the possibility of using hyperpolarized spins to cool a single mechanical mode. Numerical examples suggest that cooling would be negligible for resonators of size scale  $\sim 10 \mu\text{m}$  or larger. In the regime characterized by these examples, substantial cooling requires sufficiently strong spin-resonator coupling that neither a mechanical mode nor a spin mode can be distinguished in the spin-resonator system; instead, the modes of the system include equal contributions from the spins and from the mechanical resonator. The spin-resonator correlations responsible for cooling make a significant contribution to the symmetric correlation function of the resonator coordinate, with the result that the noisy "thermal torque" acting on the resonator is increased rather than diminished by the presence of the hyperpolarized spins.

## Chapter 2

# Description of the nanoscale spin-resonator system

### 1 Average Hamiltonian

We begin by obtaining an interaction-frame Hamiltonian for a system consisting of a torsional mechanical resonator coupled to a collection of isochronous spins that interact only with the resonator. The field at the spins is the sum of a static applied field and the field of the magnetic mechanical resonator. Let  $\theta$  be the resonator's angular coordinate, with equilibrium position corresponding to  $\theta = 0$ , and let  $\mathbf{B}_a$  and  $\mathbf{B}_h(\theta)$  represent the applied field and the field of the resonator, respectively. We define

$$\mathbf{B}(\theta) = \mathbf{B}_a + \mathbf{B}_h(\theta)$$

to be the total field at the spins, and simplify notation by letting  $\mathbf{B}$ ,  $\mathbf{B}_h$ , and  $d\mathbf{B}/d\theta$  stand for  $\mathbf{B}(0)$ ,  $\mathbf{B}_h(0)$ , and  $\{d\mathbf{B}/d\theta\}(0)$ , respectively. The positive  $z$ -axis is chosen to lie in the direction of  $\mathbf{B}$ , and the  $x$ -axis is chosen so that  $d\mathbf{B}/d\theta$  lies in the  $xz$ -plane; i.e.,  $d\mathbf{B}/d\theta$  has nonzero components along only the  $x$ -axis and the  $z$ -axis. The Hamiltonian is written in units of rad/s as

$$H = -\gamma \mathbf{I} \cdot \mathbf{B}(\theta) + H_{\text{osc}}, \quad (2.1)$$

where  $H_{\text{osc}}$  is the Hamiltonian for the harmonic oscillator,  $\gamma$  is the gyromagnetic ratio, and  $\mathbf{I}$  is the spin operator. In analyzing the Hamiltonian, we approximate  $\mathbf{B}(\theta)$  by its first-order Taylor series:

$$\mathbf{B}(\theta) \approx \mathbf{B} + \left( \frac{d\mathbf{B}}{d\theta} \right) \theta. \quad (2.2)$$

Our first-order approximation to  $\mathbf{B}(\theta)$  is completely characterized by the three constants  $B_z$ ,  $dB_x/d\theta$ , and  $dB_z/d\theta$ . For oscillators which have

$$B_z(\theta) = B_z(-\theta),$$

the derivative  $dB_z/d\theta$  is zero at  $\theta = 0$ , and we limit the discussion to oscillators having this property. The first-order approximation to  $\mathbf{B}(\theta)$  is

$$B_x(\theta) = \frac{dB_x}{d\theta} \theta, \quad (2.3)$$

$$B_y(\theta) = 0, \quad (2.4)$$

and

$$B_z(\theta) = B_z. \quad (2.5)$$

Equations 2.3 through 2.5 allow us to express the Hamiltonian as

$$H = \left( -\gamma \frac{dB_x}{d\theta} \right) I_x \theta + H_0,$$

where  $H_0$  would be the Hamiltonian for a system in which the spins and oscillator are uncoupled:

$$H_0 = \omega_0 I_z + H_{\text{osc}} \quad (2.6)$$

$$\omega_0 \equiv -\gamma B_z. \quad (2.7)$$

Making the substitutions

$$\begin{aligned}\theta &= \frac{1}{\sqrt{2}\beta} (a + a^\dagger), \\ I_x &= \frac{1}{2} (I_+ + I_-)\end{aligned}$$

yields

$$H = H_0 + g (I_+ a^\dagger + I_- a + I_+ a + I_- a^\dagger). \quad (2.8)$$

In (2.8),  $I_+$ ,  $I_-$  are the respective raising and lowering operators for the spins,  $a^\dagger$  and  $a$  are the respective raising and lowering operators for the mechanical oscillator, and the constants  $\beta$  and  $g$  are given by

$$\begin{aligned}\beta &\equiv \sqrt{\frac{I_h \omega_h}{\hbar}}, \\ g &\equiv \frac{-\gamma}{2\sqrt{2}\beta} \frac{dB_x}{d\theta},\end{aligned} \quad (2.9)$$

where  $I_h$  is oscillator's moment of inertia and  $\omega_h$  is the mechanical frequency.

Using the operator  $\exp(-iH_0 t/\hbar)$  to switch to the interaction frame and applying the identities

$$\begin{aligned}e^{i\omega_h t a^\dagger} a e^{-i\omega_h t a^\dagger} &= a e^{-i\omega_h t}, \\ e^{i\omega_0 t I_z} I_+ e^{-i\omega_0 t I_z} &= I_+ e^{i\omega_0 t}\end{aligned}$$

transforms the Hamiltonian to

$$\tilde{H} = g [e^{i(\omega_h + \omega_0)t} I_+ a^\dagger + e^{-i(\omega_h + \omega_0)t} I_- a + e^{-i(\omega_h - \omega_0)t} I_+ a + e^{i(\omega_h - \omega_0)t} I_- a^\dagger].$$

If the gyromagnetic ratio is positive, resonance between the Larmor and mechanical frequencies corresponds to the condition

$$\omega_h = -\omega_0, \quad (2.10)$$

since  $\omega_h > 0$  and  $\omega_0 < 0$ . At resonance, the average Hamiltonian, which we denote by  $V$ , is

$$V = g (I_+ a^\dagger + I_- a). \quad (2.11)$$

This Hamiltonian is often referred to as the Jaynes-Cummings Hamiltonian. It has been studied extensively in quantum optics, since it governs the interaction between a two-level atom and a mode of the electromagnetic field [4]. In the current context, it can be interpreted as governing an interaction in which one rotating component of the resonator's transverse field is resonant with the Larmor frequency and induces transitions between spin eigenstates. This resonant transverse field can be considered roughly analogous to the applied transverse field which rotates spins during an NMR pulse.

The use of the first-order expression (2.2) as an approximation to  $\mathbf{B}(\theta)$  yields a model in which  $B_z$  does not vary as the mechanical resonator moves. The model excludes physical effects caused by fluctuations in  $B_z$  associated with the mechanical motion, such as the resonator's contribution to transverse spin relaxation by "secular broadening" (i.e., transverse relaxation due to fluctuations in the longitudinal field). To include such effects in our analysis, we expand the field to second order in  $\theta$ , limiting the discussion to resonators for which the properties

$$\begin{aligned} B_x(\theta) &= -B_x(-\theta) \\ B_y(\theta) &\equiv 0 \end{aligned}$$

imply that

$$\frac{d^2 B_x}{d\theta^2} = \frac{d^2 B_y}{d\theta^2} = 0$$

at  $\theta = 0$ . The average Hamiltonian in the interaction frame is then

$$V' = g (I_+ a^\dagger + I_- a) + f I_z (a^\dagger a - n_{\text{th}}), \quad (2.12)$$

where

$$f = -\gamma \frac{d^2 B_z}{d\theta^2} \frac{\hbar}{2I_h \omega_h}$$

and  $n_{\text{th}}$  is the thermal number of quanta in the resonator. In deriving (2.12), we have used the interaction frame defined by  $H_0 = \omega_0 I_z + \omega_h (a^\dagger a + 1/2)$ , where

$$\omega_0 = -\gamma B_z + f (n_{\text{th}} + 1/2). \quad (2.13)$$

The terms proportional to  $f$  in (2.12) and (2.13) arise because the value of  $B_z$  depends on the number of quanta in the resonator. In the case where

$$\frac{d^2 B_z}{d\theta^2} < 0,$$

for instance, the value of  $B_z$  is greatest when the resonator is in equilibrium position, and motion away from equilibrium decreases  $B_z$ . In the interaction-frame Hamiltonian, the resonator's contribution to  $B_z$  consists of terms which vary at frequency  $\pm 2\omega_h$  as well as a time-independent term that depends on the the number of quanta  $a^\dagger a$  in the resonator. Fluctuations in  $a^\dagger a$  away from the thermal value  $n_{\text{th}}$  correspond to a fluctuating value of  $B_z$  at the spins. In the presence of this fluctuating field, the mean value of the Larmor frequency is given by (2.13). Using this value of  $\omega_0$  in defining  $H_0$  ensures that  $\langle V' \rangle = 0$ , where the average is taken over the thermal reservoir that damps the resonator.

## 2 Equations of motion for spin operators

### 2.1 Reduced master equation for the spins

In the case where the sample consists of spins  $1/2$ , evolution under the Hamiltonian (2.11) can be characterized using results available in the quantum optics literature. When a single atom interacts with an undamped electromagnetic mode of a resonant cavity, an initial state function that has  $n$  quanta in the mode and that has the

spin in its excited state evolves in time by periodically exchanging a single quantum between spin and mode at frequency  $2g\sqrt{n+1}$  [4]. When  $N$  atoms are present in the undamped cavity, with all atoms initially excited, the system evolves "quasi-periodically," as the excitation initially present in the spins is transferred between the atoms and the resonant mode with a frequency of order [5]

$$g \times \text{field amplitude} \approx g\sqrt{\langle a^\dagger a \rangle}, \quad (2.14)$$

where  $\langle a^\dagger a \rangle$  is the mean number of quanta in the cavity mode, including thermal quanta and quanta donated by the atoms to the cavity mode. For a cavity at zero Kelvins, this frequency is of order  $g\sqrt{N}$ , where  $N$  is the number of atoms in the cavity [5]. If the cavity mode is weakly damped, oscillations in the excitation of the atoms gradually decay as quanta are dissipated from the mode. Increasing the strength of the damping eventually suppresses the oscillations, and the atoms decay monotonically when the rate constant for dissipation of quanta is large compared to the frequency at which quanta would cycle between atoms and the resonator in the absence of damping [5]. Since the rate constant for dissipation of quanta can be written as  $2/\tau_h$ , where  $\tau_h$  is the decay time of the mechanical resonator's position coordinate (or "ringdown time"), the condition that guarantees oscillations will be suppressed is

$$g\sqrt{\langle a^\dagger a \rangle} \ll \frac{2}{\tau_h}. \quad (2.15)$$

In this regime, the evolution of the atomic system can be described by a reduced master equation which does not explicitly include the resonator's degrees of freedom [5], and the resonator can be considered a reservoir which damps the atomic system. For a resonator at zero Kelvins, the condition (2.15) which allows the use of a reduced master equation is written more explicitly as [6]

$$g\sqrt{N} \ll \frac{2}{\tau_h}. \quad (2.16)$$

These results can be carried over directly to a system consisting of spins 1/2 which

evolve under a spin Hamiltonian  $H_s$  while interacting with a damped mechanical resonator. The evolution of the spin system is governed by the master equation [5]

$$\begin{aligned} \frac{d}{dt}\rho_s = & -i[H_s, \rho_s] - \frac{1}{2}R_0(n_{\text{th}} + 1)[I_-I_+, \rho_s]_+ + R_0(n_{\text{th}} + 1)I_+\rho_s I_- \\ & - \frac{1}{2}R_0n_{\text{th}}[I_+I_-, \rho_s]_+ + R_0n_{\text{th}}I_-\rho_s I_+, \end{aligned} \quad (2.17)$$

where

$$R_0 = 2g^2\tau_h.$$

The anticommutator  $[\cdot, \cdot]_+$  is defined by

$$[A, B]_+ = AB + BA.$$

Both  $H_s$  and the spin density matrix  $\rho_s$  are expressed in the interaction frame in which the Hamiltonian  $H_0$  of equation (2.6) has been eliminated, and the resonator field is assumed to be identical at all spins. Note that spin-lattice interactions are not included, since (2.17) is derived by considering an undamped system of atoms which interact with a damped electromagnetic mode. At very low temperatures, where the spin-lattice relaxation is "frozen out," equation (2.17) can be used to investigate the question of whether spin-resonator relaxation governed by the Hamiltonian of equation (2.11) can efficiently cool the spins toward thermal equilibrium with the resonator.

Note that (2.17) was derived by adding the term  $-i[H_s, \rho_s]$ , which governs unitary evolution under  $H_s$ , to a relaxation superoperator derived under the assumption that  $H_s = 0$ . The discussion in this thesis is limited to the regime in which this step is valid. To characterize this regime, note first that resonator-induced relaxation depends on weak correlations which develop between spins and resonator. The resonator "remembers" an interaction with the spins for a time period of order  $\tau_h$ . In a simple visualization of the relaxation, we can consider that a spin-resonator correlation survives during a period of order  $\tau_h$  and is then annihilated. The new spin-resonator correlation which then develops is determined by the instantaneous

state of the spins. Spin relaxation can thus be visualized as occurring during time periods of order  $\tau_h$ , with the relaxation during a given time period depending only on the state of the spins at the beginning of that period. If the time scale of the spin evolution associated with  $H_s$  is long compared to  $\tau_h$ , then there is little error in adopting the point of view that the spins are at every instant relaxing just as they would if  $H_s$  were absent, while  $H_s$  slowly modulates the spin state. In this regime, we can obtain a master equation by adding the unitary term  $-i[H_s, \rho_s]$  to the relaxation superoperator  $\Lambda$  derived under the assumption that  $H_s = 0$ . During a time step during which evolution due to  $H_s$  is negligible, for instance, such a master equation correctly predicts that relaxation is governed by  $\Lambda$ , while the presence of the unitary term allows for the slow modulation of the spin state.

This argument can be formalized by considering the general derivation given in reference [7] of the master equation for a system  $A$  coupled to a reservoir  $R$ . The interaction Hamiltonian can be written as

$$V = V_A V_R,$$

where  $V_A$  acts on  $A$  and  $V_R$  acts on  $R$ . In the absence of the coupling  $V$ , the lab-frame Hamiltonians  $H_A$  and  $H_R$  govern  $A$  and  $R$ , respectively. These Hamiltonians are eliminated from the evolution equations by a switch from the lab frame to an interaction frame, and second-order time-dependent perturbation theory is used to obtain an interaction-frame expression for the evolution of  $A$  and  $R$  during a time step  $\Delta t$ . A partial trace is taken over the reservoir degrees of freedom, and the resulting expression is simplified using the assumption that  $\Delta t \gg \tau_h$  and the assumption that the reservoir is only weakly perturbed from thermal equilibrium by the interaction with  $A$ . A similar derivation can be carried out in the case where the switch from the lab frame to the interaction frame does not completely eliminate the Hamiltonian  $H_A$  but rather leaves a "secular" term  $H_s$ . A second-order expression for the evolution of the full density matrix for  $A$  and  $R$  yields terms quadratic in  $V$ , terms which are proportional to  $V$  and  $H_s$ , as well as terms quadratic in  $H_s$ . A partial trace over the

reservoir degrees of freedom eliminates the terms which are linear in  $V$ , due to the assumption that the thermal average of  $V_R$  over the reservoir states is zero. (This condition can always be achieved by adding a term  $\langle V_R \rangle V_A$  to the Hamiltonian  $H_A$  and then defining  $V = V_A V'_R$ , where  $V'_R = V_R - \langle V_R \rangle$ .) The terms depending on the square of  $V$  are unaffected by the presence of  $H_s$ , and they yield the same relaxation superoperator that would be obtained in the absence of  $H_s$ . The remaining terms yield a second-order approximation to the unitary evolution of  $A$  associated with  $H_s$ . If this second-order approximation is valid throughout the time step  $\Delta t$ , then the resulting master equation for  $A$  includes the same relaxation superoperator which would be obtained in the absence of  $H_s$ , along with the additional term  $-i[H_s, \rho_s]$ . The relaxation superoperator can therefore be calculated without consideration of  $H_s$  if the evolution associated with  $H_s$  is sufficiently slow that it can be approximated by second-order perturbation theory during the time step  $\Delta t$ .

We consider a simple example in which  $H_s = 0$ . Multiplying the master equation (2.17) by  $I_z$  and taking the trace gives the derivative of  $\langle I_z \rangle(t)$ :

$$\frac{d}{dt} \langle I_z \rangle = R_0 (n_{\text{th}} + 1) \langle I_- I_+ \rangle - R_0 n_{\text{th}} \langle I_+ I_- \rangle. \quad (2.18)$$

$$= -R_0 (2n_{\text{th}} + 1) \langle I_z \rangle + R_0 \langle I_x^2 + I_y^2 \rangle. \quad (2.19)$$

If only a single spin is present, then

$$I_x^2 = I_y^2 = 1/4,$$

and we obtain

$$\frac{d}{dt} \langle I_z \rangle = -R_0 (2n_{\text{th}} + 1) \left( \langle I_z \rangle - \frac{1/2}{2n_{\text{th}} + 1} \right).$$

This equation describes the exponential relaxation of  $\langle I_z \rangle$  toward thermal equilibrium with the resonator, and the rate constant is

$$R_h = R_0 (2n_{\text{th}} + 1).$$

Since  $R_h = R_0$  at when  $n_{th} = 0$ , we can consider  $R_0$  to be the rate constant in the limiting case  $T \rightarrow 0$ .

The interaction-frame equations of motion for the transverse spin components are

$$\frac{d}{dt} \langle I_x \rangle = -\frac{1}{2} R_h \langle I_x \rangle - R_0 \left\langle \frac{1}{2} (I_x I_z + I_z I_x) \right\rangle, \quad (2.20)$$

$$\frac{d}{dt} \langle I_y \rangle = -\frac{1}{2} R_h \langle I_y \rangle - R_0 \left\langle \frac{1}{2} (I_y I_z + I_z I_y) \right\rangle. \quad (2.21)$$

For a sample consisting of a single spin 1/2, we have

$$I_x I_z + I_z I_x = I_y I_z + I_z I_y = 0,$$

and

$$\frac{d}{dt} \langle I_x \rangle = -\frac{1}{2} R_h \langle I_x \rangle, \quad (2.22)$$

$$\frac{d}{dt} \langle I_y \rangle = -\frac{1}{2} R_h \langle I_y \rangle. \quad (2.23)$$

We can interpret the transverse relaxation with rate constant  $R_h/2$  as lifetime broadening associated with the spin transitions induced by the resonator.

## 2.2 Full master equation for the spin-resonator system

In analyzing resonator-induced relaxation, it is often convenient to use a master equation which includes the resonator's degrees of freedom. If the effects of the spin lattice are neglected, the full master equation for the spin-resonator density matrix  $\rho$  in the interaction frame is [5]

$$\frac{d}{dt} \rho = -i [H_s + V, \rho] + \Lambda \rho, \quad (2.24)$$

where  $V$  is the average Hamiltonian (2.11) governing the spin-resonator interaction, and  $\Lambda$  is the relaxation superoperator for the damped mechanical resonator [8]:

$$\begin{aligned} \Lambda\rho = & -\frac{n_{\text{th}}+1}{\tau_h} [a^\dagger a, \rho]_+ + 2\frac{n_{\text{th}}+1}{\tau_h} a\rho a^\dagger \\ & -\frac{n_{\text{th}}}{\tau_h} [aa^\dagger, \rho]_+ + 2\frac{n_{\text{th}}}{\tau_h} a^\dagger\rho a. \end{aligned} \quad (2.25)$$

Equations (2.19) through (2.21) can be obtained for arbitrary values of  $I$  from the full master equation by using a method presented in Appendix A to derive a "coarse-grained" derivative, i.e., the average rate of change during a time step  $\Delta t$  which is long compared to  $\tau_h$  but short compared to the time needed for spin relaxation. The error associated with the use of the rotating-frame approximation (i.e., the use of an average Hamiltonian obtained by neglecting the off-resonant components of the transverse field) to obtain equations of motion for spin operators can be estimated by replacing the average Hamiltonian used during the time step  $\Delta t$  with a Magnus expansion [9]. The average Hamiltonian (2.11) is the zero-order term in this expansion, and the first-order term is smaller than the average Hamiltonian by a factor of order  $g/\omega_h$ .

The method given in Appendix A can be used to correct the spin equations of motions to include "secular broadening" associated with the fluctuations in  $B_z$  caused by the mechanical motion. Replacing (2.11) by (2.12) as the interaction Hamiltonian does not affect the equation of motion for  $\langle I_z \rangle$ , but equations (2.20) and (2.21) become

$$\begin{aligned} \frac{d}{dt} \langle I_x \rangle &= -\frac{1}{2} R_h \langle I_x \rangle - R_0 \left\langle \frac{1}{2} (I_x I_z + I_z I_x) \right\rangle \\ &\quad - \frac{1}{2} f^2 \tau_h n_{\text{th}} (n_{\text{th}} + 1) \langle I_x \rangle, \\ \frac{d}{dt} \langle I_y \rangle &= -\frac{1}{2} R_h \langle I_y \rangle - R_0 \left\langle \frac{1}{2} (I_y I_z + I_z I_y) \right\rangle \\ &\quad - \frac{1}{2} f^2 \tau_h n_{\text{th}} (n_{\text{th}} + 1) \langle I_y \rangle. \end{aligned}$$

Appendix B uses a numerical example to demonstrate that

$$f^2 \tau_h n_{\text{th}} (n_{\text{th}} + 1) \ll R_h$$

for the low-temperature nanoscale regime of interest. In this regime, (2.11) may be used as the interaction Hamiltonian, since the corrections introduced by the switch from (2.11) by (2.12) are negligible.

A similar approach can be used to derive equations of motion in the case where the spins' Larmor frequency is separated from the mechanical frequency by an offset  $\beta$ :

$$\omega_0 = -\omega_h + \beta.$$

Appendix C shows that if the spins all experience the same off-resonant field, the rate of longitudinal relaxation is given by

$$\frac{d\langle I_z \rangle}{dt} = \{R_0(n_{\text{th}} + 1)\langle I_- I_+ \rangle - R_0 n_{\text{th}}\langle I_+ I_- \rangle\} \frac{1}{1 + (\beta\tau_h)^2}. \quad (2.26)$$

A rate equation for longitudinal relaxation is also given for the case where the resonator's field varies across the sample. These results can be used to estimate the sample volume which can be cooled toward thermal equilibrium by a mechanical resonator.

### 3 Spontaneous and stimulated transitions

Agarwal has shown that spontaneous emission from a two-level atom into the vacuum is governed by the operator which is written in our notation as  $I_- I_+$  [10]. Since (2.18) can be expressed as

$$\frac{d}{dt}\langle I_z \rangle = R_0\langle I_- I_+ \rangle + R_0 n_{\text{th}}\langle I_- I_+ \rangle - R_0 n_{\text{th}}\langle I_+ I_- \rangle, \quad (2.27)$$

it is natural to interpret the terms  $R_0\langle I_- I_+ \rangle$ ,  $R_0 n_{\text{th}}\langle I_- I_+ \rangle$ , and  $R_0 n_{\text{th}}\langle I_+ I_- \rangle$  as characterizing processes analogous to spontaneous emission, stimulated emission, and stimulated absorption, respectively. More precisely, the term  $R_0(n_{\text{th}} + 1)$  and  $R_0 n_{\text{th}}\langle I_+ I_- \rangle$  are expected to give the respective rates at which the spins donate energy to an oscillator and receive energy from it.

The conjecture can be verified using the general formulas derived in reference [7] for the coefficients of a master equation. The interaction-frame master equation is written as

$$\frac{d}{dt}\rho_{ab}(t) = \sum_{c,d} \exp\{i(\omega_{ab} - \omega_{cd})t\} \mathcal{R}_{abcd} \rho_{cd}(t),$$

where  $\rho_{ij}$  is an element of the density matrix expressed in the energy eigenbasis, and  $\mathcal{R}_{abcd}$  is a constant which characterizes the rate of transfer from  $\rho_{cd}$  to  $\rho_{ab}$ . The eigenfrequency of spin eigenstate  $|a\rangle$  is denoted by  $\omega_a$ , and the difference of two such eigenfrequencies by

$$\omega_{ab} = \omega_a - \omega_b.$$

A spin transition from state  $|b\rangle$  to state  $|c\rangle$  changes the respective populations  $\rho_{bb}$ ,  $\rho_{cc}$  of the states, and  $\mathcal{R}_{cbb}$  is the rate constant for this transition. In the case where the transition  $b \rightarrow c$  involves the donation of a quantum from the spins to the resonator, we find by applying the general formulas of reference [7] that

$$\mathcal{R}_{cbb} = g^2 |\langle c | I_+ | b \rangle|^2 \int_{-\infty}^{\infty} \exp(i\omega_{bc}\tau) \langle a(\tau) a^\dagger(0) \rangle d\tau. \quad (2.28)$$

The correlation function  $\langle a(\tau) a^\dagger(0) \rangle$  appearing in the integrand can be approximated as

$$\begin{aligned} \langle a(\tau) a^\dagger(0) \rangle &= \langle a(\tau) a^\dagger(0) \rangle \exp(-i\omega_h\tau) \exp(-\tau/\tau_h) \\ &= (n_{\text{th}} + 1) \exp(-i\omega_h\tau) \exp(-\tau/\tau_h). \end{aligned}$$

When the difference frequency  $\omega_{bc}$  is resonant with the mechanical frequency, the integrand of (2.28) is equal to  $(n_{\text{th}} + 1) \exp(-\tau/\tau_h)$ , and we obtain

$$\mathcal{R}_{cbb} = 2g^2\tau_h (n_{\text{th}} + 1) |\langle c | I_+ | b \rangle|^2. \quad (2.29)$$

In the case where the Hamiltonian governing the spins is  $\omega_0 I_z$ , the energy eigenstates can be chosen to consist of angular momentum manifolds, with  $I_+$  and  $I_-$

the raising and lowering operators within each manifold. In this basis,  $\langle c | I_+ | b \rangle$  is nonzero only if  $I_+ | b \rangle = | c \rangle$ , and in this case

$$\begin{aligned} |\langle c | I_+ | b \rangle|^2 &= 1 \\ &= \langle b | I_- I_+ | b \rangle, \end{aligned}$$

and

$$\mathcal{R}_{cbb} = R_0 (n_{\text{th}} + 1) \langle b | I_- I_+ | b \rangle.$$

Summing over all transitions  $b \rightarrow c$  for which  $\langle c | I_+ | b \rangle$  is nonzero shows that the rate at which quanta are donated to the resonator is

$$\sum_{\langle c | I_+ | b \rangle \neq 0} \mathcal{R}_{cbb} \rho_{bb} = R_0 (n_{\text{th}} + 1) \langle I_- I_+ \rangle.$$

Since temperature  $T_h = 0$  gives  $n_{\text{th}} = 0$ , we find that  $R_0 \langle I_- I_+ \rangle$  is the rate of spontaneous emission, while

$$R_0 (n_{\text{th}} + 1) \langle I_- I_+ \rangle - R_0 \langle I_- I_+ \rangle = R_0 n_{\text{th}} \langle I_- I_+ \rangle$$

is the rate of stimulated emission. Similar arguments can be used to demonstrate that  $R_0 n_{\text{th}} \langle I_+ I_- \rangle$  is the rate at which quanta are donated to the spins, i.e., the rate of stimulated absorption.

The contribution of spontaneous and stimulated transitions to longitudinal relaxation can be highlighted by expressing equation (2.27) in the form

$$\frac{d}{dt} \langle I_z \rangle = -2R_0 n_{\text{th}} \langle I_z \rangle - R_0 \{ \langle I_z \rangle - \langle I_x^2 + I_y^2 \rangle \}.$$

The term proportional to  $n_{\text{th}}$  is due to stimulated transitions. In the absence of spontaneous emission, stimulated transitions would cause  $\langle I_z \rangle$  to relax exponentially to zero. The remaining contribution is due to spontaneous emission, which drives  $\langle I_z \rangle$  toward the instantaneous value of  $\langle I_x^2 + I_y^2 \rangle$ . In the case where a single spin

$1/2$  interacts with the resonator, spontaneous emission drives  $\langle I_z \rangle$  toward  $1/2$ . In the general case, spin-spin correlations affect the value of  $\langle I_x^2 + I_y^2 \rangle$  and hence the contribution of spontaneous emission to the relaxation of  $\langle I_z \rangle$ .

## 4 Physical interpretation of the cooling process

Reference [7] presents a physical interpretation of the energy exchange which occurs between a system  $\mathcal{A}$  and a thermal reservoir  $\mathcal{R}$  which is weakly-coupled to  $\mathcal{A}$  and damps its motion. Two types of processes contribute: 1) Processes in which system  $\mathcal{A}$  responds linearly to fluctuations in  $\mathcal{R}$ , and 2) Processes in which  $\mathcal{R}$  responds linearly to the motion of  $\mathcal{A}$  and damps this motion. In the case where  $\mathcal{A}$  is a single atom and  $\mathcal{R}$  is an isotropic and homogeneous radiation field, stimulated emission and absorption are shown to depend on the first type of process, while spontaneous emission is shown to include equal contributions from both types. In particular, the response of the atom to vacuum fluctuation and the response of the electromagnetic field to the motion of the electrons contribute equally to spontaneous emission. The atom continually loses energy as the radiation field responds to its motion (the "radiation reaction"), while the atom can either gain or lose energy when acted upon by vacuum fluctuations. If a two-level atom is in its excited state, vacuum fluctuations and the radiation reaction both transfer energy from the atom to the field at an equal rate. When the atom is in its ground state, however, vacuum fluctuations tend to induce atomic transitions to the excited state, thereby increasing the atom's energy, while the energy transfer due to the radiation reaction cancels the effect of the vacuum fluctuations.

The derivations used in justifying this interpretation can be adapted to yield a similar interpretation of the energy exchanges between a single spin  $1/2$  and a damped mechanical resonator. Consider as an example a problem in which the initial spin density matrix  $\rho_s$  is diagonal in the product-state eigenbasis. It follows from (2.17) that  $\rho_s$  will remain diagonal as the spin relaxes, since the derivative of  $\rho_s$  is itself diagonal. (This can be verified directly using matrix representations of

$I_-$  and  $I_+$ .) In this case, the mean transverse dipole is zero during the relaxation, and it is the fluctuations in the transverse dipole which drive the mechanical motion. The fluctuations are damped as they drive the resonator, and the resulting transfer of energy from spin to resonator is a mechanical analog of the radiation reaction. When  $T_h = 0$  and the spin is in its ground state, no transitions occur, since spin fluctuations drive the resonator and donate energy to it at the same rate that zero-point fluctuations return energy to the spin. If the spin is in the excited state, spin fluctuations and zero-point motion both contribute equally to spontaneous emission.

This interpretation is consistent with the idea that transverse spin fluctuations continue to occur even when a system is in its ground state. Consistent with this interpretation is the convention that the mean square fluctuation of a complex operator  $T = T_1 + iT_2$  be defined as [11]

$$\begin{aligned} |\Delta T|^2 &\equiv \frac{1}{2} \langle TT^\dagger + T^\dagger T \rangle - \langle T \rangle \langle T^\dagger \rangle \\ &= (\Delta T_1)^2 + (\Delta T_2)^2. \end{aligned} \quad (2.30)$$

Under this convention, the mean square fluctuations in the resonator's complex amplitude in thermal equilibrium are

$$|\Delta a|^2 = |\Delta a^\dagger|^2 = n_{\text{th}} + 1/2,$$

while the thermal fluctuations in the transverse spin are given by

$$|\Delta I_+|^2 = |\Delta I_-|^2 = \langle I_x^2 + I_y^2 \rangle.$$

For a system consisting of a resonator at  $T_h = 0$  and a spin 1/2 in its ground state, we have

$$\begin{aligned} |\Delta a|^2 &= 1/2, \\ |\Delta I_+|^2 &= 1/2. \end{aligned}$$

Definition (2.30) is not appropriate in all cases, however. Although a spin 1/2 in its ground state coupled to a mode at  $T_h = 0$  can be visualized as actively exchanging energy with the mode, no net radiation into or out of the mode will be detectable. Note also that the results presented in 2.3 imply that the radiation emitted by transverse spin fluctuations is characterized by the operator  $I_- I_+$ , rather than by  $|\Delta I_+|^2$ . In studying "radiative transverse fluctuations" of a mechanical oscillator or a spin system, an alternative to definition (2.30) may be used. If we let  $T$  denote the complex operator which removes a quantum from the radiating system (i.e.,  $I_+$  in the case of radiating spins or  $a$  in the case of a radiating mode), the radiative fluctuations of the spins and the resonator are characterized by

$$|\Delta' T|^2 \equiv \langle T^\dagger T \rangle - \langle T \rangle \langle T^\dagger \rangle. \quad (2.31)$$

For a resonator or a spin system in a thermal state, definition (2.31) yields the respective operators

$$\begin{aligned} \langle a^\dagger a \rangle &= n_{\text{th}}, \\ \langle I_- I_+ \rangle &= \langle I_x^2 + I_y^2 \rangle - \langle I_z \rangle. \end{aligned}$$

At zero Kelvins, the radiative fluctuations defined by these operators are zero.

The physical interpretation of energy exchange given in reference [7] can also be used to explain the appearance of the resonator's ringdown time  $\tau_h$  in the rate constant

$$R_0 = 2g^2 \tau_h. \quad (2.32)$$

When subject to a time-dependent input  $x(t)$ , the response  $y(t)$  of a linear system can be expressed as

$$y(t) = \int_{-\infty}^{+\infty} x(t') h(t-t') dt', \quad (2.33)$$

where  $h(t-t')$  gives the response at time  $t$  to a unit impulse applied at time  $t'$ . In using (2.33) to explain the appearance of  $\tau_h$  in equation (2.32), we consider the

two types of process which contribute to energy exchange between the spins and the damped resonator. For processes in which the spins respond linearly to resonator fluctuations, the linear system of equation (2.33) is the spin sample, the input  $x(t)$  is the fluctuating field of the mechanical resonator, and  $\tau_h$  is the correlation time of  $x(t)$ . Short  $\tau_h$  limits the rate of stimulated emission and absorption by limiting the time period during which the spins experience the steady periodic field that induces transitions. For processes in which the damped resonator responds linearly to spin motion and damps this motion (i.e., the mechanical analog of the "radiation reaction" mentioned above), the decay time of the impulse response  $h(t)$  is  $\tau_h$ , and so  $\tau_h$  limits the time period during which the mechanical response can "ring up."

Note that the derivation of equation (2.32) depends on the assumption that  $\tau_h$  is much shorter than the correlation time of the transverse sample dipole, and as a result,  $\tau_h$  is the only correlation time which appears in this equation. If the transverse spin correlation time is short enough to have a significant effect in determining the time period during which the linear response of the spins and resonator can accumulate, then the rate constant  $R_0$  must be modified to take account of the effects of spin fluctuations. This could be done by adding a superoperator for spin relaxation to the spin-resonator master equation and then performing a derivation similar to that of Appendix A. The discussion in section 2 of chapter 7 illustrates a method of including the effects of spin relaxation in an approximate way without using an explicit expression for the spin relaxation superoperator.

## 5 Semiclassical model

The motion of spin systems can often be visualized using a semiclassical model in which each spin component has a definite value at all times. Such a model can be considered a formalization of the "finger physics" pictures that are used to visualize spin evolution. We present a semiclassical model of the spin-resonator system which can be used to visualize the spin-resonator interaction and also to distinguish the relaxation governed by (2.18) from so-called radiation damping [12]. The semiclassical

spin  $\mathbf{I}^c$  is governed by the equation

$$\frac{d}{dt}\mathbf{I}^c = \gamma\mathbf{I}^c \times \mathbf{B}, \quad (2.34)$$

i.e.,  $\mathbf{I}^c$  precesses around the instantaneous field at frequency

$$\omega_0 = -\gamma B.$$

The magnetic dipole associated with  $\mathbf{I}^c$  is

$$\boldsymbol{\mu}^c = \gamma\hbar\mathbf{I}^c.$$

A classical damped mechanical resonator is coupled to the spin system by the Hamiltonian

$$W = -\boldsymbol{\mu}^c \cdot \mathbf{B}(\theta),$$

and the torque exerted on the resonator by the dipole is

$$-\frac{\partial W}{\partial \theta} = \frac{dB_x}{d\theta}\mu_x^c.$$

Precession of  $\mathbf{I}^c$  around the applied field causes  $\mu_x^c$  to vary sinusoidally. The mechanical oscillator thus responds to a resonant driving torque, and energy can be transferred from the spins to the oscillator by this driving torque. The resonant rotating component of the oscillator's field simultaneously exerts a torque on the spins and causes spin rotation toward or away from the static applied field. As in the derivative of the quantum mechanical equations of motion, coarse-grained relaxation equations can be found by integrating the motion over a time step  $\Delta t$  which is long compared to  $\tau_h$  but short compared to spin relaxation time.

Appendix D derives an equation of motion for  $\langle I_z^c \rangle$ , where the average is taken

over a statistical ensemble of spin-resonator systems:

$$\frac{d\langle I_z^c \rangle}{dt} = -2R_0 \frac{\langle E_h^c \rangle}{\hbar\omega_h} \langle I_z^c \rangle + R_0 \langle I_-^c I_+^c \rangle. \quad (2.35)$$

In (2.35),  $I_+^c, I_-^c$  are defined as

$$I_\pm^c = I_x^c \pm iI_y^c,$$

and  $\langle E_h^c \rangle$  is the mean thermal energy of the classical resonator. From equation (2.18), we can obtain a formally equivalent equation for longitudinal relaxation of the quantum mechanical system:

$$\frac{d\langle I_z \rangle}{dt} = -2R_0 \frac{\langle E_h \rangle}{\hbar\omega_h} \langle I_z \rangle + R_0 \langle I_- I_+ \rangle, \quad (2.36)$$

where

$$\langle E_h \rangle = \hbar\omega_h n_{\text{th}}$$

can be considered the mean thermal energy of the quantum resonator, with zero-point energy excluded.

The formal equivalence between (2.35) and (2.36) masks the fact that the commutation properties of the quantum operators can yield distinctly nonclassical relaxation in the quantum system. Writing the two equations in the form

$$\frac{d\langle I_z^c \rangle}{dt} = -2R_0 \frac{\langle E_h^c \rangle}{\hbar\omega_h} \langle I_z^c \rangle + R_0 \langle (I_x^c)^2 + (I_y^c)^2 \rangle, \quad (2.37)$$

$$\frac{d\langle I_z \rangle}{dt} = -2R_0 \frac{\langle E_h \rangle}{\hbar\omega_h} \langle I_z \rangle + \{R_0 \langle I_x^2 + I_y^2 \rangle - R_0 \langle I_z \rangle\} \quad (2.38)$$

highlights the failure of the semiclassical model to characterize correctly the spontaneous emission which is responsible for polarizing the spins in the quantum system at low temperatures. As shown in section 3, the terms in curly brackets on the right side of (2.38) are due to spontaneous emission. Section 4 interprets spontaneous emission as including equal contributions from the spins' response to zero-point fluctuations

of the resonator's field, and the resonator's response to transverse spin fluctuations that are present even in a perfectly polarized sample. Since these phenomena are not present in the semiclassical model, it is not surprising that spontaneous emission is not correctly characterized by this model. Equations (2.35) and (2.36) show that discrepancies between the quantum and semiclassical models can be expected when

$$\frac{\langle E_h \rangle}{\hbar\omega_h} = n_{\text{th}}$$

has order of magnitude unity or less, as well as when  $\langle I_x^2 + I_y^2 \rangle$  differs significantly from the value that would be calculated if each spin component had a definite value simultaneously.

As an illustration, we compare the semiclassical phenomenon called "radiation damping" with the longitudinal polarization of a spin 1/2 by a cold resonator. Magnetization precessing in an inductive coil excites current oscillations within the coil circuit, and radiation damping occurs when the field generated within the coil by the oscillating current is strong enough to rotate the magnetization into alignment with the static applied field, thereby shortening the precession period. In the case where spins are coupled to a mechanical rather than an inductive resonator, the analogous phenomenon occurs when the mechanical response to precessing spins creates a resonant field which rotates the spins.

Abragam has derived a rate equation for radiation damping using a model equivalent to our semiclassical model [12]. Adopting the language and notation of our semiclassical model, we can say that Abragam derives the rate equation by assuming that a single semiclassical dipole  $\mu^c$  interacts with a classical resonator in which thermal fluctuations can be neglected, i.e., a classical resonator at temperature  $T_h = 0$ . The equation of motion for  $\langle I_z^c \rangle$  during radiation damping can therefore be obtained from (2.37) by setting  $\langle E_h^c \rangle$  to zero:

$$\frac{d\langle I_z^c \rangle}{dt} = R_0 \langle (I_x^c)^2 + (I_y^c)^2 \rangle. \quad (2.39)$$

Equation (2.39) implies that  $d\langle I_z^c \rangle / dt$  is zero if the semiclassical dipole is aligned with the negative  $z$ -axis, and that  $d\langle I_z^c \rangle / dt$  takes on its maximum value when the dipole lies in the transverse plane. This is consistent with the fact that it is the transverse dipole which drives the mechanical motion and thereby induces the resonant field responsible for radiation damping.

For purposes of comparison, note that the quantum mechanical equation of motion is

$$\frac{d\langle I_z \rangle}{dt} = R_0 \langle I_x^2 + I_y^2 \rangle - R_0 \langle I_z \rangle \quad (2.40)$$

when the resonator is at zero Kelvins. Consider an example in which the spin sample consists of a single spin  $1/2$ . Since

$$I_x^2 + I_y^2 = 1/2,$$

equation (2.40) reduces to

$$\frac{d\langle I_z \rangle}{dt} = -R_0 (\langle I_z \rangle - 1/2). \quad (2.41)$$

The evolution governed by (2.41) is distinctly different from that governed by (2.39). If the spin is aligned with the negative  $z$ -axis, for instance,  $d\langle I_z \rangle / dt$  takes on its maximum possible value, and the derivative decreases linearly as  $\langle I_z \rangle$  is increased, reaching zero when the spin is oriented along the positive  $z$ -axis. Since  $I_x^2 + I_y^2$  is a constant,  $d\langle I_z \rangle / dt$  depends only on  $\langle I_z \rangle$ . In particular, since a polarized spin  $1/2$  initially precessing in the transverse plane has the same initial value of  $\langle I_z \rangle$  as a spin which is initially completely unpolarized, the evolution of  $\langle I_z \rangle$  is the same in both cases.

The most striking difference between the semiclassical and quantum models is that only the quantum mechanical model allows for the polarization of a sample of spins which all experience the same field. Equation (2.34) implies that the derivative  $d\mathbf{I}^c / dt$  is perpendicular to  $\mathbf{I}^c$ , and it follows that this equation of motion describes rotation of  $\mathbf{I}^c$ . The magnitude  $|\mathbf{I}^c|$  cannot change as a result of the spin-resonator

interaction. The quantum model does allow polarization, as can be seen from equation (2.41). For a single spin  $1/2$ , relaxation of  $\langle I_z \rangle$  toward thermal equilibrium proceeds independently of  $I_x$  and  $I_y$ . As we will see in chapter 3, resonator-induced polarization is also possible for a system of  $N$  spins.

## 6 Polarization of spins using an inductive resonator

Reference [13] demonstrates that mechanical detection of NMR signals is more sensitive than inductive detection for sufficiently small samples, with mechanical detection typically becoming more sensitive when the sample radius is on the order of tens of microns to hundreds of microns. We extend this result by presenting a numerical estimate which suggests that a nanoscale inductive resonator would not efficiently cool a nanoscale spin sample.

### 6.1 Rate constant for longitudinal relaxation

An classical  $LC$  circuit is governed by the Hamiltonian

$$H = \frac{p^2}{2L} + \frac{q^2}{2C},$$

where  $q$  is charge,  $L$  is inductance, and  $C$  is capacitance. The inductive oscillator has the coordinate  $q$ , and the conjugate momentum is

$$p = L\dot{q},$$

where  $\dot{q}$  is the current flowing in the circuit. For a sufficiently long solenoid, the solenoid's field at the spins, which we will denote by  $B_y$ , is

$$\begin{aligned} B_y &= \mu_0 n \dot{q} \\ &= \frac{\mu_0 n}{L} p, \end{aligned}$$

where  $n$  is the number of turns per unit length. We will assume that the inductive resonator's field at the spins can be written in the form

$$\mathbf{B}_s(p) = \left( 0, \frac{dB_y}{dp} p, 0 \right),$$

with

$$\frac{dB_y}{dp} = \frac{\mu_0 n}{L}.$$

This assumption yields the following Hamiltonian (in units of rad/s) for the spin-resonator system:

$$H = \omega_0 I_z + \omega_h (a^\dagger a + 1/2) - \gamma I_y \frac{dB_y}{dp} p.$$

Substituting

$$p = i \sqrt{\frac{L\hbar\omega_h}{2}} (a^\dagger - a)$$

and

$$I_h = \frac{1}{2i} (I_+ - I_-)$$

into the Hamiltonian gives

$$\begin{aligned} H &= \omega_0 I_z + \omega_h (a^\dagger a + 1/2) \\ &\quad - \frac{\gamma}{2} \frac{dB_y}{dp} \sqrt{\frac{L\hbar\omega_h}{2}} (a^\dagger - a) (I_+ - I_-). \end{aligned}$$

In the interaction frame, the term in the Hamiltonian which survives averaging is

$$V = -\frac{\gamma}{2} \frac{dB_y}{dp} \sqrt{\frac{L\hbar\omega_h}{2}} (I_+ a^\dagger + I_- a). \quad (2.42)$$

Equation (2.42) shows that for both inductive and mechanical resonators, the spin-resonator Hamiltonian in the interaction frame takes the same form. For the inductive resonator, we define

$$g_{\text{induct}} = -\frac{\gamma}{2} \frac{dB_y}{dp} \sqrt{\frac{L\hbar\omega_h}{2}}.$$

Longitudinal relaxation of the spins will be governed by the rate constant

$$R_{\text{induct}} = 2g_{\text{induct}}^2 \tau_{\text{induct}} (2n_{\text{th}} + 1), \quad (2.43)$$

where the ringdown time  $\tau_{\text{induct}}$  of the inductive resonator is given by

$$\tau_{\text{induct}} = 2L/R,$$

with  $R$  the resistance in the inductive circuit. Equation (2.43) can be written more explicitly as

$$R_{\text{induct}} = (\gamma\mu_0 n)^2 \frac{\hbar\omega_h}{2R} (2n_{\text{th}} + 1).$$

## 6.2 Comparison of mechanical and inductive resonators

In comparing mechanical and inductive resonators, we first consider the way in which  $g^2$  scales with size. If  $\omega_h$  varies as  $1/r$ , we find that

$$\begin{aligned} g_{\text{mech}}^2 &\propto \frac{1}{I_h \omega_h} \\ &\propto 1/r^4, \end{aligned}$$

and

$$\begin{aligned} g_{\text{induct}}^2 &\propto \frac{n^2 \omega_h}{L} \\ &\propto 1/r^4. \end{aligned}$$

However, if  $\omega_h$  is assumed to be determined by a fixed field which does not vary during the scaling, we obtain

$$\begin{aligned} g_{\text{mech}}^2 &\propto 1/r^5, \\ g_{\text{induct}}^2 &\propto 1/r^3. \end{aligned}$$

At a given frequency, the the strength of the spin-resonator coupling depends more strongly on size if the resonator is mechanical.

The spin-relaxation rate depends on the resonator ringdown time as well as the coupling strength, and a quantitative comparison of spin relaxation rates for mechanical and inductive resonators is not possible because the dependence of mechanical ringdown time on size and temperature is poorly understood. We can, however, make simple estimates which suggest that inductive resonators would not efficiently cool spins. The resistance  $R$  of a coil is scale invariant if the skin depth is smaller than the radius of the wire used in the windings of the coil, while  $R$  scales as  $1/r$  in the regime where the current flows uniformly through the wire [13]. Cooling an exceptionally pure conductor to a temperature of a few Kelvins or below can increase its conductivity by a factor of up to  $10^6$  [14], which would yield a skin depth for copper of a few nanometers at 200 MHz. In order to make an estimate advantageous to inductive cooling, we assume that  $R$  is scale invariant, setting aside the question of whether a nanoscale inductor of this purity could be fabricated. This assumption yields

$$\tau_{\text{induct}} = 2L/R \propto r$$

and

$$g_{\text{induct}}^2 \tau_{\text{induct}} \propto 1/r^2. \quad (2.44)$$

The longitudinal relaxation rate constant  $R_{\text{induct}}$  for the example coils presented in reference [13] were calculated using the assumption that the resonator's conductivity increased by a factor of  $10^6$  over that of room-temperature copper due to cooling of the coil to mK temperatures:

$$R_{\text{induct}} \approx 3 \times 10^{-11} \text{ s}^{-1}.$$

These example coils have length and diameter of order  $50 \mu\text{m}$ . Scaling down these dimensions by a factor of  $10^3$  under the assumption that (2.44) holds would increase  $R_{\text{induct}}$  by six orders of magnitude, yielding a rate constant that is negligible compared

to the value

$$R_h \sim 1 \text{ s}^{-1}$$

obtained from numerical examples presented in section 6 of chapter 5.

## Chapter 3

# Resonator-induced spin relaxation

## 1 Trapping of the spin system due to angular momentum conservation

The idea that the transverse field of a mechanical resonator can polarize  $N$  spins might at first glance seem surprising or implausible, since we would in general expect a resonant transverse field to rotate a system of spins without polarizing it. Indeed, if we replace the resonator's field with a time-dependent applied transverse field and consider a set of noninteracting spins which evolve under this applied field, the evolution operator is simply a rotation of the spin system. This follows from the fact that at each instant, the system's Hamiltonian is the generator of a rotation operator. When the transverse field is that of a resonator which interacts with the spins, however, the spins can be polarized by the field. For instance, if the spins are initially at a higher temperature than the resonator, then heat transfer between spins and resonator must occur as the spin-resonator system moves toward equilibrium, and the spins become polarized as they are cooled by the resonator.

A spin system coupled to a resonator at zero Kelvins will not necessarily relax to its ground state, however. The Hamiltonian (2.1) commutes with  $\mathbf{I}^2$ , and spin angular momentum will be conserved during the relaxation if the spin Hamiltonian  $H_s$  also commutes with  $\mathbf{I}^2$ . The ground state of a system of spins has the maximum possible value of  $\mathbf{I}^2$ , and angular momentum conservation would prohibit most initial

spin distributions from relaxing to this state. For example, a distribution of  $N$  spins  $1/2$  contains only one angular momentum manifold with  $I = N/2$ . The ground state of the spin system is the low-energy state of this manifold. Relaxation under the spin-resonator interaction does not transfer population between angular momentum systems of different  $I$ , and if the initial state of the spins has population in any of the angular momentum manifolds with  $I < N/2$ , then spin-resonator relaxation will not transfer this population to the angular momentum manifold containing the ground state. Rather, the population belonging to a given angular momentum manifold will be transferred to the lowest energy state belonging to that manifold and will remain "trapped" in this state. In particular, if the initial distribution of  $N$  spins  $1/2$  is completely disordered, then all states of all angular momentum manifolds are equally populated, and spin relaxation induced by a resonator at zero Kelvins under the constraint of angular momentum conservation will leave population trapped in the ground state of each manifold, yielding an eventual spin polarization of [15]

$$P_{\text{trap}} = \frac{1}{2^{N-1}N} \sum_J^{N/2} \frac{N! (2J+1)^2}{(N/2+J+1)! (N/2-J)!}$$

$$\approx \sqrt{2/N}, \quad N \gg 1. \quad (3.1)$$

To illustrate this "trapping," we consider an example presented by Dicke [16]. A single spin  $1/2$  initially in its excited state will eventually relax to the ground state by spontaneous emission, as a result of the coupling between the spin and the resonant modes of the electromagnetic field. If two spins  $1/2$  are separated from each other by a distance which is small compared to the radiation frequency  $|\omega_0|$ , however, then the system interacting with the electromagnetic modes contains a singlet and a triplet, and the singlet cannot radiate to the field. If the initial state has one spin  $1/2$  in the excited state  $|-\rangle$  and the other in the state  $|+\rangle$ , then the singlet and triplet initially have the same population. The triplet decays by spontaneous emission, while the population of the singlet remains trapped. After the triplet has fully decayed, the

probability of detecting an excited spin is  $1/2$ , and only half the population is in the ground state of the two-spin system.

In addition to pointing out that a system coupled to the electromagnetic field can become trapped in a nonradiative state that differs from the ground state, Dicke showed that coherent spontaneous emission, or "super-radiance," can occur in a collection of two-level atoms which share the same coupling to the electromagnetic field. For example, he showed that the largest rate at which a gas of  $N$  two-level atoms can radiate by spontaneous emission is [16]

$$I = \frac{N}{2} \left( \frac{N}{2} + 1 \right) I_0. \quad (3.2)$$

In (3.2),  $I_0$  is the rate of radiation when only one atom is present and in its excited state. A model in which each atom radiates independently would have emission proportional to  $N$ , whereas the super-radiance described by equation (3.2) is proportional to  $N^2$ . The surprising nature of this result can be understood by expressing it in the language of the spin-resonator system. If a collection of  $N$  spins  $1/2$  is initially aligned along a transverse axis and then precesses in unison, the transverse dipole moment which drives the resonator is proportional to  $N$ , and the spontaneous emission rate is proportional to  $N^2$ . However, if the spin system is initially in the eigenstate having  $I_z = 0$ ,  $I = N/2$ , then the spontaneous emission rate is also proportional to  $N^2$ , in spite of the fact that the expected value of the transverse dipole moment is identically zero. A number of theoretical and experimental studies of super-radiance have been performed, and the subject is reviewed in reference [17].

For both trapped states and super-radiant states, correlated motion changes the nature of spontaneous emission dramatically from what would be observed in a system of spins radiating independently. For a system of  $N$  spins  $1/2$  interacting with a mechanical resonator and simultaneously evolving under the interaction-frame Hamiltonian  $H_s$ , the contribution to spin relaxation associated with spin-spin correlations can be highlighted by writing the equations of motion for the Cartesian spin compo-

nents as

$$\begin{aligned}\frac{d}{dt} \langle I_z \rangle &= -i \langle [I_z, H_s] \rangle - R_h \left\{ \langle I_z \rangle - \frac{N/2}{2n_{\text{th}} + 1} \right\} - R_0 \langle N/2 - I_x^2 - I_y^2 \rangle, \\ \frac{d}{dt} \langle I_x \rangle &= -i \langle [I_x, H_s] \rangle - \frac{1}{2} R_h \langle I_x \rangle - R_0 \left\langle \frac{1}{2} (I_x I_z + I_z I_x) \right\rangle, \\ \frac{d}{dt} \langle I_y \rangle &= -i \langle [I_y, H_s] \rangle - \frac{1}{2} R_h \langle I_y \rangle - R_0 \left\langle \frac{1}{2} (I_y I_z + I_z I_y) \right\rangle.\end{aligned}$$

In each of these equations, the term proportional to  $R_0$  is zero if the components of distinct spins are uncorrelated. In an ensemble of  $N$  spins  $1/2$  which relax without developing spin-spin correlations, the relaxation induced by the resonator is thus exponential, with a rate constant proportional to  $R_h$ . It is correlations of the form  $\langle I_{x,j} I_{x,k} \rangle$ ,  $\langle I_{y,j} I_{y,k} \rangle$ ,  $\langle I_{x,j} I_{z,k} \rangle$ , and  $\langle I_{y,j} I_{z,k} \rangle$  which are responsible for phenomena such as trapping and super-radiance.

## 2 Indirect spin-spin interaction

The semiclassical equation introduced in section 5 of chapter 2 can be used to visualize the way in which an indirect spin-spin interaction develops as a result of the spins' coupling to the same resonator. We consider an example in which the classical resonator is at zero Kelvins, with no direct interaction between spins. In the absence of coupling between spins and resonator, the spins simply precess around the static field, while the resonator is motionless. In the coupled system, the resonator quickly achieves a steady-state response to the torque exerted on it by the spins, and energy is donated from spins to resonator by means of this driving torque. The driven mechanical motion creates a resonant transverse field which rotates the spins, thereby changing their energy. As the spins drive the resonator, the oscillating field associated with the mechanical motion causes the energy of the spins to change.

An indirect spin-spin interaction arises because the resonator's field is the sum of its steady-state response to all spins. The field torque associated with the resonator's linear response to spin  $j$  acts on spin  $k$ , and so the state of spin  $j$  affects the field acting

on spin  $k$ . The torque acting on spin  $k$  due to the driving of the resonator by spin  $j$  can be interpreted as an indirect torque exerted on spin  $k$  by spin  $j$ , and the indirect torques which link each pair of spins cause the development of spin-spin correlations during mechanical cooling. In order to quantify the strength of the indirect torques, we consider the state of the spin-resonator system during a time step  $\Delta t \gg \tau_h$  which is short compared to the time needed for the spin-resonator interaction to change the spin state. If the initial orientation of semiclassical spin  $j$  at  $t = 0$  is given by angles  $\phi_j$  and  $\alpha_j$ , with  $\phi_j$  the azimuthal angle and  $\alpha_j$  the angle between the spin and the  $z$ -axis, then the resonator's steady state motion during  $\Delta t$  is

$$\theta(t) = \frac{dB_x}{d\theta} \gamma \hbar I \frac{\tau_h}{2I_h \omega_h} \sum_j \sin \alpha_j \sin(\omega_h t + \phi_j),$$

where we have assumed that all spins experience the same field and have Larmor frequency  $\omega_0 = -\omega_h$ . (In order to simplify notation in this section, we have dropped the superscript  $c$  used to distinguish semiclassical variables from analogous quantum operators.) The transverse field is

$$\frac{dB_x}{d\theta} \theta(t) = \left( \frac{dB_x}{d\theta} \right)^2 \gamma \hbar I \frac{\tau_h}{2I_h \omega_h} \sum_j \sin \alpha_j \sin(\omega_h t + \phi_j), \quad (3.3)$$

and since this field is established quickly and changes negligibly in amplitude during the time step  $\Delta t$ , we can consider the  $j$ th term in this sum to be the effective field of spin  $j$  experienced by the other spins. The amplitude of this effective field is

$$B_{j,\text{eff}} = \left( \frac{dB_x}{d\theta} \right)^2 \gamma \hbar \frac{\tau_h}{2I_h \omega_h} (I \sin \alpha_j).$$

In a reference frame rotating around the  $z$ -axis at the Larmor frequency of the spins, the resonant component of this effective field has magnitude  $B_{j,\text{eff}}/2$ , and the precession frequency of spin  $k$  in a resonant field of this magnitude is

$$\gamma B_{j,\text{eff}}/2 = R_0 I_{j,\text{trans}},$$

where

$$I_{j,\text{trans}} \equiv I \sin \alpha_j$$

is the magnitude of the transverse component of spin  $j$ . We see that the semiclassical model predicts that spin  $j$  indirectly exerts a torque on spin  $k$  which in the absence of any other interactions would cause spin  $k$  to precess at frequency  $R_0 I_{j,\text{trans}}$ .

When the transverse components of individual spins are distributed randomly in the plane, the indirect torques exerted on a spin  $k$  by the remaining spins do not add coherently. Although the sum  $Z$  of the resonant effective fields exerted on spin  $k$  by the other spins has an expected value of zero, its actual value during the time step  $\Delta t$  will in general have an order of magnitude comparable to the standard deviation of  $S$ . Consider a frame rotating around the  $z$ -axis with spin  $k$  during  $\Delta t$  and having its  $x$ -axis aligned with the transverse component of spin  $k$ . Assume that spins are initially independent and have identical probability distributions, with the distribution of  $\phi_j$  flat and uncorrelated with  $\alpha_j$ . It follows from (3.3) that the root-mean-square value of  $\gamma Z$  is

$$\gamma Z = \sqrt{N-1} R_0 \bar{I}_{\text{trans}},$$

where  $\bar{I}_{\text{trans}}$  is the root-mean-square value of  $I_{j,\text{trans}}$ .

If a spin system is completely disordered or has weak Zeeman order at the beginning of  $\Delta t$ , the sum of the indirect torques exerted on spin  $k$  by the other spins would cause spin  $k$  to precess with a frequency of order  $R_0 I \sqrt{N}$ . If the spins are all aligned in the transverse plane at the beginning of  $\Delta t$ , the indirect torques on spin  $k$  add coherently, and the precession frequency of spin  $k$  due to the sum of the indirect torques is of order  $R_0 I N$ . (In this case, the uniform rotation of  $\mathbf{I}$  toward the static applied field would be the mechanical analog of "radiation damping.") We define  $T_{\text{corr}}$  to be the characteristic evolution time of each spin in the net field exerted on it

indirectly by all of the other spins:

$$\begin{aligned} T_{\text{corr}} &\approx 1/(R_0IN), \text{ spins aligned along transverse axis,} \\ T_{\text{corr}} &\approx 1/(R_0I\sqrt{N}), \text{ disordered system.} \end{aligned} \tag{3.4}$$

We can expect that relaxation associated with these indirect torques will be disrupted if they vary sinusoidally with a period substantially less than  $T_{\text{corr}}$ . Consider, for instance, an example where two semiclassical spins whose Larmor frequencies differ by  $\delta\omega$  are initially aligned along the  $x$ -axis. In a frame rotating with spin 1, the indirect torque exerted by spin 2 will initially tend to rotate spin 1 toward  $B_z$ , but after a time  $t = \pi/\delta\omega$ , the two spins will be aligned in opposite directions in the transverse plane, and the indirect torque on spin 1 will tend to rotate it away from  $B_z$ . More generally, we can expect that for a system of  $N$  spins, a perturbation which reverses the signs of the indirect torques within a time  $T_{\text{perturb}}$  will partially disrupt the contribution of spin-spin correlations to relaxation if  $T_{\text{perturb}}$  is of the order of  $T_{\text{corr}}$  or smaller. If  $T_{\text{perturb}} \ll T_{\text{corr}}$ , the contribution of the indirect torques should be effectively suppressed.

### 3 Modification of the relaxation processes by the spin Hamiltonian

Arguments based on the semiclassical model suggest that a resonator at zero Kelvins will induce the spins to relax exponentially to the ground state if the indirect spin-spin torques are modulated sufficiently quickly by terms in the spin Hamiltonian. To move beyond this conjecture and characterize resonator-induced relaxation under a given spin Hamiltonian requires an analysis of the way in which perturbations to the spin Hamiltonian modify the coefficients of the master equation. In order to clarify the nature of the arguments being presented, we frame the discussion in this section in terms of general properties of the master equation. Sections 4 and 5 apply the results of this section to the problems of longitudinal and transverse spin relaxation.

Reference [7] derives a general expression for the master equation which governs a small system  $S$  interacting with a large reservoir  $R$ . The sets  $\{|a\rangle\}$ ,  $\{|\mu\rangle\}$  are respective orthonormal bases of  $S$ ,  $R$ , and would be energy eigenstates in the absence of the coupling between  $S$  and  $R$ . The eigenfrequency of a state  $|a\rangle$  is denoted by  $\omega_a$ , and the difference of two such eigenfrequencies by

$$\omega_{ab} = \omega_a - \omega_b.$$

For the discussion in sections 3, 4, and 5, it will be convenient to define the interaction frame as one in which the only surviving terms in the Hamiltonian are those which characterize interactions between  $S$  and  $R$ . Note that this definition differs from the one used for equation (2.24), which was defined so as to eliminate only the terms  $\omega_0 I_z$  and  $\omega_h (a^\dagger a + 1/2)$  from the Hamiltonian. The interaction-frame master equation for  $S$  can be written as

$$\frac{d}{dt} \rho_{ab}(t) = \sum_{c,d} \exp\{i(\omega_{ab} - \omega_{cd})t\} \mathcal{R}_{abcd} \rho_{cd}(t), \quad (3.5)$$

where  $\mathcal{R}_{abcd}$  is time-independent.

Perturbations in the Hamiltonian  $H_s$  of the small system  $S$  can affect equation (3.5) by perturbing the constants  $\mathcal{R}_{abcd}$  as well as the difference frequencies  $\omega_{ab}$ . We will find that these two types of changes in the master equation have different effects on spin relaxation. Each coefficient  $\mathcal{R}_{abcd}$  can be expressed as a sum of terms of the form

$$M_1 M_2 \int_0^\infty g(\tau) \exp(i\omega_{nm}\tau) d\tau,$$

where  $M_1$  and  $M_2$  are matrix elements of operators acting on  $S$  which contribute to the interaction Hamiltonian, and  $g(\tau)$  is a reservoir correlation function. If the eigenfrequencies  $\{\omega_a\}$  are perturbed while the eigenstates  $\{|a\rangle\}$  do not change, the matrix elements  $M_1$  and  $M_2$  are unaffected by the perturbation; if, in addition, the perturbation in the frequencies  $\omega_{nm}$  is small compared to the spectral width of the correlation functions  $g(\tau)$ , then  $\mathcal{R}_{abcd}$  will be unaffected by the perturbation. Since

correlation times of a reservoir are in general extremely short, we will consistently consider the spectral width of  $g(\tau)$  to be large compared to any perturbations in  $\omega_{nm}$ . Under these conditions, perturbing the eigenfrequencies but not the eigenstates leaves  $\mathcal{R}_{abcd}$  unmodified in (3.5). By way of contrast, perturbations to  $H_s$  which modify the eigenstates can change the values of the matrix elements  $M_1$  and  $M_2$ , thereby modifying the coupling constants  $\mathcal{R}_{abcd}$  which characterize the physical processes occurring during the correlation time of the reservoir.

The difference  $(\omega_{ab} - \omega_{cd})$  in the oscillation frequencies of lab-frame density matrix elements appears in the interaction-frame relaxation equation as an oscillation in the phase of the coupling responsible for transfer from  $\rho_{cd}$  to  $\rho_{ab}$ . If the frequency difference  $|\omega_{ab} - \omega_{cd}| \ll 2\pi\mathcal{R}_{abcd}$  is perturbed to a value much larger than  $2\pi\mathcal{R}_{abcd}$ , then the transfer from  $\rho_{cd}$  to  $\rho_{ab}$  characterized by  $\mathcal{R}_{abcd}$  will be suppressed. More precisely, the physical processes responsible for such transfer will continue to occur, but the relative phase of lab-frame density matrix elements will vary within a period which is short compared to the characteristic time  $1/\mathcal{R}_{abcd}$  required for the transfers to cause a non-negligible change in  $\rho_{ab}$ , and the fast phase variation will ensure that the sum of the transfers to  $\rho_{ab}$  continually stays near zero. Under these conditions, the coefficient  $\mathcal{R}_{abcd}$  will not contribute to the evolution of  $\rho_{ab}$ .

Reference [7] derives formulas which are helpful in interpreting the processes associated with the various coupling constants  $\mathcal{R}_{abcd}$ . If  $c \neq a$ , for instance, then  $\mathcal{R}_{aacc}$  can be expressed as

$$\mathcal{R}_{aacc} = \frac{2\pi}{\hbar} \sum_{\mu} p_{\mu} \sum_{\nu} |\langle \nu, a | V | \mu, c \rangle|^2 \delta(E_{\mu} + E_c - E_{\nu} - E_a). \quad (3.6)$$

Here  $\delta$  is the Dirac delta function,  $E_i$  is an energy eigenvalue for the system or reservoir,  $V$  is the interaction Hamiltonian coupling the system to the reservoir,  $p_{\mu}$  is the thermal population of state  $\mu$ , and  $\mu, \nu$  range over the orthonormal basis of  $R$ . This equation is interpreted to mean that  $\mathcal{R}_{aacc}$  gives the summed probability per unit time that a state from the continuum  $\{|\mu, c\rangle\}$  makes the transition to the continuum  $\{|\nu, a\rangle\}$ , where  $a$  and  $c$  are fixed, while  $\mu, \nu$  range over the orthonormal

basis of  $R$ . This interpretation is highlighted by the use of the notation

$$\Gamma_{c \rightarrow a} \equiv \mathcal{R}_{aacc}.$$

Reference [7] also shows that the relaxation of coherences  $\rho_{ab}$  is governed by the constants

$$\begin{aligned} \Gamma_{ab} &= \Gamma_{ab}^{\text{nonad}} + \Gamma_{ab}^{\text{ad}}, \\ \Gamma_{ab}^{\text{nonad}} &= \frac{1}{2} \left( \sum_{n \neq a} \Gamma_{a \rightarrow n} + \sum_{n \neq b} \Gamma_{b \rightarrow n} \right), \\ \Gamma_{ab}^{\text{ad}} &= \frac{2\pi}{\hbar} \sum_{\mu} p_{\mu} \sum_{\nu} \delta(E_{\mu} - E_{\nu}) \\ &\quad \times \frac{1}{2} (|\langle \nu, a | V | \mu, a \rangle|^2 + |\langle \nu, b | V | \mu, b \rangle|^2 - 2 \text{Re} \langle \mu, a | V | \nu, a \rangle \langle \nu, b | V | \mu, b \rangle). \end{aligned} \quad (3.7)$$

The constant  $\Gamma_{ab}^{\text{nonad}}$  is interpreted as giving the rate at which transitions away from  $|a\rangle$  and  $|b\rangle$  disrupt the coherence between these states and cause "nonadiabatic" relaxation, while the "adiabatic" constant  $\Gamma_{ab}^{\text{ad}}$  characterizes damping of a coherence due to interactions in which the system  $A$  does not change state. When  $A$  represents a spin system, we would expect  $\Gamma_{ab}^{\text{nonad}}$  and  $\Gamma_{ab}^{\text{ad}}$  to be associated with "lifetime broadening" and "secular broadening," respectively. (Lifetime broadening is transverse spin relaxation caused by spin transitions which shorten the lifetime of a coherence, while secular broadening is caused by fluctuations in  $B_z$  which modulate the precession frequency of the spins.) Consistent with this interpretation is the fact that  $\Gamma_{ab}^{\text{ad}} = 0$  if fluctuations in  $B_z$  are excluded from the model of the spin-resonator system by the use of the Jaynes-Cummings Hamiltonian (2.11) as the interaction Hamiltonian. This can be seen by noting first that

$$\begin{aligned} \langle \nu, b | I_+ a^\dagger | \mu, b \rangle &= 0, \\ \langle \nu, b | I_- a | \mu, b \rangle &= 0, \end{aligned}$$

for any eigenstate  $|b\rangle$  of a secular spin Hamiltonian, since  $I_+$  and  $I_-$  do not couple

states within a given eigenspace of  $I_z$ . It follows that

$$\langle \nu, b | V | \mu, b \rangle = 0 \quad (3.8)$$

for each energy eigenstate  $|b\rangle$ , which implies  $\Gamma_{ab}^{\text{ad}} = 0$ . In discussing the relaxation of coherences due to spin-resonator interactions, we will therefore consider only nonadiabatic relaxation, and we will simplify notation by dropping the label "nonadab."

An interpretation of the coupling constants  $\mathcal{R}_{abcd}$ , with  $a \neq c$ ,  $b \neq d$ , will be helpful in our analysis of spin relaxation. Reference [7] derives the formula

$$\begin{aligned} \mathcal{R}_{abcd} = & \frac{2\pi}{\hbar} \sum_{\mu} p_{\mu} \sum_{\nu} \langle \mu, d | V | \nu, b \rangle \langle \nu, a | V | \mu, c \rangle \\ & \times \delta(E_{\mu} + E_c - E_{\nu} - E_a). \end{aligned} \quad (3.9)$$

In suggesting an interpretation for (3.9), we note first that it is not a formula for a transition amplitude, so we cannot immediately associate the product  $\langle \mu, d | V | \nu, b \rangle \langle \nu, a | V | \mu, c \rangle$  with a process in which a transition from  $|\mu, c\rangle$  to  $|\nu, a\rangle$  is followed by a transition from  $|\nu, b\rangle$  to  $|\mu, d\rangle$ . If it were correct to interpret in this way the matrix elements which characterize relaxation processes, then the product

$$|\langle \nu, a | V | \mu, c \rangle|^2 = \langle \mu, c | V | \nu, a \rangle \langle \nu, a | V | \mu, c \rangle$$

appearing in (3.6) should be associated with a process in which a transition from  $|\mu, c\rangle$  to  $|\nu, a\rangle$  is followed by a transition from  $|\nu, a\rangle$  back to  $|\mu, c\rangle$ ; since we associate  $\mathcal{R}_{aacc}$  with one-way transfer from  $|\mu, c\rangle$  to  $|\nu, a\rangle$ , this interpretation would be problematic. We can obtain an unproblematic interpretation of (3.9) by first recalling that the equation of motion for a density matrix  $\rho$  can be written as

$$\frac{d}{dt}\rho(t) = (-iH)\rho(t) + \rho(t)(iH). \quad (3.10)$$

The factor  $(-iH)$  in the product  $(-iH)\rho(t)$  is obtained from the evolution operator

$e^{-iHt}$  responsible for evolving the kets forward in time, while the factor  $(iH)$  in the product  $\rho(t)(iH)$  is associated with the evolution of the bras. If we use first-order perturbation theory to study the motion of  $\rho$ , we can interpret the results in terms of two sets of processes: those in which the kets evolve while the bras are unchanged, and those in which the bras evolve while the kets are unchanged. Similarly, evolution of  $\rho$ , as calculated using second-order perturbation theory, can be interpreted in terms of four types of processes, each associated with one of the terms in the double commutator

$$i^2 [[\rho, H(t_1)], H(t_2)] = -\rho H(t_1) H(t_2) + H(t_1) \rho H(t_2) + H(t_2) \rho H(t_1) - H(t_2) H(t_1) \rho. \quad (3.11)$$

For instance, the term  $\rho H(t_1) H(t_2)$  is associated with processes in which bras are evolved in two consecutive steps, while  $H(t_1) \rho H(t_2)$  is associated with processes in which the kets evolve during the first step and the bras during the second.

Note as well that the transfers of probability amplitude associated with  $H(t_1)$  and  $H(t_2)$  each involve a phase change of magnitude  $90^\circ$ . This can be seen by examining (3.10), in which the respective factors of  $-i$  and  $i$  yield phase changes of opposite sign for the transfers associated with evolution of the kets and the bras. The factor  $(-iH)\rho dt$ , for example, represents a change to  $\rho$  in which the term added to a given element  $\rho_{jk}$  is

$$-i \sum_{|n\rangle} \langle j | H | n \rangle \rho_{nk}.$$

This can be interpreted to mean that the interaction characterized by the matrix element  $\langle j | H | n \rangle$  causes a transfer to occur from  $\rho_{nk}$  to  $\rho_{jk}$ , while the factor  $-i$  yields a phase change of  $-90^\circ$ . Note that for processes in which a bra evolves during one step and a ket evolves during the other, the phase changes occurring during the two steps will cancel. If kets are evolved twice or bras are evolved twice, however, the phase change associated with the process will be  $180^\circ$ . In particular, probability amplitude which is transferred by such processes will change sign.

The physical process associated with a product  $M_1 M_2$  of matrix elements can

be interpreted by determining whether bras or kets were evolving during the two consecutive stages of motion. We find that the coefficient  $\mathcal{R}_{abcd}$  given by (3.9) depends on processes in which the ket  $|c\rangle$  makes a transition to  $|a\rangle$  during one stage of motion, while the bra  $\langle d|$  makes a transition to  $\langle b|$  during the other. Although the distinction between bras and kets is helpful in making sense of formulas such as (3.9), we can simplify language and notation by neglecting to distinguish between bras and kets in discussing physical processes; for instance, we will consider (3.9) to characterize processes in which  $|c\rangle \rightarrow |a\rangle$  and  $|d\rangle \rightarrow |b\rangle$  without a change of phase. This simplification is motivated by the idea that we can consider these processes to be occurring within an ensemble of systems, with each system represented by a linear combination of kets. The appearance of bras in our formalism can be considered an artifact of the choice to represent the ensemble by a matrix rather than a collection of state functions.

In analyzing spin relaxation due to spin-resonator interactions, we will find that coefficients such as  $\mathcal{R}_{abad}$ , with  $b \neq d$ , play an important role. The arguments given in reference [7] can be extended to yield formulas for these coefficients and obtain an interpretation of the processes characterized by them. When  $V$  represents the spin-resonator interaction Hamiltonian, we find that  $\mathcal{R}_{abad}$  characterizes processes in which probability amplitude is transferred first from  $|d\rangle$  to  $|m\rangle$  and then from  $|m\rangle$  to  $|b\rangle$ , with  $m \neq b, d$ , and the matrix elements associated with these processes are

$$M_{abad} = \langle d, \mu | V | m, \nu \rangle \langle m, \nu | V | b, \mu \rangle. \quad (3.12)$$

During the two steps, the transferred probability amplitude changes phase by  $180^\circ$ . In the general case,  $\mathcal{R}_{abad}$  also depends on matrix elements of the form  $\langle a, \mu | V | a, \nu \rangle \langle d, \nu | V | b, \mu \rangle$ , but it follows from (3.8) that these products are zero for the Jaynes-Cummings Hamiltonian.

## 4 Longitudinal relaxation

In this section, we analyze in greater detail the processes which cause spin population to be trapped away from the ground state during resonator-induced spin polarization, as well as the mechanisms by which such trapping could be disrupted by the presence of additional terms in the spin Hamiltonian.

### 4.1 Noninteracting spins

We first consider a system of  $N$  noninteracting spins  $1/2$  which have identical Larmor frequencies. The eigenstates  $\{|a\rangle\}$  can be chosen as product states. Longitudinal relaxation can occur due to direct couplings  $\mathcal{R}_{aacc}$  between populations, and it can also occur when two populations are coupled to the same coherence: simultaneous transfer from  $\rho_{aa}$  to  $\rho_{bd}$  and from  $\rho_{bd}$  to  $\rho_{cc}$  yields indirect transfer from  $\rho_{aa}$  to  $\rho_{cc}$ . Appendix E presents a proof that if these indirect transfers are eliminated, then  $\langle I_z \rangle$  relaxes exponentially to thermal equilibrium with rate constant  $R_h$ , regardless of initial conditions. The proof depends on a selection rule, namely, the fact that the matrix element  $\langle \nu, a | V | \mu, c \rangle$  will be nonzero only if eigenstates  $|a\rangle$ ,  $|c\rangle$  differ by exactly one spin flip. When the matrix element is nonzero, then the transfer between populations which it characterizes can be calculated as if the other spins were absent.

#### 4.1.1 Two spins

While the single-spin flips associated with direct coupling between populations do not introduce spin-spin correlations, such correlations can be introduced as the result of couplings between populations and coherences. Consider, for example, a system of

two noninteracting spins with basis set

$$|1\rangle \equiv |++\rangle \quad (3.13)$$

$$|2\rangle \equiv |+-\rangle \quad (3.14)$$

$$|3\rangle \equiv |-+\rangle \quad (3.15)$$

$$|4\rangle \equiv |--\rangle. \quad (3.16)$$

Writing out explicit expressions [7] for the coefficients of the master equation governing this system shows that for each state  $i$ , the coefficients  $\mathcal{R}_{ii23}$ ,  $\mathcal{R}_{23ii}$ ,  $\mathcal{R}_{ii32}$ , and  $\mathcal{R}_{32ii}$ , which couple coherences to populations, have the same order of magnitude as coefficients which couple populations directly, and since  $\omega_{23} = \omega_{32} = \omega_{ii} = 0$ , the time-dependent exponential terms appearing in (3.5) do not modulate into the coupling between the population  $\rho_{ii}$  and the coherences  $\rho_{23}$  and  $\rho_{32}$ . Note that  $\mathcal{R}_{23ii}$  and  $\mathcal{R}_{32ii}$  in particular are responsible for converting populations into coherent superpositions of product states and can therefore introduce spin-spin correlations into the system.

For  $i = 2, 3$ , these coefficients tend to introduce a negative correlation between states 2 and 3. For instance, it follows from the last paragraph of section 3 that  $\mathcal{R}_{2322}$  is associated with processes in which probability amplitude is first transferred from  $|2\rangle$  to  $|m\rangle$  and then from  $|m\rangle$  to  $|3\rangle$ , where  $m = 1$  or  $m = 4$ , with the probability amplitude changing sign during the two transfers. The change in sign during transfer of probability amplitude from  $|2\rangle$  to  $|3\rangle$  introduces a negative correlation between the two states. More formally, we can say that since

$$\mathcal{R}_{2322} = -R_0 (n_{\text{th}} + 1/2)$$

is negative, it tends to introduce a negative correlation between states 2 and 3. Similar processes are associated with the coefficients  $\mathcal{R}_{23ii}$  and  $\mathcal{R}_{32ii}$ , for  $i = 2, 3$ , and these coefficients have the same value.

In the case where an initially disordered sample relaxes to a trapped state due to its

interaction with a resonator at zero Kelvins, we can view these processes as continually renewing the probability amplitude of the coherent superposition  $(|+-\rangle - |-+\rangle)/\sqrt{2}$ , thereby preventing it from decaying due to the single-spin flips which occur as population is transferred between product-state populations. An alternative point of view would be that the transfers which occur between populations and the coherences  $\rho_{23}$  and  $\rho_{32}$  constitute an indirect coupling between product-state populations which depletes the ground state and renews the populations of states 2 and 3. For instance,  $\mathcal{R}_{1123}$  and  $\mathcal{R}_{1132}$  are associated with processes in which both  $|2\rangle$  and  $|3\rangle$  make a transition to the ground state. Because of the negative correlation which is maintained between states 2 and 3, the product of the probability amplitudes simultaneously transferred from  $|2\rangle$  to  $|1\rangle$  and from  $|3\rangle$  to  $|1\rangle$  tends to be negative, which decreases the population of the ground state. The population which disappears from the ground state as a result of its coupling to the coherences  $\rho_{23}$  and  $\rho_{32}$  is simultaneously added to the populations of states 2 and 3 because of their coupling to the same coherences.

Note that this simple analysis of spin trapping has not taken into account all couplings between coherences and populations. However, the coefficients which take  $\rho_{11} \rightarrow \rho_{23}$ ,  $\rho_{11} \rightarrow \rho_{32}$ ,  $\rho_{23} \rightarrow \rho_{44}$ , and  $\rho_{32} \rightarrow \rho_{44}$  are insignificant at 0 K, since they depend on transitions in which the resonator donates a quantum to the spins. (Indeed, the coupling constants associated with these transfers are proportional to  $n_{\text{th}}$ .) In addition, transfers from  $\rho_{44}$  to  $\rho_{23}$  and  $\rho_{32}$ , although relevant in the early stages of spin-trapped relaxation, are negligible in later stages, since the population of  $|--\rangle$  is entirely depleted by the single-spin flips that couple it to the populations of  $|+-\rangle$  and  $|-+\rangle$ . In the product-state basis, spin trapping can be interpreted in terms of the processes which contribute to  $\mathcal{R}_{ii23}$ ,  $\mathcal{R}_{23ii}$ ,  $\mathcal{R}_{ii32}$ , and  $\mathcal{R}_{32ii}$ .

Spin trapping can be suppressed by a perturbation  $H_1$  to the spin Hamiltonian  $H_s$  that changes the eigenfrequencies but not the eigenstates. The fastest transfers between the ground state and the coherences  $\rho_{23}$ ,  $\rho_{32}$  are governed by the rate constant

$R_0 (n_{\text{th}} + 1)$ , and if the lab-frame coherences oscillate in phase with a frequency

$$|\omega_{23}| \gg 2\pi R_0 (n_{\text{th}} + 1),$$

then the couplings between populations and coherences will not contribute to the relaxation of the populations. Under these conditions, the spin-spin flips will cause the longitudinal relaxation to proceed exponentially with rate constant  $R_h$ .

#### 4.1.2 $N$ spins

A similar result holds for an initially disordered system of  $N$  spins. The matrix elements of the interaction Hamiltonian  $V$  allow for two types of processes which can create spin-spin correlations by transferring the populations of product states into coherent superpositions of states. If  $a \neq b, c$ , then transfer from  $\rho_{aa}$  to coherence  $\rho_{bc}$  can occur by a process involving the two transitions  $|a\rangle \rightarrow |b\rangle$  and  $|a\rangle \rightarrow |c\rangle$ . The selection rule obtained from (3.9) is

$$\langle a, \mu | V | b, \nu \rangle \langle c, \nu | V | a, \mu \rangle \neq 0, \quad (3.17)$$

where  $\mu$  and  $\nu$  label states of the reservoir. This rule requires that  $|b\rangle$  and  $|c\rangle$  each differ from  $|a\rangle$  by exactly one spin flip, and the transitions  $|a\rangle \rightarrow |b\rangle$  and  $|a\rangle \rightarrow |c\rangle$  both involve spin flips in the same direction, since both transitions have the reservoir moving from  $|\mu\rangle$  to  $|\nu\rangle$ . We can conclude that  $\rho_{bc}$  is a zero-quantum coherence between states which differ by two spin flips in opposite directions. A second type of process which can create spin-spin correlations occurs when  $a = b$  or  $a = c$ . Without loss of generality, we suppose that  $a = b$ ,  $a \neq c$ . The processes contributing to the development of spin-spin correlations involve transfer from  $|a\rangle \rightarrow |m\rangle$  and then from  $|m\rangle \rightarrow |c\rangle$  during the correlation time of the reservoir, and (3.12) implies that these processes are allowed if

$$\langle a, \mu | V | m, \nu \rangle \langle m, \nu | V | c, \mu \rangle \neq 0. \quad (3.18)$$

Rule (3.18) implies that the two transitions  $|a\rangle \rightarrow |m\rangle$  and  $|m\rangle \rightarrow |c\rangle$  involve a spin flip in opposite directions, since the first is accompanied by the reservoir transition  $|\mu\rangle \rightarrow |\nu\rangle$  and the second by the transition  $|\nu\rangle \rightarrow |\mu\rangle$ , and since the interaction Hamiltonian  $V$  only couples product states which differ by a single spin flip. For this case as well,  $\rho_{bc}$  is a zero-quantum coherence between states differing by a "flip-flop."

The development of resonator-induced spin-spin correlations in an initially disordered system depends on transfer from product-state populations to zero-quantum "flip-flop" coherences. If the periods of such coherences are short compared to the time required for this transfer, the cumulative effect of the transfers will be negligible, and no coherences will be excited. In this case, we can consider the populations to be coupled only to populations, which yields a problem for which the longitudinal relaxation proceeds exponentially with rate constant  $R_h$ . Note that as the number  $N$  of spins is increased, the number of processes which contribute to coefficients such as  $\mathcal{R}_{acaa}$  increases, since many states  $|m\rangle$  become accessible to  $|a\rangle$  as intermediates in the transition to  $|c\rangle$ . In addition, the rate at which coherent superpositions of product states are renewed by these processes in general depends on the instantaneous value of many elements in the density matrix, as well as on the value of many coupling constants. It is therefore not immediately obvious how large the frequencies of the "flip-flop" zero-quantum coherences must be in order to suppress the cumulative effect of the processes responsible for spin-trapping.

We can obtain a rough estimate of the time  $T_{\text{trap}}$  required for the resonator to induce spin-spin correlations in an initially disordered system. For large  $N$ , equation (3.1) implies that

$$\langle I_z \rangle_{\text{trap}} \approx \sqrt{\frac{N}{2}} \quad (3.19)$$

is the final value of  $\langle I_z \rangle$  when the resonator is at zero Kelvins. Substituting (3.19) into the relaxation equation for  $\langle I_z \rangle$  and setting the derivative equal to zero yields

$$0 \approx -R_0 \langle I_z \rangle_{\text{trap}} + R_0 \langle I_x^2 + I_y^2 \rangle_{\text{trap}},$$

from which it follows that

$$\langle I_x^2 + I_y^2 \rangle_{\text{trap}} \approx \sqrt{\frac{N}{2}}.$$

Our estimate of the time  $T_{\text{trap}}$  depends on the claim that  $\langle I_x^2 + I_y^2 \rangle$  decreases monotonically from  $N/2$  to  $\sqrt{N/2}$  as spin-spin correlations develop. In supporting this claim, we use a basis of angular momentum eigenstates  $|I, M\rangle$ , where  $M$  denotes the eigenvalue for the operator  $I_z$ . The states  $|I, M\rangle$  are also eigenstates of the operator  $I_x^2 + I_y^2$ :

$$\begin{aligned} (I_x^2 + I_y^2) |I, M\rangle &= (I_- I_+ + I_z) |I, M\rangle \\ &= \{I(I+1) - M^2\} |I, M\rangle. \end{aligned}$$

Note that within each angular momentum manifold, the value of  $\langle I_x^2 + I_y^2 \rangle$  varies as  $-M^2$ . A completely disordered system has equal population in each state  $|I, M\rangle$ , and resonator-induced relaxation eventually moves the entire population to the state with  $M = I$ . It is clear that once the bulk of the population of a given angular momentum manifold has been transferred to states with positive  $M$ , continued spontaneous emission from the spins to the resonator's mode will decrease  $\langle I_x^2 + I_y^2 \rangle$ , since emission from a state with positive  $M$  increases the value of  $M$ . For several values of  $I$  between  $I = 2$  and  $I = 100$ , we have used the formulas for the spontaneous emission rate of states  $|I, M\rangle$  [16] to simulate the mechanical cooling of a single angular momentum system in which all states  $|I, M\rangle$  initially have equal population. In these simulations,  $\langle I_x^2 + I_y^2 \rangle$  decreased monotonically throughout the cooling process. It is reasonable to conclude that monotonic decrease of  $\langle I_x^2 + I_y^2 \rangle$  would occur for any value of  $\dot{I}$ , which implies that  $\langle I_x^2 + I_y^2 \rangle$  decreases monotonically in a disordered spin system.

This conclusion allows us to obtain a lower bound on the time required for resonator-induced spin-spin correlations to develop. We rewrite the longitudinal relaxation equation as

$$\frac{d}{dt} \langle I_z \rangle \approx -R_0 (\langle I_z \rangle - \langle I_x^2 + I_y^2 \rangle), \quad (3.20)$$

and note that  $\langle I_z \rangle$  increases exponentially toward the instantaneous value of  $\langle I_x^2 + I_y^2 \rangle$ . If  $\langle I_x^2 + I_y^2 \rangle$  were constant during the spin-trapped cooling, the polarization would evolve exponentially, with a rate constant independent of  $N$ . When  $\langle I_x^2 + I_y^2 \rangle$  decreases from  $N/2$  down to  $\sqrt{2/N}$ , however, the derivative of  $\langle I_z \rangle$  is decreased by the presence of resonator-induced spin-spin correlations. We might guess that  $\langle I_z \rangle$  initially follows the relaxation curve predicted for a system in which such correlations are suppressed, but then flattens out as  $\langle I_z \rangle$  takes on a value of order  $\langle I_z \rangle_{\text{trap}}$ . (Note that if  $\langle I_z \rangle_{\text{trap}}$  is significantly smaller than the thermal value of  $\langle I_z \rangle$ , then the resulting curve can be interpreted as fast, coherent relaxation to the trapped state, since  $\langle I_z \rangle$  relaxes to  $\langle I_z \rangle_{\text{trap}}$  much faster than a function decaying exponentially toward  $\langle I_z \rangle_{\text{trap}}$  with rate constant  $R_h$ .) Since it follows from (3.20) that the magnitude of  $d\langle I_z \rangle / dt$  decreases with time, a lower bound  $T_{\text{trap}}$  on the time required for this coherent relaxation to occur can be obtained using the initial value of the derivative:

$$\begin{aligned} T_{\text{trap}} &= \left( \langle I_z \rangle_{\text{trap}} \right) / \frac{d\langle I_z \rangle}{dt} (0) \\ &= \frac{1}{R_0 \sqrt{N/2}}. \end{aligned} \quad (3.21)$$

Simulations of spin-trapped cooling presented in section 2.1 of chapter 6 suggest that for an initially disordered sample,  $T_{\text{trap}}$  is a good estimate of the time required for  $\langle I_z \rangle$  to relax from zero to a value which differs from  $\langle I_z \rangle_{\text{trap}}$  by a factor of order unity. Note as well that since we are considering spins 1/2, (3.21) is consistent with the estimate (3.4) obtained from the semiclassical model.

For an initially disordered system of noninteracting spins which all experience the same field, we can also consider  $T_{\text{trap}}$  to be a lower bound on the time required for the resonator-induced spin-spin correlations to develop fully. This follows from the fact that  $\langle I_x^2 + I_y^2 \rangle$  depends strongly on  $M$ , since transitions between states of different  $M$  causes changes in both  $\langle I_z \rangle$  and  $\langle I_x^2 + I_y^2 \rangle$ . We can conclude that if all "flip-flop" zero-quantum coherences oscillate within a period of time  $\lesssim T_{\text{trap}}$ , then spin trapping of an initially disordered sample will be partially disrupted, since the relative phase of the populations and these coherences will vary on the time scale needed for transfers

between coherences and populations to induce spin-spin correlations. If the periods of these coherences are much less than  $T_{\text{trap}}$ , then spin trapping should be effectively suppressed.

## 4.2 Dipole-dipole coupled spins

### 4.2.1 Two spins

We turn our attention to the longitudinal relaxation of a system of spins coupled by the secular dipolar Hamiltonian  $H_D$ , beginning with a system of two spins. If no chemical shifts are present, then the eigenstates of the system are given by the set  $B \equiv \{|p\rangle, |q\rangle, |r\rangle, |s\rangle\}$ , where

$$|p\rangle \equiv |++\rangle, \quad (3.22)$$

$$|q\rangle \equiv (|+-\rangle + |-+\rangle) / \sqrt{2}, \quad (3.23)$$

$$|r\rangle \equiv |--\rangle, \quad (3.24)$$

$$|s\rangle \equiv (|+-\rangle - |-+\rangle) / \sqrt{2}. \quad (3.25)$$

When the master equation is projected onto this basis set, we find that there is no coupling between populations and coherences, and the population  $\rho_{ss}$  does not relax at all. These results, which can be obtained by considering the matrix elements of the interaction Hamiltonian  $V$ , do not depend on the exact eigenfrequencies of the system. Indeed, if the eigenfrequencies are perturbed, then the longitudinal relaxation will be unaffected, since transfer between populations is unaffected by such perturbations. In particular, longitudinal relaxation does not depend on the strength of the dipolar coupling.

For a system in which one of the two spins has a chemical shift, the longitudinal relaxation depends strongly on the relative magnitude of the chemical shift and the dipolar coupling. If  $H_D$  is much larger than the chemical shift Hamiltonian  $H_{\text{shift}}$ , then the spin eigenstates are approximately those of the set  $B$ , and the longitudinal relaxation is only weakly affected by the presence of the chemical shift. If  $H_{\text{shift}} \gg$

$H_D$ , then the eigenstates are perturbed product states, and the longitudinal relaxation will proceed exponentially with rate constant  $R_h$ , provided that  $|\omega_{23}|$  is sufficiently large to disrupt transfer between coherences and populations, where

$$\begin{aligned} |2\rangle &\equiv |+-\rangle, \\ |3\rangle &\equiv |-+\rangle, \end{aligned}$$

as in (3.13) through (3.16). If  $n_{\text{th}} \ll 1$ , as in the case of the example resonator presented in table 5.3, then the condition

$$|\omega_{23}| \gg 2\pi R_0 \tag{3.26}$$

is sufficient to guarantee that the contribution of spin-spin correlations to longitudinal relaxation is suppressed, regardless of initial conditions. This follows from the fact that the terms coupling populations to coherences between  $|2\rangle$  and  $|3\rangle$  have magnitude  $\lesssim R_0$  when  $n_{\text{th}} \ll 1$ . In the limit where  $H_{\text{shift}} \gg H_D$ , we can consider  $H_D$  to be a perturbation of  $H_{\text{shift}}$  and use first-order perturbation theory to find  $\omega_2$  and  $\omega_3$ . From

$$\begin{aligned} H_{\text{shift}} &= \omega_{\text{shift}} I_{z,1}, \\ H_D &= \omega_{dd} (3I_{z,1} I_{z,2} - \mathbf{I}_1 \cdot \mathbf{I}_2), \end{aligned}$$

we obtain

$$\omega_1 \approx \omega_0 + \frac{1}{2} (\omega_{\text{shift}} + \omega_{dd}), \tag{3.27a}$$

$$\omega_2 \approx \frac{1}{2} (\omega_{\text{shift}} - \omega_{dd}), \tag{3.27b}$$

$$\omega_3 \approx \frac{1}{2} (-\omega_{\text{shift}} - \omega_{dd}), \tag{3.27c}$$

$$\omega_4 \approx -\omega_0 + \frac{1}{2} (-\omega_{\text{shift}} + \omega_{dd}), \tag{3.27d}$$

which allows us to express (3.26) as

$$|\omega_{\text{shift}}| \gg 2\pi R_0.$$

An alternative way of understanding the ineffectiveness of a small chemical-shift difference in modifying the relaxation of the dipole-coupled system is to transform  $H_{\text{shift}}$  into the rotating frame in which the fast evolution due to the secular dipolar coupling is absent. In this rotating frame, the time-independent component of  $H_{\text{shift}}$  is proportional to  $I_z$ , and therefore has no effect on relaxation. Using the language of the semiclassical model introduced in the first section, we can say that the component of  $H_{\text{shift}}$  which survives averaging due to oscillations induced by the dipolar coupling does not modulate the indirect spin-spin torques responsible for coherent relaxation.

#### 4.2.2 Three spins

We now consider a system of three spins which are coupled by the secular dipolar Hamiltonian

$$\begin{aligned} H_D = & \omega_{12} (3I_{z,1}I_{z,2} - \mathbf{I}_1 \cdot \mathbf{I}_2) + \omega_{13} (3I_{z,1}I_{z,3} - \mathbf{I}_1 \cdot \mathbf{I}_3) \\ & + \omega_{23} (3I_{z,2}I_{z,3} - \mathbf{I}_2 \cdot \mathbf{I}_3). \end{aligned}$$

The rules for addition of angular momenta allow a collection of three spins  $1/2$  to be represented as a single angular momentum  $I = 3/2$  and two angular momenta  $I = 1/2$ . For our purposes, it is convenient to define one of the  $I = 1/2$  angular

momentum systems to be

$$|1/2, +\rangle = \{(\omega_{13} - \omega_{23})|++-\rangle + (\omega_{23} - \omega_{12})|+-+\rangle + (\omega_{12} - \omega_{13})| - + +\rangle\} \frac{1}{C}, \quad (3.28)$$

$$|1/2, -\rangle = \{(\omega_{13} - \omega_{23})|--+\rangle + (\omega_{23} - \omega_{12})|-+-\rangle + (\omega_{12} - \omega_{13})|+--\rangle\} \frac{-1}{C}, \quad (3.29)$$

$$C \equiv (\omega_{12} - \omega_{13})^2 + (\omega_{12} - \omega_{23})^2 + (\omega_{13} - \omega_{23})^2.$$

The states of this angular momentum system are also eigenstates of  $H_D$ :

$$H_D |1/2, +\rangle = H_D |1/2, -\rangle = 0.$$

Population which begins in one of these states can only move between the two states during the mechanical cooling, since the matrix elements of the spin-resonator interaction Hamiltonian  $V$  ensure that the population of any angular momentum system is not coupled to the population of any other spin eigenstate or to any coherences between eigenstates. For an initially disordered system cooled by a resonator at 0 K, one-fourth of the population will eventually be trapped in the nondecaying state  $|1/2, +\rangle$ . As in the case of two spins, additional terms in the spin Hamiltonian can only be effective in suppressing this spin trapping if they significantly perturb the spin eigenstates. Since  $H_D$  does not in general commute with the Hamiltonian which shifts the Larmor frequencies of distinct spins by different amounts, chemical shifts of magnitude comparable to the dipolar coupling would modify the eigenstates sufficiently to break the selection rule responsible for trapping the population away from the ground state.

In order to determine whether the population of the remaining  $I = 1/2$  manifold will quickly reach the ground state during spin-resonator relaxation, we considered ten example systems having randomly generated coupling constants  $\omega_{ij}$ . For five of these examples, the value of each  $\omega_{ij}/2\pi$  was a uniformly distributed random number between 1 kHz and 2 kHz, and for the remaining five examples,  $\omega_{ij}/2\pi$  was uniformly

$(\omega_{12}, \omega_{13}, \omega_{23}) / 2\pi$	$p$
(1476, 352, 1843) Hz	0.85
(1871, 1834, 811) Hz	0.92
(1787, 116, 821) Hz	0.78
(1626, 20, 706) Hz	0.76
(406, 397, 278) Hz	0.98

Table 3.1: Mixing of angular momentum systems.

distributed between 0 Hz and 2 kHz. In the cases where  $1 \text{ kHz} \leq \omega_{ij}/2\pi \leq 2 \text{ kHz}$ , each spin eigenstate had at least 95% of its population in a single angular momentum manifold. In these systems,  $H_D$  induces only weak mixing of the angular momentum manifolds, and we would expect that the population would first relax quickly to the low-energy state of each manifold, and would then relax slowly as population is transferred from one of  $I = 1/2$  manifolds to the  $I = 3/2$  manifold. Simulations of relaxation in a three-spin system confirmed this conjecture, and section 2.2 of chapter 6 presents similar simulations for four-spin systems. After the population of each angular momentum system (or "manifold") has reached the low-energy state of the manifold, the rate of longitudinal relaxation depends on the efficiency with which  $H_D$  couples manifolds.

Choosing  $0 \text{ Hz} \leq \omega_{ij}/2\pi \leq 2 \text{ kHz}$  generally gave more effective mixing of the two angular momentum manifolds. We found that for a given set of values  $\omega_{ij}$ , the mixing of the two angular momentum systems could be characterized by just one probability  $p$ . Calculation of the eigenstates for these systems shows that for each eigenstate  $|a\rangle$  which includes contributions from both manifolds, the probability of detecting angular momentum  $I_a$  is  $p$ , where  $I_a$  is the angular momentum of the manifold making the dominant contribution to  $|a\rangle$ , and  $p$  is independent of  $|a\rangle$ . Table 3.1 shows that mixing was most effective when the values of  $\omega_{ij}$  were well separated.

### 4.2.3 $N$ spins

For larger systems, we note first that since  $H_D$  commutes with  $I_z$ , it can only couple states having the same value of  $I_z$ . We thus consider two limiting cases. When resonator-induced relaxation within a manifold is fast compared to the rate at which

$H_D$  transfers population between manifolds, then the population of a manifold will quickly decay to the low-energy state of that manifold and then slowly be transferred to unpopulated states having the same value of  $I_z$  but belonging to manifolds of higher angular momentum. In the opposite limit,  $H_D$  will quickly equalize the population of all states which have the same value of  $I_z$ . Resonator-induced transfers of population to low-energy states within a manifold immediately results in compensating transfers that equalize the populations of all states within a given eigenspace of  $I_z$ . Section 2.2 of chapter 6 presents simulations of longitudinal relaxation for this regime.

Note that if the spin system were temporarily moved out of the large applied field, the nonsecular part of the dipolar Hamiltonian would be "turned on," and we could expect a spin temperature to be established, so that the system could be viewed as an ensemble of independent spins. If the secular dipolar Hamiltonian is found to couple angular momentum systems too weakly for efficient cooling, moving the spin-resonator system adiabatically in and out of the high field might speed up the relaxation. When the spins have been moved out of the high field, a low spin temperature would correspond to a strong dipole order. Moving the system adiabatically back into the high field would convert the dipolar order of the thermal spin system to Zeeman order, and interactions with the resonator could then cool the system for a period of time until the ground states of the angular momentum systems have accumulated excess population and the cooling has slowed. The changes in the field at the spins would need to be slow enough that the entropy of the spin system would not change as the field varies. If the spin temperature could be repeatedly re-established on a time scale short compared to the time needed for resonator-induced spin-spin correlations to develop, then the spins could be considered independent during the relaxation. In the limiting case where the time needed to re-establish the spin temperature is negligible, longitudinal relaxation would proceed exponentially with a time constant  $1/R_h$ .

## 5 Transverse relaxation of freely-precessing spins

For sufficiently large  $N$ , we expect "radiation damping" to rotate the magnetization away from the transverse axis and toward the longitudinal axes, causing the transverse magnetization to decay more quickly than it would if only a single spin were present. As Abragam points out, this process is reversible and is not properly considered a form of relaxation [12]. However, the resonator could also induce fast, irreversible transverse relaxation. We can see this by considering a two-spin system with the basis of eigenstates given by equations (3.13) through (3.16), which we restate here for convenience:

$$\begin{aligned} |1\rangle &\equiv |++\rangle, \\ |2\rangle &\equiv |+-\rangle, \\ |3\rangle &\equiv |-+\rangle, \\ |4\rangle &\equiv |--\rangle. \end{aligned}$$

The rotating-frame evolution equation for a coherence  $\rho_{ab}$  is

$$\frac{d}{dt}\rho_{ab}(t) = \sum_{c,d} \exp\{i(\omega_{ab} - \omega_{cd})t\} \mathcal{R}_{abcd} \rho_{cd}(t),$$

and the cumulative effect on  $\rho_{ab}$  of the physical processes characterized by the coupling  $\mathcal{R}_{abcd}$  will be negligible if

$$|\omega_{ab} - \omega_{cd}| \gg 2\pi\mathcal{R}_{abcd},$$

due to fast variation in the phase of lab-frame coherences. Assume for the sake of simplicity that frequency differences  $|\omega_{12} - \omega_{cd}|$  suppress couplings between  $\rho_{12}$  and other terms of the density matrix so that the relaxation of  $\rho_{12}$  is governed by the

single constant

$$\begin{aligned}
\Gamma_{12} &= \frac{1}{2} \left( \sum_{n \neq 1} \Gamma_{1 \rightarrow n} + \sum_{n \neq 2} \Gamma_{2 \rightarrow n} \right) \\
&= \frac{1}{2} (\Gamma_{1 \rightarrow 2} + \Gamma_{1 \rightarrow 3} + \Gamma_{2 \rightarrow 1} + \Gamma_{2 \rightarrow 4}) \\
&= \frac{R_0}{2} \{n_{\text{th}} + n_{\text{th}} + (n_{\text{th}} + 1) + n_{\text{th}}\} \\
&= \frac{R_0}{2} (4n_{\text{th}} + 1).
\end{aligned}$$

The damping constant  $\Gamma_{12}$  includes contributions from four transitions; by way of contrast, note that for a single spin, the damping constant for a coherence between the states  $|+\rangle$ ,  $|-\rangle$  includes contributions from only two transitions,  $|+\rangle \rightarrow |-\rangle$  and  $|-\rangle \rightarrow |+\rangle$ , and has magnitude  $(R_0/2)(2n_{\text{th}} + 1)$ . At temperatures for which  $n_{\text{th}}$  is of order unity or larger, the two-spin single-quantum coherence will decay much more quickly than the single-spin coherence.

The reasoning used in this example can be extended to suggest that the damping constant for a single-quantum coherence between product states will increase in magnitude as  $N$  is increased. An increase in the damping constants for single-quantum coherences does not always imply that the rate of transverse relaxation increases, however. Consider, for instance, a system of two spins for which the spin Hamiltonian is

$$H = \omega_0 I_z + \omega_{\text{shift}} I_{z,1},$$

with

$$|\omega_{\text{shift}}| \gg 2\pi R_0 (n_{\text{th}} + 1).$$

The coherences in the set  $Z_2 = \{\rho_{12}, \rho_{34}\}$  have the same frequency, since they both involve a flip of spin 2; similarly, the coherences  $Z_1 = \{\rho_{13}, \rho_{24}\}$  both involve a flip of spin 1. Physical processes which cause transfer from a coherence in  $Z_1$  to one in  $Z_2$  have no cumulative effect on the relaxation of  $Z_2$  coherences, since the phase difference between a  $Z_1$  coherence and a  $Z_2$  coherence cycles quickly during the time required for the transfer to accumulate. The coupling between the two coherences of

$Z_1$  is significant, however, and the relaxation equations for  $\rho_{12}$  and  $\rho_{34}$  can be written as

$$\begin{aligned}\frac{d}{dt}\rho_{12} &= -R_0 \left( n_{\text{th}} + \frac{1}{2} \right) \rho_{12} + \{-R_0 n_{\text{th}} \rho_{12} + R_0 (n_{\text{th}} + 1) \rho_{34}\}, \\ \frac{d}{dt}\rho_{34} &= -R_0 \left( n_{\text{th}} + \frac{1}{2} \right) \rho_{34} + \{R_0 n_{\text{th}} \rho_{12} - R_0 (n_{\text{th}} + 1) \rho_{34}\}.\end{aligned}$$

Note that the first term on the right side of each equation tends to yield exponential relaxation with rate constant  $R_0 (n_{\text{th}} + \frac{1}{2})$ , while the second is responsible for reversible transfer between  $\rho_{12}$  and  $\rho_{34}$ . Adding together these two equations yields

$$\frac{d}{dt}(\rho_{12} + \rho_{34}) = -R_0 \left( n_{\text{th}} + \frac{1}{2} \right) (\rho_{12} + \rho_{34}).$$

The other coherences which contribute to  $\langle I_x \rangle$  can similarly be paired to form sums which decay exponentially, and we find that

$$\frac{d}{dt} \langle I_x \rangle = -R_0 \left( n_{\text{th}} + \frac{1}{2} \right) \langle I_x \rangle. \quad (3.30)$$

This result can be generalized to  $N$  spins. If the product states are eigenstates of the spin Hamiltonian, then each single-quantum coherence involves a flip of just one spin. Group the single-quantum coherences into sets  $Z_k$ , where the coherences in set  $Z_k$  are between states which differ by a flip of spin  $k$ . If the eigenfrequencies of the product states are such that all couplings between coherences within a set  $Z_k$  are preserved, while all couplings responsible for transfer between a  $Z_k$  coherence and another coherence are suppressed by frequency differences, then equation (3.30) holds. A simple spin Hamiltonian which meets these conditions is

$$H = \omega_0 I_z + \sum_{i=1}^n \omega_i I_{z,i}, \quad (3.31)$$

provided the spacing between Larmor frequencies of distinct spins is sufficiently large.

These conditions can be stated more transparently in terms of the physical processes

responsible for transfer between coherences. Consider first a single-quantum coherence  $\rho_{ab}$  in  $Z_k$ . The matrix elements of the Jaynes-Cummings Hamiltonian allow transfer from  $\rho_{ab}$  to other coherences by two types of processes: 1) Processes associated with two transitions,  $|a\rangle \rightarrow |c\rangle$  and  $|b\rangle \rightarrow |d\rangle$ , with both transitions involving a flip of spin  $j$  in the same direction, for some  $j \neq k$ , and 2) Processes such as  $|a\rangle \rightarrow |m\rangle \rightarrow |c\rangle$ , in which one transition has spin  $i$  flipping up and the other has spin  $j \neq i$  flipping down. The first type of process couples a coherence  $\rho_{ab}$  in  $Z_k$  to other coherences in  $Z_k$ , while the second type couples  $\rho_{ab}$  to coherences in  $Z_j$ , for  $j \neq k$ , as well as to triple-quantum coherences. If the eigenfrequencies are such that the couplings associated with the first type of process are preserved, while those associated with the second type of process are suppressed, then (3.30) holds. This result is derived in Appendix F.

Section 2.2 of chapter 6 presents simulations which show that "turning on" the dipolar coupling can increase the rate of resonator-induced transverse relaxation in a four-spin system. A similar result can be obtained analytically for a system of two spins, as we now show. First, note that if all couplings allowed by the matrix elements of the interaction Hamiltonian  $V$  contribute to spin relaxation, the transverse relaxation is not governed by a single exponential. This can be illustrated by using the spin Hamiltonian

$$H = \omega_0 I_z,$$

and the basis set  $B$ :

$$\begin{aligned} |p\rangle &\equiv |++\rangle, \\ |q\rangle &\equiv (|+-\rangle + |-+\rangle) / \sqrt{2}, \\ |r\rangle &\equiv |--\rangle, \\ |s\rangle &\equiv (|+-\rangle - |-+\rangle) / \sqrt{2}. \end{aligned}$$

We have

$$\langle I_x \rangle = \frac{1}{\sqrt{2}} (\rho_{pq} + \rho_{qr} + \rho_{qp} + \rho_{rq}).$$

The coefficients of the master equation can be found by calculating the matrix elements of  $V$ , and for a resonator at zero Kelvins, we find that

$$\begin{aligned} \langle I_x \rangle (t) = & \frac{1}{\sqrt{2}} \{ \rho_{pq} (0) + \rho_{qp} (0) \} \exp (-R_0 t) \\ & + \frac{1}{\sqrt{2}} \{ \rho_{qr} (0) + \rho_{rq} (0) \} \{ 2 \exp (-R_0 t) - \exp (-2R_0 t) \}. \end{aligned} \quad (3.32)$$

For this system, curves for transverse relaxation are sums of exponentials having rate constants  $R_0$  and  $2R_0$ , rather than a single exponential with rate constant  $R_0/2$ , as would be expected for lifetime broadening.

If additional terms in the spin Hamiltonian perturb the difference frequencies  $\omega_{pq}$  and  $\omega_{qr}$  so as to yield a sufficiently large frequency difference  $|\omega_{pq} - \omega_{qr}|$ , the physical processes previously responsible for the reversible transfer between  $\rho_{pq}$  and  $\rho_{qr}$  will instead produce irreversible loss of order. Transfers away from a given coherence decrease the magnitude of that coherence without increasing the magnitude of any other coherences, due to fast variation in the relative phase of coherences. A single-quantum coherence  $\rho_{ab}$  will then decay at a rate determined by the damping constant  $\Gamma_{ab}$ , which may be calculated by evaluating the transition probabilities for all allowed transitions  $|a\rangle \rightarrow |m\rangle$  and  $|b\rangle \rightarrow |n\rangle$ . If the two spins are coupled by a sufficiently strong dipolar Hamiltonian, we have

$$\begin{aligned} \langle I_x \rangle (t) = & \frac{1}{\sqrt{2}} \{ \rho_{pq} (0) + \rho_{qp} (0) \} \exp \{ -R_0 t \} \\ & + \frac{1}{\sqrt{2}} \{ \rho_{qr} (0) + \rho_{rq} (0) \} \exp \{ -2R_0 t \}. \end{aligned} \quad (3.33)$$

"Turning on" the dipolar coupling increases the rate of transverse relaxation by changing the interaction-frame equation for  $\langle I_x \rangle (t)$  from (3.32) to (3.33). If all spins are initially aligned with the  $x$ -axis, for instance, then the initial values of the coherences  $\rho_{pq}$ ,  $\rho_{qr}$ ,  $\rho_{qp}$ ,  $\rho_{rq}$  are equal, and the contribution  $\{ \rho_{qr} (t) + \rho_{rq} (t) \}$  to  $\langle I_x \rangle (t)$  decays more quickly when the dipolar coupling is present.

Resonator-induced transverse relaxation faster than that expected for a single spin can be distinguished from radiation damping. Since radiation damping rotates the

sample dipole, it causes growth in  $\langle I_z \rangle$  that is simultaneous with the decay of the transverse dipole. However, fast transverse relaxation may occur even under conditions which guarantee that longitudinal relaxation will proceed exponentially with rate constant  $R_h$ . If the frequencies of "flip-flop" zero-quantum coherences between product states differ sufficiently from zero, the contribution of spin-spin correlations to longitudinal relaxation will be suppressed, regardless of the initial conditions. If, in addition, degeneracies among the frequencies of single-quantum coherences are sufficiently perturbed, the rate of transverse relaxation will be determined by the damping constants  $\Gamma_{ab}$ , which tend to increase in magnitude as the number of spins is increased.

A two-spin system having weak dipolar coupling and a large chemical shift offset between the spins would satisfy these conditions. When the chemical shift offset is much larger than the dipolar coupling, the energy eigenstates are weakly perturbed product states, and the resonator will induce exponential longitudinal relaxation with rate constant  $R_h$  if the offset is large enough to suppress the couplings between product-state populations and zero-quantum coherences. When a weak dipolar coupling is also present, the rate of transverse relaxation can be characterized using (3.27a) through (3.27d) to estimate the frequencies of single quantum coherences. We have

$$\begin{aligned}\omega_{12} &\approx \omega_0 + \omega_{dd}, \\ \omega_{13} &\approx \omega_0 + \omega_{\text{shift}} + \omega_{dd}, \\ \omega_{24} &\approx \omega_0 + \omega_{\text{shift}} - \omega_{dd}, \\ \omega_{34} &\approx \omega_0 - \omega_{dd},\end{aligned}$$

where the eigenfunctions are weakly perturbed from those given in (3.13) through (3.16). If

$$|\omega_{dd}| \gg \pi R_0,$$

then all transfer between single-quantum coherences will be suppressed due to the fast

variation in the relative phase between each pair of coherences, and the damping constants for single-quantum coherences will determine the rate of transverse relaxation.

We find that

$$\begin{aligned} \langle I_x \rangle = & \frac{1}{2} (\rho_{12} + \rho_{21} + \rho_{13} + \rho_{31}) \exp \left\{ -\frac{1}{2} R_0 t \right\} \\ & + \frac{1}{2} (\rho_{42} + \rho_{24} + \rho_{43} + \rho_{34}) \exp \left\{ -\frac{3}{2} R_0 t \right\}. \end{aligned} \quad (3.34)$$

Section 2.2 of chapter 6 presents a simulation of a four-spin system for which the chemical-shift offset between spins is large compared to the dipolar coupling. Although the large spacing of the chemical shifts yields longitudinal relaxation with time constant  $1/R_h$ , as discussed in section 4, the presence of the dipolar coupling accelerates the transverse relaxation induced by the resonator. The transverse dipole decays in a fraction of the time required for transverse relaxation of a single-spin sample.

## 6 Transverse relaxation during spin-locking

Resonator-induced longitudinal relaxation between transients is potentially useful as a substitute for spin-lattice relaxation, but fast transverse relaxation induced by the resonator is generally undesirable, since it would tend to shorten the lifetime of the signal. In this section, we show that spin-locking can in principle be used to limit resonator-induced transverse relaxation to exponential relaxation with rate constant

$$T_{1\rho}^{-1} = R_h/2. \quad (3.35)$$

We begin from the reduced master equation (2.17) for the spin system:

$$\begin{aligned} \frac{d}{dt}\rho_s &= -i[H_s, \rho_s] - \frac{1}{2}R_0(n_{\text{th}} + 1)[I_- I_+, \rho_s]_+ + R_0(n_{\text{th}} + 1)I_+ \rho_s I_- \\ &\quad - \frac{1}{2}R_0 n_{\text{th}}[I_+ I_-, \rho_s]_+ + R_0 n_{\text{th}} I_- \rho_s I_+, \\ H_s &= H_{\text{secular}}^{\text{int}} + \omega_1 I_y, \end{aligned} \quad (3.36)$$

where  $H_{\text{secular}}^{\text{int}}$  is the secular internal Hamiltonian, and  $\omega_1 I_y$  is the Hamiltonian for the spin-locking field. We switch to a reference frame in which the fast motion associated with  $\omega_1 I_y$  has been eliminated. (We shall refer to this frame as the "toggling frame.") The density matrix in the toggling frame can be written as

$$\begin{aligned} \rho'_s &= U_1^{-1}(t) \rho_s U_1(t), \\ U_1(t) &= \exp(-i\omega_1 I_y t), \end{aligned}$$

and it follows from (3.36) that the time derivative of  $\rho'_s$  is

$$\begin{aligned} \frac{d}{dt}\rho'_s &= -i[H_{\text{toggling}}^{\text{int}}, \rho'_s] \\ &\quad - \frac{1}{2}R_0(n_{\text{th}} + 1)[I'_- I'_+, \rho'_s]_+ + R_0(n_{\text{th}} + 1)I'_+ \rho'_s I'_- \\ &\quad - \frac{1}{2}R_0 n_{\text{th}}[I'_+ I'_-, \rho'_s]_+ + R_0 n_{\text{th}} I'_- \rho'_s I'_+, \end{aligned} \quad (3.37)$$

where

$$\begin{aligned} H_{\text{toggling}}^{\text{int}} &= U_1^{-1}(t) H_{\text{secular}}^{\text{int}} U_1(t), \\ I'_+ &= U_1^{-1}(t) I_+ U_1(t), \\ I'_- &= U_1^{-1}(t) I_- U_1(t). \end{aligned}$$

From (3.37) we obtain the equation of motion for  $\langle I_y \rangle$  in the toggling frame:

$$\begin{aligned} \frac{d}{dt} \langle I_y \rangle &= -i \langle [I_y, H_{\text{toggling}}^{\text{int}}] \rangle \\ &\quad - \frac{1}{2} R_0 (n_{\text{th}} + 1) \langle [I_y, I'_- I'_+]_+ \rangle + R_0 (n_{\text{th}} + 1) \langle I'_- I_y I'_+ \rangle \\ &\quad - \frac{1}{2} R_0 n_{\text{th}} \langle [I_y, I'_+ I'_-]_+ \rangle + R_0 n_{\text{th}} \langle I'_+ I_y I'_- \rangle. \end{aligned} \quad (3.38)$$

Equation (3.38) can be written as

$$\frac{d}{dt} \langle I_y \rangle = -\frac{1}{2} R_h \langle I_y \rangle - i \langle [I_y, H_{\text{toggling}}^{\text{int}}] \rangle + \langle L_{\text{osc}} I_y \rangle, \quad (3.39)$$

where  $L_{\text{osc}}$  is a superoperator which averages to zero during a time period of length  $2\pi/\omega_1$ . For sufficiently large  $\omega_1$ , only the first term on the right side of (3.39) makes a nonnegligible contribution to the evolution, since the time average of the remaining terms is zero. The fact that the commutator on the right side of (3.39) averages to zero can be established by noting that  $H_{\text{toggling}}^{\text{int}}$  is obtained by performing a rotation of  $H_{\text{secular}}^{\text{int}}$  around the  $y$ -axis in spin space, and the time average of  $H_{\text{toggling}}^{\text{int}}$  is invariant under infinitesimal rotations around the same axis. Spin-locking can therefore be used to limit the rate of resonator-induced transverse relaxation, provided  $\omega_1$  is large enough to average the internal Hamiltonian and the relaxation superoperator in the toggling frame. Section 2.2 of chapter 6 presents a simulation of an artificial four-spin system for which spin-locking yields transverse relaxation closely approximating an exponential curve with rate constant  $R_h/2$ .

## Chapter 4

# Sensitivity of spin detection by a nanoscale resonator

### 1 Definition of signal-to-noise ratio for measurement of an amplitude

Since the term "signal-to-noise ratio" is attached to a variety of different measures of sensitivity, we begin by defining the measures that we will use and by obtaining general formulas for signal-to-noise ratio (SNR). In this section and the following one, we motivate and propose a general definition of SNR which can be used to compare methods which measure the amplitude of a signal with methods which yield a continuous record of a signal.

We assume that the measurement of a signal amplitude is performed by passing the noisy signal through a linear filter. An alternative method often used to extract information from noisy data is least-squares fitting. Appendix G shows that if the noise is white, then least-squares fitting yields an amplitude estimate identical to one obtained from an optimal filter, but for more general types of noise, least-square fitting yields an amplitude estimate which would be obtained using a non-optimal filter. Use of a linear filter is therefore the more powerful method of extracting the signal amplitude.

The noisy signal entering the filter  $\mathcal{K}$  can be written as

$$f(t) = m(t) + n(t),$$

where  $m(t)$  is the useful signal and  $n(t)$  is the noise. The output of the filter is

$$\phi(t) = \mu(t) + \nu(t),$$

where  $\mu(t)$  and  $\nu(t)$  would be the respective outputs if  $m(t)$  and  $\nu(t)$  were passed through  $\mathcal{K}$  individually. The signal  $m(t)$  has the form

$$m(t) = Gm_0(t), \tag{4.1}$$

with  $m_0(t)$  a known real-valued function and  $G$  the unknown constant to be measured. For simplicity, we refer to  $G$  as an amplitude, although the analysis method we characterize here does not require that  $G$  be nonnegative.

Let  $\mu_0(t)$  be the output obtained by passing  $m_0(t)$  through  $\mathcal{K}$ . Since  $m_0(t)$  is a known function, and the properties of  $\mathcal{K}$  are assumed to be known, the function  $\mu_0(t)$  can in principle be calculated. If it could be arranged that  $\nu(t_0) = 0$  at a particular time  $t_0$ , then  $G$  could be found by taking the ratio of the filtered output  $\mu(t_0)$  to the calculated value  $\mu_0(t_0)$ :

$$G = \mu(t_0) / \mu_0(t_0).$$

In the general case, where it cannot be arranged that  $\nu(t_0) = 0$ , a reasonable strategy would be to minimize the value of  $\nu(t_0)$  and then to estimate  $G$  as

$$\frac{\phi(t_0)}{\mu_0(t_0)} = G + \frac{\nu(t_0)}{\mu_0(t_0)}. \tag{4.2}$$

The estimate of  $G$  obtained in this way is a random variable which will be denoted by  $X$ .

Given this strategy for estimating  $G$ , the signal-to-noise ratio (SNR) of the mea-

surement can be defined as

$$SNR = \frac{\langle X \rangle}{\sigma_X}, \quad (4.3)$$

where  $\langle X \rangle$  is the mean value of  $X$  and  $\sigma_X$  is its standard deviation. The optimal filter is the one which minimizes SNR. To determine the characteristics of this filter, we first seek an explicit formula for  $\sigma_X$ , or equivalently for the variance  $\sigma_X^2$ . Since  $X$  is the sum of two random variables  $G$  and  $\nu(t_0)/\mu_0(t_0)$ , the variance  $\sigma_X^2$  can also be written as a sum:

$$\sigma_X^2 = \sigma_G^2 + \sigma_{\text{noise}}^2. \quad (4.4)$$

Here  $\sigma_G^2$  is the variance of  $G$ , and  $\sigma_{\text{noise}}^2$  is the variance of  $\nu(t_0)/\mu_0(t_0)$ .

To analyze  $\sigma_{\text{noise}}^2$ , we assume that  $n(t)$  is a stationary random process with zero mean and that the filter  $\mathcal{K}$  is linear and time-invariant. These assumptions imply that the mean value  $\langle \nu(t) \rangle$  equals zero and that the variance

$$\langle (\nu(t) - \langle \nu(t) \rangle)^2 \rangle \equiv \langle \nu^2 \rangle$$

is independent of time, with

$$\langle X \rangle = \langle G \rangle, \quad (4.5)$$

$$\sigma_X^2 = \sigma_G^2 + \frac{\langle \nu^2 \rangle}{[\mu_0(t_0)]^2}. \quad (4.6)$$

If the filter  $\mathcal{K}$  is implemented as a causal system, the the time  $t_0$  must occur after the signal  $m(t)$  has completely died out. Since we are using  $\mathcal{K}$  merely as an aid in estimating sensitivity, however, we consider the filter to be a purely mathematical operation performed on the signal, rather than a causal filter, and we simplify notation by setting  $t_0 = 0$  and defining  $\mu \equiv \mu(0)$ ,  $\mu_0 \equiv \mu_0(0)$ ,  $\nu \equiv \nu(0)$ , and  $\phi \equiv \phi(0)$ . The most general expression for the signal-to-noise ratio of an amplitude measurement is then found by substituting equations (4.6) and (4.5) into (4.3):

$$SNR = \frac{\langle G \rangle}{\sqrt{\sigma_G^2 + \langle \nu^2 \rangle / \mu_0^2}}. \quad (4.7)$$

Note that the only term in this expression which depends on the choice of filter is  $\langle \nu^2 \rangle / \mu_0^2$ . Since  $\sigma_G^2$  and  $\langle \nu^2 \rangle / \mu_0^2$  are both nonnegative, the optimal filter will be the one giving the maximum value of

$$r \equiv \mu_0^2 / \langle \nu^2 \rangle.$$

Reference [18] derives a formula for the transfer function  $K(\omega)$  of the filter which maximizes  $r$ . Define  $C_n(t)$  and  $S_n(\omega)$  to be the respective autocorrelation function and double-sided spectral density of the input noise  $n(t)$ , and let  $M_0(\omega)$  be the Fourier transform of  $m_0(t)$ . We give explicit formulas in order to establish the conventions we will be using:

$$\begin{aligned} M_0(\omega) &= \int_{-\infty}^{\infty} e^{-i\omega t} m_0(t) dt, \\ m_0(t) &= \frac{1}{2\pi} \int_{-\infty}^{\infty} e^{i\omega t} M_0(\omega) d\omega, \\ \mu_0(t) &= \frac{1}{2\pi} \int_{-\infty}^{\infty} e^{i\omega t} K(\omega) M_0(\omega) d\omega, \\ C_n(t) &= \langle n(t) n(0) \rangle, \\ S_n(\omega) &= \int_{-\infty}^{\infty} e^{-i\omega t} C_n(t) dt, \\ \langle n^2 \rangle &= \frac{1}{2\pi} \int_{-\infty}^{\infty} S_n(\omega) d\omega, \\ \langle \nu^2 \rangle &= \frac{1}{2\pi} \int_{-\infty}^{\infty} |K(\omega)|^2 S_n(\omega) d\omega. \end{aligned}$$

These definitions are discussed in reference [19]. In addition, Appendix H presents an introduction to the spectral density, specifically tailored to its use in SNR calculations.

The value  $r$  which we wish to maximize is

$$r = \frac{\left( \int_{-\infty}^{\infty} K(\omega) M_0(\omega) d\omega \right)^2}{2\pi \int_{-\infty}^{\infty} |K(\omega)|^2 S_n(\omega) d\omega}. \quad (4.8)$$

The Schwartz inequality, applied to an appropriate space of functions such as  $L_2$ ,

yields

$$\left| \int_{-\infty}^{\infty} K(\omega) M_0(\omega) d\omega \right|^2 \leq \int_{-\infty}^{\infty} |K(\omega)|^2 S_n(\omega) d\omega \int_{-\infty}^{\infty} \frac{|M_0(\omega)|^2}{S_n(\omega)} d\omega.$$

Dividing both sides of the inequality by the denominator of (4.8) gives

$$r \leq \frac{1}{2\pi} \int_{-\infty}^{\infty} \frac{|M_0(\omega)|^2}{S_n(\omega)} d\omega. \quad (4.9)$$

If we take

$$K(\omega) = c \frac{M_0^*(\omega)}{S_n(\omega)}, \quad (4.10)$$

then  $r$  reaches the maximum value given by the right side of (4.9), since

$$\mu_0^2 = c^2 \left( \frac{1}{2\pi} \int_{-\infty}^{\infty} \frac{|M_0(\omega)|^2}{S_n(\omega)} d\omega \right)^2 \quad (4.11)$$

$$\langle \nu^2 \rangle = c^2 \frac{1}{2\pi} \int_{-\infty}^{\infty} \frac{|M_0(\omega)|^2}{S_n(\omega)} d\omega. \quad (4.12)$$

The transfer function  $K(\omega)$  given in equation (4.10) yields an optimal filter.

This transfer function is particularly simple if the noise  $n(t)$  is white, with

$$S_n(\omega) = S_n = \text{constant}.$$

The choice [18]

$$c = S_n \quad (4.13)$$

gives

$$K(\omega) = M_0^*(\omega).$$

Passing  $f(t)$  into the filter produces output

$$\phi(t) = \int_{-\infty}^{\infty} f(t') m_0(t' - t) dt'. \quad (4.14)$$

The amplitude estimate  $X$  is given by

$$X = \frac{1}{\mu_0} \left( \int_{-\infty}^{\infty} f(t') m_0(t') dt' \right), \quad (4.15)$$

and the SNR by

$$SNR = \frac{\langle G \rangle}{\sqrt{\sigma_G^2 + S_n/\mu_0}}, \quad (4.16)$$

where

$$\mu_0 = \int_{-\infty}^{\infty} m_0^2(t) dt. \quad (4.17)$$

## 2 Generalization to measurement of a continuous signal

Definition (4.7) can be generalized in a natural way to characterize the sensitivity of measurement in which  $Q$  samples of a continuous signal are obtained from each shot of an experiment. We proceed heuristically by considering an example in which a real signal  $s(t)$  is sampled during a time period  $T$ . Two methods of sampling are used, with each method yielding identical statistical information. Imposing the requirement that the sensitivity of the two sampling methods be equal leads to a natural extension of definition (4.7).

The signal  $s(t)$  will be sampled at  $N$  pre-determined points. Method 1 measures one point of  $s(t)$  per shot, while method 2 measures all  $N$  sampled points during a single shot of the experiment. Assume that normally distributed white noise gives a sampled point of  $s(t)$  a variance  $\sigma_j^2$  for a single-shot measurement, with  $j = 1, 2$  for methods 1 and 2, respectively. Let  $f_j(t)$  denote the averaged measurement of  $s(t)$  obtained using method  $j$ , and let  $Z_j$  denote the number of times that each point is sampled using method  $j$ . Note that method 1 requires  $NZ_1$  transients, while method 2 requires  $Z_2$  transients.

We seek to define a "single-shot sensitivity" for each method such that the sensitivity for  $f_j$  is equal to the single-shot sensitivity times the number of transients. In

the case where the number of sampled points is

$$N = 1,$$

applying definition (4.3) to  $f_1$  would yield

$$\begin{aligned} \text{SNR of } f_1 &= \frac{|\text{mean value of } f_1|}{\text{standard deviation of } f_1} \\ &= \frac{|s|}{\sigma_1/\sqrt{Z_1}}, \end{aligned}$$

which is not proportional to the number  $Z_1$  of transients observed. If we square this expression, however, we do obtain a measure of sensitivity which is proportional to  $Z_1$ :

$$(\text{SNR of } f_1)^2 = Z_1 \frac{s^2(t)}{\sigma_1^2}. \quad (4.18)$$

We can therefore proceed heuristically by generalizing this expression; that is, we assume that a meaningful measure of sensitivity can be defined which is proportional to the number of points sampled and which reduces to (4.18) in the case where  $N = 1$ . If  $N > 1$ , the sensitivity of  $f_1$  is given by

$$(\text{SNR of } f_1)^2 = \sum Z_1 \frac{s^2(t)}{\sigma_1^2} = N Z_1 \frac{\langle s^2(t) \rangle}{\sigma_1^2}, \quad (4.19)$$

where the sum and the average are both taken over the  $N$  sampled points. Extending this to case where  $\sigma_1^2$  depends on  $t$  gives

$$(\text{SNR of } f_1)^2 = \sum Z_1 \frac{s^2(t)}{\sigma_1^2(t)} = N Z_1 \left\langle \frac{s^2(t)}{\sigma_1^2(t)} \right\rangle. \quad (4.20)$$

Note that the "single-shot sensitivity" of method 1 can then be written as

$$\frac{(\text{SNR of } f_1)^2}{\text{number of transients}} = \left\langle \frac{s^2(t)}{\sigma_1^2(t)} \right\rangle,$$

which yields

$$\text{single-shot SNR of method 1} = \sqrt{\left\langle \frac{s^2(t)}{\sigma_1^2(t)} \right\rangle}. \quad (4.21)$$

In seeking a similar expression for  $f_2$ , consider an example in which  $\sigma_1^2(t) = \sigma_2^2(t)$  and  $Z_1 = Z_2$ . The statistical information obtained using the two methods can be considered identical in this case, since each point is sampled the same number of times with the same distribution of noise. It follows that

$$\begin{aligned} (\text{SNR of } f_2)^2 &= (\text{SNR of } f_1)^2 \\ &= NZ_1 \frac{\langle s^2(t) \rangle}{\sigma_1^2} \\ &= NZ_2 \frac{\langle s^2(t) \rangle}{\sigma_2^2}. \end{aligned}$$

The "single-shot sensitivity" of method 2 is then found to be

$$\frac{(\text{SNR of } f_2)^2}{\text{number of transients}} = N \frac{\langle s^2(t) \rangle}{\sigma_2^2}.$$

The natural extension to the case of time-dependent noise would be

$$\text{single-shot SNR of method 2} = \sqrt{N \left\langle \frac{s^2(t)}{\sigma_2^2(t)} \right\rangle}. \quad (4.22)$$

These results can be written in a unified way as

$$SNR_{\text{real}} = \sqrt{QM \left\langle \frac{s^2(t)}{\sigma^2(t)} \right\rangle}, \quad (4.23)$$

where  $Q$  is the number of points sampled per transient,  $M$  is the total number of transients, and the average runs over all sampled points. We have included the subscript "real" as a reminder that the discussion has so far been limited to real-valued signals. In extending this definition to the case of a complex signal  $s(t) = a(t) + ib(t)$ , we adopt the point of view that in sampling the complex signal, we are seeking information about a real-valued function, such as the real component of a spectrum.

In addition, we assume that sampling a point of  $a(t)$  or  $b(t)$  contributes equally to the sensitivity with which we can measure this real-valued function. For the purpose of characterizing the sensitivity of the measurement, we consider the  $N$  sampled complex points equivalent to  $2N$  sampled real points which measure a real-valued function. We can therefore define the SNR for a method which samples complex points by letting  $Q$  represent the total number of real points sampled per transient, and by letting the average inside the radical run over all sampled real points:

$$\begin{aligned} SNR_{\text{complex}} &= \sqrt{(QM) \frac{1}{2N} \sum \left( \frac{a^2(t)}{\sigma_a^2(t)} + \frac{b^2(t)}{\sigma_b^2(t)} \right)} \\ &= \sqrt{\frac{QM}{2} \left\langle \frac{a^2(t)}{\sigma_a^2(t)} + \frac{b^2(t)}{\sigma_b^2(t)} \right\rangle}. \end{aligned} \quad (4.24)$$

In (4.24), both the sum and the average are taken over the  $N$  sampled points of the complex function, and  $\sigma_a^2(t)$ ,  $\sigma_b^2(t)$  are the variances for respective measurements of  $a(t)$ ,  $b(t)$  without signal averaging.

### 3 Comparison with a standard definition

We wish to compare (4.24) with a standard definition given by Ernst in reference [20]. Consider first a nondecaying complex signal  $s(t)$  which contains a single Fourier component that is sampled during a time period  $T$ :

$$s(t) = s_k e^{i\omega_k t}, \quad 0 \leq t \leq T.$$

Normally-distributed, channel-independent white noise is assumed, which gives the measured values of  $\text{Re } s(t)$  and  $\text{Im } s(t)$  the same time-independent variance  $\sigma^2$ , and each transient is assumed to yield  $N$  sampled complex points. Since  $Q = 2N$  and  $|s(t)| = |s_k|$ , we have

$$SNR = \frac{|s_k|}{\sigma/\sqrt{NM}}. \quad (4.25)$$

(To simplify notation, we have dropped the subscript "complex.") For a real spectrum containing one peak, Ernst defined the SNR as the ratio of peak height to root-mean-square noise in the real components of the spectrum [20]. In order to compare this definition with (4.25), we assume that the signal  $s(t)$  is "properly phased," that is, we assume that  $s_k$  is real and positive. The peak height in our real spectrum is thus  $s_k$ . Let  $x(n)$  represent the complex noise present in the  $n^{\text{th}}$  sampled point after averaging, and let the Fourier components of  $x$  be denoted by  $x_m$ . For each  $n$ , the mean value of  $|x(n)|^2$  is  $2\sigma^2/M$ , since the real and imaginary parts of the noise have the same mean-square value  $\sigma^2/M$  after averaging. It follows that

$$\begin{aligned} \left\langle \sqrt{\frac{1}{N} \sum |x_m|^2} \right\rangle &= \left\langle \sqrt{\frac{1}{N^2} \sum |x(n)|^2} \right\rangle \\ &= \left\langle \sqrt{\frac{1}{N^2} \left( N \frac{2\sigma^2}{M} \right)} \right\rangle \\ &= \sqrt{2} \left( \sigma / \sqrt{NM} \right). \end{aligned}$$

We see that the root-mean-square noise in the real spectrum is  $\sigma/\sqrt{NM}$ , and that (4.25) can be written as

$$SNR = \frac{\text{peak height in real spectrum}}{\text{rms noise in real spectrum}}, \quad (4.26)$$

so that (4.24) agrees with Ernst's definition for this particular example.

We generalize the example by supposing that  $s(t)$  is an arbitrary bounded complex signal which is sampled at  $N$  points within the interval  $0 \leq t \leq T$ . Assume as before that the noise in the measurement is white and independent of channel. In order to avoid introducing the unnecessary assumption that  $N$  complex points are sampled per transient, we define  $Z$  to be the number of averages performed in estimating each complex point of  $s(t)$ . The total number of real samples obtained during the measurement is

$$QM = 2NZ.$$

We have

$$\begin{aligned} SNR &= \sqrt{ZN \left\langle \frac{a^2(t) + b^2(t)}{\sigma^2} \right\rangle} \\ &= \frac{\sqrt{\langle |s(t)|^2 \rangle}}{\sigma/\sqrt{ZN}}. \end{aligned} \quad (4.27)$$

Let  $s_k$  represent the  $k^{\text{th}}$  Fourier component of  $s(t)$ , and note that

$$\begin{aligned} \sqrt{\langle |s(t)|^2 \rangle} &= \sqrt{\frac{1}{N} \sum |s(t)|^2} \\ &= \sqrt{\sum |s_k|^2}. \end{aligned}$$

With  $x(n)$  and  $x_m$  defined as in the previous example, we find that the mean value of  $|x(n)|^2$  is  $2\sigma^2/Z$ , and

$$\begin{aligned} \left\langle \sqrt{\frac{1}{N} \sum |x_m|^2} \right\rangle &= \left\langle \sqrt{\frac{1}{N^2} \sum |x(n)|^2} \right\rangle \\ &= \left\langle \sqrt{\frac{1}{N^2} \left( N \frac{2\sigma^2}{Z} \right)} \right\rangle \\ &= \sqrt{2} \left( \sigma/\sqrt{NZ} \right). \end{aligned}$$

The root-mean-square noise in the real spectrum is therefore  $\sigma/\sqrt{ZN}$ . It follows that

$$(SNR)^2 = \frac{\text{sum of all squared real and imaginary Fourier components of the signal}}{\text{mean-square noise in real spectral components}}. \quad (4.28)$$

Equation (4.28) highlights the difference between Ernst's definition of SNR and the one we have proposed. For this example, Ernst's definition could be obtained from (4.28) by discarding from the sum in the numerator the squares of all real and imaginary Fourier components with the exception of the largest real Fourier component.

We end this section by considering the limitations of our proposed definition. Note first that the SNR is determined once we know the total number of real-valued

samples taken, and the average ratio

$$\langle R \rangle = \left\langle \frac{\text{signal magnitude squared}}{\text{variance in measured value}} \right\rangle,$$

where the average is taken over all real-valued samples. For any experiment being considered, the SNR we obtain will be the same as if we had made  $QM$  independent measurements of a single, real-valued random variable  $f$  for which the ratio

$$\frac{\text{mean value of } f}{\text{standard deviation of } f} = \sqrt{\langle R \rangle}.$$

This observation highlights a condition necessary for the validity of our definition: the noise in the  $QM$  real-valued samples must be statistically independent. If the noise in different sampled points is correlated (as in the case of spin noise during a single transient, for instance), then knowledge of these correlations could in general be used to increase the effectiveness with which information could be extracted from the measurement; that is, an analysis that takes account of the correlations should give a higher value of SNR than one which does not. In this case, we would expect our definition of SNR to underestimate the sensitivity of the measurement.

Another limitation of our definition is that it does not take account of the method we use in obtaining information from the spectrum; for instance, our definition of SNR does not specifically tell us how effectively we can obtain the frequency of a given peak in the spectrum. To highlight this point, we suppose that the signal  $s(t)$  is a decaying exponential which will be sampled at intervals  $\Delta t$  during some time interval  $0 \leq t \leq T$ . How far toward zero should  $s(t)$  be allowed to decay before the sampling is terminated? In seeking an optimal  $T$ , we begin by recalling the definition of the discrete Fourier transform  $s_k$  of a function  $s(n)$  which is defined on a set of  $N$

integers:

$$s(n) = \sum_k s_k \exp \{i(2\pi k/N) n\} \quad (4.29)$$

$$s_k = \frac{1}{N} \sum_n s(n) \exp \{-i(2\pi k/N) n\}. \quad (4.30)$$

Given a time  $T_0$  such that  $|s(t)|$  is close to zero for  $t \geq T_0$ , we can see from equation (4.30) that the height of each peak in the spectrum will be decreased by a factor of 2 if we sample during a period of length  $2T_0$  rather than a period of length  $T_0$ . (Doubling the length of the sampling period doubles the value of  $N$  appearing in the denominator on the right side of (4.30), but it does not significantly change the value of the sum.) In the limit of large  $T$ , the height of each peak is proportional to  $1/T$ . The root-mean-square noise in the spectrum, however, does not decrease as quickly as the height of the spectrum, as can be seen from the relation

$$\frac{1}{N} \sum_n |x(n)|^2 = \sum_m |x_m|^2, \quad (4.31)$$

where  $x(n)$  is the noise in the  $n^{\text{th}}$  sampled point, and  $x_m$  is a Fourier component. If the value of  $N$  is doubled, the left side of (4.31) does not change, while the number of Fourier components  $x_k$  is doubled. It follows that the root-mean-square noise in the spectrum, which can be written as

$$\text{rms spectral noise} = \sqrt{\frac{1}{N} \sum_m |x_m|^2},$$

varies as  $1/\sqrt{T}$  in the limit of long  $T$ , and that the peak height becomes arbitrarily small in relation to the root-mean-square noise as  $T \rightarrow \infty$ .

Our definition of SNR claims that the sensitivity of the measurement does not change as  $T$  increases from  $T_0$  toward infinity. This can be seen by noting that (4.27)

gives

$$\begin{aligned} SNR &= \frac{\sqrt{\langle |s(t)|^2 \rangle}}{\sigma/\sqrt{ZN}} \\ &= \frac{\sqrt{\sum |s(t)|^2}}{\sigma/\sqrt{Z}}, \end{aligned}$$

where the sum is over the  $N$  sampled points. Taking additional samples for which  $|s(t)|^2 \approx 0$  does not affect the SNR.

To understand this property of our SNR definition, note that the ratio in (4.28) does not change as  $T \rightarrow \infty$ . Although the peak height becomes small relative to the root-mean-square noise, the sum of the signal's squared Fourier components does not become small relative to the mean-square noise. For long  $T$ , the statistical information about each peak is spread over a larger number of Fourier components separated by very small frequency increments. Although decreasing the peak height relative to the noise certainly makes the spectrum less pretty, it is not clear a priori whether a given method for extracting the position of a peak (for example) would be sensitive to the value of  $T$ , provided  $T$  is not pathologically long. To answer a question of this sort, it would be necessary to move beyond the general arguments we used in characterizing sensitivity and consider particular methods of extracting information from the spectrum.

## 4 Signal-to-noise ratio for amplitude detection

### 4.1 Definition of the signal

The BOOMERANG scheme for force-detected NMR spectroscopy [13, 21, 22] detects a single point of the free-induction decay (FID) for each measured transient. In this scheme, a conventional NMR pulse sequence is applied to the spins, and the spins precess freely for a period of time without being coupled to the resonator. At time  $t_1$  during the FID, a transverse component  $\langle I_x(t_1) \rangle$  is measured by using  $\langle I_x(t_1) \rangle$  to

drive the mechanical resonator. The driven spin component exerts a resonant driving force on the mechanical oscillator, and the resulting mechanical motion is detected. Analysis of the mechanical motion yields a measurement of  $\langle I_x(t_1) \rangle$ . By repeating the measurement for a range of values  $t_1$ , a record of the spins' time evolution is obtained, and Fourier analysis yields an NMR spectrum. This detection scheme is discussed in more detail in section 1 of chapter 5. In the current section, we derive a SNR formula for BOOMERANG detection in the case where the spin-resonator coupling has the form of equation (2.11).

In applying the SNR formula derived in section 1 to such detection schemes, we can define the signal  $m(t)$  either in terms of the resonator's position coordinate or in terms of the torque exerted on the resonator by the spins. The analysis is simpler if the signal is defined as a torque, since the functional form of  $m(t)$  is independent of the resonator's ringdown time  $\tau_h$ . The driving torque is modulated by spin precession in the transverse plane, and it decays as  $\langle I_x \rangle$  and  $\langle I_y \rangle$  relax to zero. In obtaining a simple sensitivity estimate, we can consider the torque to be a single decaying sinusoid. However, the functional form of the resonator's response depends on the relative lengths of  $\tau_h$  and the time period during which the torque is exerted. In general,  $\langle \theta(t) \rangle$  will include an initial period of "ringing up," as well as a delayed response to changes in the amplitude of the driving torque, and so the functional form of  $\langle \theta(t) \rangle$  will not always be well-approximated by a decaying sinusoid, even if the driving torque has that form. For sufficiently short  $\tau_h$ , negligible error will be introduced by considering the resonator to be continually driven at steady-state, and since our analysis of resonator-induced spin relaxation assumed that  $\tau_h$  is short compared to spin relaxation times, there is no inconsistency in analyzing sensitivity under the assumption of short  $\tau_h$ . The assumption of short  $\tau_h$  is unnecessary, however, and we can obtain more general results by defining the signal in terms of the torque exerted by the spins. (It should be pointed out that although it is convenient for purposes of sensitivity analysis to define the signal as a torque, it may not be the preferred method of analyzing experimental data. A practical protocol for data analysis would need to take account of the details of the experiment.)

For an experiment involving a macroscopic resonator and a large number of spins, the torque exerted by the spins is a clearly defined concept, since the resonator's evolution can be analyzed using classical mechanics, which includes explicit reference to forces and torques. In the current context, however, we are deriving SNR formulas which will be used to characterize the sensitivity of a low-temperature, high-frequency resonator interacting with a small spin sample, and so a quantum mechanical description is needed. In this context, an unproblematic definition of the torque can be made using the lab-frame master equation for the spin-resonator system:

$$\frac{d\rho}{dt} = -i[H_{\text{osc}} - \gamma\mathbf{I} \cdot \mathbf{B}(\theta), \rho] + \Lambda\rho, \quad (4.32)$$

where the relaxation superoperator  $\Lambda$  is given by (2.25). Evolution equations for the coordinate  $\langle\theta(t)\rangle$  and the conjugate momentum  $\langle p_\theta(t)\rangle$  can be obtained by multiplying equation (4.32) by  $\theta$  and  $p_\theta$ , respectively, and taking the trace:

$$\frac{d\langle\theta\rangle}{dt} = \frac{\langle p_\theta\rangle}{I_h} - \frac{\langle\theta\rangle}{\tau_h}, \quad (4.33)$$

$$\frac{d\langle p_\theta\rangle}{dt} = -k\langle\theta\rangle - \frac{\langle p_\theta\rangle}{\tau_h} + \left\langle \mu \cdot \frac{d}{d\theta} \mathbf{B}(\theta) \right\rangle, \quad (4.34)$$

where  $\mu$  is the sample dipole. Note that in deriving the second equation, we used the identity

$$[p_\theta, F(\theta)] = -i\hbar dF/d\theta,$$

which follows from  $[\theta, p_\theta] = i\hbar$ . Equations (4.33) and (4.34) have the same form as the equations of motion for a classical torsional oscillator driven by a torque  $\langle \mu \cdot \frac{d}{d\theta} \mathbf{B}(\theta) \rangle$ , and we can consider this to be the torque exerted by the spins. Approximating  $\mathbf{B}_h(\theta)$  by an expression first-order in  $\theta$  as in section 1 of chapter 2 yields the simpler expression

$$m(t) = \gamma\hbar \frac{dB_x}{d\theta} \langle I_x(t) \rangle. \quad (4.35)$$

Equation (4.35) defines the signal which would be detected in a noiseless experiment.

In studying the sensitivity of NMR methods which detect  $\langle I_x(t) \rangle$ , we assume that

$$\langle I_x(t) \rangle = \begin{cases} \langle I_x(0) \rangle e^{-t/\tau_s} \cos \omega_h t & t \geq 0 \\ 0 & t < 0 \end{cases}. \quad (4.36)$$

Time  $t = 0$  corresponds to the beginning of a detection period during which the mechanical oscillator experiences a resonant driving torque. The decay time of the transverse dipole during the detection period is denoted by  $\tau_s$ . The signal can be expressed in the form

$$m(t) = Gm_0(t),$$

where

$$G = \gamma \hbar \frac{dB_x}{d\theta} \langle I_x(0) \rangle, \\ m_0(t) = \begin{cases} e^{-t/\tau_s} \cos \omega_h t & t \geq 0 \\ 0 & t < 0 \end{cases}. \quad (4.37)$$

The method developed in section 1 will be used to estimate the sensitivity with which  $G$  can be measured.

## 4.2 Definition of the noise

Equations (4.3) and (4.4) of section 1 give the SNR of the amplitude estimate  $X$  as

$$SNR = \frac{\langle G \rangle}{\sqrt{\sigma_G^2 + \sigma_{\text{noise}}^2}}.$$

Note first that since

$$G = \gamma \hbar \frac{dB_x}{d\theta} \langle I_x(0) \rangle \quad (4.38)$$

is an ensemble average, it has a definite value, rather than being a random variable, and so

$$\sigma_G^2 = 0.$$

The variance of  $X$  is equal to  $\sigma_{\text{noise}}^2$ , which can be calculated if the spectral density  $S_n(\omega)$  of the noise is known.

In deriving an expression for  $S_n(\omega)$ , we begin by defining the noisy signal  $f(t) = m(t) + n(t)$ . Continuous observation of the resonator yields a measured coordinate  $\theta_{\text{obs}}(t)$ . Given  $\theta_{\text{obs}}(t)$ , in addition to measured values of  $I_h$ ,  $\omega_h$ , and  $\tau_h$ , equations (4.33) and (4.34) can be used to calculate the driving torque which would cause the expected value of the resonator's coordinate to equal  $\theta_{\text{obs}}(t)$ . This calculated driving torque is the noisy signal  $f(t)$ . Equivalently, the noise  $n(t)$  can be defined as the torque which would produce mean displacement  $\delta\theta_{\text{obs}}(t)$  in the resonator, where  $\delta\theta_{\text{obs}}(t)$  is given by

$$\delta\theta_{\text{obs}}(t) = \theta_{\text{obs}}(t) - \langle\theta(t)\rangle,$$

and the average  $\langle\theta(t)\rangle$  is taken over an ensemble of spin-resonator systems.

Spin fluctuations and the thermal fluctuations in  $\theta$  are two intrinsic noise sources. In addition, quantum mechanics imposes limitations on the sensitivity with which motion can be detected. Section 4.3 presents formulas for the spectral density of the noise introduced by thermal fluctuations in  $\theta$  and the noise introduced by the motion detector. Section 4.4 derives an expression for the spectral density of the spin noise.

### 4.3 Spectral density of the instrument noise

The evolution of the Heisenberg operator  $\theta(t)$  is given to first order in  $\theta$  by the quantum Langevin equation

$$I_h \frac{d^2}{dt^2} \theta(t) + \frac{2I_h}{\tau_h} \frac{d}{dt} \theta(t) + k\theta(t) = \gamma \hbar \frac{dB_x}{d\theta} I_x(t) + N'(t), \quad (4.39)$$

where  $N'(t)$  is a fluctuating thermal torque. The quantum Langevin equation for a damped resonator is derived in reference [23], and a similar derivation can be carried out when  $\theta(t)$  is coupled to  $I_x(t)$ . Equation (4.39) shows that the intrinsic fluctuations  $\theta$  for the spin-resonator system can be characterized in terms of a thermal torque. The spectral distribution of the thermal torque is calculated using the

symmetric correlation function

$$C_{N'}(t_1, t) = \frac{1}{2} \langle N'(t) N'(t_1) + N'(t_1) N'(t) \rangle,$$

which can be expressed as [23]

$$C_{N'}(t_1, t) = \frac{2I_h}{\tau_h} \frac{1}{\pi} \int_0^\infty \hbar\omega \coth\left(\frac{\hbar\omega}{2k_B T_h}\right) \cos[\omega(t - t_1)] d\omega. \quad (4.40)$$

Equation 4.40 implies that the double-sided spectral density  $S_{N'}(\omega)$  of  $N'(t)$  is given by

$$S_{N'}(\omega) = \frac{4I_h}{\tau_h} \hbar\omega \left( \frac{1}{2} + n_{\text{th}}(\omega) \right), \quad \omega \geq 0, \quad (4.41)$$

where  $n_{\text{th}}(\omega)$  is the number of thermal quanta in an oscillator of frequency  $\omega$  at temperature  $T_h$ . (Since a double-sided spectral density is an even function of  $\omega$ , it suffices to specify its values for  $\omega \geq 0$ .)

If  $\hbar\omega_h \ll k_B T_h$ , then (4.41) is closely approximated by the classical expression

$$S_{N'}(\omega) = \frac{4I_h k_B T_h}{\tau_h}.$$

At frequencies of order 50 MHz or higher and temperatures of order 10 mK, which are achievable in a dilution refrigerator, mechanical zero-point motion makes a non-negligible contribution to the intrinsic fluctuations characterized by (4.41), since  $n_{\text{th}}(\omega_h)$  is of order unity or less. In this regime, quantum mechanics imposes limitations on the sensitivity with which  $\langle \theta(t) \rangle$  can be measured. In the limit where the temperature approaches zero Kelvins, the spectral density of the thermal torque is

$$S_{N'}(\omega, 0) = \frac{4I_h}{\tau_h} \hbar\omega \left( \frac{1}{2} \right).$$

Quantum-limited detection of the oscillator's motion occurs when the noise added by the detector is equivalent to the noise resulting from the thermal torque at zero Kelvins [24]. Letting  $S_{\text{QL}}(\omega)$  denote the spectral density of the quantum-limited "noise torque," which includes contributions from the thermal torque as well as the

noise added by the detector, we have

$$S_{\text{QL}}(\omega) = \frac{4I_h}{\tau_h} \hbar \omega \left( \frac{1}{2} + \frac{1}{2} + n_{\text{th}}(\omega) \right), \omega \geq 0.$$

The nature of this quantum limit is clarified by remarks presented in references [11] and [24]. Achievement of quantum-limited detection sensitivity requires that the strength of the coupling between oscillator and detector be optimally tuned. For overly weak coupling, the detector's response to the mechanical motion becomes small compared to the detector's intrinsic fluctuations, while for overly strong coupling, the "back-action," or perturbation of the mechanical oscillator due to its coupling to the detector, becomes large relative to the intrinsic mechanical fluctuations characterized by  $S_{N'}(\omega)$  [24]. The minimal noise added to the signal by an optimal detection scheme can be interpreted as the zero-point motion of an internal mode of the detector [11].

In characterizing the performance of a real detector, we let  $S_{\text{inst}}(\omega)$  denote the spectral density of "instrument noise," that is, the noise not present in the spin sample itself, and we assume that  $S_{\text{inst}}(\omega)$  can be expressed in the form

$$S_{\text{inst}}(\omega) = \frac{4I_h}{\tau_h} \hbar \omega \left( A_{\text{det}} + \frac{1}{2} + n_{\text{th}}(\omega) \right), \omega \geq 0. \quad (4.42)$$

(In practice, this will be equivalent to the assumption that the detector adds white noise, since  $S_{\text{inst}}(\omega)$  is flat in the bandwidth of interest for NMR signals.) We could say that in this case the noise added by the resonator is  $2A_{\text{det}}$  times the quantum limit. More conventional (but less straightforward) is the use of noise temperature  $T_N$ , for which different authors give inconsistent definitions [11, 24]. A simple approach might be to define  $T_N$  by the equation

$$A_{\text{det}} + \frac{1}{2} + n_{\text{th}}(\omega_h, T_h) = \frac{1}{2} + n_{\text{th}}(\omega_h, T_h + T_N), \quad (4.43)$$

or

$$A_{\text{det}} = n_{\text{th}}(\omega_h, T_h + T_N) - n_{\text{th}}(\omega_h, T_h),$$

where  $A_{\text{det}}$  is defined as in (4.42), and where the temperature dependence of  $n_{\text{th}}$  has been highlighted by expressing its argument as  $(\omega_h, T_h)$ . From (4.43) we see that the noise temperature can be roughly interpreted as the increase in resonator temperature needed to account for the noise added by the detector. A weakness of this definition is that the detector's noise temperature depends on the amount of noise at the input (i.e., the temperature of the resonator), which implies that noise temperature does not characterize the "intrinsic" properties of the detector. Differing attempts to correct this weakness lead to inconsistent definitions of noise temperature.

We follow reference [25] in defining the quantum-limited noise temperature  $T_{QL}$  by

$$T_{QL} = \frac{\hbar\omega_h}{k_B \ln 3}. \quad (4.44)$$

Equation (4.44) is obtained by defining the noise temperature  $T_N$  in reference to an oscillator at 0 K, so that

$$A_{\text{det}} = n_{\text{th}}(\omega_h, T_N).$$

Schwab et al. have reported detection of mechanical motion with [25]

$$T_N = 18T_{QL},$$

which gives

$$A_{\text{det}} = 16. \quad (4.45)$$

In adding noise to simulations of detected spectra in section 1 of chapter 6, we assume that the detector has this value of  $A_{\text{det}}$ , so that the "noise torque" associated with thermal fluctuations and detector noise has spectral density

$$S_{\text{inst}}(\omega) = \frac{4I_h}{\tau_h} \hbar\omega \left( 16 + \frac{1}{2} + n_{\text{th}}(\omega) \right), \quad T_N = 18T_{QL}, \quad \omega \geq 0.$$

#### 4.4 Spectral density of the spin noise

Superimposed on  $m(t)$  is a noise torque  $T'(t)$  associated with fluctuations of  $I_x(t)$ . In quantifying these fluctuations, we use a simple model in which they are treated as a stationary random process with zero mean during the period in which the resonator's position is being monitored. The properties of this random process are calculated using a high-temperature limit, without consideration of the pulse sequence used during the NMR experiment. In certain cases, this model could overestimate the spin noise. Consider, for instance, an experiment in which the longitudinal magnetization of a highly-polarized sample is rotated by  $90^\circ$  to lie along the  $x$ -axis at the beginning of the detection period. The variance in  $I_x$  at the beginning of the detection period is then equal to the variance in  $I_z$  just before the rotation. If the spin sample is at a temperature of  $\sim 10$  mK and is in an applied field of order 10 T, the variance in  $I_z$  is significantly less than the high-temperature limit, and the spin noise could be overestimated as a result.

The spectral distribution of the spin noise can be quantified by means of the symmetric correlation function

$$C_I(t_1, t) = \frac{1}{2} \langle I_x(t) I_x(t_1) + I_x(t_1) I_x(t) \rangle.$$

Use of the quantum regression theorem [7] in combination with equation (4.36) gives

$$C_I(t_1, t) = \langle I_x^2 \rangle e^{-|t-t_1|/\tau_s} \cos(\omega_h |t - t_1|).$$

Note that the value of the time constant  $\tau_s$  for decay of the transverse spin dipole will depend on whether the spins precess freely or are spin-locked. For the mean-square fluctuation  $\langle I_x^2 \rangle$  we use the value  $N/4$ , appropriate for a sample of  $N$  spins  $1/2$  in thermal equilibrium. The symmetric correlation of the spin-noise torque  $T'(t)$  is in

this way approximated as

$$\begin{aligned} C_{T'}(t_1, t) &= \frac{1}{2} \langle T'(t) T'(t_1) + T'(t_1) T'(t) \rangle \\ &= \left( \gamma \hbar \frac{dB_x}{d\theta} \right)^2 \frac{N}{4} e^{-|t-t_1|/\tau_s} \cos(\omega_h |t - t_1|), \end{aligned}$$

and the spectral density  $S_{T'}(\omega)$  as

$$S_{T'}(\omega) = \left( \gamma \hbar \frac{dB_x}{d\theta} \right)^2 \frac{N}{4} \int_{-\infty}^{\infty} e^{-i\omega t} e^{-|t|/\tau_s} \cos(\omega_h t) dt. \quad (4.46)$$

## 4.5 SNR formula for amplitude detection

In order to simplify the analysis, we will calculate SNR using a filter which is optimal if spin noise is negligible compared to the thermal torque  $N'(t)$  and the detector noise. The transfer function  $K(\omega)$  is

$$K(\omega) = c \frac{M_0^*(\omega)}{S_{\text{inst}}(\omega)},$$

where  $S_{\text{inst}}(\omega)$  is given by equation (4.42), and  $M_0(\omega)$  is the Fourier transform of the unit amplitude signal defined by (4.37). The curve  $M_0(\omega)$  has complex Lorentzian peaks at  $\pm\omega_h$ . The magnitude of  $S_{\text{inst}}$  varies by at most a few percent over the range of frequencies for which  $M_0(\omega)$  is non-negligible, assuming that  $\omega_h/2\pi$  is in the range of 50 MHz to 1 GHz, with

$$T_h \geq 10 \text{ mK},$$

$$\tau_s \geq 1 \mu\text{s},$$

$$A_{\text{det}} \leq 10^3.$$

We will therefore approximate  $S_{\text{inst}}(\omega)$  by  $S_{\text{inst}}(\omega_h)$  and consider the noise to be white. The constant  $c$  is chosen as in equation 4.13:

$$c = S_{\text{inst}}(\omega_h).$$

When the noisy signal  $f(t) = m(t) + n(t)$  is passed into filter  $\mathcal{K}$ , the output  $\phi(t) = \mu(t) + \nu(t)$  is given by equation (4.14) as

$$\phi(t) = \int_{-\infty}^{\infty} f(t') m_0(t' - t) dt'.$$

The amplitude estimate  $X$  is given by equations (4.15) and (4.17):

$$X = \frac{\int_{-\infty}^{\infty} m_0(t) f(t) dt}{\int_{-\infty}^{\infty} m_0^2(t) dt}.$$

The SNR formula (4.7) can be expressed as

$$SNR = \frac{\langle X \rangle}{\sqrt{\sigma_{\text{inst}}^2 + \sigma_{\text{spin}}^2}},$$

where  $\sigma_{\text{inst}}^2$ ,  $\sigma_{\text{spin}}^2$  are the respective variances introduced into the measurement by instrument noise and spin noise:

$$\sigma_{\text{inst}}^2 = \frac{1}{\mu_0^2} \left( \frac{1}{2\pi} \int_{-\infty}^{\infty} |M_0(\omega)|^2 S_{\text{inst}}(\omega) d\omega \right), \quad (4.47)$$

$$\sigma_{\text{spin}}^2 = \frac{1}{\mu_0^2} \left( \frac{1}{2\pi} \int_{-\infty}^{\infty} |M_0(\omega)|^2 S_{T'}(\omega) d\omega \right), \quad (4.48)$$

$$\begin{aligned} \mu_0 &= \int_{-\infty}^{\infty} m_0^2(t) dt \\ &\approx \frac{\tau_s}{4}. \end{aligned}$$

Evaluation of the integrals appearing in (4.47) and (4.48) yields

$$\begin{aligned} \sigma_{\text{inst}}^2 &= S_{\text{inst}}(\omega_h) \frac{4}{\tau_s}, \\ \sigma_{\text{spin}}^2 &= \frac{N}{2} \left( \gamma \hbar \frac{dB_x}{d\theta} \right)^2. \end{aligned}$$

The mean value  $\langle X \rangle = G$  is given by equation (4.38):

$$\langle X \rangle = \gamma \hbar \frac{dB_x}{d\theta} \langle I_x \rangle.$$

Here  $\langle I_x \rangle$  is a mean transverse spin component at the beginning of the time period during which the torque on the mechanical resonator has the form of a decaying sinusoid. The value of  $\langle I_x \rangle$  depends on the sequences of pulses and delays used to encode information about the microscopic environment of the spins into the motion of the transverse spin dipole. For the SNR estimate, we assume that the value of  $\langle I_x \rangle$  at the beginning of the FID is  $PN/2$ , where  $P$  is the polarization of the spin sample just before the beginning of the pulse sequence. The time-dependence of  $\langle I_x \rangle$  during the sampled portion of the FID is characterized by the function  $s_0(t)$ , which is defined by the equation

$$\langle I_x(t_1) \rangle = \frac{PN}{2} s_0(t_1). \quad (4.49)$$

To characterize the sensitivity of a single measurement of  $\langle I_x \rangle$  as a means of detecting the FID, we use equation (4.21), which can be expressed in this case as

$$\text{single-shot SNR} = \frac{(PN/2) \sqrt{\langle s_0^2(t_1) \rangle}}{\sqrt{\sigma_{\text{inst}}^2 + \sigma_{\text{spin}}^2}}.$$

The single-shot SNR for detection of an FID by measurement of an amplitude  $\langle I_x \rangle$  is

$$\begin{aligned} \text{single-shot SNR} &= \frac{(PN/2) (\gamma \hbar dB_x/d\theta) \sqrt{\langle s_0^2(t_1) \rangle}}{\sqrt{S_{\text{inst}}(\omega_h) (4/\tau_s) + (N/2) (\gamma \hbar dB_x/d\theta)^2}}, \quad (4.50) \\ S_{\text{inst}}(\omega_h) &= \frac{4I_h}{\tau_h} \hbar \omega_h \left( A_{\text{det}} + \frac{1}{2} + n_{\text{th}}(\omega_h) \right). \end{aligned}$$

Note that the spectral density  $S_{\text{inst}}(\omega_h)$  is a double-sided spectral density. Equation (4.50) could be expressed in terms of a single-sided spectral density  $S_{\text{inst}}^s(\omega_h)$  by making the substitution  $S_{\text{inst}}(\omega_h) = S_{\text{inst}}^s(\omega_h)/2$ .

If the amplitude measurement is performed by spin-locking the transverse spin dipole, with resonator-induced relaxation responsible for decay of the spin-locked signal, then the results of section 6 of chapter 3 imply that

$$\tau_s = 2/R_h,$$

provided the spin-locking field is strong enough to average both the internal spin Hamiltonian and the spin relaxation superoperator associated with spin-resonator interactions. If, in addition, instrument noise is much larger than spin noise, then (4.50) can be simplified to yield

$$\begin{aligned} \text{single-shot } SNR &= \frac{(PN/2) (\gamma \hbar dB_x/d\theta) \sqrt{\langle s_0^2(t_1) \rangle}}{\sqrt{S_{\text{inst}}(\omega_h) (2R_h/\tau_s)}} \\ &= \frac{PN \sqrt{\langle s_0^2(t_1) \rangle}}{4 \sqrt{(A_{\text{det}} + \frac{1}{2} + n_{\text{th}}) (n_{\text{th}} + \frac{1}{2})}}. \end{aligned} \quad (4.51)$$

In this case, the SNR is independent of the resonator parameters  $\tau_h$ ,  $I_h$ , and  $dB_x/d\theta$ . We can interpret (4.51) as stating that if the resonator ringdown time, moment of inertia, and field derivative  $dB_x/d\theta$  are considered to be "knobs" which can be varied, then changes in transverse relaxation due to lifetime broadening will compensate exactly for changes in the signal strength and the Brownian noise as these knobs are turned. The only resonator parameter which appears in the SNR expression is the thermal number of quanta  $n_{\text{th}}$ , which is determined by the resonator frequency  $\omega_h$  and the temperature  $T_h$ .

## 5 Signal-to-noise ratio for detection of a continuous signal

If the freely-precessing transverse spin dipole drives the resonator throughout the FID, then detection of a single transient yields a measurement of the time-dependent function  $\langle I_x(t) \rangle$  rather than a single amplitude  $\langle I_x(t_1) \rangle$ . In characterizing the sensitivity of this method, we assume that a sampling interval  $\Delta t$  has been chosen, and that broadband noise with spectral density  $S_{\text{inst}}(\omega_h)$  is present in the measurement, with  $S_{\text{inst}}(\omega_h)$  given by equation (4.42). This noise is filtered before the noisy signal is sampled, and we assume for the sake of simplicity that an ideal bandpass filter eliminates all noise outside a frequency range of width  $(1/\Delta t)$  Hz, and that the filtered

noise introduces an identical variance  $\sigma^2$  to each real-valued sample.

The definitions of the signal and the noise are similar to those given in sections 4.1 and 4.2. The signal  $s(t)$  is defined as the torque which would produce mean displacement  $\langle \theta(t) \rangle$  in the resonator, where the average is quantum statistical. Noise is present in the measurement due to the fact that

$$\theta_{\text{obs}}(t) \neq \langle \theta(t) \rangle,$$

with  $\theta_{\text{obs}}(t)$  the observed displacement. The noisy signal  $f(t)$  is defined as the torque needed to produce a mean displacement equal to  $\theta_{\text{obs}}(t)$ , and the noise  $n(t)$  is given by

$$n(t) = f(t) - s(t).$$

Detection of a single transient yields a measurement of the driving torque exerted by the spins throughout the FID, and the signals from two transients can be combined to yield a complex signal, as in conventional NMR spectrometers. We will consider  $s(t)$  to be complex, with two transients required to sample the full curve  $s(t)$ .

Using equation (4.27), the signal-to-noise ratio can be expressed as

$$SNR = \frac{\sqrt{\sum |s(t)|^2}}{\sigma/\sqrt{Z}},$$

where the sum is over the sampled complex points, with each point sampled  $Z$  times. We assume that the sampling interval is so short compared to the decay time of  $|s(t)|^2$  that the average appearing underneath the radical can be approximated as an integral:

$$\begin{aligned} \sum |s(t)|^2 &= \frac{1}{\Delta t} \sum |s(t)|^2 \Delta t \\ &\approx \frac{1}{\Delta t} \int_0^\infty |s(t)|^2 dt \\ &\equiv \frac{1}{\Delta t} \langle |s(t)|^2 \rangle. \end{aligned}$$

We obtain

$$SNR \approx \frac{\sqrt{\langle |s(t)|^2 \rangle}}{\sqrt{\sigma^2 \Delta t / Z}}. \quad (4.52)$$

In the case where instrument noise is the dominant noise source, the variance introduced by this noise in a bandwidth of  $(1/\Delta t)$  Hz is

$$\sigma^2 = \frac{S_{\text{inst}}(\omega_h)}{\Delta t}. \quad (4.53)$$

Substituting this expression into (4.52) and noting that  $2Z$  transients were observed yields

$$\text{single-shot } SNR \approx \frac{\sqrt{\langle |s(t)|^2 \rangle}}{\sqrt{2S_{\text{inst}}(\omega_h)}}. \quad (4.54)$$

For convenience in comparing the sensitivity of different detection schemes, we express  $s(t)$  in the form

$$s(t) = \left(\frac{PN}{2}\right) \left(\gamma \hbar \frac{dB_x}{d\theta}\right) \{s_a(t) + i s_b(t)\}. \quad (4.55)$$

If

$$\begin{aligned} \langle |s_a(t) + i s_b(t)|^2 \rangle &= \langle s_a^2(t) \rangle + \langle s_b^2(t) \rangle \\ &= 2 \langle s_a^2(t) \rangle, \end{aligned}$$

then (4.54) can be written as

$$\text{single-shot } SNR \approx \frac{(PN/2) (\gamma \hbar dB_x/d\theta) \sqrt{\langle s_a^2(t) \rangle}}{\sqrt{S_{\text{inst}}(\omega_h)}}. \quad (4.56)$$

## 6 Comparison of detection sensitivities

### 6.1 Dependence of sensitivity on the energy in the signal

The signal-to-noise ratios given in equations (4.50) and (4.56) can be compared in the case where instrument noise is dominant in (4.50). Dropping spin noise from (4.50)

and taking the ratio of the two expressions gives

$$\begin{aligned} \left( \frac{\text{single-shot } SNR \text{ amplitude detection}}{\text{single-shot } SNR \text{ continuous signal}} \right)^2 &= \frac{\langle s_0^2(t_1) \rangle}{(4/\tau_s) \langle s_a^2(t) \rangle} \\ &= \frac{\langle s_0^2(t_1) \rangle \langle m_0^2(t) \rangle}{\langle s_a^2(t) \rangle}. \end{aligned} \quad (4.57)$$

Note that  $\langle s_0^2(t_1) \rangle$  is an average over a set of times  $t_1$  at which spin-locking was applied to obtain an amplitude measurement, and the signal  $s_0$  corresponds to free spin precession in the absence of spin-resonator interaction. By way of contrast, the signal  $s_a$  appearing in the denominator of (4.57) corresponds to free spin precession in the presence of coupling to a mechanical resonator. Equation (4.57) can be interpreted as the ratio of the mean energies in the signals which drive the resonator in the two types of detection, with the average being taken over all transients. During continuous detection, the energy in the signal torque is proportional to  $\langle s_a^2(t) \rangle$ , while during an amplitude measurement, the resonator is driven by a signal torque proportional to  $m_0(t)$  and having energy proportional to  $\langle m_0^2(t) \rangle$ . The proportionality constant for the spin-locked signal depends on the value of

$$\langle I_x(t_1) \rangle \propto s_0(t_1),$$

and the average  $\langle s_0^2(t_1) \rangle$  includes the effect of this variation on detection sensitivity.

To further clarify the content of (4.57), we consider an example in which  $s(t)$  has the form of a single decaying exponential with time constant  $T_2$ :

$$s(t) = \left( \frac{PN}{2} \right) \left( \gamma \hbar \frac{dB_x}{d\theta} \right) \exp \{ (i\omega_0 - 1/T_2) t \}, \quad t \geq 0,$$

with the time constant  $\tau_s$  for the decay of  $m_0(t)$  given by  $T_{1\rho}$ , the time constant for the decay of a spin-locked signal:

$$\tau_s = T_{1\rho}.$$

During amplitude measurements, the value of  $\langle I_x(t_1) \rangle$  is sampled only at times  $t_1$  when the FID has not decayed significantly. For this example, the ratio of equation

(4.57) can be expressed as

$$\left( \frac{\text{single-shot } SNR \text{ amplitude detection}}{\text{single-shot } SNR \text{ continuous signal}} \right)^2 = \frac{T_{1\rho}/2}{T_2}. \quad (4.58)$$

The factor of 2 difference arises from the fact that the initial amplitude of the signal for continuous detection does not vary between measurements, while the initial signal amplitude for spin-locked detection varies sinusoidally as  $t_1$  is varied between shots.

## 6.2 Effect of resonator-induced transverse relaxation

Equations (4.57) and (4.58) show that the relative sensitivities of spin-locked detection and detection of freely-precessing spins are determined by the time constants for decay of the transverse spin. At mK temperatures, the precessing transverse spin of a solid sample containing only a few spins (e.g., two or three spins) is expected to relax slowly in the absence of spin-resonator interactions, since in this case transverse relaxation depends on spin-lattice interactions which are "frozen out" at low temperatures. The coupling between the spins and the mechanical resonator will induce transverse relaxation, thereby limiting the sensitivity with which the spectrum can be detected. Consider an example in which the sample contains only a single spin  $1/2$  and the resonator is at zero Kelvins. If interaction with the mechanical resonator is the dominant source of transverse relaxation, then it follows from equations (2.22) and (2.23) that the time constant for transverse relaxation is  $2/R_h$ . The signal  $s(t)$  which drives the resonator is

$$s(t) = \left( \frac{P}{2} \right) \left( \gamma \hbar \frac{dB_x}{d\theta} \right) \exp \{ (i\omega_0 - R_h/2) t \}, \quad t \geq 0,$$

and the single-shot SNR given by (4.56) evaluates to

$$\text{single-shot } SNR = \frac{P}{4\sqrt{(n_{\text{th}} + \frac{1}{2})(n_{\text{th}} + \frac{1}{2} + A_{\text{det}})}}, \quad (\text{free precession}). \quad (4.59)$$

Equation (4.59) can be compared with the sensitivity for spin-locked detection

given by (4.51):

$$\text{single-shot } SNR = \frac{PN \sqrt{\langle s_0^2(t_1) \rangle}}{4 \sqrt{(n_{\text{th}} + \frac{1}{2}) (A_{\text{det}} + \frac{1}{2} + n_{\text{th}})}}, \quad (\text{spin locking}),$$

where  $N = 1$  and

$$s_0(t_1) = \cos(\omega_0 t_1).$$

Note that since the spins and the resonator are out of resonance until the spin-locking field is applied, the resonator is assumed not to induce transverse relaxation before spin-locking begins, and so negligible decay in  $s_0(t_1)$  is also assumed. Since

$$\sqrt{\langle s_0^2(t_1) \rangle} = \frac{1}{\sqrt{2}},$$

we have

$$\frac{\text{single-shot } SNR \text{ free precession}}{\text{single-shot } SNR \text{ spin locking}} = \sqrt{2}. \quad (4.60)$$

Equation (4.60) is consistent with (4.58), since our assumptions have yielded

$$T_{1\rho} = T_2 = 2/R_h.$$

We next consider examples of two-spin systems in which a  $90^\circ$  pulse applied to a system in thermal equilibrium leaves the mean dipole aligned with the  $x$ -axis. For simplicity, the resonator is assumed to be at zero Kelvins. For a two-spin system in which the dipolar couplings are large compared to the difference in the chemical shift at the two spins, the energy eigenstates can be approximated as

$$\begin{aligned} |p\rangle &\equiv |++\rangle, \\ |q\rangle &\equiv (|+-\rangle + |-+\rangle) / \sqrt{2}, \\ |r\rangle &\equiv |--\rangle, \\ |s\rangle &\equiv (|+-\rangle - |-+\rangle) / \sqrt{2}. \end{aligned}$$

It follows from equation (3.33) that if the resonator is at zero Kelvins, the signal  $s(t)$  driving the resonator during detection of freely precessing spins can be written as

$$s(t)/G = \frac{1}{2} \exp\{(i\omega_{pq} - 1/T_{pq})t\} + \frac{1}{2} \exp\{(i\omega_{qr} - 1/T_{qr})t\}, \quad t \geq 0, \quad (4.61)$$

$$T_{pq}^{-1} = R_0,$$

$$T_{qr}^{-1} = 2R_0.$$

If the peaks associated with these two coherences do not overlap appreciably, then

$$\frac{1}{G^2} \int_0^\infty |s(t)|^2 dt \approx \frac{(T_{pq} + T_{qr})/2}{4}. \quad (4.62)$$

Note that for a signal  $s(t)$  which has two frequency components decaying exponentially with arbitrary time constant  $T'$ , we have

$$\frac{1}{G^2} \int_0^\infty |s(t)|^2 dt = \frac{T'}{4}, \quad (4.63)$$

provided that the frequency difference between the two components is much greater than  $1/T'$ . Comparing (4.62) and (4.63), we see that the effective decay time associated with (4.61) is

$$T_{\text{eff,dd}} = (T_{pq} + T_{qr})/2$$

$$= \frac{3}{4R_0}.$$

By comparing this with the time constant  $2/R_0$  for a single-spin system, we see that the decay time has decreased by  $3/8$ . In the case where the chemical shift offset of one spin is much larger than the dipolar coupling, equation (3.34) can be used to obtain a similar result. The effective time constant is

$$T_{\text{eff,dd+shift}} = \left( \frac{2}{R_0} + \frac{2}{3R_0} \right) / 2$$

$$= \frac{4}{3R_0},$$

which is smaller than  $2/R_0$  by a factor of  $2/3$ .

These examples have shown that resonator-induced transverse relaxation can make a nonnegligible change in signal lifetime as the sample size is increased from  $N = 1$  to  $N = 2$ . Simulations of resonator-induced transverse relaxation in four-spin systems are presented in section 2.2 of chapter 6, and those simulations suggest that the effective decay time of a freely-precessing signal decreases sharply as the number of dipole-dipole coupled spins is increased above two. By way of contrast, the decay time of the spin-locked signal does not depend on the size of the sample, provided the spin-locking field is strong enough to average both the internal Hamiltonian and the superoperator for resonator-induced relaxation. Ideal spin-locked detection is more sensitive than detection of free precession, even in the case of the two spin sample having  $T_{\text{eff,dd}} = 3/(4R_0)$ :

$$\begin{aligned} \frac{\text{single-shot } SNR \text{ free precession}}{\text{single-shot } SNR \text{ spin locking}} &= \sqrt{2}\sqrt{3/8} \\ &= \sqrt{3/4}. \end{aligned}$$

As sample size is increased, we may expect that detection of free precession will be substantially less sensitive than spin-locked detection, even if the number of spins is small enough that spin locking would not be needed to extend the lifetime of the signal in the absence of resonator-induced relaxation.

## 7 Dependence of signal-to-noise ratio and acquisition time on resonator parameters

In the case where instrument noise is dominant and the spin-locked signal decays exponentially with rate constant  $R_h/2$ , the single-shot SNR is given by (4.51) as

$$\text{single-shot } SNR = \frac{PN\sqrt{\langle s_0^2(t_1) \rangle}}{4\sqrt{(A_{\text{det}} + \frac{1}{2} + n_{\text{th}})(n_{\text{th}} + \frac{1}{2})}}.$$

Given a sample of  $N$  spins and a pulse sequence which yields signal  $s_0(t_1)$ , the dependence of  $SNR$  on resonator parameters can be expressed as

$$\text{single-shot } SNR \propto \frac{P}{\sqrt{(A_{\text{det}} + \frac{1}{2} + n_{\text{th}}) (n_{\text{th}} + \frac{1}{2})}}, \quad (4.64)$$

$$P = \tanh\left(\frac{\hbar\omega_h}{2k_B T_h}\right),$$

$$n_{\text{th}} = \left(\exp\left(\frac{\hbar\omega_h}{k_B T_h}\right) - 1\right)^{-1}.$$

The only resonator parameter which contributes to  $P$  and  $n_{\text{th}}$  is the ratio  $\omega_h/T_h$  of frequency to temperature. If this ratio is increased, polarization increases and  $n_{\text{th}}$  decreases, and both of these changes improve SNR. In general, therefore, sensitivity improves when the frequency increases or the temperature decreases. However, the limiting values of  $P$  and  $n_{\text{th}}$  in the high-frequency, low-temperature limit are

$$P \rightarrow 1,$$

$$n_{\text{th}} \rightarrow 0.$$

For the example resonator presented in chapter 5, the values

$$T_h = 10 \text{ mK}, \quad (4.65)$$

$$\omega_h/2\pi = 630 \text{ MHz} \quad (4.66)$$

give

$$P = 0.91,$$

$$n_{\text{th}} = 0.05.$$

In this regime, SNR is near the value high-frequency, low-temperature limit.

Decreasing the  $\omega_h/T_h$  by a factor of three (e.g., by increasing  $T_h$  to 30 mK) gives

$$P = 0.46,$$

$$n_{\text{th}} = 0.6.$$

In the case where the noise added by the motion detector is substantially larger than the noise associated with the zero-point motion of the resonator ( $A_{\text{det}} \gg 1/2$ ), this change in  $\omega_h/T_h$  decreases the right side of (4.64) by a factor of approximately 2.8. We see that although the regime defined by (4.65) and (4.66) is near optimal, SNR is sensitive to changes in  $\omega_h/T_h$  within this regime.

The time required to acquire a spectrum is more sensitive to resonator parameters than the SNR is. Consider a problem in which the time needed per transient is proportional to  $1/R_h$ ; for example, a problem in which both the decay of the spin-locked signal and the longitudinal relaxation occur during a time proportional to  $1/R_h$ , with the pulse sequence requiring a negligible period of time per transient. Since the number of transients  $Z$  needed to detect  $\langle I_x(t_1) \rangle$  with acceptable accuracy at a given point  $t_1$  is proportional to  $1/(SNR)^2$ , acquisition time is minimized if the resonator is designed to yield a minimal value of

$$\frac{1}{R_h (SNR)^2}$$

or, equivalently, a maximal value of

$$\begin{aligned} (SNR)^2 R_h &\propto \frac{P^2}{\left(A_{\text{det}} + \frac{1}{2} + n_{\text{th}}\right)} g^2 \tau_h \\ &\propto \frac{P^2}{\omega_h \left(A_{\text{det}} + \frac{1}{2} + n_{\text{th}}\right)} \frac{(dB_x/d\theta)^2}{I_h} \tau_h. \end{aligned} \quad (4.67)$$

The dependence of  $\tau_h$  on other resonator parameters is poorly understood. If this dependence is neglected, then (4.67) can be used to analyze the way in which acquisition time depends on  $\omega_h$ ,  $I_h$ , and  $dB_x/d\theta$ . The dependence on  $I_h$  and  $dB_x/d\theta$  is simple: acquisition time is proportional to  $I_h$  and inversely proportional to  $(dB_x/d\theta)^2$ .

The dependence of acquisition time on frequency is entirely contained in the function

$$f(\omega_h) = \frac{P^2}{\omega_h (A_{\text{det}} + \frac{1}{2} + n_{\text{th}})}.$$

The choice  $A_{\text{det}} = 16$ , which is explained in the discussion preceding (4.45), along with  $T_h = 10$  mK, causes  $f(\omega_h)$  to have a maximum around  $\omega_h/2\pi = 450$  MHz, but the peak is fairly flat, and the value of  $f(\omega_h)$  stays within 10% of the peak value for frequencies between 300 MHz and 700 MHz. If quantum-limited detection is assumed, the peak is shifted to around 525 MHz, while  $f(\omega_h)$  stays within 10% of its peak value over the range 375 MHz to 775 MHz.

## 8 Signal-to-noise ratio for a product of correlated measurements

Reference [13] presents a SNR analysis for CONQUEST, a scheme in which an NMR spectrum is obtained by measuring a spin correlation function. The analysis in this reference does not include thermal noise in the mechanical resonator or noise added to the measurement during detection of the mechanical motion. In order to compare quantitatively the sensitivity of different techniques for NMR spectroscopy of nanoscale samples, we extend the sensitivity analysis of CONQUEST to include these forms of noise.

### 8.1 Definition of the signal and the noise

Since we are specifically interested in measurements which could be done with a nanoscale torsional mechanical resonator coupled to the transverse sample dipole, it will be convenient to modify the convention established in reference [13] by considering  $I_x$  rather than  $I_z$  to be the spin component measured in the CONQUEST experiment. In particular, we consider that a single shot of the experiment yields a measurement

of the Heisenberg operator

$$S_2(t_1, 0) = I_x(t_1) I_x(0) \quad (4.68)$$

$$\equiv \left( U_0^\dagger I_x U_0 \right) I_x, \quad (4.69)$$

where  $U_0$  is the spin-system evolution operator for the time period beginning at time  $t = 0$  and ending at  $t = t_1$ . In order to simplify the discussion, we follow reference [13] in assuming that  $U_0$  corresponds to free precession of the sample dipole at frequency  $\omega$ , so that

$$\begin{aligned} I_x(t_1) &= U_0^\dagger I_x(0) U_0 \\ &= I_x(0) \cos \omega t - I_y(0) \sin \omega t \\ &= I_x \cos \omega t_1 - I_y \sin \omega t_1. \end{aligned} \quad (4.70)$$

Spin noise is analyzed in reference [13] by considering that each measurement is represented by a projection operator which acts on the spin system. In order to quantify the effects of instrument noise on the measurements, we replace this model with one in which a period of spin motion governed by the evolution operator  $U$  is sandwiched between two periods of spin-resonator evolution. The resonator is continuously observed throughout the experiment, with  $\theta_{\text{obs}}(t)$  denoting the observed value of the resonator coordinate.

In proposing a method for quantifying the information available in  $\theta_{\text{obs}}(t)$ , we are guided by consideration of the method defined in sections 4.1 and 4.2 for analyzing the SNR of an amplitude measurement. The noisy signal  $f(t)$  was defined as the torque which would produce expected displacement  $\theta_{\text{obs}}(t)$  in the resonator, for all  $t$ , while the "noiseless signal"  $m(t)$  was defined as the torque which would produce expected displacement  $\langle \theta(t) \rangle$  in the resonator, where the average is quantum statistical. The information to be extracted by analysis of  $f(t)$  was the amplitude of  $m(t)$ , or equivalently, the value  $m(0)$  at the beginning of the detection period. In order to filter out instrument noise, we multiplied  $f(t)$  by  $m_0(t)$  and integrated, where  $m_0(t)$

has the same functional form as  $m(t)$  but unit amplitude.

For CONQUEST, we propose an analogous method of analyzing SNR. Given  $\theta_{\text{obs}}(t)$ , we find the torque  $g(t)$  which would produce expected displacement  $\theta_{\text{obs}}(t)$  in the resonator. Our definition of the signal can be motivated by considering equation (4.39), the quantum Langevin equation for a damped resonator interacting with a spin sample:

$$\begin{aligned} I_h \frac{d^2}{dt^2} \theta(t) + \frac{2I_h}{\tau_h} \frac{d}{dt} \theta(t) + k\theta(t) &= \gamma \hbar \frac{dB_x}{d\theta} I_x(t) + N'(t) \\ &\equiv T(t) + N'(t). \end{aligned}$$

The operator  $N'(t)$  is a rapidly fluctuating torque of mean zero, and  $T(t)$  can be identified with the torque exerted by the spins at time  $t$ . The noisy torque  $g(t)$  includes contributions from  $T(t)$  and  $N'(t)$ , as well as from noise added during the detection of the resonator's mechanical motion. Define  $N_{\text{inst}}(t)$  to be the torque associated with instrument noise, including both thermal noise and noise in the motion detector, and assume that the spectral density of  $N_{\text{inst}}(t)$  is given by (4.42). We wish to obtain from  $g(t)$  a measurement of

$$\langle I_x(t_1) I_x(0) \rangle = \left( \frac{1}{\gamma \hbar dB_x/d\theta} \right)^2 \langle T(t_1) T(0) \rangle. \quad (4.71)$$

If the noiseless signal is defined by

$$m(t', t'') = \langle T(t') T(t'') \rangle,$$

and the noisy signal by

$$f(t', t'') = g(t') g(t''),$$

then the optimal measurement protocol for CONQUEST will be the one which minimizes the variance in the estimate of

$$m(t_1, 0) = \langle T(t_1) T(0) \rangle \quad (4.72)$$

obtained by filtering  $f(t', t'')$ . Error will be introduced in the measurement due to the presence of the noise:

$$n(t', t'') = f(t', t'') - m(t', t'').$$

## 8.2 SNR formula

By analogy with the method of data analysis derived in section 1, we seek to express the signal  $m(t', t'')$  in the form

$$m(t', t'') = G_1 m_0(t', t''),$$

where  $m_0(t', t'')$  is a known function and  $G_1$  is the value we wish to estimate. The estimate of  $G_1$  will be given by the random variable

$$X = \frac{\int_{-\infty}^{\infty} \int_{-\infty}^{\infty} f(t', t'') m_0(t', t'') dt' dt''}{\int_{-\infty}^{\infty} \int_{-\infty}^{\infty} m_0^2(t', t'') dt' dt''}.$$

In determining the functional form of  $m(t', t'')$ , we neglect spin relaxation and fluctuations occurring during the interval  $0 \leq t \leq t_1$ . It follows from (4.70), (4.71), and (4.72) that

$$m(t_1, 0) = \left( \gamma \hbar \frac{dB_x}{d\theta} \right)^2 \{ \langle I_x^2(0) \rangle \cos \omega t_1 - \langle I_x(0) I_y(0) \rangle \sin \omega t_1 \} \quad (4.73)$$

$$= \left( \gamma \hbar \frac{dB_x}{d\theta} \right)^2 \langle I_x^2(0) \rangle \cos \omega t_1, \quad (4.74)$$

where we have assumed in moving from (4.73) to (4.74) that at time  $t = 0$ , the spin density matrix  $\rho_s$  is a multiple of the identity.

For simplicity, we assume that the spins exert negligible torque on the resonator during the interval  $0 < t < t_1$ , and so  $m(t', t'') = 0$  if either  $t'$  or  $t''$  lies in this interval. If  $t'$  and  $t''$  lie outside this interval, then  $m(t', t'')$  is proportional to the correlation function

$$C_I(t', t'') = \langle I_x(t') I_x(t'') \rangle.$$

In obtaining an estimate of  $C_I$ , we let  $U(t', t'')$  denote the lab-frame evolution operator for the spins, with  $U(t_1, 0) = U_0$ , the operator appearing in (4.69). Since we have taken  $\rho_s(0)$  to be a multiple of the identity,  $\rho_s(0)$  commutes with all spin operators, and  $C_I$  can be written as

$$\begin{aligned} C_I(t', t'') &= \text{Tr} \{ I_x(t') I_x(t'') \rho_s(0) \} \\ &= \text{Tr} \{ U(0, t') I_x U(t', 0) U(0, t'') I_x U(t'', 0) \rho_s(0) \} \\ &= \text{Tr} \{ U(t'', t') I_x U(t', t'') I_x \rho_s(0) \}. \end{aligned} \quad (4.75)$$

Equation (4.75) implies that  $C_I$  can be evaluated as the correlation function of a spin system which is completely disordered at time  $t''$ .

If  $t', t''$  are both less than 0 or both greater than  $t_1$ , then  $U$  is the evolution operator for the spins as they drive the resonator. For simplicity, we assume that the spins are spin-locked during this period. A simple method of approximating  $C_I$  for these values of  $t', t''$  is to assume that  $\tilde{C}_I$ , the correlation function in the rotating frame, is given by

$$\tilde{C}_I(t', t'') = \langle I_x^2 \rangle \exp(-|t' - t''|/T_{1\rho}),$$

where  $T_{1\rho}$  is the decay time of  $I_x$  during spin-locking. We can then approximate the lab-frame correlation function as

$$C_I(t', t'') = \langle I_x^2 \rangle \exp(-|t' - t''|/T_{1\rho}) \cos(\omega_h t') \cos(\omega_h t''), \quad (4.76)$$

for  $t', t'' < 0$ , and

$$\langle I_x(t') I_x(t'') \rangle = \langle I_x^2 \rangle \exp(-|t' - t''|/T_{1\rho}) \cos(\omega_h(t' - t_1)) \cos(\omega_h(t'' - t_1)) \quad (4.77)$$

if  $t', t'' > t_1$ . Note that we have assumed that during spin-locking, components of sample dipole which are not spin-locked decay so quickly that we can neglect their contribution to the lab-frame correlation function.

If  $t'' < 0$  and  $t' > t_1$ , we obtain

$$\begin{aligned}\langle I_x(t') I_x(t'') \rangle &= \langle U(t'', t') I_x U(t', t'') I_x \rangle \\ &= \left\langle U(t'', 0) U_0^\dagger U(t_1, t') I_x U(t', t_1) U_0 U(0, t'') I_x \right\rangle,\end{aligned}$$

with the average taken for a density matrix which is a multiple of the identity. Again, this is a lab-frame correlation function, and the simplest way to approximate it is to consider first the correlation function  $\tilde{C}_I$  in a particular rotating frame. For times during which the spin-locking field is present, the  $x$ -axis of this rotating frame is parallel to the resonant rotating component of the spin-locking field, while the  $z$ -axes of the rotating and lab frames are identical. During the period  $0 \leq t \leq t_1$ , the axes of the rotating and lab frames are identical (that is, the rotating frame does not rotate). In this rotating frame, we can approximate the correlation function by

$$\tilde{C}_I(t', t'') = \langle I_x^2 \rangle \cos(\omega t_1) \exp\{-(|t' - t''| - t_1)/T_{1\rho}\}. \quad (4.78)$$

Roughly speaking, equation (4.78) expresses the idea that in comparing  $I_x$  at times  $t''$  and  $t'$  within the rotating frame, we average over a set of hypothetical, idealized measurements, and for each measurement, the following sequence of events occurs: 1)  $I_x$  is sampled at time  $t''$ , 2) Fluctuations in  $I_x$  occur during the spin-locking which lasts from  $t = t''$  to  $t = 0$ , 3) A rotation of the spin system is performed which replaces  $I_x(0)$  with  $I_x(0) \cos \omega t_1 - I_y(0) \sin \omega t_1$  as the spin component along the  $x$ -axis, 4) Fluctuations in this spin component occur during the spin-locking which lasts from  $t_1$  to  $t'$ , and 5)  $I_x$  is once again sampled. Our unpolarized system has  $\langle I_x I_y \rangle = 0$ , and so the transverse dipole  $-I_y(0) \sin \omega t_1$  directed along the  $x$ -axis at time  $t_1$  makes no contribution to the average of these hypothetical measurements, while the effect of the fluctuations occurring during a period of length  $(|t' - t''| - t_1)$  is exponential decay with time constant  $T_{1\rho}$ . To obtain the lab-frame correlation functions from (4.78), we once again assume that components of the sample dipole which are not

spin-locked may be neglected, and we write

$$C_I(t', t'') = \langle I_x^2 \rangle \cos(\omega t_1) \exp\{-(|t' - t''| - t_1)/T_{1\rho}\} \cos(\omega_h(t' - t_1)) \cos(\omega_h t''). \quad (4.79)$$

Note that when  $t' < 0$  and  $t'' > t_1$ , we similarly obtain

$$C_I(t', t'') = \langle I_x^2 \rangle \cos(\omega t_1) \exp\{-(|t' - t''| - t_1)/T_{1\rho}\} \cos(\omega_h t') \cos(\omega_h(t'' - t_1)). \quad (4.80)$$

Examination of (4.76), (4.77), (4.79), and (4.80) shows that only in the case where  $t'$  and  $t''$  lie on opposite sides of the time interval  $0 < t < t_1$  does our approximate expression for  $m(t', t'')$  contain information about the precession frequency  $\omega$  of the spins. In searching for an optimal method of estimating  $m(t_1, 0)$ , we may therefore simplify the analysis by considering  $m$  to be zero in regions where  $t', t''$  are both less than 0 or both greater than  $t_1$ . Making the assumption that  $t_1 \ll T_{1\rho}$ , we drop  $t_1$  from the exponential factor appearing in (4.79) and (4.80), and we further simplify notation by redefining  $m(t', t'')$  as

$$m(t', t'') = \begin{cases} \langle T(t') T(t'' + t_1) \rangle & (t', t'') \text{ in quadrant II} \\ \langle T(t' + t_1) T(t'') \rangle & (t', t'') \text{ in quadrant IV} \\ 0 & \text{otherwise} \end{cases}$$

That is, at points where the correlation function contains spectroscopic information, we define  $m$  as if the time period governed by the evolution operator  $U$  had length zero, which is a natural choice of notation within a model which neglects spin fluctuations during this time period. Our approximate expression for  $m(t', t'')$  then becomes

$$m(t', t'') = \left( \gamma \hbar \frac{dB_x}{d\theta} \right)^2 \langle I_x^2 \rangle \cos(\omega t_1) \exp(-|t' - t''|/T_{1\rho}) \cos(\omega_h t') \cos(\omega_h t'')$$

at all points  $(t', t'')$  lying in quadrant II or quadrant IV of the plane. The estimate

$f(t', t'')$  of the useful signal is also redefined so that

$$f(t', t'') = m(t', t'') + n(t', t'') \quad (4.81)$$

for all points  $(t', t'')$  in the plane, including points at which  $m(t', t'') = 0$ .

The information which we wish to extract from a single shot of a CONQUEST experiment is an estimate of

$$G_1 \equiv \left( \gamma \hbar \frac{dB_x}{d\theta} \right)^2 \langle I_x^2 \rangle \cos(\omega t_1). \quad (4.82)$$

Our simplified notation for  $m(t', t'')$  allows us to define  $m_0(t', t'')$  by the equation

$$m(t', t'') = G_1 m_0(t', t'').$$

The analysis used to find the optimal linear filter for transverse BOOMERANG can be carried over without substantial modification to show that the optimal estimate of  $G_1$  is given by

$$X = \frac{\int_{-\infty}^{\infty} \int_{-\infty}^{\infty} f(t', t'') m_0(t', t'') dt' dt''}{\int_{-\infty}^{\infty} \int_{-\infty}^{\infty} m_0^2(t', t'') dt' dt''} \quad (4.83)$$

if the noise is white.

The noise in the function  $f(t', t'') = g(t')g(t'')$  will include contributions from the products  $T(t')T(t'')$  of spin torques, the products  $N_{\text{inst}}(t')N_{\text{inst}}(t'')$  of torques associated with instrument noise, and the products  $T(t')N_{\text{inst}}(t'')$  and  $N_{\text{inst}}(t'')T(t')$  of one spin torque and one torque associated with instrument noise. We shall assume that the dominant noise source contributing to  $g(t')g(t'')$  comes from the product  $N_{\text{inst}}(t')N_{\text{inst}}(t'')$ . This would occur for a problem in which

$$\int_{-\infty}^{\infty} \int_{-\infty}^{\infty} T(t')T(t'')m_0(t', t'') dt' dt''$$

and

$$\int_{-\infty}^{\infty} \int_{-\infty}^{\infty} T(t')N_{\text{inst}}(t'')m_0(t', t'') dt' dt''$$

are substantially smaller than

$$\int_{-\infty}^{\infty} \int_{-\infty}^{\infty} N_{\text{inst}}(t') N_{\text{inst}}(t'') m_0(t', t'') dt' dt'',$$

that is, a problem in which the products  $T(t')T(t'')$  and  $T(t')N_{\text{inst}}(t'')$  have much smaller components in the relevant frequency domain than  $N_{\text{inst}}(t')N_{\text{inst}}(t'')$ . An example of such a problem would be the two-spin system of section 1.2 of chapter 6, with the spectrum detected by the example resonator of table 5.3 and the noise temperature  $T_N = 18T_{QL}$ . A more general SNR expression could be obtained by estimating the spectral densities of the noise contributions due to the products  $T(t')T(t'')$  and  $T(t')N_{\text{inst}}(t'')$ .

The instrument noise characterized by equation (4.42) is flat within the spectral range of interest, and so the instrument noise at distinct sampled times  $t' \neq t''$  can be considered independent. The unfiltered noise  $n(t', t'')$  can therefore be approximated as the product of two normally distributed random variables, denoted by  $n_{\text{inst}}(t')$  and  $n_{\text{inst}}(t'')$ :

$$n(t', t'') = n_{\text{inst}}(t') n_{\text{inst}}(t'').$$

The correlation function  $C_n$  of the noise is defined as

$$\begin{aligned} C_n(t'_1, t''_1, t'_2, t''_2) &= \langle n(t'_1, t''_1) n(t'_2, t''_2) \rangle \\ &= \langle n_{\text{inst}}(t'_1) n_{\text{inst}}(t''_1) n_{\text{inst}}(t'_2) n_{\text{inst}}(t''_2) \rangle. \end{aligned}$$

Note that the four random variables  $n_{\text{inst}}(t'_j)$ ,  $n_{\text{inst}}(t''_j)$  may be considered independent, since we are not concerned with the small subset of sampled points at which two or more of the times are identical. We thus have

$$\begin{aligned} C_n(t'_1, t''_1, t'_2, t''_2) &= \langle n_{\text{inst}}(t'_1) n_{\text{inst}}(t'_2) \rangle \langle n_{\text{inst}}(t''_1) n_{\text{inst}}(t''_2) \rangle \\ &= C_{\text{inst}}(t'_2 - t'_1) C_{\text{inst}}(t''_2 - t''_1), \end{aligned}$$

where  $C_{\text{inst}}(t)$  is the correlation function of the instrument noise  $n_{\text{inst}}(t)$ . We can

thus write  $C_n$  as a function of two variables:

$$C_n(t', t'') = C_{\text{inst}}(t') C_{\text{inst}}(t'').$$

The double-sided spectral density  $S_n(\omega', \omega'')$  of  $n$  is

$$S_n(\omega', \omega'') = S_{\text{inst}}(\omega') S_{\text{inst}}(\omega''),$$

where  $S_{\text{inst}}(\omega)$  is given by equation (4.42).

The variance introduced into the estimate  $X$  by instrument noise is

$$\sigma_{\text{inst}}^2 = \frac{(S_{\text{inst}}(\omega_h))^2}{\int_{-\infty}^{\infty} \int_{-\infty}^{\infty} m_0^2(t', t'') dt' dt''}. \quad (4.84)$$

Note that noise at points  $(t', t'')$  lying in the first and third quadrants makes no contribution to the estimate  $X$ , since  $m_0$  is zero in these regions. Since

$$\int_{-\infty}^{\infty} \int_{-\infty}^{\infty} m_0^2(t', t'') dt' dt'' \approx \frac{T_{1\rho}^2}{16},$$

we have

$$\sigma_{\text{inst}}^2 = \left( \frac{4S_{\text{inst}}(\omega_h)}{T_{1\rho}} \right)^2. \quad (4.85)$$

It follows from equations (4.82) and (4.85) that the SNR is

$$\begin{aligned} SNR_{\text{CONQUEST}} &= \frac{(\gamma \hbar dB_x/d\theta)^2 \langle I_x^2 \rangle \cos(\omega t_1)}{(4S_{\text{inst}}(\omega_h)/T_{1\rho})} \\ &= N \left( \frac{\gamma \hbar dB_x}{2 d\theta} \right)^2 \frac{1}{4S_{\text{inst}}/T_{1\rho}}. \end{aligned} \quad (4.86)$$

### 8.3 Comparison of the first-order and second-order methods

In comparing the sensitivity of the "first-order" method which measures a single value of  $\langle I_x(t_1) \rangle$  and the "second-order" method which measures  $\langle I_x(t_1) I_x(0) \rangle$ , we consider detection at a single point  $t_1$  for which  $\cos(\omega t_1) = 1$ . If spin-locking is used to detect

$\langle I_x(t_1) \rangle$ , the results of section 4.5 imply that the single-shot SNR is

$$SNR_{\text{BOOM}} = PN \frac{\gamma \hbar dB_x}{2 d\theta} \sqrt{\frac{1}{4S_{\text{inst}}/T_{1\rho}}}, \quad (4.87)$$

where the subscript "BOOM" highlights the fact that this method of measuring an NMR spectrum is a version of the BOOMERANG scheme for force-detected spectroscopy in the absence of field gradients [13]. Comparison of (4.86) and (4.87) shows that for a sample consisting of a single spin with polarization  $P = 1$ , we have

$$SNR_{\text{CONQUEST}} = (SNR_{\text{BOOM}})^2.$$

In this case, the contribution of instrument noise to the measurement of  $\langle I_x(t_1) I_x(0) \rangle$  equals the product of the instrument noise for independent measurements of  $\langle I_x(t_1) \rangle$  and  $\langle I_x(0) \rangle$ .

More generally, we have

$$\begin{aligned} SNR_{\text{CONQUEST}} &= \frac{1}{P^2 N} (SNR_{\text{BOOM}})^2 \\ &= \left( \frac{SNR_{\text{BOOM}}}{P^2 N} \right) SNR_{\text{BOOM}} \end{aligned} \quad (4.88)$$

if instrument noise is dominant. Equation (4.88) may be considered a generalization of the result that when spin noise is dominant [13],

$$\begin{aligned} SNR_{\text{BOOM}} &= P\sqrt{N}, \\ SNR_{\text{CONQUEST}} &= \frac{1}{\sqrt{1 + (1 - 2/N)}} \\ &\approx 1, \end{aligned}$$

since (4.88) holds in this case as well. When (4.88) holds, e.g., when either the spin noise or instrument noise can be neglected, the second-order method is more sensitive

than the first-order method provided that

$$SNR_{\text{BOOM}} \geq P^2 N. \quad (4.89)$$

When instrument noise is dominant, (4.89) can be expressed as

$$\frac{\gamma \hbar dB_x}{2 d\theta} \sqrt{\frac{1}{4S_{\text{inst}}/T_{1\rho}}} \geq P. \quad (4.90)$$

Equation (4.90) implies that the second-order method is preferred if the sample polarization  $P$  is less than the single-shot SNR for detecting a single spin which is aligned along the  $x$ -axis at the beginning of the detection period.

# Chapter 5

## Resonator design

### 1 Description of the resonator and the detection scheme

Figure 5.1 shows a resonator that we propose to use for NMR study of nanoscale samples. The design has a spin sample placed between magnetic cylinders, with the sample enclosed by a silicon "paddle" which separates the two cylinders. Torsional motion of the beam causes the magnetic "sandwich" to rotate, and a transverse field at right angles to the beam develops as a result of the rotation. Since the sample rotates with the sandwich, there is no relative motion between the spins and the magnetic cylinders. The field at the spins changes as the resonator moves, however, and so the spins are coupled to the mechanical coordinate.

The mechanical resonator can be used to polarize spins and detect their spectrum at low temperatures. Between transients, the resonator induces longitudinal spin relaxation. At mK temperatures, the spin-lattice interactions which restore the spins to thermal equilibrium between transients become "frozen out," and the time constant  $T_1$  for relaxation to equilibrium increases by orders of magnitude over the room temperature value. Slow relaxation of the spins to thermal equilibrium translates to a pathologically long delay between transients, which makes acquisition of many transients impractical. Resonator-induced longitudinal relaxation replaces spin-lattice relaxation as a means of restoring the spin system to equilibrium between

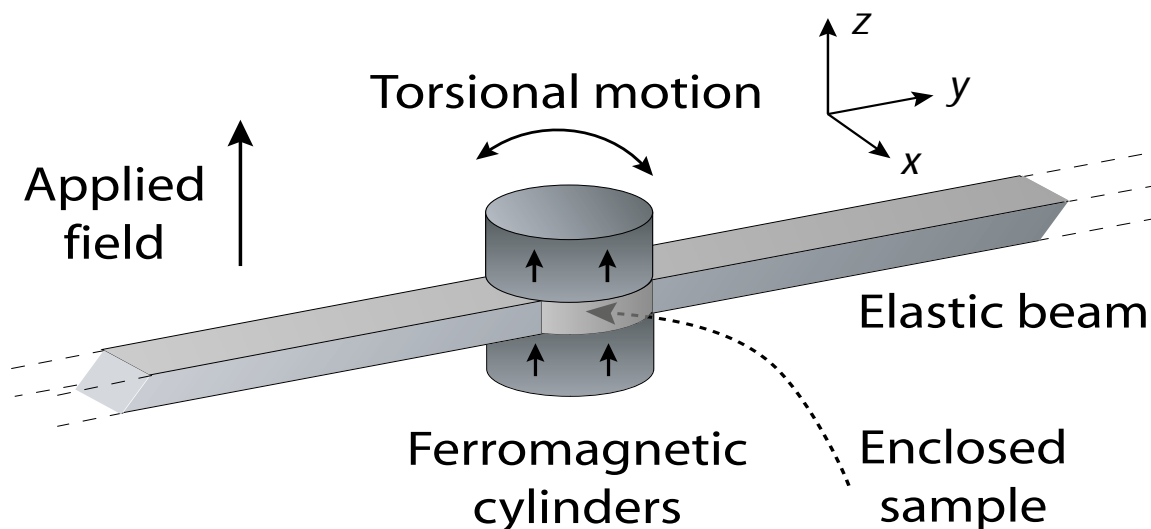


Figure 5.1: Torsional resonator for force-detected NMR spectroscopy. The sample is “sandwiched” between ferromagnetic cylinders, and it rotates with the sandwich about the axis of the torsional beam. The transverse spin dipole couples to the mechanical coordinate through the oscillating transverse field generated by the rotating sandwich.

transients.

In addition to inducing longitudinal relaxation, the resonator can be used to detect the NMR spectrum. The BOOMERANG scheme for force-detected NMR spectroscopy [2, 13, 21, 22] detects a single point of the free-induction decay for each measured transient. In this scheme, a conventional NMR pulse sequence is applied to the spins, and the spins then precess freely for a period of time without being coupled to the resonator. At time  $t_1$  during the FID, a component  $\langle I_x(t_1) \rangle$  of the sample’s transverse spin is measured by using this component to drive the mechanical resonator. For the resonator shown in figure 5.1, this scheme could be realized by moving the Larmor frequency out of resonance with the mechanical frequency during the NMR pulse sequence and the period of free spin precession, and then performing a  $\pi/2$  pulse to store  $\langle I_x(t_1) \rangle$  along  $z$  while the Larmor frequency is brought back into resonance with the mechanical frequency. An additional  $\pi/2$  pulse returns  $\langle I_x(t_1) \rangle$  to the transverse plane, at which point it is spin-locked. The spin-locked transverse dipole exerts a driving force on the mechanical resonator, and the resulting mechan-

ical motion is detected. Analysis of the mechanical motion yields a measurement of  $\langle I_x(t_1) \rangle$ . By repeating the measurement for a range of values  $t_1$ , a record of the spins' time evolution is obtained, and Fourier analysis yields an NMR spectrum.

This measurement scheme extracts information by analyzing the mechanical response to torques exerted by the spin sample. It is therefore essential that the applied radiofrequency (RF) field not drive the resonator during the spin-locking. This goal can be achieved by applying the RF in pulses along the length of the torsion beam. A magnetic field directed along the length of the beam does not drive the torsional motion, so an ideal applied field would drive only the spins without imparting motion to the resonator. If imperfections in the fabricated structures cause the resonator to be driven by the applied RF, the mechanical response to the spins can be separated from the mechanical response to the applied RF by applying the spin-locking field in pulses. Between pulses, excitation which has been imparted to the resonator by the applied field will decay quickly on the time scale required for decay of the precessing transverse spin dipole. After the excitation due to the applied field has decayed, the mechanical motion observed up to the beginning of the next RF pulse will be due to driving by the spins. (Pulsed spin-locking of a solid sample is discussed in reference [26].)

Detection of the torsional motion might be accomplished by means of a single-electron transistor (SET). A scheme for SET detection of translational mechanical motion has been demonstrated experimentally at a level of sensitivity near the quantum limit [25]. Mechanical motion changes the state of the SET by modulating the gate capacitance. This scheme might be adapted for the detection of torsional motion by capacitively coupling electrodes to the magnetic sandwich, with the coupling designed in such a way that the capacitance is modulated by the mechanical motion.

The resonator design shown in figure 5.1 can be modified for purposes of magnetic resonance imaging. Figure 5.2 shows a resonator design which is appropriate for imaging a small sample. The sample is placed a hole in the silicon paddle, and the gradient created by the magnetic cylinder selects a resonant section of the sample for imaging. Scanning the applied field shifts the position of the resonant section being

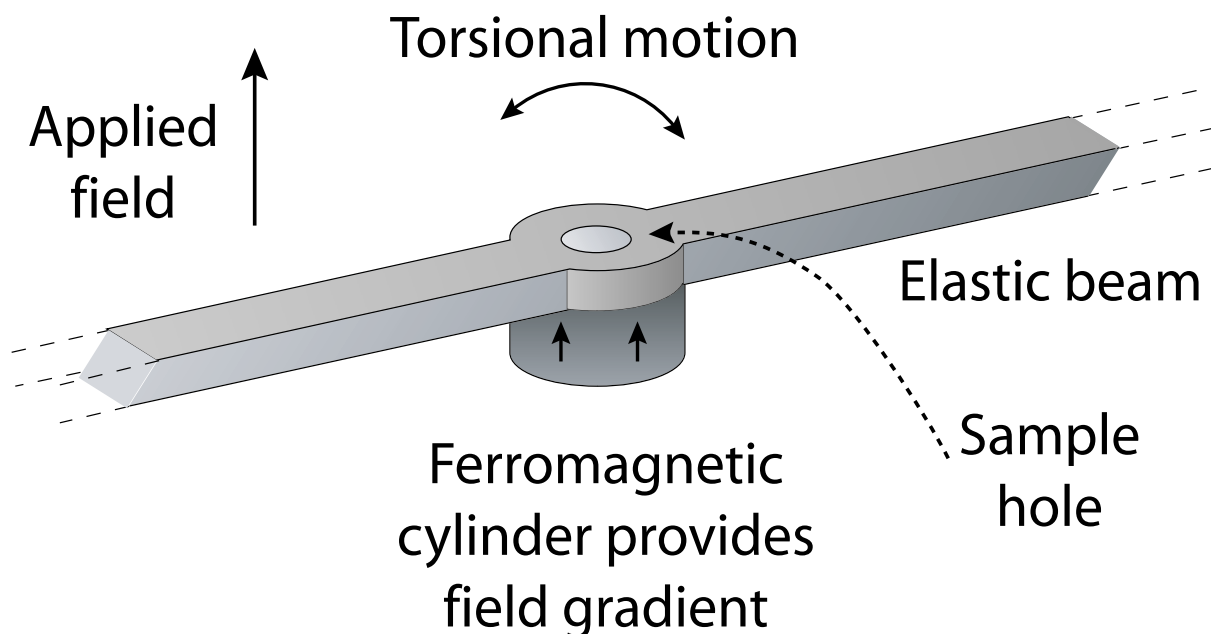


Figure 5.2: Torsional resonator for force-detected NMR imaging. The cylinder creates a field gradient which selects a resonant slice of the sample for imaging, and the transverse spin dipole couples to the mechanical coordinate through the oscillating transverse field generated by the moving cylinder.

detected and allows imaging of the sample.

## 2 Selection of the resonator design

The resonator design shown in figure 5.1 was selected after alternative designs were considered. Three types of mechanical motion were considered: 1) Radial motion of a magnet along a line connecting the magnet to the spins, 2) Horizontal motion of a magnet placed above the spins, and 3) Rotation of a hollow magnet or an array of magnets around an axis passing through the spins. The figure of merit used to compare different designs was the magnitude of the coupling constant  $g$  defined by equation (2.9). Since the rate constant for longitudinal relaxation of a single spin is

$$R_h = 2g^2\tau_h(n_{\text{th}} + 1)$$

$$\propto g^2,$$

the magnitude of  $g$  characterizes the efficiency with which a particular form of mechanical motion can cool spins. We found that the cooling efficiency of these three types of motion was similar, with the magnitude of  $g$  varying by a factor of order unity between resonator designs.

The choice to use a torsional resonator was motivated by the fact that spins can be coupled to torsional mechanical motion without the need for relative motion between the sample and nearby magnets. Surface friction between nearby moving parts can decrease cooling efficiency as well as detection sensitivity, since damping decreases the magnitude of the mechanical response to forces or torques exerted by the spins. Relative motion between the sample and nearby moving parts is unavoidable if the mechanical motion is translational, but it can be eliminated by the use of a torsional resonator. This can be seen by noting first that the spins drive the resonator only if mechanical motion modulates the interaction between the spins and moving magnets. If both the sample and the magnets move in unison along a straight line, with no relative motion occurring between sample and magnets, the spin-magnet interactions are not modulated by the motion. By way of contrast, consider an idealized example in which an array of magnets creates a uniform field at the spin sample. If both the magnets and the sample are rotated together, with no relative motion occurring between sample and magnets, the spins experience a rotating field, and the interaction between the spin degrees of freedom and the magnet array is modulated as the array rotates. Use of a torsional resonator therefore eliminates the need for relative motion between the sample and nearby moving magnets.

Two types of torsional resonators were considered. In addition to the design shown in figure 5.1, we studied a design in which the sample is placed at the center of a short magnetic tube, with the axis of the tube aligned with the applied field. The tube's axis rotates out of alignment with the applied field as the resonator moves out of equilibrium position. The design of figure 5.1 was selected instead in order to create a more homogeneous field at the spins.

Our initial estimates of  $g$  were based on a simplified model in which the ferromagnetization of the resonator rotates with the resonator itself, regardless of the

magnitude of the static applied field. Calculations of  $g$  based on this model suggested that for the size scale at which efficient cooling might be achieved, nanoscale mechanical resonators would have frequencies corresponding to the Larmor frequency of hydrogen in a large applied field. Since a large applied field would tend to keep the ferromagnetization aligned with the applied field rather than rotating with the resonator, the simplified model we were using was of doubtful validity in the regime of interest, and we considered instead a model in which the magnetization remains continually aligned with the applied field as the resonator moves. As discussed in section 5.1, we found that the strength of the spin-resonator coupling was increased by the switch from a model which assumed infinitely hard magnetic materials to a model which assumed soft magnetic materials. Section 4 discusses the validity of our assumption that the magnetization remains aligned with the applied field as the resonator moves.

### 3 Condition for resonance between the spins and the resonator

Efficient energy transfer from spin to resonator can only occur if the precession frequency of the spins is resonant with the mechanical frequency. In deriving the interaction Hamiltonian in section 1 of chapter 2, the resonance condition was expressed as

$$\omega_0 = -\omega_h, \tag{5.1}$$

since  $\omega_h$  is positive by definition, and since

$$\omega_0 = -\gamma B_z$$

is negative in the common case where  $\mathbf{B}$  is parallel to the positive  $z$ -axis yields and  $\gamma$  is positive. Note, however, that the sign of  $-\gamma B_z$  depends on the choice of coordinate axes; if the coordinate axes are rotated so that the  $z$ -axis is directed opposite  $\mathbf{B}$ , the

sign of  $-\gamma B_z$  changes, while the physical resonance between spins and mechanical oscillator is unchanged. It follows that the resonance condition could be written as

$$\omega_0 = \pm\omega_h, \quad (5.2)$$

with the sign determined by the choice of reference frames rather than by the physical nature of the problem.

In designing a device for which spin precession is resonant with mechanical motion, we express (5.2) as

$$\omega_0^2 = \omega_h^2, \quad (5.3)$$

or equivalently

$$\gamma^2 B_z^2 = \frac{k_h}{I_h}, \quad (5.4)$$

where  $k_h$  and  $I_h$  are the respective spring constant and moment of inertia. If the mechanical energy and the energy of the electromagnetic field energy both vary as the resonator moves, then the  $k_h$  and  $I_h$  will each include a contribution associated with the electromagnetic field as well as a contribution associated with the mechanical motion. Appendix J shows by means of a numerical example that the contribution to  $I_h$  associated with the electromagnetic field is negligible. An expression for the electromagnetic contribution to  $k_h$  is derived in Appendix K. This contribution is determined by the dependence of magnetostatic energy  $U_{\text{mag}}$  on the resonator's coordinate, where

$$U_{\text{mag}} = -\boldsymbol{\mu} \cdot \mathbf{B}_a - \frac{1}{2} \int \mathbf{M} \cdot \mathbf{B}_h d^3x. \quad (5.5)$$

In (5.5),  $\mathbf{B}_a$  is the applied field,  $\mathbf{B}_h$  is the resonator's magnetic field, and  $\mathbf{M}$ ,  $\boldsymbol{\mu}$  are its respective magnetization and dipole moment. The magnetic spring constant  $k_{\text{mag}}$  is given by

$$k_{\text{mag}} = \frac{d^2 U_{\text{mag}}}{d\theta^2}. \quad (5.6)$$

In general, both terms on the right side of (5.5) can contribute to  $k_{\text{mag}}$ , but simplifications are possible in two limiting cases. For a sufficiently hard magnetic

material or a sufficiently weak applied field,  $\mathbf{M}$  remains constant within a reference frame fixed in the resonator. In this case, the second term on the right side of (5.5) does not depend on the resonator coordinate  $\theta$  and may be dropped for purposes of finding  $k_{\text{mag}}$ . If the applied field lies along the positive or negative  $z$ -axis and the dependence of  $\mu_z$  on  $\theta$  is given by

$$\mu_z(\theta) = \mu_z \cos \theta,$$

equation (5.6) becomes

$$k_{\text{mag}} = \mu_z B_{a,z}. \quad (5.7)$$

In the opposite limit, the applied field is sufficiently large that  $\mu$  remains aligned with  $\mathbf{B}_a$  as the resonator moves, and it is the second term of (5.5) which determines  $k_{\text{mag}}$ , since  $\mu \cdot \mathbf{B}_a$  is constant. In this limit,  $k_{\text{mag}}$  is a constant which does not depend on the exact value of  $B_a$ :

$$k_{\text{mag}} = \frac{d^2}{d\theta^2} \left\{ -\frac{1}{2} \int \mathbf{M} \cdot \mathbf{B}_h d^3x \right\}. \quad (5.8)$$

The resonance condition (5.4) can be written in the form

$$\gamma^2 |\mathbf{B}_a + \mathbf{B}_h|^2 = \frac{k_{\text{beam}} + k_{\text{mag}}}{I_h}, \quad (5.9)$$

where  $k_{\text{beam}}$  is the spring constant of the elastic suspension. The applied field may be considered the variable determined by the solution of this equation. In evaluating resonator designs, we used (5.7) or (5.8) as the magnetic spring constant. Finite-element software (Maxwell 3D v11, Ansoft Corporation, Pittsburgh) was used to compute the magnetic spring constant given by (5.8).

In general, equation (5.9) has more than one solution. If the magnetic spring constant is given by (5.7), for instance, there are always two solutions to (5.9). In the examples we considered, one of the solutions corresponded to an applied field which was sufficiently large that protons at 10 mK would be highly polarized in the

field. We used this solution in our initial comparison of different resonator designs.

## 4 Model of the resonator's magnetization

The resonator was modelled as having uniform magnetization  $\mathbf{M}$  which remains continually aligned with the applied field  $\mathbf{B}_a$ . In this section we justify that approximation using analytic expressions for the demagnetizing field which is present within uniformly-magnetized spheroids of soft magnetic material. In keeping with our use of the notation  $\mathbf{B}_h$  for the resonator's field, we also will use  $\mathbf{B}_h$  to denote the field of a given spheroid.

### 4.1 Uniform magnetization

The field  $\mathbf{B}_h$  within a uniformly-magnetized spheroid is itself uniform and is given by [27]

$$\mathbf{B}_h = -\mu_0 (N_a M_x, N_a M_y, N_c M_z) + \mu_0 \mathbf{M}. \quad (5.10)$$

Here the  $x$ -axis,  $y$ -axis, and  $z$ -axis coincide with the spheroid axes of length  $a$ ,  $a$ , and  $c$ , respectively, and  $N_a$ ,  $N_c$  are constants which depend only on the ratio  $r = c/a$  [27]. In the limiting case where  $r \rightarrow 0$  (thin disc), we have

$$N_a \rightarrow 0,$$

$$N_c \rightarrow 1,$$

while in the case  $r \rightarrow \infty$  (long rod), we have

$$N_a \rightarrow 1/2,$$

$$N_c \rightarrow 0.$$

Equation (5.5) gives the magnetostatic energy  $U_{\text{mag}}$  of the spheroid:

$$U_{\text{mag}} = -\boldsymbol{\mu} \cdot \mathbf{B}_a - \frac{1}{2} \int \mathbf{M} \cdot \mathbf{B}_h d^3x.$$

Consider the problem of finding the shape which minimizes the magnetostatic energy of a spheroid of a given volume and magnetization in the absence of an applied field. From (5.10), we have

$$U_{\text{mag}} = -\frac{1}{2}\mu_0 \int \mathbf{M} \cdot \mathbf{M} d^3x + \frac{1}{2}\mu_0 \int (N_a M_x^2 + N_a M_y^2 + N_c M_z^2) d^3x,$$

and since the constants  $N_a, N_c$  are nonnegative,

$$U_{\text{mag}} \geq -\frac{1}{2}\mu_0 \int \mathbf{M} \cdot \mathbf{M} d^3x.$$

The minimum magnetostatic energy

$$U_{\text{min}} = -\frac{1}{2}\mu_0 \int \mathbf{M} \cdot \mathbf{M} d^3x$$

is achieved, for instance, in the limiting case of a arbitrarily long, thin rod, with  $\mathbf{M}$  lying along the axis of the rod. We can use  $U_{\text{min}}$  as an estimate of the minimum magnetostatic energy which can be achieved by a given volume of magnetization  $\mathbf{M}$ . The term  $-\mu_0 (N_a M_x, N_a M_y, N_c M_z)$  appearing in (5.10) can be considered a "demagnetizing field," since it raises the energy of a uniformly-magnetized structure above  $U_{\text{min}}$  and introduces the possibility that the low-energy configuration of  $\mathbf{M}$  may be nonuniform.

The field required to saturate a magnet to a state of uniform magnetization is often characterized in terms of the demagnetizing field which exists within the magnet [27]. If the magnetization is nonuniform due to demagnetizing fields within the magnet, application of an external field stronger than the demagnetizing fields is expected to saturate the magnet [27]. Since the demagnetizing field within the ferromagnetic

cylinders of the mechanical resonator is at most of order

$$\mu_0 M \leq 2 \text{ T},$$

it is reasonable to model the mechanical resonator's magnetization as uniform when the applied field is of order 10 T or more, as in the examples we have considered.

Even in the absence of an applied field, exchange interactions will produce uniform magnetization in a sufficiently small particle. Since exchange energy is increased when  $\mathbf{M}$  varies over small distances within a magnet, the exchange energy associated with variation in  $\mathbf{M}$  across a nanoscale magnet eventually becomes larger than the magnetostatic energy associated with uniform magnetization [28], with the result that the low-size limit for multidomain particles is in the range 20-800 nm [29]. Both the dimensions of the resonator's ferromagnetic cylinders and the magnitude of the applied field suggest that the magnetization should be modelled as uniform.

## 4.2 Magnetization constant in the lab frame

In addition to considering the resonator's magnetization to be uniform, we model it as remaining continually aligned with the applied field. The error associated with this simplifying assumption can be estimated by using equations (5.10) and (5.5) to estimate the angle by which  $\mathbf{M}$  would rotate away from  $\mathbf{B}_a$  during the mechanical motion. As in section 4.1, we consider a uniformly magnetized spheroid for which the  $x$ -axis,  $y$ -axis, and  $z$ -axis coincide with the spheroid axes of length  $a$ ,  $a$ , and  $c$ . The applied field  $\mathbf{B}_a$  lies in the  $xz$ -plane at an angle  $\theta$  from the  $z$ -axis. Let  $\phi$  denote the angle between  $\mathbf{M}$  and the  $z$ -axis when  $\mathbf{M}$  is oriented so as to minimize magnetostatic energy. We wish to derive an expression for  $\phi(\theta)$ , the angle by which the magnetization rotates away from the spheroid  $z$ -axis when the applied field is rotated through angle  $\theta$ .

We can find  $\phi$  by minimizing the energy  $U_{\text{mag}}$  given by equation (5.10), or equiv-

alently, by minimizing  $U_{\text{mag}}/V$ , where  $V$  is the volume of the spheroid:

$$\frac{U_{\text{mag}}}{V} = -\mathbf{M} \cdot \mathbf{B}_a - \frac{1}{2}\mathbf{M} \cdot \mathbf{B}_h.$$

Since the demagnetizing  $H$ -field is given by

$$\begin{aligned} \mathbf{H}_d &= -(N_a M_x, 0, N_c M_z) \\ &= -(N_a M \sin \phi, 0, N_c M \cos \phi), \end{aligned}$$

we have

$$\mathbf{B}_h = \mu_0 M ((1 - N_a) \sin \phi, 0, (1 - N_c) \cos \phi)$$

and

$$-\frac{1}{2}\mathbf{M} \cdot \mathbf{B}_h = \frac{1}{2}\mu_0 M^2 [(N_a - N_c) \sin^2 \phi + (N_c - 1)].$$

The angle between  $\mathbf{M}$  and  $\mathbf{B}_a$  has magnitude  $|\theta - \phi|$ , and so

$$\mathbf{M} \cdot \mathbf{B}_a = M B_a \cos(\theta - \phi).$$

Dropping from the expression for  $E/V$  any terms which do not vary with  $\phi$ , we obtain

$$U_{\text{mag}}/V = \frac{1}{2}\mu_0 M^2 (N_a - N_c) \sin^2 \phi - M B_a \cos(\theta - \phi).$$

Making the definition

$$K_u \equiv \frac{1}{2}\mu_0 M^2 (N_a - N_c)$$

allows us to write the energy density as

$$U_{\text{mag}}/V = K_u \sin^2 \phi - M B_a \cos(\theta - \phi). \quad (5.11)$$

Stationary points occur when

$$0 = \frac{\partial}{\partial \phi} (U_{\text{mag}}/V) = 2K_u \sin \phi \cos \phi - M B_a \sin(\theta - \phi). \quad (5.12)$$

We can consider the equation

$$2K_u \sin \phi \cos \phi = MB_a \sin(\theta - \phi)$$

to define  $\phi(\theta)$ , and implicit differentiation can be used to derive a series expression for  $\phi(\theta)$ . Defining

$$A = \frac{2K_u}{MB_a},$$

we find that the first and second derivatives of  $\phi$  evaluated at  $\theta = 0$  are

$$\begin{aligned} \phi'(0) &= \frac{1}{A+1}, \\ \phi''(0) &= 0. \end{aligned} \tag{5.13}$$

The second order Taylor series for  $\phi(\theta)$  is

$$\phi(\theta) \approx \frac{\theta}{A+1}. \tag{5.14}$$

In the case where  $M = 2.3 \text{ T}/\mu_0$  and  $B_a = 15 \text{ T}$ , with the ratio of spheroid axes  $r = c/a$  of order 2, for instance, equation (5.14) predicts that  $\mathbf{M}$  rotates away from the applied field through an angle roughly 5% of the angle  $\theta$  between the spheroid and  $\mathbf{B}_a$ .

The calculations we have presented do not include dynamic effects: the magnet is held motionless in a static field, and the low-energy orientation of  $\mathbf{M}$  is found. In reality, the orientation of the applied field (as seen from a reference frame fixed in the magnet) will be changing at a frequency on the order of 500 MHz. However, simple estimates can be used to show that in this range of frequencies, the problem of finding the state of the magnetization can be treated as a static one. In investigating dynamic effects on the evolution of  $\mathbf{M}$ , we consider a lab frame which has the  $z$ -axis aligned with the field. Within this reference frame, each ferromagnetic dipole experiences a static applied field and a varying field due to the changing orientation of the resonator. A first correction to the model in which all fields are static can be

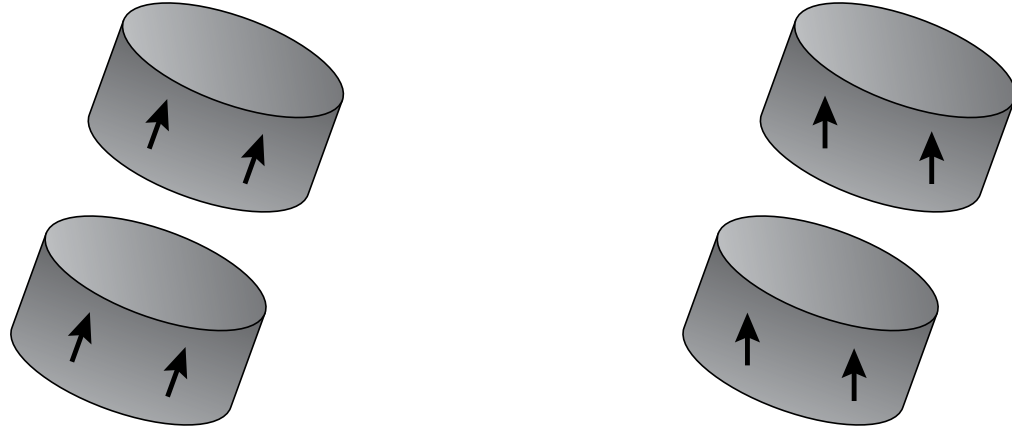
made by supposing that ferromagnetic dipoles experiences a static field along  $z$  and a transverse field oscillating at around 500 MHz. We can estimate the importance of dynamic effects by comparing the AC susceptibility of the particle at this frequency to the DC susceptibility. This model problem is equivalent to experiments done in studying ferromagnetic resonance (FMR), and results from the literature of this field show that the resonator's AC susceptibility at this frequency is very close to its DC susceptibility. Ferromagnetic resonance peaks occur in a higher range of frequencies than NMR peaks, due to the larger gyromagnetic ratio of the electron, and the linewidths observed in FMR experiments are typically only a small fraction of the resonance frequency [30]. Frequencies of  $\sim 500$  MHz are far enough from FMR resonance frequencies that the AC susceptibility of the resonator's ferromagnetic cylinders can be considered equal to the DC susceptibility in this frequency range.

## 5 Strength of the spin-resonator coupling

### 5.1 Effect of soft magnetic material on the coupling strength

Figure 5.3 shows the configuration of  $\mathbf{M}$  in the resonator's ferromagnetic cylinders when the "sandwich" shown in figure 5.1 has rotated through a substantial angle. The angle of rotation is highly exaggerated in order to highlight the difference between the configurations for hard and soft magnetic materials. Hard magnetization rotates with the cylinders, while soft magnetization remains aligned vertically with the field. Examination of this figure might initially suggest that the spin-resonator coupling, which is proportional to the transverse field linear in  $\theta$ , will be weak if soft magnetic materials are used, since it might appear that a larger transverse field will develop if the magnetization rotates with the cylinders.

Finite-element simulations have shown, however, that the soft oscillator in figure 5.3 has the larger transverse field. A rationalization for this result can be seen in figure 5.4. The magnetization in the soft magnetic material can be expressed as the sum of two components, one parallel to the cylinder axis and one perpendicular to



## Hard oscillator

## Soft oscillator

Figure 5.3: Comparison of magnetization orientation for hard and soft magnetic materials. The ferromagnetic cylinders are those of the oscillator in figure 5.1 after it has rotated through a substantial angle about its torsional axis. The orientation of the cylinder magnetization for hard and soft magnetic materials is shown.

it. The fields generated by these two components add constructively at the location of the spins. The field generated by each of the components can be rationalized by replacing each of the four cylinders on the right side of the figure by a single dipole which has the same orientation as the cylinder's magnetization. The field lines of these dipoles give a qualitative estimate of the contribution that each cylinder makes to the field at the center of the sandwich.

The ideas expressed in figure 5.4 can be demonstrated analytically if the cylinders in the figure are replaced by two identical spheroids (either prolate or oblate). Suppose that the sandwich has rotated through an angle  $\theta$  away from the vertical applied field  $\mathbf{B}_a$ . If the magnetization  $M$  remains aligned with  $\mathbf{B}_a$ , then we can consider the resonator field at the spins to be the superposition of two fields, one generated by magnetization  $M \cos \theta$  aligned along the sandwich axis, and the other generated by magnetization  $M \sin \theta$  aligned at right angles to the axis. Reference [31] gives analytic expressions for the fields external to uniformly magnetized ellipsoids, and it can be shown that that the magnetization aligned with the sandwich axis generates

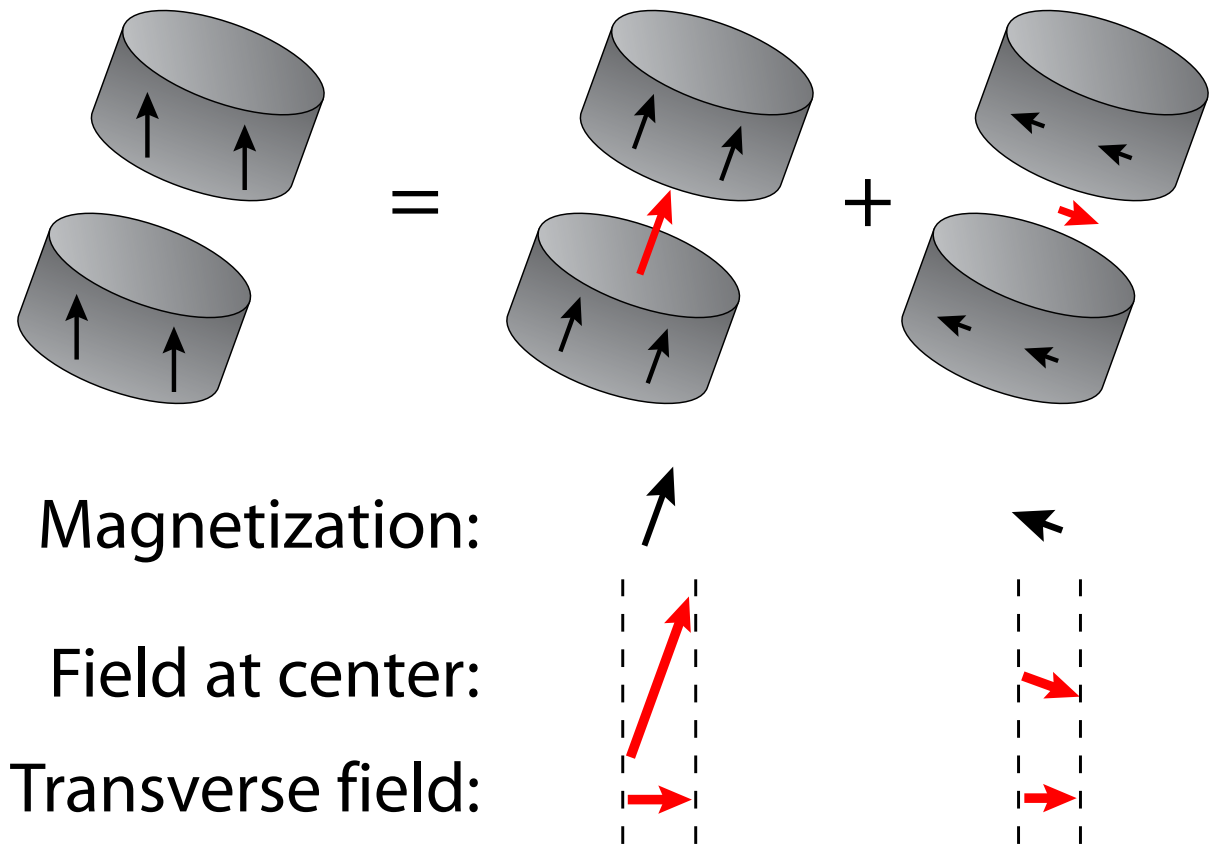


Figure 5.4: Comparison of the transverse field for hard and soft magnetic materials. The ferromagnetic cylinders are those of the oscillator in figure 5.1. In the case where the cylinders are composed of soft magnetic material, the transverse field which couples to the nuclear spins can be expressed as the sum of two components that add constructively. If the cylinders are composed of hard magnetic materials, only the first of these components is present. As a result, soft magnetic materials yield a strong coupling to the spins.

at the spins a field  $\mathbf{B}_1$  parallel to itself, while the magnetization at right angles to the resonator axis generates a field  $\mathbf{B}_2$  antiparallel to itself. Expressed in the unrotated Cartesian components of the lab frame, these two fields are

$$\begin{aligned}\mathbf{B}_1 &= B_h \cos \theta (\sin \theta, 0, \cos \theta), \\ \mathbf{B}_2 &= \frac{1}{2} \sin \theta (\cos \theta, 0, -\sin \theta).\end{aligned}$$

From these formulas we obtain

$$\frac{dB_x}{d\theta} = \frac{3B_h}{2} \cos 2\theta$$

and

$$\frac{d^2 B_z}{d\theta^2} = -3B_h \cos 2\theta.$$

Evaluating at  $\theta = 0$  gives

$$\frac{dB_x}{d\theta} = \frac{3B_h}{2}, \tag{5.15}$$

$$\frac{d^2 B_z}{d\theta^2} = -3B_h. \tag{5.16}$$

By way of contrast, a magnetically hard sandwich would have

$$B_x(\theta) = B_h \sin \theta,$$

$$B_z(\theta) = B_h \cos \theta,$$

as well as

$$\begin{aligned}\frac{dB_x}{d\theta} &= B_h, \\ \frac{d^2 B_z}{d\theta^2} &= -B_h\end{aligned}$$

at  $\theta = 0$ . We see that switching from an ideal magnetically hard resonator to an ideal magnetically soft resonator increases the magnitude of  $dB_x/d\theta$  by a factor of

$3/2$ , and the magnitude of  $d^2B_z/d\theta^2$  by a factor of 3. The factor of  $3/2$  in (5.15) is due to the fact that the contribution to  $dB_x/d\theta$  made by  $\mathbf{B}_2$  is half the size of the contribution made by  $\mathbf{B}_1$ .

The data from finite-element simulations is consistent with the hypothesis that (5.15) and (5.16) continue to be valid for the configuration of soft magnets shown in figure 5.3, which contains two cylinders rather than two spheroids. The finite-element software package Maxwell 3D v11 (Ansoft Corporation, Pittsburgh) was used to calculate  $B_x(\theta)$  and  $B_z(\theta)$  after rotating the sandwich axis away from the applied field up to  $5^\circ$  in steps of  $1^\circ$ , and curve-fitting was used to estimate  $dB_x/d\theta$  and  $d^2B_z/d\theta^2$ . These calculations were done for each sandwich geometry tested during the optimization described in section 6, and for geometries in which cylinders of diameter 100 nm and height 50 nm were separated by distances ranging from 5 nm to 50 nm. For each geometry that was simulated, the data points for  $B_x(\theta)$  lay essentially on a straight line, and the value of  $dB_x/d\theta$  obtained by curve fitting was within about 1% of the computed value of  $3B_h/2$ . Substantial random residuals were seen when quadratic curves were fitted to computed plots of  $B_z(\theta)$  in order to estimate  $d^2B_z/d\theta^2$ , which may be used to rationalize the fact that computed values of  $d^2B_z/d\theta^2$  differed from  $-3B_h$  by up to 15%. Adopting the hypothesis that (5.15) and (5.16) are valid for resonators of the type shown in figure 5.1 allows us to express the field  $\mathbf{B}(\theta)$  to second order in  $\theta$  as

$$\mathbf{B}(\theta) = \mathbf{B}_a + B_h \left( \frac{3}{2}\theta, 0, 1 - 3\theta^2 \right).$$

## 5.2 Upper bound on the torque between the spins and the resonator

Since detection sensitivity is enhanced if the torque acting between spins and resonator is increased, an estimated upper bound on the attainable torque per spin is helpful in evaluating resonator designs. A simple estimate can be made using the model introduced in section 5.1, which replaces the resonator's two cylinders with

spheroids. Since the strength of the spin-resonator torque is given by

$$G = \mu_x dB_x/d\theta,$$

it follows from equation (5.15) that largest possible torque will be obtained when  $dB_x/d\theta$  reaches its maximal value.

The formulas given in reference [31] can be used to express  $G$  in the form

$$G/\mu_x = \mu_0 MV K_{\text{geom}},$$

where  $V$  is the volume of the magnetic material, and  $K_{\text{geom}}$  depends on the shape of the spheroids as well as the distance between them. Given the constraints that  $M$  and  $V$  are fixed, and that a gap must exist between the two spheroids, the maximal value of  $G/\mu_x$  can be found by optimizing  $K_{\text{geom}}$ . We found that  $G/\mu_x$  achieves its maximal value in the limiting case where the spheroids become arbitrarily long and thin. The maximal value is independent of the volume of the spheroids and is given by

$$(G/\mu_x)_{\text{max}} = 3\mu_0 M. \quad (5.17)$$

For the example resonator presented in table 5.3 of section 6, the value of  $\mu_0 M$  is 2.3 T, and the limiting value of  $G/\mu_x$  is 7 T, which is larger by a factor of 4 than the value calculated for the resonator.

Note that when the spheroids are nearly touching, the dependence of  $G/\mu_x$  on shape anisotropy of the spheroids is weak. If the spheroids are prolate, and if the long axis of each is just twice the length of the short axes, for instance, the value of  $G/\mu_x$  is 83% of the limiting value given by (5.17) when the separation between spheroids is negligible. Even in the case where the shape anisotropy is zero and the resonator is composed of two spheres separated by a negligible gap, we have  $G/\mu_x$  equal to 67% of the upper limit.

## 6 Optimization of example resonators

Two different optimizations of the magnetic "sandwich" shown in figure 5.1 were performed. For the first optimization, the separation  $S$  between the ferromagnetic cylinders and the diameter  $D$  of the sandwich were constrained by

$$S \geq 50 \text{ nm}, \quad (5.18)$$

$$D \geq 100 \text{ nm}, \quad (5.19)$$

and for the second optimization,  $S$  and  $D$  were constrained by

$$S \geq 25 \text{ nm}, \quad (5.20)$$

$$D \geq 50 \text{ nm}. \quad (5.21)$$

Both optimizations had the same constraints on the width  $w$  and thickness  $t$  of the rectangular cross-section of the torsional beam:

$$w \geq 50 \text{ nm},$$

$$t \geq 50 \text{ nm},$$

and the silicon paddle separating the two ferromagnetic cylinders was constrained to have the same diameter as the cylinders. The resonator's ringdown time was fixed at  $\tau_h = 6 \mu\text{s}$  during the optimizations.

In characterizing the sensitivity associated with a particular choice of dimensions for the magnetic sandwich, the beam dimensions which maximize the SNR formula (4.50) were found, where the decay time of the spin-locked signal was fixed at 1 s. This optimization was performed before we had investigated the way in which resonator-induced relaxation affects the lifetime of a spin-locked signal. For all of the resonators we considered, the time-constant  $2/R_h$  for resonator-induced decay of the spin-locked signal was greater than 1 s. Our optimization can therefore be considered to incorporate an assumption that factors other than resonator-induced relaxation limit

the period of time during which spin-locking can be performed. Since (4.51) shows that SNR is independent of all resonator parameters other than  $\omega_h/T_h$  in an ideal spin-locking field, an alternative approach to designing the resonator would be to minimize acquisition time using expressions given in section 7 of chapter 4.

The optimal beam must have

$$w = t = 50 \text{ nm}.$$

This can be seen by noting that, given a resonator of frequency  $\omega_h$  and a beam with width or thickness greater than 50 nm, we could decrease the beam's moment of inertia without changing  $\omega_h$  by switching to a shorter beam that has a 50 nm  $\times$  50 nm cross-section; this decrease in the moment of inertia would increase the resonator's sensitivity. The optimization of beam dimensions for a given magnetic sandwich therefore involved varying the beam length  $l$  in steps of 100 nm to find the optimal frequency  $\omega_h$ . The applied field  $B_a$  was then chosen to satisfy the resonance condition determined by beam length.

In performing the optimizations, we assumed a sample consisting of a single spin 1/2. As a result, the instrument noise characterized by  $S_{\text{inst}}(\omega)$  was substantially larger than the spin noise. The optimal geometry of the magnetic sandwich was not sensitive to the changes in  $A_{\text{det}}$ . The same geometry was obtained when the motion detection was assumed to be quantum-limited or to have a noise temperature  $T_N = 18T_{QL}$ . (The quantum-limited noise temperature  $T_{QL}$  is discussed in section 4.3 of chapter 4.)

Sensitivity is in general optimal when the cylinders are as close together as possible. Decreasing the separation between the magnets improves SNR in two ways: 1) The resonator's moment of inertia is decreased, which decreases  $S_{\text{inst}}(\omega)$ , and 2) The field  $B_h$  at the center of the sandwich is increased, which increases the size of the torque acting between spins and resonator, since this torque is proportional to

$$\frac{dB_x}{d\theta} = \frac{3}{2}B_h. \quad (5.22)$$

Length $L$	Diameter $D$	Beam length	Single-shot SNR	$1/R_h$	$B_a$
35 nm	100 nm	1600 nm	0.109	3.6 s	14 T

Table 5.1: Selected parameters for a resonator optimized with a separation of 50 nm between magnetic cylinders.

Length $L$	Diameter $D$	Beam length	Single-shot SNR	$1/R_h$	$B_a$
40 nm	55 nm	2200 nm	0.236	0.91 s	20 T

Table 5.2: Selected parameters for a resonator optimized with a separation of 25 nm between magnetic cylinders.

(Equation (5.22) is explained in section 5.1.) It was this observation which motivated us to perform optimizations with different constraints on the separation  $S$ . The optimal designs associated with the different constraints (5.18) and (5.20) were found by varying the diameter  $D$  and the length  $L$  of each ferromagnetic cylinder in steps of 5 nm, while keeping the separation  $S$  between them fixed at the minimum value. The two dimensions  $D$  and  $L$  were varied until the SNR given by (4.50) reached its maximum value. For each choice of cylinder dimensions, the Maxwell 3D v11 software package (Ansoft Corporation, Pittsburgh) was used to calculate  $B_h$  and  $dB_x/d\theta$ . Magnetic spring constants were not calculated, since initial numerical tests found the magnetic spring constant to be negligible compared to the elastic spring constant.

Tables 5.1 and 5.2 show the results of the two optimizations. The values of single-shot SNR assume detection of a single spin which has been cooled by the resonator to a temperature of 10 mK. Quantum-limited motion detection is included in the estimate by setting

$$A_{\text{det}} = 1/2.$$

For each of these designs, SNR changes by less than 1% in response to a change of 5 nm in  $L$  or  $D$  within the constraints set by (5.18) through (5.21). Note that constraint (5.21) may be considered superfluous, since the optimal design in table 5.2 is not limited by this constraint.

A modified version of the resonator presented in table 5.2 will be used for numerical

examples. The applied field of 20 T can be reduced without significantly changing the resonator's sensitivity. We modified the design by lowering the applied field and simultaneously increasing the beam length until SNR has decreased by 5% from the optimal value given in table 5.2. This procedure yields an applied field of 14 T and a beam length of  $3.5 \mu\text{m}$  for the example resonator. Tables 5.3 and 5.4 give additional details regarding the resonator. In table 5.4, equation (4.50) is used to calculate the the SNR for detecting  $\langle I_x(t_1) \rangle$  at an instant when

$$\langle I_x(t_1) \rangle = \frac{PN}{2}.$$

In evaluating SNR, we use the assumption

$$T_{1\rho} = 1 \text{ s}$$

which defined the optimization. The alternative assumption that resonator-induced relaxation is responsible for decay of the spin-locked signal would yield

$$T_{1\rho} = 2/R_h = 1.5 \text{ s}.$$

Note that the entry " $N$  at spin-noise limit" in table 5.4 gives the number of spins  $N$  at which the spin noise equals the instrument noise. This number is a natural measure of the instrument noise associated with the resonator, since instrument noise becomes dominant as the number of spins is decreased below this number. Note as well that the volume  $4.4 \text{ nm}^3$  in table 5.3 represents a cylinder of diameter 2 nm and height 1.4 nm within which the field of the magnetic sandwich differs by no more than 25 kHz from the field  $B_h$  at the center of the sandwich. An ice sample filling this volume would contain  $\sim 300$  protons. Note that this sample is sufficiently small to satisfy the condition that guarantees that oscillatory energy exchange between spins and resonator will be suppressed. Since the number of thermal quanta  $n_{\text{th}} \ll 1$ , we

Magnet length $L$	40 nm
Magnet diameter $D$	55 nm
Separation $S$ between magnets	25 nm
Magnetization $\mathbf{M}$	$2.3 \text{ T} / \mu_0$
Magnet density	$7900 \text{ kg} / \text{m}^3$
Beam cross-section	$50 \text{ nm} \times 50 \text{ nm}$
Beam length	$3.5 \mu\text{m}$
Beam stiffness constant $C_{44}$	$7.96 \times 10^{10} \text{ N} / \text{m}^2$
Density of beam and paddle	$2.33 \times 10^3 \text{ kg} / \text{m}^3$
Sandwich moment of inertia	$2.1 \times 10^{-33} \text{ kg m}^2$
Beam moment of inertia	$4.2 \times 10^{-33} \text{ kg m}^2$
Frequency $\omega_h/2\pi$	628 MHz
Ringdown time $\tau_h$	$6.0 \mu\text{s}$
Quality factor	11,800
Applied field	13.6 T
Resonator field $B_h$	1.1 T
Transverse derivative $dB_x/d\theta$	1.6 T
Coupling constant $g$	$313 \text{ s}^{-1}$
Rate constant $1/R_h$	0.77 s
Sample polarization $P$	0.91
Volume where $ \Delta\omega  \leq 25 \text{ kHz}$	$4.4 \text{ nm}^3$
Resonator temperature $T_h$	10 mK
Thermal quanta $n_{\text{th}}$	0.05

Table 5.3: Parameters for the optimized example resonator.

	Quantum limited detection ( $T_N = T_{QL}$ )	$T_N = 18T_{QL}$
$SNR$ for a single spin	0.224	0.0602
$N$ when $SNR = 1$	6 spins	18 spins
$N$ at spin noise limit	7 spins	112 spins
$SNR$ at spin noise limit	1.2	4.8

Table 5.4: Sensitivity of the optimized example resonator.

can use (2.16) to verify that such oscillations are suppressed:

$$\begin{aligned}
 g\sqrt{N} &= (313 \text{ s}^{-1}) \sqrt{300} \\
 &\approx 5.4 \times 10^3 \text{ s}^{-1} \\
 &\ll 330 \times 10^3 \text{ s}^{-1} \\
 &= \frac{2}{\tau_h}.
 \end{aligned}$$

The frequency offset 25 kHz was chosen based on an estimate that sample spins having a frequency spread of 50 kHz could be rotated uniformly by RF pulses. Note that line broadening proportional to the field inhomogeneity across the sample can be eliminated, for example, by the use of pulse sequences which select zero-quantum coherences or multiquantum heteronuclear coherences whose frequency does not shift in response to an offset in a static applied field [32]. Note as well that equation (2.26) implies that spins whose Larmor frequency is out of resonance with  $\omega_h$  by 25 kHz are cooled more slowly by the resonator between transients. An offset of

$$\beta = 2\pi \times 25 \text{ kHz}$$

from resonance decreases the cooling rate by a factor of

$$\frac{1}{1 + (\beta\tau_h)^2} \approx 0.5.$$

## 7 Use of non-metallic magnetic material

A requirement of the scheme we have proposed is that the mechanical resonator be exposed to RF magnetic fields during the NMR pulse sequence as well as during spin-locking. If the ferromagnetic material of the cylinders is metallic, eddy currents will be induced in the metallic cylinders by the RF fields. Appendix M presents an example which illustrates the way in which the resulting temperature change  $\Delta T_h$  is determined by physical parameters which depend strongly on the dimensions and

temperature of the resonator. Estimates of the order of magnitude of these parameters based on the limited information available in the literature leave open the possibility that the temperature change  $\Delta T_h$  could substantially decrease detection sensitivity if conducting ferromagnetic materials are used.

A possible solution to the problem of eddy-current heating is the use of dielectric material as the source of the resonator's field. A natural candidate for such a material would be an insulator that contains magnetic ions. Even if the material is paramagnetic rather than ferromagnetic, magnetic ions would remain aligned with the applied field at low temperatures, yielding time-independent magnetization in the lab frame, as in the model discussed in section 4. At fields of order 10 T and mK temperatures, ferromagnetic material is not necessarily a requirement for the resonator design or the numerical examples we have presented.

Ions with partially filled f-orbitals can have relatively large angular momenta, in part due to the fact that the orbital angular momentum of the tightly-bound f-orbitals is not quenched by the crystal field. Lanthanide oxides are natural candidates for non-metallic magnetic materials to be used in force-detected NMR, and EuO is particularly promising, since it has a large saturation magnetization of  $2.41 \text{ T}/\mu_0$  at 0 K [33], and since it has been prepared as an epitaxial thin film on Si [34] as well as in the form of nanocrystals [35, 36]. Although the saturation magnetization of the nanocrystals and epitaxial thin films were not measured, the Curie law susceptibility of the nanocrystals showed that each  $\text{Eu}^{2+}$  ion in these materials has a moment of  $\sim 7$  Bohr magnetons [35, 36], as in the bulk compound [33].

At room temperature EuO is a semiconductor with a resistivity many orders of magnitude larger than that of metals, and the resistivity increases as the temperature is lowered [37]. At temperatures below 77 K, EuO is ferromagnetic [33]. Doping with excess Eu causes a metal-insulator transition to occur around the Curie temperature, but low-temperature bulk resistivities observed by Shapira and coworkers for doped EuO were at least three orders of magnitude larger than the room-temperature conductivity of Fe [38]. Since the power dissipation due to eddy-current heating is inversely proportional to resistivity, the estimate presented in Appendix M suggests

that eddy-current heating should be negligible even for the "metallic" form of doped EuO.

## Chapter 6

# Simulations of spectra and spin relaxation

### 1 Simulations of two-spin spectra

We have simulated the noisy spectra of two-spin systems in order to characterize the sensitivity of the example resonator presented in table 5.3. Simulations had normally distributed noise added to each sampled point of the FID, with the variance of the noise determined by equation (4.50) in the case of spin-locked detection, and equation (4.53) in the case of freely-precessing spins. The value

$$A_{\text{det}} = 16$$

was used to characterize noise in the motion detector, as in the measurements reported in reference [25]. This value of  $A_{\text{det}}$  renders the spin noise negligible in comparison to instrument noise. For detection of freely-precessing spins, resonator-induced relaxation was included in the simulation by writing GAMMA programs [39] which simulated the motion of the spin system under the reduced master equation (2.17). For spin-locked detection using the scheme described in section 1 of chapter 5, no relaxation was included in the simulation. (This detection scheme measures a single point  $\langle I_x(t_1) \rangle$  of the FID with each shot of the measurement, and the spins are off resonance from the mechanical oscillator until time  $t_1$ .) We assumed that transverse decay of a two-spin system in a lattice at 10 mK would be negligible during the range

of values  $t_1$  sampled during spin-locked measurements, which included times up to 3 s after the beginning of the FID. As in the optimization described in section 6 of chapter 5, we used

$$T_{1\rho} = 1 \text{ s},$$

rather than assuming that resonator-induced relaxation was responsible for the decay of the spin-locked signal, which would have yielded

$$T_{1\rho} = 2/R_h = 1.5 \text{ s}.$$

## 1.1 Noninteracting spins

For a system of two noninteracting spins coupled to the mechanical resonator, the discussion of section 5 of chapter 3 suggests that a chemical-shift difference of

$$\delta\omega/2\pi = 200 \text{ Hz}$$

would yield the same time constant for resonator-induced transverse relaxation of the freely precessing dipole that would be observed for a single spin:

$$2/R_h = 1.5 \text{ s}.$$

Under these conditions, section 6 of chapter 4 shows that detection of the freely precessing transverse dipole is more sensitive than spin-locked detection, particularly if the lifetime of the spin-locked signal is shortened from  $2/R_h$  to 1 s. Indeed, equations (4.50) and (4.56) predict that under these conditions, detection of freely-precessing spins will be more sensitive than spin-locked detection by a factor of about 1.75. Figures 6.1 and 6.2 are consistent with this prediction, since the peaks at 100 Hz and 300 Hz stand out more sharply from the noise in the case where the freely-precessing spins drive the magnet than in the case of spin-locked detection.

Each of these spectra requires 32,000 transients. In estimating the time required to obtain the spectra, note first that the time constant for resonator-induced longi-

Detection of the free precession of noninteracting spins

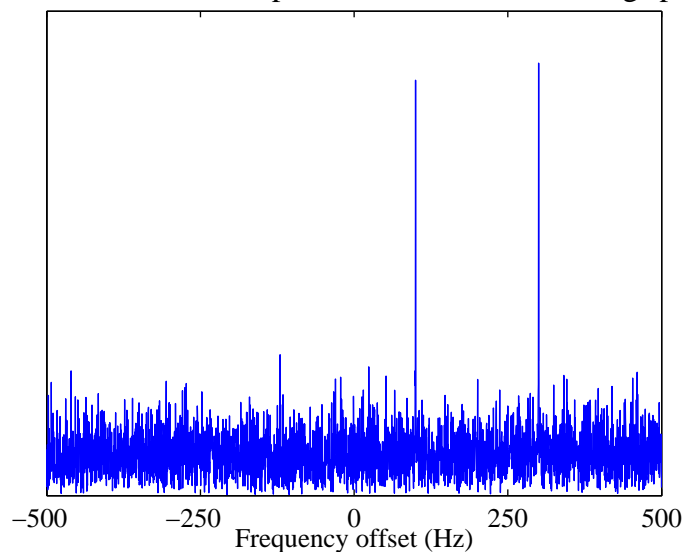


Figure 6.1: Simulated spectrum of two noninteracting spins detected without spin-locking. The spin Hamiltonian is  $H = (100 \text{ Hz}) I_{1z} + (300 \text{ Hz}) I_{2z}$ . Transverse relaxation induced by the example resonator of table 5.3 is included in the simulation of the noiseless FID, and normally distributed instrument noise associated with detection by the same resonator is added to the FID. Thermal polarization is assumed at the beginning of each transient. The acquisition time is  $\sim 50 \text{ h}$ .

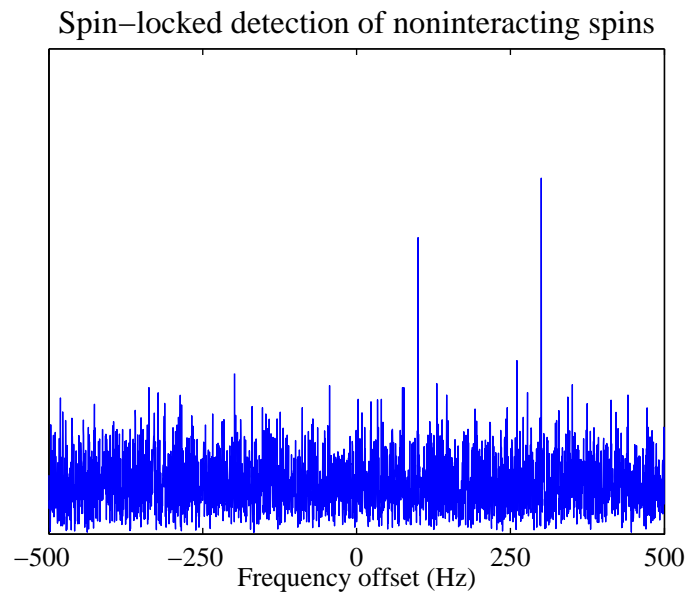


Figure 6.2: Simulated spectrum of two noninteracting spins detected with spin-locking, with  $T_{1\rho} = 1$  s. The spin-resonator system is the same as in figure 6.1, but resonator-induced transverse relaxation is eliminated from the simulation. Acquisition time for the spectrum is  $\sim 60$  h. Figures 6.1 and 6.2 are consistent with the prediction that for this system, detection of freely-precessing spins is more sensitive than spin-locked detection by a factor of about 1.75.

tudinal relaxation between transients is

$$1/R_h = 0.77 \text{ s}, \quad (6.1)$$

and we estimate the relaxation time between transients as  $3/R_h = 2.3 \text{ s}$ , for consistency with the assumption that thermal polarization is present at the beginning of each transient. For both figures, the detection period for a single transient lasts 3 s. In the case where freely precessing magnetization is detected, this is twice the time constant  $2/R_h$  for resonator-induced transverse relaxation (chosen after experimenting with simulated FIDs of different lengths in order to produce peaks clearly differentiated from the noise), while in the case of spin-locked detection, this is  $3T_{1\rho}$  (an assumed value for the protocol used to analyze the resonator's detected mechanical motion). The acquisition time for figure 6.1 is therefore

$$(2.3 \text{ s} + 3 \text{ s}) \times 32000 \approx 50 \text{ h}.$$

For the spin-locked detection simulated in figure 6.2, an initial period of free precession which precedes the detection period is also required, and the average length of this period is 1.5 s, which gives an acquisition time of

$$(2.3 \text{ s} + 3 \text{ s} + 1.5 \text{ s}) \times 32000 \approx 60 \text{ h}.$$

## 1.2 Vinyl bromide

Reference [40] has studied the structure of dibromoethylene adsorbed on a silicon surface and proposed the two structures shown in figure 6.3. We simulated spin-locked detection of one of these structures, adsorbed vinyl bromide, using the example resonator. Standard bond angles and bond lengths were used to estimate the Hamiltonian for dipolar coupling. A chemical shift difference was incorporated into the Hamiltonian by using the value 0.6 ppm given in the literature for vinyl bromide

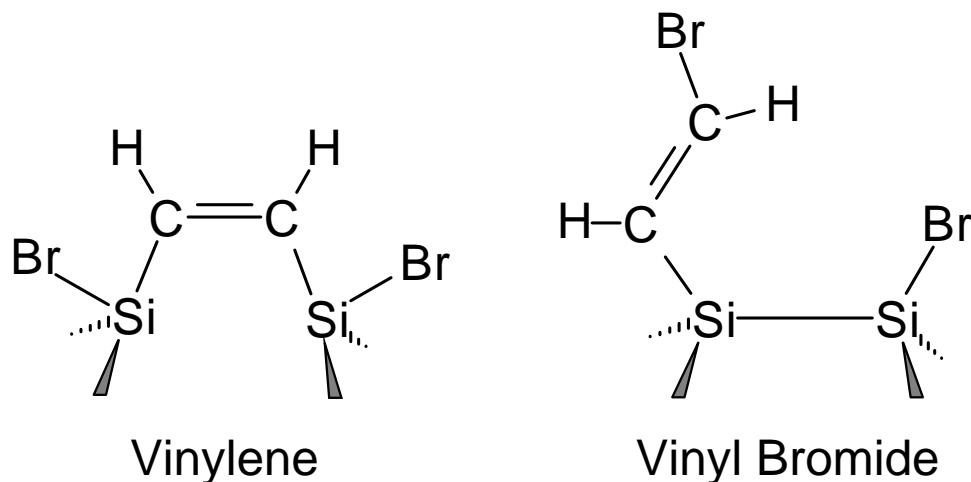


Figure 6.3: Two possible structures for dibromoethylene adsorbed on a silicon surface, proposed by reference [40].

in deuterated dichloromethane [41]. The spin Hamiltonian obtained in this way is

$$H_{\text{vinyl bromide}} = (0.6) (628 \text{ Hz}) I_{z,1} + (1840 \text{ Hz}) (2I_{z,1}I_{z,2} - I_{x,1}I_{x,2} - I_{y,1}I_{y,2}).$$

Figure 6.4 shows the simulated spectrum, for which the acquisition time is  $\sim 60$  h, as in figure 6.2. Since the dipolar coupling is sensitive to variations in geometry such as those shown in figure 6.3, this simulation suggests the possibility of chemical studies in which NMR spectroscopy is used with single-spin sensitivity.

## 2 Simulations of spin relaxation

Chapter 3 analyzes resonator-induced spin relaxation in samples containing more than one spin. Here we present GAMMA simulations [39] which illustrate and extend the results obtained in that section. The resonator used for these simulations has parameters similar to those given in table 5.3, although simplifications have been made to facilitate the interpretation of the graphs. For simulations of spin relaxation, the rate constant for spontaneous emission is  $R_0 = 1 \text{ s}^{-1}$ , the Larmor frequency has a magnitude of 600 MHz, and the temperature is approximately zero Kelvins, i.e., we

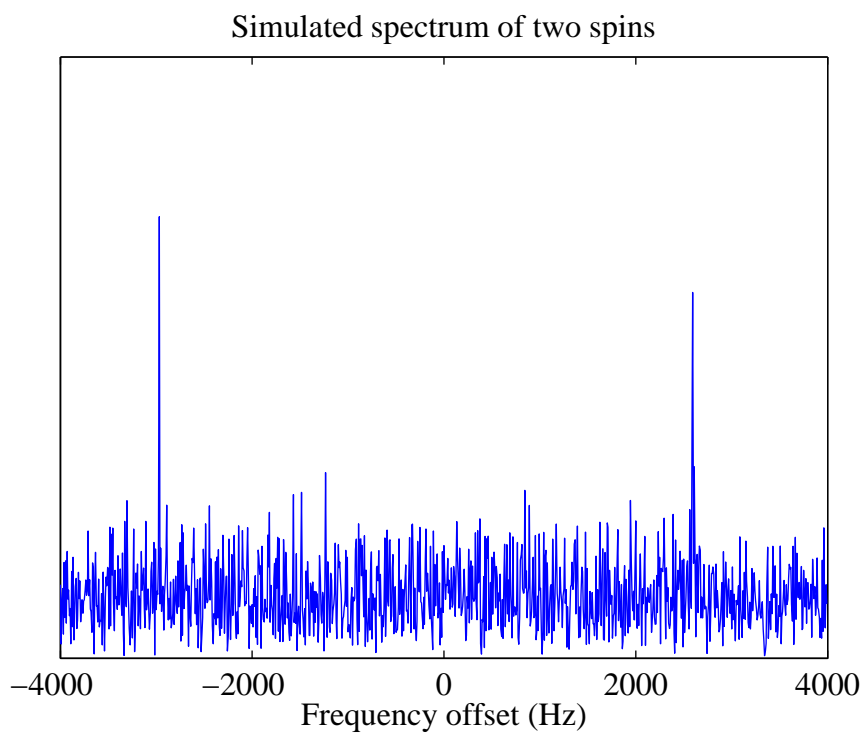


Figure 6.4: Simulated spectrum of a single molecule of adsorbed vinyl bromide, detected with spin-locking. The FID contains 1024 sampled complex points, averaged during 32,000 transients. Thermal polarization is assumed at the beginning of each transient. Acquisition time for this spectrum is  $\sim 60$  h.

have set  $n_{\text{th}} < 10^{-4}$  in equation (2.17). The interaction frame used for simulations of the relaxation of  $\langle I_x \rangle$  is defined as follows: the interaction-frame reduced density matrix for the spins  $\rho_s(t)$  is found by evolving the spin system forward in time for a period  $t$  from the initial state  $\rho_s(0)$  using the full evolution superoperator corresponding to equation (2.17), and then evolving the spins backward in time for the same period using the superoperator for evolution under the full spin Hamiltonian without relaxation.

## 2.1 Relaxation of noninteracting spins

Figure 6.5 presents the results of two simulations performed in order to test the estimate (3.21) of the time  $T_{\text{trap}}$  required for an initially disordered system to approach its spin-trapped equilibrium state:

$$T_{\text{trap}} = \frac{1}{R_0 \sqrt{N/2}}.$$

Note that  $T_{\text{trap}}$  also characterizes the time required for resonator-induced spin-spin correlations to develop, and it can be used to estimate the frequency at which indirect spin-spin torques must be modulated if spin trapping is to be suppressed. The solid and dashed curves show the relaxation of two systems of noninteracting spins which all experience the same field while relaxing from an initially disordered state, with the respective systems having  $N = 144$  and  $N = 36$  spins. The curves are normalized to take the value 1 when a system has relaxed to its spin-trapped equilibrium state. Figure 6.5 suggests that (3.21) works reasonably well as an estimate of the characteristic time required for  $\langle I_z \rangle$  to approach its equilibrium value. For both curves, the time  $t = T_{\text{trap}}$  corresponds to a point at which the system has relaxed to about 70% of its spin-trapped polarization.

The semiclassical model used to estimate  $T_{\text{trap}}$  suggests that chemical-shift offsets could reverse the sign of indirect spin-spin torques, thereby allowing resonator-induced relaxation to be characterized by a rate constant, and the simulations shown in figures 6.6 through 6.9 are consistent with this hypothesis. In figures 6.6 and 6.7, the

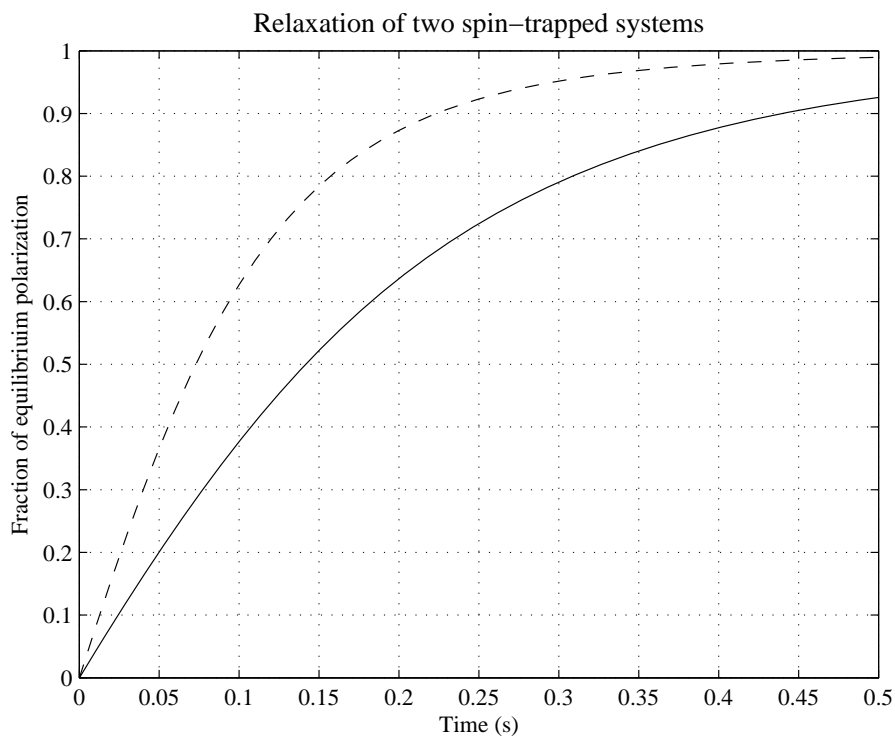


Figure 6.5: The solid and dashed curves show the respective relaxation of noninteracting systems having  $N = 36$  and  $N = 144$ , with  $R_0 = 1 \text{ s}^{-1}$ . The curves are normalized to take the value 1 when a system has relaxed to its spin-trapped equilibrium state. For each curve, the time  $t = \left(R_0 \sqrt{N/2}\right)^{-1}$  corresponds to a point at which the system has relaxed to about 70% of its spin-trapped polarization.

spins are initially aligned along the  $x$ -axis. The dashed curves show resonator-induced longitudinal and transverse relaxation, while the solid curves show the ideal longitudinal and transverse relaxation which would be observed if the relaxation were exponential with the respective rate constants  $R_0$  and  $R_0/2$  that govern the relaxation of an isolated spin interacting with the resonator. The dotted curve in each figure displays the evolution of  $\langle N/2 - I_x^2 - I_y^2 \rangle$ . Since the relaxation equation for  $\langle I_z \rangle$  can be expressed as

$$\frac{d}{dt} \langle I_z \rangle = -R_h \left\{ \langle I_z \rangle - \frac{N/2}{2 \langle n_{\text{th}} \rangle + 1} \right\} - R_0 \langle N/2 - I_x^2 - I_y^2 \rangle,$$

a plot of  $\langle N/2 - I_x^2 - I_y^2 \rangle$  displays the instantaneous contribution of indirect spin-spin torques to longitudinal relaxation. Adding chemical shift offsets spaced in steps of 1 Hz causes the indirect spin-spin torques to be modulated quickly enough that the contribution of these torques to the relaxation is effectively suppressed, and the simulated relaxation closely follows the exponential curves.

Figures 6.8 and 6.9 show longitudinal relaxation from a completely disordered initial state. Note that in figure 6.9, the spacing of chemical shift frequencies in steps of 1 Hz is sufficient to suppress completely the contribution of the indirect torques to longitudinal relaxation. The value of  $\langle N/2 - I_x^2 - I_y^2 \rangle$ , which shows the instantaneous contribution of indirect spin-spin torques, oscillates without ever becoming large enough to affect the relaxation substantially. By way of contrast, the same spacing of chemical shift frequencies leaves noticeable wiggles in the simulated curves of figure 6.7, and  $\langle N/2 - I_x^2 - I_y^2 \rangle$  initially oscillates between much larger values. These differences can be rationalized by noting that when the spins are initially disordered, the indirect torques do not add coherently, and modulation of these torques during a period of one or two seconds is sufficient to suppress their contribution to longitudinal relaxation. In the case where the spins are initially aligned along the  $x$ -axis, the indirect torques add coherently, and the effect of these torques can be seen even when their contribution is modulated within a similar time period.

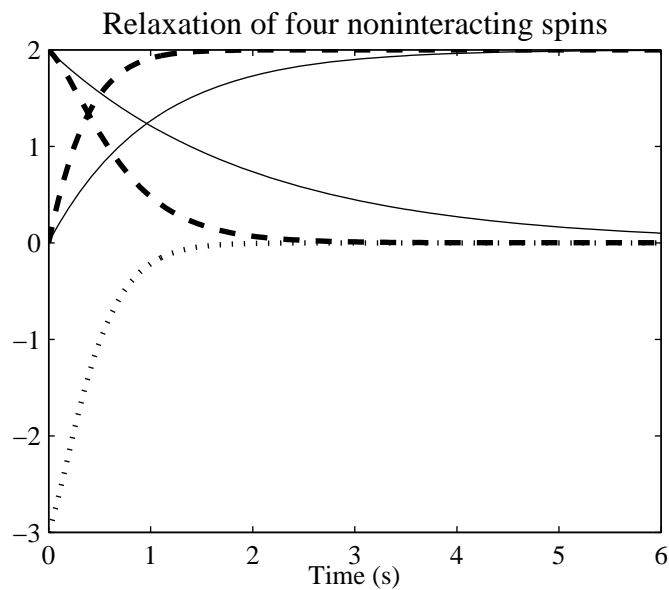


Figure 6.6: Relaxation of four isochronous spins which are initially aligned along the  $x$ -axis. The dashed curves show the simulated relaxation of  $\langle I_x \rangle$  and  $\langle I_z \rangle$ , while the solid curves show ideal exponential longitudinal and transverse relaxation with respective time constants  $1/R_0$  and  $2/R_0$ . The dotted curve shows the evolution of  $\langle N/2 - I_x^2 - I_y^2 \rangle$ , which determines the instantaneous contribution of indirect spin-spin torques to longitudinal relaxation.

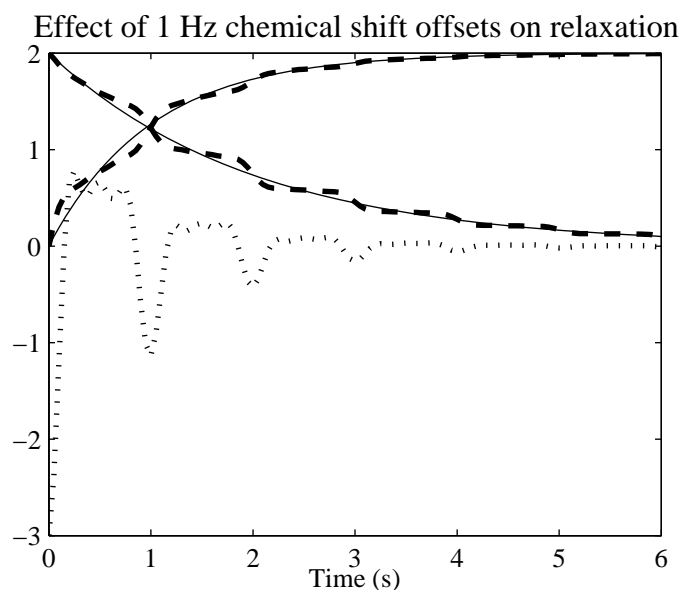


Figure 6.7: Adding chemical shift offsets spaced in steps of 1 Hz causes the indirect spin-spin torques to be modulated quickly enough that their contribution to relaxation is effectively suppressed.

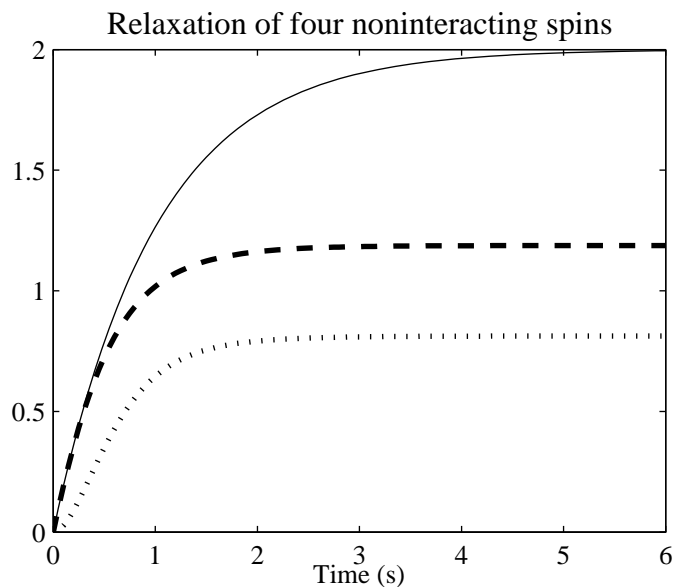


Figure 6.8: Relaxation of four noninteracting spins which experience the same field and are initially completely disordered. The dashed curve shows the simulated relaxation of  $\langle I_z \rangle$ , while the dotted curve shows the evolution of  $\langle N/2 - I_x^2 - I_y^2 \rangle$ . The solid curve shows exponential longitudinal relaxation with time constant  $1/R_0$ .

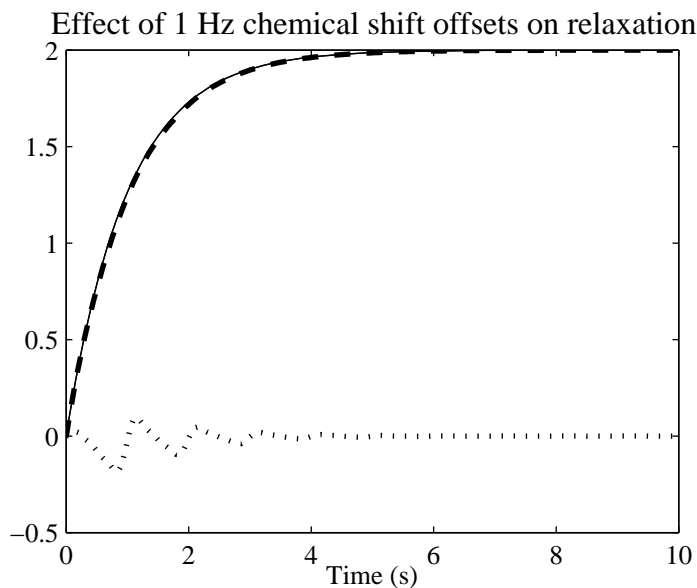


Figure 6.9: Adding chemical shift offsets spaced in steps of 1 Hz causes the indirect spin-spin torques to be modulated quickly enough that their contribution to relaxation is completely suppressed, and the simulated curve closely follows the ideal exponential curve.

## 2.2 Relaxation of dipole-dipole coupled spins

Figures 6.10, 6.11, and 6.12 show GAMMA simulations of the relaxation of four-spin systems coupled by the dipolar Hamiltonian. The spin Hamiltonian for these simulations has the form

$$\begin{aligned}
 H &= \omega_0 I_z + H_D, \\
 H_D &= \sum_{i>j} \omega_{ij} (3I_{z,i}I_{z,j} - \mathbf{I}_i \cdot \mathbf{I}_j).
 \end{aligned}
 \tag{6.2}$$

In these figures, the dotted curve corresponds to a system in which the dipolar coupling was eliminated by choosing  $\omega_{ij} = 0$  for all  $i, j$ . The system characterized by the dash-dot curve has a Hamiltonian obtained by letting each  $\omega_{ij}/2\pi$  be randomly chosen, with a flat probability distribution between 1 kHz and 2 kHz. The Hamiltonian yielding the dash-dash relaxation curves was obtained by broadening the distribution of  $\omega_{ij}/2\pi$  to lie between 0 Hz and 2 kHz. The solid curves show ideal exponential relaxation with the rate constants for longitudinal relaxation and transverse relaxation given by  $R_0$  and  $R_0/2$ , respectively.

Longitudinal relaxation of an initially disordered system is shown in figure 6.10. The dipole-dipole coupled systems show two different time scales for relaxation, with a short initial period of fast relaxation being followed by a longer period of slow relaxation. Extending the simulations to  $t = 150$  s shows that the systems effectively remain trapped away from the ground state.

This behavior can be rationalized using results obtained in section 4 of chapter 3 for a system of three dipole-dipole coupled spins. The rules for addition of angular momenta allow a collection of three spins  $1/2$  to be represented as a single particle with  $I = 3/2$  and two particles with  $I = 1/2$ . Equations (3.28) and (3.29) show that one of the  $I = 1/2$  particles (or "manifolds") can be defined in such a way that its two states  $|1/2, +\rangle$ ,  $|1/2, -\rangle$  are eigenstates of  $H_D$ . As the spins interact with the cold mechanical resonator, the combined population of this manifold will be transferred to the lower-energy state  $|1/2, +\rangle$  within a time period of order  $R_0$  and then remain

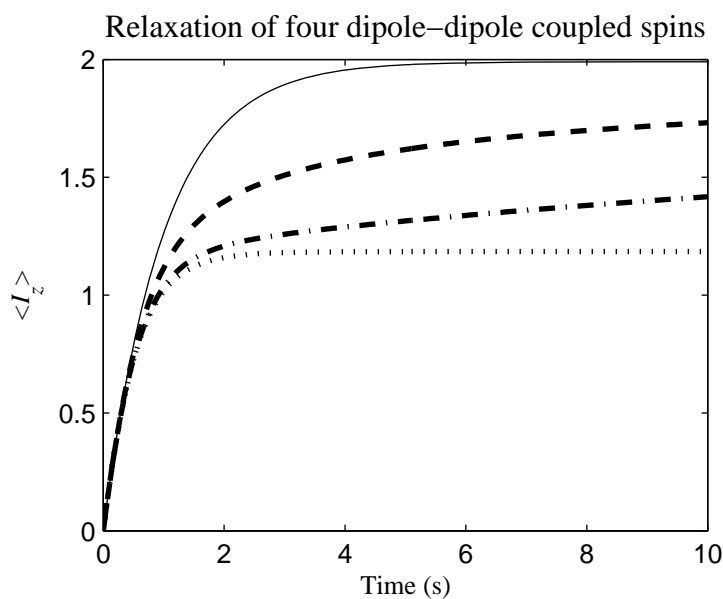


Figure 6.10: Longitudinal relaxation of four dipole-dipole coupled spins from an initially disordered state. For the dash-dot curve, the dipolar Hamiltonian was obtained by letting the frequencies  $\omega_{ij}/2\pi$  of equation (6.2) be randomly chosen, with a flat probability distribution between 1 kHz and 2 kHz. For the dash-dash curve, the frequencies  $\omega_{ij}/2\pi$  were randomly selected between 0 Hz and 2 kHz. For purposes of comparison, the solid curve shows exponential relaxation with time constant  $1/R_0$ , and the dotted curve shows the relaxation of a system of noninteracting spins.

in that state indefinitely. Table 3.1 shows that  $H_D$  does not strongly couple the remaining  $I = 1/2$  manifold with the  $I = 3/2$  manifold unless the magnitudes of the dipolar couplings are well separated. When the coupling between angular momentum manifolds is weak, two different time scales of relaxation are expected. An initial period of fast relaxation occurs as population is transferred to the lowest-energy state of each manifold, and this is followed by a period of slow relaxation as population is slowly transferred to the  $I = 3/2$  manifold and then relaxes to the ground state of the spin system. Simulated relaxation of three-spin systems confirms these expectations.

The four-spin simulations of figure 6.10 can be rationalized by the hypothesis that the relaxation is governed by similar processes. The systems appear to relax quickly from a disordered state to a state in which the population of each manifold is in the manifold's ground state. Relaxation out of this trapped state occurs on a slower time scale as population is transferred between manifolds with different values of  $I$ . In figure 6.10, the efficiency of transfer between manifolds of different  $I$  separates the three simulated curves after an initial period in which they relax at the same rate. Extending the simulation to  $t = 150$ s suggests that the systems represented by the dash-dash curve and the dash-dot curve effectively become trapped away from the ground state. A system of four spins  $1/2$  yields one  $I = 2$  manifold, three  $I = 1$  manifolds, and two  $I = 0$  manifolds. The dash-dash curve can be rationalized by the hypothesis that population is trapped in the two  $I = 0$  manifolds, while the dash-dot curve can be rationalized by the hypothesis that population is trapped in the two  $I = 0$  manifolds and one of the  $I = 1$  manifolds. Both curves become flat at a value a fraction of a percent below the trapped value predicted by these hypotheses.

The discussion in section 5 of chapter 3 analyzes the way in which the resonator can induce fast transverse relaxation in a system of two or more spins. A coherence  $\rho_{ab}$  between states  $|a\rangle$  and  $|b\rangle$  can be disrupted when the system makes a transition away from one of these states. Transitions do not necessarily decrease the order within a system, however. A transition from  $|a\rangle$  to  $|c\rangle$  might replenish a coherence  $\rho_{cb}$  at the same time that it depletes  $\rho_{ab}$ , leaving the sum  $\rho_{ab} + \rho_{cb}$  unchanged. If a perturbation changes the frequency of  $\rho_{ab}$  or  $\rho_{cb}$  so that their relative phase varies

during the time needed for non-negligible transfer from  $\rho_{ab}$  to  $\rho_{cb}$ , however, then transfer from  $\rho_{ab}$  to  $\rho_{cb}$  depletes  $\rho_{ab}$  without replenishing  $\rho_{cb}$ , since the terms added to  $\rho_{cb}$  during different time steps interfere destructively. An addition to the spin Hamiltonian which perturbs the degeneracies of distinct coherences can therefore transform reversible transfer between coherences into irreversible decay, and in this way modify the rate of resonator-induced transverse relaxation. In section 5 of chapter 3, this was illustrated using analytic expressions for the transverse decay of two-spin systems.

Figure 6.11 shows that the presence of dipolar couplings can substantially accelerate transverse relaxation in a four-spin system. The solid curve shows ideal exponential relaxation with time constant

$$2/R_0 = 2 \text{ s},$$

and the dotted curve shows the simulated relaxation of a system of four noninteracting isochronous spins. Addition of the dipolar Hamiltonian  $H_D$  increases the relaxation rate, with the magnitude of the change depending on the spacing of the frequencies  $\omega_{ij}$  which appear in (6.2). The fast transverse relaxation induced by the resonator in these examples would significantly decrease the sensitivity of a scheme which detects freely precessing spins

The tendency of the dipolar Hamiltonian  $H_D$  to accelerate transverse relaxation cannot be interpreted as radiation damping, which is associated with rotation of a sample dipole rather than true decay. This is demonstrated by figure 6.12, which shows the longitudinal relaxation of four-spin systems having the spins initially aligned with the  $x$ -axis. The dotted curve shows longitudinal relaxation in the absence of  $H_D$ , while the dash-dash curve corresponds to the same Hamiltonian  $H_D$  as the dash-dash curves in figures 6.10 and 6.11. The solid curve shows exponential relaxation with a time constant  $1/R_0$ . "Turning on" the dipolar coupling slows down longitudinal decay at the same time that it accelerates transverse decay; hence, it is not associated with simple rotation of the sample dipole.

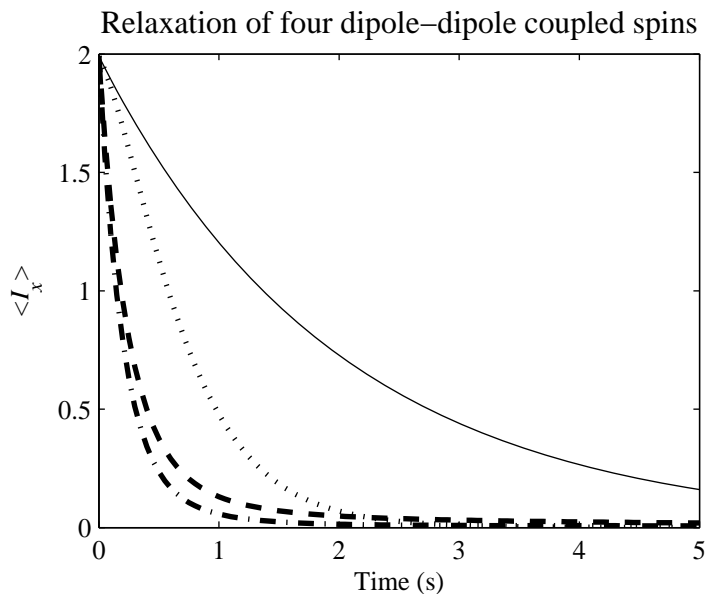


Figure 6.11: Transverse relaxation of four dipole-dipole coupled spins which are initially aligned with the  $x$ -axis. For the dash-dot curve, the dipolar Hamiltonian was obtained by letting the frequencies  $\omega_{ij}/2\pi$  of equation (6.2) be randomly chosen, with a flat probability distribution between 1 kHz and 2 kHz. For the dash-dash curve, the frequencies  $\omega_{ij}/2\pi$  were randomly selected between 0 Hz and 2 kHz. For purposes of comparison, the solid curve shows exponential relaxation with time constant  $2/R_0$ , and the dotted curve shows the relaxation of a system of noninteracting spins. This figure shows that "turning on" the dipolar interaction can accelerate resonator-induced transverse relaxation.

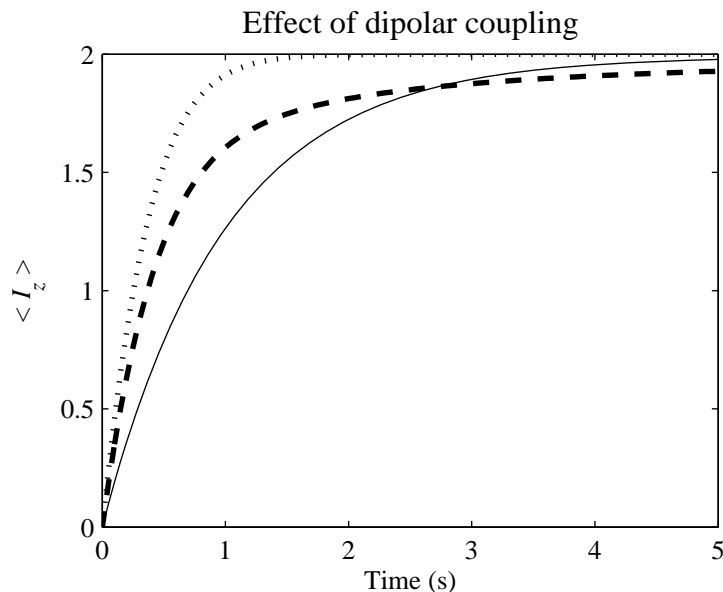


Figure 6.12: Longitudinal relaxation of four-spin systems. The solid curve shows exponential relaxation with time constant  $1/R_0$ . The dash-dash curve represents a dipole-dipole coupled system, and the dotted curve represents a system of noninteracting spins. "Turning on" the dipolar coupling slows down longitudinal decay.

Figure 6.13 reinforces the distinction between radiation damping and fast transverse relaxation induced by the resonator. In section 5 of chapter 3, we studied transverse relaxation of a two-spin sample having a weak dipolar coupling and a large chemical shift offset between the spins. We showed that the large chemical shift offset guaranteed that longitudinal relaxation would proceed exponentially with time constant  $1/R_h$  (or  $1/R_0$  in the case where the resonator is at zero Kelvins), while the presence of the dipolar coupling accelerated the transverse relaxation induced by the resonator. Figure 6.13 extends the results of that section by presenting simulated relaxation of a four-spin system which has a chemical-shift offset of  $j \times 4000$  Hz added to spin  $j$ , in addition to the same dipolar coupling  $H_D$  which yielded the dash-dash curves in figures 6.10 through 6.12. For purposes of comparison with the simulation, the longitudinal and transverse relaxation predicted for a single-spin sample is shown using solid curves. Simulated longitudinal relaxation is only slightly perturbed from that of a single spin, while the transverse dipole relaxes in a fraction of the time

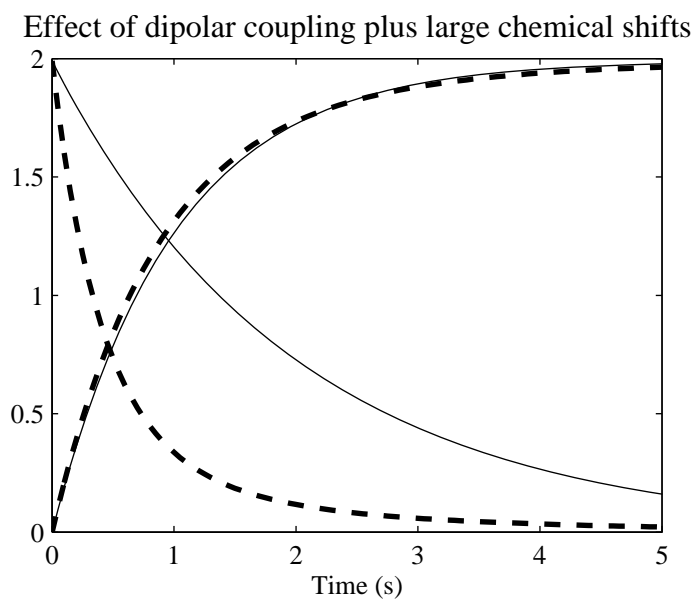


Figure 6.13: Relaxation of a four-spin system which includes dipolar couplings smaller than the spacing of chemical shift offsets. All spins are initially aligned along the  $x$ -axis. Solid curves show ideal exponential longitudinal and transverse relaxation with respective time constants  $1/R_0$  and  $2/R_0$ . The dashed curves show the simulated relaxation of  $\langle I_x \rangle$  and  $\langle I_z \rangle$ . The transverse relaxation is accelerated by the presence of the dipolar coupling, while the longitudinal relaxation closely follows the ideal exponential curve, due to the presence of large chemical shift offsets.

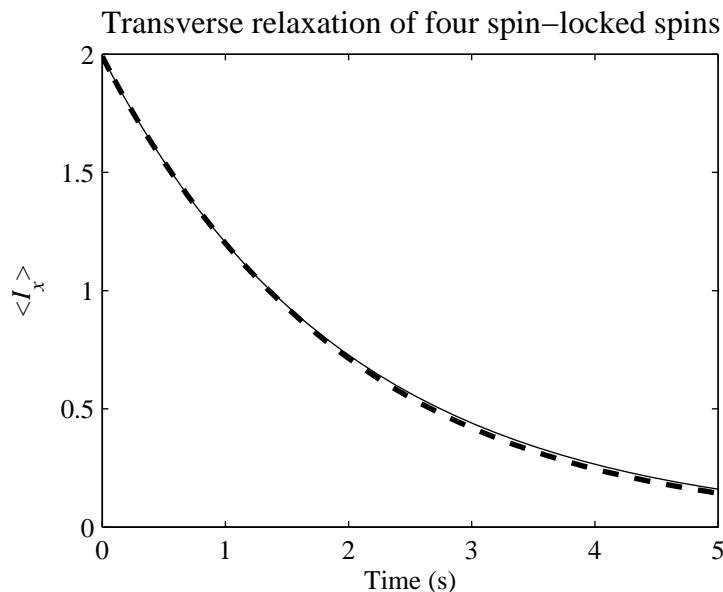


Figure 6.14: Resonator-induced relaxation of a spin-locked sample of four dipole-dipole coupled spins. The solid curve shows the predicted exponential transverse relaxation with time constant  $2/R_0$ .

required for transverse relaxation of a single spin.

Figure 6.14 illustrates the result (3.35) obtained in section 6 of chapter 3:

$$T_{1\rho} = R_h/2.$$

The dash-dash curve shows simulated relaxation of a spin-locked system of four dipole-dipole coupled spins. The internal spin Hamiltonian is the same dipolar Hamiltonian  $H_D$  used for the dash-dash curves in figures 6.10 through 6.12, and  $\omega_1/2\pi = 10$  kHz. The solid curve shows exponential relaxation with time constant  $R_0/2 = R_h/2$ . We see from figure 6.14 that spin-locking with a Rabi frequency of 10 kHz is sufficient to average both  $H_D$  and the superoperator for resonator-induced relaxation, thereby suppressing the fast transverse relaxation shown in figure 6.11.

The qualitative character of resonator-induced longitudinal relaxation of  $N \gg 1$  dipole-dipole coupled spins depends on the efficiency with which the Hamiltonian  $H_D$  transfers populations between angular momentum manifolds corresponding to differ-

ent values of  $I$ . In the limiting case where transfers between manifolds occur quickly,  $H_D$  equalizes the population of all states within a given eigenspace of  $I_z$ . Resonator-induced transfers of population to low-energy states within a manifold immediately result in compensating transfers between manifolds as the population of all states within each eigenspace of  $I_z$  are equalized. Figures 6.15 and 6.16 present simulations of longitudinal relaxation for this limiting case. The dashed curves show simulations in which population is equalized among all states of each  $I_z$  eigenspace at the end of each 0.01 s time step of resonator-induced relaxation. (For these figures, the initial state is completely disordered, and the simulation includes no spin-spin interactions during the time steps.) The solid curves show ideal exponential relaxation with rate constant  $R_0$ . In spite of the fact that the number of angular momentum manifolds having small  $I$  is vastly greater than the number of manifolds having  $I$  near  $N/2$  for these systems, the simulations suggest that efficient redistribution within eigenspaces of  $I_z$  can result in fast longitudinal relaxation to a polarization near 1.

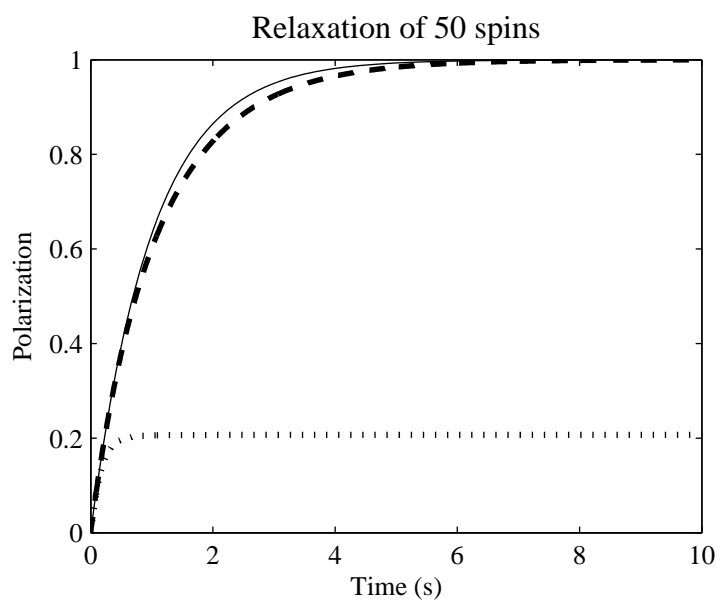


Figure 6.15: Resonator-induced longitudinal relaxation of 50 spins from a disordered state. The dashed curve shows simulated relaxation in the regime where dipolar interactions efficiently redistribute population within each eigenspace of  $I_z$  during the relaxation. For purposes of comparison, the dotted curve shows relaxation of noninteracting spins to a trapped state, and the solid curve shows ideal exponential relaxation with time constant  $1R_0$ .

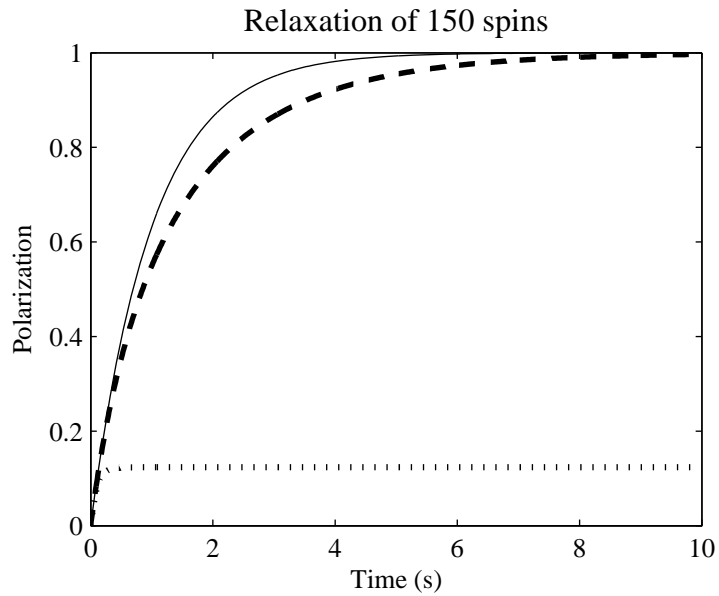


Figure 6.16: Resonator-induced longitudinal relaxation of 150 spins from a disordered state. As in figure 6.15, the dashed curve shows simulated relaxation in the regime where dipolar interactions efficiently redistribute population within each eigenspace of  $I_z$  during the relaxation. The dotted curve shows relaxation of noninteracting spins to a trapped state, and the solid curve shows ideal exponential relaxation with time constant  $1R_0$ .

# Chapter 7

## Cooling a single mode with hyperpolarized spins?

### 1 Hyperpolarized spins as a cold bath

The simulations presented in chapter 6 are based on the assumption that all modes of the mechanical oscillator are cooled to  $\sim 10$  mK by a dilution refrigerator. An alternative approach would be to extract energy from the single resonant mode, thereby cooling it to a temperature below that of the sample and the oscillator's remaining modes. A promising method for removing energy from a single mode is to use negative feedback to reduce the amplitude of the mode's thermal motion. Such "feedback cooling" of a single mechanical mode from a base temperature of 2.2 K down to 3 mK has been demonstrated experimentally [42].

We have considered the possibility of using cold spins to absorb the mode's energy. If a stream of hyperpolarized xenon nuclei passes by a warm mechanical oscillator whose frequency is resonant with the Larmor frequency of xenon, the spin-resonator interaction governed by the Hamiltonian (2.11) would cause the resonator to be cooled toward the spin temperature of the xenon. The scheme of using hyperpolarized spins to cool a resonator was particularly interesting to us because of the possibility of detecting entropy exchange between spins and resonator at sizes substantially larger than nanoscale. Numerical examples such as those presented in section 6 of chapter 5 suggest that a nanoscale resonator is needed to achieve measurable cooling of a spin

system; we investigated the possibility that cooling of a larger resonator by many hyperpolarized spins might be detectable.

In studying the system consisting of a warm mechanical oscillator coupled to hyperpolarized spins, we begin with a heuristic example in which the spins are modelled as a cold bath which damps the oscillator. The oscillator is also coupled to a warm bath, and the master equation for the damped oscillator is

$$\frac{d}{dt}\rho = \frac{1}{i\hbar} [H_{\text{osc}}, \rho] + \Lambda_h \rho + \Lambda_c \rho, \quad (7.1)$$

where  $H_{\text{osc}}$  is the Hamiltonian for the undamped oscillator, and  $\Lambda_h, \Lambda_c$  are the superoperators associated with damping by the warm and cold baths, respectively. The formula for the relaxation superoperator associated with damping of a harmonic oscillator by a thermal bath [8] allows us to write  $\Lambda_h$  explicitly as

$$\begin{aligned} \Lambda_h \rho = & -\frac{n_h + 1}{\tau_h} [a^\dagger a, \rho]_+ + 2\frac{n_h + 1}{\tau_h} a \rho a^\dagger \\ & - \frac{n_h}{\tau_h} [a a^\dagger, \rho]_+ + 2\frac{n_h}{\tau_h} a^\dagger \rho a, \end{aligned} \quad (7.2)$$

where  $n_h$  is the number of quanta the resonator would have in equilibrium with the warm bath, and  $\tau_h$  would be the ringdown time of the resonator if only the warm bath were present. By replacing  $n_h$  and  $\tau_h$  by analogous quantities  $n_c$  and  $\tau_c$  associated with the cold bath, we obtain an explicit expression for  $\Lambda_c$ . Letting  $\Lambda_\infty$  denote the sum  $\Lambda_h + \Lambda_c$ , we find that

$$\begin{aligned} \Lambda_\infty \rho = & -\frac{n_\infty + 1}{\tau_\infty} [a^\dagger a, \rho]_+ + 2\frac{n_\infty + 1}{\tau_\infty} a \rho a^\dagger \\ & - \frac{n_\infty}{\tau_\infty} [a a^\dagger, \rho]_+ + 2\frac{n_\infty}{\tau_\infty} a^\dagger \rho a, \end{aligned}$$

where

$$\frac{1}{\tau_\infty} = \frac{1}{\tau_h} + \frac{1}{\tau_c}, \quad (7.3)$$

$$n_\infty = \frac{\tau_h n_c + \tau_c n_h}{\tau_h + \tau_c}. \quad (7.4)$$

The system consisting of the resonator in contact with two baths is formally equivalent to a system in which only a single bath is present, with  $\tau_\infty$  the ringdown time of the oscillator and

$$T_\infty = \frac{\hbar\omega_h}{k_B \ln(1 + 1/n_\infty)}$$

the temperature of the bath. The spectral density of the thermal torque can be obtained by substituting  $\tau_\infty$  and  $n_\infty$  into equation (4.41):

$$\begin{aligned} S_{N'} &= \frac{4I_h \hbar\omega_h}{\tau_\infty} \left( \frac{1}{2} + n_\infty \right) \\ &= \frac{4I_h \hbar\omega_h}{\tau_h} \left( \frac{1}{2} + n_h \right) + \frac{4I_h \hbar\omega_h}{\tau_c} \left( \frac{1}{2} + n_c \right). \end{aligned} \quad (7.5)$$

We can interpret (7.5) to mean that the thermal torque responsible for introducing noise into the measurement is additive. Adding a cold bath will therefore not decrease the thermal torque exerted by the warm bath.

This argument highlights the possibility that the modification of a resonator's ringdown time by the cold spins could mitigate the advantages associated with cooling a single mode, but the model we used to obtain (7.5) is not in general correct for a system in which hyperpolarized spins flow past a mechanical resonator. Equation (7.1) describes relaxation associated with two baths, each of which acts independently of the other. However, we found in section 2 of chapter 2 that the rate constant for energy flow between spins and resonator depends on  $\tau_h$ , that is, on the coupling between the resonator and the warm bath. Since energy exchange between spins and resonator depends on the collective properties of the spins, resonator, and warm bath, it is problematic to represent the cold spins as an independent cold bath.

Section 2 of this chapter presents a model based on the interaction Hamiltonian

for the spin-resonator system, and sections 3 through 7 use this model to analyze the system. In summarizing here the results of this analysis, we use  $T_2$  to denote a transverse spin decay time that can include contributions from ordinary transverse relaxation as well as from the flow of spins into and out of the region of space where the Larmor frequency is resonant with the mechanical oscillator. Our attention is focused on the regime where

$$\tau_h \ll T_2, \quad (7.6)$$

that is, the regime where the fluctuations of the resonator coordinate limit the magnitude of the spin-resonator correlations which can develop. In section 3, we find that the steady-state number of quanta  $n_\infty$  in the cooled resonator can in fact be calculated using equation (7.3), which we obtained above by treating the spins as a cold bath. In the regime defined by (7.6), the constant  $\tau_c$  appearing in (7.3) is

$$\frac{1}{\tau_c} \equiv 2g^2\tau_h \langle I_z \rangle_\infty. \quad (7.7)$$

By way of contrast, the rate constant which governs cooling of spins by a single resonator at zero Kelvins is

$$R_0 = 2g^2\tau_h. \quad (7.8)$$

Since (7.7) is larger than (7.8) by a factor of  $\langle I_z \rangle_\infty$ , these equations suggest the possibility that entropy flow between spins and resonator might be most easily observed by performing an experiment in which hyperpolarized spins cool a resonator. Section 4 presents numerical examples to characterize the regime in which cooling may be possible, however, and for these examples,  $g^2$  scales so strongly with size that cooling becomes negligible at size scales of order  $10 \mu\text{m}$  or larger.

Since (7.3) can be used to calculate  $n_\infty$ , it is tempting to conclude that the cold spins can be treated as a cold bath. Section 5 shows, however, that in the numerical examples where substantial cooling is possible, the spins and resonator are so strongly coupled that one cannot distinguish a mechanical mode or a spin mode. Instead, the two modes of the spin-resonator system include equal contributions from the

spins and the mechanical resonator. It is only in the limit of weak spin-resonator coupling and short  $T_2$  that (7.7) can be used to calculate the decay time of the mechanical mode. In general, the mechanical response to an external torque is also incorrectly predicted by the model which treats the hyperpolarized spins as a cold bath. Indeed, in the case where (7.6) holds, the mechanical resonator could be considered a device for transducing an external mechanical torque at frequency  $\omega_h$  into precessing magnetization of hyperpolarized spins, since the energy donated by the external torque ends up as transverse spin excitation. For sufficiently strong spin-resonator coupling, however, we find that a resonant mechanical response can be obtained by driving the mechanical oscillator at one of the two eigenfrequencies  $\omega_h \pm d$  of the spin-resonator system, where  $d \approx 1/\sqrt{\tau_h \tau_c}$ .

Section 7 uses the symmetric autocorrelation function for the oscillator's mechanical coordinate to characterize quantitatively the mechanical fluctuations. Equation (7.5) is obtained in the limit of weak spin-resonator coupling and short  $T_2$ . In the regime where (7.6) holds and substantial cooling is possible, the strong spin-resonator correlations which are responsible for cooling make a large contribution to mechanical fluctuations. As a result, the mechanical thermal noise is not decreased by the coupling to the hyperpolarized spins; indeed we find that when  $n_\infty \gg 1/2$  and  $n_\infty \gg n_c$ , the thermal torque at the eigenfrequencies  $\omega_h \pm d$  becomes larger than it would be at  $\omega_h$  in the absence of the hyperpolarized spins. In this regime, as well as in the regime where the spins behave as a cold bath, the noisy thermal torque acting on the resonator is not decreased by the presence of the cold spins.

## 2 Model of the spin-resonator system

In analyzing a system consisting of a damped mechanical resonator and hyperpolarized spins which flow past it, we will use the master equation

$$\frac{d}{dt}\rho = \frac{1}{i\hbar} [H_0 + V, \rho] + \Lambda_h \rho + \Lambda_s \rho, \quad (7.9)$$

where  $H_0$ ,  $V$ , and  $\Lambda_h$  are given respectively by (2.6), (2.11), and (2.25):

$$\begin{aligned}
H_0 &= \omega_0 I_z + \omega_h \left( a^\dagger a + \frac{1}{2} \right), \\
V &= g (I_+ a^\dagger + I_- a), \\
\Lambda_h \rho &= -\frac{n_h + 1}{\tau_h} [a^\dagger a, \rho]_+ + 2\frac{n_h + 1}{\tau_h} a \rho a^\dagger \\
&\quad - \frac{n_h}{\tau_h} [a a^\dagger, \rho]_+ + 2\frac{n_h}{\tau_h} a^\dagger \rho a.
\end{aligned} \tag{7.10}$$

(Note that for consistency with the notation used in section 1 of this chapter, we have used  $n_h$  rather than  $n_{\text{th}}$  to denote the thermal number of quanta in the warm bath which damps the resonator.) In order to reveal the fundamental properties of the spin-resonator system without complicating the analysis, we will assume that spins are perfectly resonant with the mechanical oscillator within a certain region of space but far off resonance outside of this region. The spin operators  $I_z$ ,  $I_+$ , and  $I_-$  act only on the spins in the resonant region.

The superoperator  $\Lambda_s$  governs the decay of  $\mathbf{I}$  due to spin-spin interactions, spin-lattice interactions, and the flow of spins into and out of the resonant region. For our purposes, it is sufficient to approximate the effects of  $\Lambda_s$  in an ad hoc way by assuming that it causes relaxation of  $\langle I_z \rangle$  toward a hyperpolarized value  $PN/2$  with a time constant denoted by  $T_1$ , and relaxation of transverse magnetization toward zero with a time constant denoted by  $T_2$ . In addition, we assume that  $\Lambda_s$  causes relaxation of  $\langle I_+ a^\dagger - I_- a \rangle$  toward zero, with time constant  $T_2$ . These assumptions can be formally expressed as

$$\text{Tr} \{ (\Lambda_s \rho) I_z \} = -\frac{1}{T_1} \left( \langle I_z \rangle - \frac{1}{2} PN \right), \tag{7.11}$$

$$\text{Tr} \{ (\Lambda_s \rho) I_\pm \} = -\frac{1}{T_2} \langle I_\pm \rangle, \tag{7.12}$$

$$\text{Tr} \{ (\Lambda_s \rho) (I_+ a^\dagger - I_- a) \} = -\frac{1}{T_2} \langle I_+ a^\dagger - I_- a \rangle. \tag{7.13}$$

The relaxation of  $\langle I_z \rangle$  toward the hyperpolarized value  $PN/2$  can be associated with the flow of spins through the resonator, and so  $T_1$  is determined by the flow rate. In

the case where the transverse decay described by equation (7.12) is due to the flow of spins, equation (7.13) can be motivated by the idea that the flow of spins during  $\Delta t$  causes a fraction of the spins in the cavity to be reset to the state having

$$\langle I_+ a^\dagger - I_- a \rangle = 0.$$

More generally, equation (7.13) can be motivated by first considering the way in which the oscillator's relaxation superoperator  $\Lambda_h$  contributes to the equation of motion of a product  $G(a, a^\dagger) F(\mathbf{I})$ , where  $g(a, a^\dagger)$  is a function of the oscillator's raising and lowering operators, and  $F(\mathbf{I})$  is an arbitrary spin operator. Using the cyclic property of the trace, we can express the term

$$\text{Tr} \{ (\Lambda_h \rho) G(a, a^\dagger) F(\mathbf{I}) \}$$

in the form

$$\text{Tr} \{ \rho [ \Lambda'_h G(a, a^\dagger) ] F(\mathbf{I}) \},$$

where

$$\begin{aligned} \Lambda'_h G &= -\frac{n_h + 1}{\tau_h} [a^\dagger a, G]_+ + 2\frac{n_h + 1}{\tau_h} a^\dagger G a \\ &\quad - \frac{n_h}{\tau_h} [a a^\dagger, G]_+ + 2\frac{n_h}{\tau_h} a G a^\dagger. \end{aligned}$$

can be obtained from  $\Lambda_h \rho$  by respectively replacing  $[a^\dagger a, \rho]_+$ ,  $[a a^\dagger, \rho]_+$ ,  $a \rho a^\dagger$ , and  $a^\dagger \rho a$  by  $[a^\dagger a, G]_+$ ,  $[a a^\dagger, G]_+$ ,  $a^\dagger G a$ , and  $a G a^\dagger$ . Consider an example in which  $G = a$ . Since

$$\Lambda'_h a = -\frac{1}{\tau_h} a,$$

we find that

$$\text{Tr} \{ (\Lambda_h \rho) a F(\mathbf{I}) \} = -\frac{1}{\tau_h} \langle a F(\mathbf{I}) \rangle.$$

Similarly, since

$$\Lambda'_h a^\dagger a = -\frac{2}{\tau_h} (a^\dagger a - n_h),$$

we have

$$\text{Tr} \{ (\Lambda_h \rho) a^\dagger a F(\mathbf{I}) \} = -\frac{2}{\tau_n} \langle (a^\dagger a - n_h) F(\mathbf{I}) \rangle.$$

These observations regarding  $\Lambda_h$  support the use of equation (7.13) as a simple way to include the effects of spin relaxation in the model of the spin-resonator system. If we assume that the spin relaxation can be characterized by a superoperator of the form

$$\Lambda_s \rho = \sum_k f_k(\mathbf{I}) \rho g_k(\mathbf{I}), \quad (7.14)$$

for some spin operators  $f_k(\mathbf{I})$ ,  $g_k(\mathbf{I})$ , then the contribution of spin relaxation to the equation of motion for  $\langle I_+ a^\dagger - I_- a \rangle$  is given by

$$\text{Tr} \{ (\Lambda_s \rho) (I_+ a^\dagger - I_- a) \} = \text{Tr} \{ \rho (\Lambda'_s I_+) a^\dagger - \rho (\Lambda'_s I_-) a \},$$

where

$$\Lambda'_s F(\mathbf{I}) = \sum_k g_k(\mathbf{I}) F(\mathbf{I}) f_k(\mathbf{I}).$$

Equation (7.12) makes the assumption that the contribution of  $\Lambda_s$  to the equation of motion for  $\langle I_\pm \rangle$  is

$$\begin{aligned} -\frac{1}{T_2} \langle I_\pm \rangle &= \text{Tr} \{ (\Lambda_s \rho) I_\pm \} \\ &= \text{Tr} \{ \rho \Lambda'_s I_\pm \} \\ &= \langle \Lambda'_s I_\pm \rangle, \end{aligned}$$

which suggests the additional assumption

$$\Lambda'_s I_\pm = -\frac{1}{T_2} I_\pm. \quad (7.15)$$

Equation (7.13) follows from the assumptions (7.14) and (7.15).

### 3 Steady-state number of quanta in the resonator

Equations of motion for expectation values can be obtained by multiplying both sides of the master equation (7.9) by an operator and taking the trace. The following interaction-frame equations can be obtained in this way:

$$\frac{d}{dt} \langle a^\dagger a \rangle = K - \frac{2}{\tau_h} (\langle a^\dagger a \rangle - n_h), \quad (7.16)$$

$$K \equiv -ig \langle I_+ a^\dagger - I_- a \rangle \quad (7.17)$$

$$\frac{d}{dt} \langle I_z \rangle = -\frac{1}{T_1} \left( \langle I_z \rangle - \frac{1}{2} PN \right) + K, \quad (7.18)$$

$$\frac{d}{dt} \langle I_+ a^\dagger - I_- a \rangle = -\frac{1}{\tau_1} \langle I_+ a^\dagger - I_- a \rangle - 4ig \langle I_z a^\dagger a \rangle + 2ig \langle I_- I_+ \rangle, \quad (7.19)$$

$$\frac{1}{\tau_1} \equiv \frac{1}{\tau_h} + \frac{1}{T_2}. \quad (7.20)$$

Note that  $K$  represents the rate at which  $\langle I_z \rangle$  changes due to the spin-resonator interaction. Equation (A.10) of Appendix A gives a formula for this rate in the limiting case where the time constants  $T_1$  and  $T_2$  are long, with  $\tau_h$  so short that the resonator is only weakly perturbed from thermal equilibrium:

$$\frac{\Delta \langle I_z \rangle}{\Delta t} = -4g^2 \tau_h n_h \langle I_z \rangle + 2g^2 \tau_h \langle I_- I_+ \rangle. \quad (7.21)$$

By using (7.16) through (7.20) to do a steady-state calculation, we can lift this restriction on  $T_1$  and  $T_2$ , and allow for the possibility that the resonator's state is strongly perturbed from equilibrium with the thermal reservoir. Setting the left side of (7.19) equal to zero and using (7.17) to eliminate  $\langle I_+ a^\dagger - I_- a \rangle$  gives

$$K_\infty = -4g^2 \tau_1 \langle I_z a^\dagger a \rangle_\infty + 2g^2 \tau_1 \langle I_- I_+ \rangle_\infty. \quad (7.22)$$

(Note that throughout this chapter, the subscript " $\infty$ " indicates a steady-state value.) The similarity between (7.21) and (7.22) is striking. The switch from  $\tau_h$  in (7.21) to  $\tau_1$  in (7.22) is due to the fact that the superoperator  $\Lambda_s$  has been included in the model, and  $\tau_1$  is replaced by  $\tau_h$  in the limit of long  $T_2$ . In both equations, the first

term on the right-hand side of the equation characterizes stimulated emission and absorption by the spins, while the second term on the right-hand side characterizes spontaneous emission.

We assume that  $\langle I_z \rangle$  is sufficiently large, and that the spins interact with the resonator for a short enough period that

$$\langle I_z a^\dagger a \rangle_\infty \approx \langle I_z \rangle_\infty \langle a^\dagger a \rangle_\infty.$$

For simplicity, we also assume that the flow of spins through the cavity is fast enough that the resonator-induced spin-spin correlations discussed in section 4 of chapter 3 remain weak:

$$\langle I_x^2 + I_y^2 \rangle \approx N/2, \quad (7.23)$$

where  $N$  is the number of spins interacting with the oscillator. These approximations allow us to express  $K_\infty$  as

$$K_\infty = -\frac{2}{\tau_c} (\langle a^\dagger a \rangle_\infty - n_c), \quad (7.24)$$

$$n_c \equiv \frac{1}{2} \left( \frac{N}{2\langle I_z \rangle_\infty} - 1 \right), \quad (7.25)$$

$$\tau_c \equiv (2g^2\tau_1 \langle I_z \rangle_\infty)^{-1}. \quad (7.26)$$

Note that equation (7.25) defines  $n_c$  to be the number of quanta in the resonator when it is at the steady-state "spin temperature," that is, the temperature defined by the values of  $N$  and  $\langle I_z \rangle_\infty$ . In the steady state, equation (7.16) can be expressed as

$$0 = -\frac{2}{\tau_c} (\langle a^\dagger a \rangle_\infty - n_c) - \frac{2}{\tau_h} (\langle a^\dagger a \rangle_\infty - n_h), \quad (7.27)$$

where  $n_c$  and  $n_h$  are the equilibrium values of  $\langle a^\dagger a \rangle$  at the respective temperatures associated with the spins and the warm bath. It is natural to interpret equation (7.27) as implying that  $2/\tau_c$  is a rate constant for the relaxation of  $\langle a^\dagger a \rangle$  toward the equilibrium value  $n_c$  determined by the "spin temperature," just as  $2/\tau_h$  is the rate constant for relaxation of  $\langle a^\dagger a \rangle$  toward the value  $n_h$ . As in the simpler analysis

presented in section 1, the steady-state number of quanta in the resonator can then be expressed as

$$\langle a^\dagger a \rangle_\infty = \frac{\tau_h n_c + \tau_c n_h}{\tau_h + \tau_c}. \quad (7.28)$$

The rate constant  $2/\tau_c$  characterizes the cooling of the resonator by many cold spins, while the rate constant  $R_0$  characterizes the cooling of spins by a single resonator at zero Kelvins:

$$\frac{2}{\tau_c} = 2g^2\tau_1 (2\langle I_z \rangle_\infty), \quad (7.29)$$

$$R_0 = 2g^2\tau_h. \quad (7.30)$$

In the case where  $T_2 \gg \tau_h$ , spin relaxation does not play a significant role in disrupting the development of spin-resonator correlations, and  $\tau_1 \approx \tau_h$ . Under these conditions, the rate constants given by (7.29) and (7.30) differ by the factor  $2\langle I_z \rangle_\infty$ , which can be considered the "effective number of spins at zero Kelvins" which are cooling the resonator. In considering numerical examples such as those presented in section 6 of chapter 5, we have found that  $R_0$  achieved values of  $\sim 1/\text{s}$  when the dimensions of the resonator's magnets are of order 100 nm or less. The presence of the additional factor  $2\langle I_z \rangle_\infty$  in equation (7.29) suggests the possibility of observing the exchange of entropy between spins and resonator at larger size scales, and in section 4 we present a numerical example to characterize the regime in which substantial cooling could be observed.

Additional support for the interpretation of  $2/\tau_c$  as a rate constant for cooling may be obtained in the case where the spins pass by the resonator quickly enough that they are only weakly perturbed from the hyperpolarized state. In this case, the method of coarse-graining introduced in Appendix A can be used to derive a formula for

$$K \equiv -ig \langle I_+ a^\dagger - I_- a \rangle$$

which is correct to second order in the coupling constant  $g$ . Equations (7.18) and (A.4), as well as equations of motion for  $I_- I_+$  and  $I_z a^\dagger a$ , are converted to integral

equations. (In determining the contribution of  $\Lambda_s$  to these equations, we assume for simplicity that the flow of spins past the resonator causes  $\langle I_z a^\dagger a \rangle$  and  ${}_1\langle I_- I_+ \rangle$  to relax with time constant  $T_1 = T_2$ .) We express  $K$  as an iterated integral and we evaluate the integral over a time step  $\Delta t$  which is long compared to  $\tau_h$  and  $T_1$ . Since  $\Delta t$  is long compared to the period of time during which spin-resonator correlations survive, we can neglect initial spin-resonator correlations. Making the approximation (7.23) then yields the expression

$$K = -2g^2\tau_1(PN) (\langle a^\dagger a \rangle - n_c), \quad (7.31)$$

which implies that

$$2g^2\tau_1(PN)$$

is the rate constant for relaxation of  $\langle a^\dagger a \rangle$  toward equilibrium with the spins. Note that this rate constant differs from that of (7.29) in replacing  $2\langle I_z \rangle_\infty$  by the hyperpolarized value of  $2\langle I_z \rangle$ . This discrepancy is a result of the use of second-order perturbation theory in calculating the rate constant. Roughly speaking, we can say that changes in  $\langle I_z \rangle$  due to interaction with the resonator are at least second-order in  $g$ . If we replace  $PN$  in (7.31) by an expression which includes effects which are second-order or higher in  $g$ , the resulting expression will include terms of 4th order or higher in  $g$ . Since the derivation of (7.31) only considers terms up to second order in  $g$ , it cannot incorporate the relaxation of  $\langle I_z \rangle$  to  $\langle I_z \rangle_\infty$ .

At this point it may be tempting to conclude that the cold spins act as a bath characterized by ringdown time  $\tau_c$  and temperature

$$T_c = \frac{\hbar\omega_h}{k_B \ln(1 + n_c^{-1})}. \quad (7.32)$$

Although this approach yields the correct values for  $\langle a^\dagger a \rangle_\infty$ , the analysis in sections 5 through 7 shows that this model yields incorrect predictions for decay times of the spin-resonator modes, the resonator's response to a driving torque, and the mechanical fluctuations. Section 5 shows that in the regime where substantial cooling has

occurred, with  $\tau_h \ll T_2$ , the spins and resonator are so strongly coupled that it is not possible to distinguish a mechanical mode or a spin mode.

## 4 Numerical example of cooling

This section presents a numerical example based on a simplified model in which polarized liquid xenon flows through a Halbach cylinder [43]. A Halbach cylinder is a circular tube of magnetic material for which the arrangement of magnetization produces a nominally uniform magnetic field within the tube and zero field outside of the tube. The Halbach cylinder is chosen to yield a simple, optimistic estimate of the size scale at which polarized spins could substantially cool a resonator, since the nominally uniform field inside the cylinder would allow a relatively large volume of cold spins to interact with the resonator. For this estimate, we set aside questions having to do with the technical feasibility of the experiment (e.g., questions about fabrication of the Halbach cylinder or its thermodynamic stability at small sizes). Our goal is simply to give a rough characterization of the regime in which polarized spins passing near a mechanical resonator could have a non-negligible effect on its temperature.

Consider a Halbach cylinder having inner radius  $R_i$ , outer radius  $R_o$ , and length  $3R_i$ , with magnetization  $1.5 \text{ T} / \mu_0$ . The cylinder is mounted on a torsional beam which runs parallel to the cylinder's axis and has width and thickness equal to the cylinder's inner radius. The torsional beam length is adjusted to the value necessary for resonance with the Larmor frequency of xenon in the field generated by the Halbach cylinder. We suppose that xenon with a natural composition of isotopes fills half the volume of the cylinder and that the polarization of  $^{129}\text{Xe}$  entering the cylinder is [44]

$$P = .70.$$

The triple point of xenon occurs at 0.81 atm and 161 K, and the boiling point of xenon at 1 atm is 165 K; within this temperature and pressure range the density of

Cylinder Dimensions	$\tau_h$	$T_h$	$T_\infty$	$\omega_h/2\pi$
$R_i = 500 \text{ nm}, R_o = 1 \mu\text{m}, L = 1.5 \mu\text{m}$	$290 \mu\text{s}$	300 K	104 K	11 MHz
$R_i = 500 \text{ nm}, R_o = 600 \text{ nm}, L = 1.5 \mu\text{m}$	1.3 ms	300 K	9 K	3 MHz

Table 7.1: Resonators cooled by hyperpolarized spins

liquid xenon is approximately  $22.6 \text{ kmol/m}^3$  [45], and we assume this density for our estimate. If the resonator's quality factor is  $Q = 10,000$ , then we obtain the results shown in table 7.1, where

$$T_\infty = \frac{\hbar\omega_h}{k_B \ln(1 + n_\infty^{-1})}, \quad (7.33)$$

$$n_\infty \equiv \langle a^\dagger a \rangle_\infty.$$

(Decreasing the ratio  $R_o/R_i$  between the outer radius and the inner radius causes  $T_\infty$  to decrease continually toward  $T_\infty \approx 8 \text{ K}$  as  $R_o \rightarrow R_i$ .)

The transverse decay time of liquid xenon has been measured at 1300 s [46], which allows us to consider  $T_2$  to be determined by the rate at which spins flow through the cylinder. For the resonators of table 7.1, the rate at which quanta are donated to the spins is such that  $\langle I_z \rangle$  changes by 0.6% or less during a time period of length  $\tau_h$ , and so we consider the interaction time between a spin and the resonator to be substantially larger than  $\tau_h$  without contradicting our assumptions that  $\langle I_z a^\dagger a \rangle_\infty \approx \langle I_z \rangle_\infty n_\infty$  and  $\langle I_x^2 + I_y^2 \rangle \approx N/2$ . The disruption of spin-resonator correlations is thus primarily due to the thermal torque which acts on the resonator, and

$$\tau_1 \approx \tau_h.$$

The value of  $T_\infty$  scales sharply with resonator size. Scaling up the first cylinder in table 7.1 by a factor of 10 and the second by a factor of 100 while retaining the assumption that  $Q = 10,000$ , gives steady-state temperatures near 300 K, as shown in table 7.2. (Note that scaling the Halbach cylinder does not change the field at the spins, and so the frequency, quality factor, and ringdown time are all held constant as we scale up the resonators in table 7.1.)

Cylinder Dimensions	$T_h$	$T_\infty$
$R_i = 5 \mu\text{m}, R_o = 10 \mu\text{m}, L = 15 \mu\text{m}$	300 K	294 K
$R_i = 50 \mu\text{m}, R_o = 60 \mu\text{m}, L = 150 \mu\text{m}$	300 K	297 K

Table 7.2: Scaled-up spin-resonator systems

It may be considered surprising that cooling becomes negligible at size scales of  $\sim 10 \mu\text{m}$ , since one might have guessed that the presence of the term  $2 \langle I_z \rangle_\infty$  in (7.29) would permit cooling to be observed at larger size scales. The nature of the scaling can be clarified by noting that

$$\begin{aligned} \frac{2}{\tau_c} &= 2g^2\tau_h (2 \langle I_z \rangle_\infty) \\ &= \frac{\hbar}{2} \left( \gamma \frac{dB_x}{d\theta} \right)^2 \frac{\tau_h}{\omega_h} \left[ \frac{\langle I_z \rangle_\infty}{I_h} \right]. \end{aligned} \quad (7.34)$$

In these numerical examples, the two terms which vary as the resonators scale up are grouped in square brackets on the right side of (7.34). The torsional beams make a negligible contribution to the moment of inertia  $I_h$  in these examples, and we need only consider the cylinder's moment of inertia in estimating  $I_h$ . Since the shape of the cylinder does not change during the scaling, we have

$$\begin{aligned} I_h &\sim r^5, \\ \langle I_z \rangle_\infty &\sim r^3, \end{aligned}$$

where  $r$  is a characteristic dimension of the cylinder, such as the inner radius. It follows that

$$\frac{2}{\tau_c} \sim r^{-2}$$

in these examples. It is the strong scaling of  $g^2$  with size which causes the cooling to become negligible as the resonator is scaled up to have dimensions of order  $10 \mu\text{m}$ . (Note that although in our example, the size dependence of  $g^2$  is determined solely by the moment of inertia, similar scaling is obtained for a translational resonator. In this case, the moment of inertia would be replaced by a mass, and the scale-invariant

Cylinder Dimensions	$2/\tau_h$	$2/\tau_c$
$R_i = 500 \text{ nm}, R_o = 1 \mu\text{m}$	$7000 \text{ s}^{-1}$	$13,000 \text{ s}^{-1}$
$R_i = 5 \mu\text{m}, R_o = 10 \mu\text{m}$	$7000 \text{ s}^{-1}$	$130 \text{ s}^{-1}$

Table 7.3: Dependence of rate constants on size

term  $dB_x/d\theta$  would be replaced by a gradient scaling as  $r^{-1}$ .) Table 7.3 shows how the rate constants  $2/\tau_c$  and  $2/\tau_h$  depend on size for the example resonator having  $R_o/R_i = 2$ .

## 5 Modes of the spin-resonator system

In estimating a "steady-state temperature"  $T_\infty$  based on the expectation value  $n_\infty$ , we did not consider the question of whether the cooled oscillator "continues to look like a mechanical oscillator" in the regime where  $T_\infty$  differs substantially from  $T_h$ . In this section, we answer that question by studying the modes of the spin-resonator system. Although most of our results will be derived from the master equation (7.9), the nature of the system can initially be clarified using a model in which spins and resonator are coupled by the lab-frame Hamiltonian

$$\mathcal{H}_{sh} = -\gamma\hbar \frac{dB_x}{d\theta} I_x \theta,$$

rather than the interaction-frame Hamiltonian

$$V = g (I_+ a^\dagger + I_- a)$$

obtained using the rotating-wave approximation. The lab-frame equations of motion are

$$\frac{d}{dt} \langle \theta \rangle = \frac{\langle p_\theta \rangle}{I_h} - \frac{\langle \theta \rangle}{\tau_h}, \quad (7.35)$$

$$\frac{d}{dt} \langle p_\theta \rangle = -I_h \omega_h^2 \langle \theta \rangle - \frac{\langle p_\theta \rangle}{\tau_h} + \gamma \hbar \frac{dB_x}{d\theta} \langle I_x \rangle, \quad (7.36)$$

$$\frac{d}{dt} \langle I_x \rangle = -\omega_0 \langle I_y \rangle - \frac{\langle I_x \rangle}{T_2}, \quad (7.37)$$

$$\frac{d}{dt} \langle I_y \rangle = \omega_0 \langle I_x \rangle - \frac{\langle I_y \rangle}{T_2} + \gamma \frac{dB_x}{d\theta} \langle I_z \theta \rangle, \quad (7.38)$$

$$\frac{d}{dt} \langle I_z \rangle = -\frac{1}{T_1} \left( \langle I_z \rangle - \frac{PN}{2} \right) - \gamma \frac{dB_x}{d\theta} \langle I_y \theta \rangle. \quad (7.39)$$

Note the formal similarity between the equations for the oscillator variables  $\langle \theta \rangle$ ,  $\langle p_\theta \rangle$  and those of the transverse spin variables  $\langle I_x \rangle$ ,  $\langle I_y \rangle$ . Indeed, we can write second-order differential equations for  $\langle \theta \rangle$  and  $\langle I_x \rangle$  which highlight the formal similarity:

$$\frac{d^2}{dt^2} \langle \theta \rangle + \frac{2}{\tau_h} \frac{d}{dt} \langle \theta \rangle + \left( \omega_h^2 + \frac{1}{\tau_h^2} \right) \langle \theta \rangle = \frac{\gamma \hbar}{I_h} \frac{dB_x}{d\theta} \langle I_x \rangle, \quad (7.40)$$

$$\frac{d^2}{dt^2} \langle I_x \rangle + \frac{2}{T_2} \frac{d}{dt} \langle I_x \rangle + \left( \omega_h^2 + \frac{1}{T_2^2} \right) \langle I_x \rangle = \omega_h \gamma \frac{dB_x}{d\theta} \langle I_z \theta \rangle. \quad (7.41)$$

For sufficiently large  $\langle I_z \rangle$  and short interaction time between each spin and the resonator, we can approximate  $\langle I_z \theta \rangle$  by  $\langle I_z \rangle \langle \theta \rangle$  and consider  $\langle I_z \rangle$  to be approximately constant. Under these conditions, the evolution of the variables  $\langle \theta \rangle$ ,  $\langle I_x \rangle$  is formally equivalent to that of two coupled oscillators, and interpreting the motion in this way can lead to an intuitive understanding of the system. We define the moment of inertia  $I_f$  of the formal oscillator associated with the variable  $\langle I_x \rangle$  to be

$$I_f = \frac{\hbar}{\omega_h \langle I_z \rangle_\infty},$$

and we rewrite (7.40) and (7.41) as

$$I_h \frac{d^2}{dt^2} \langle \theta \rangle + \frac{2I_h}{\tau_h} \frac{d}{dt} \langle \theta \rangle + I_h \left( \omega_h^2 + \frac{1}{\tau_h^2} \right) \langle \theta \rangle = \gamma \hbar \frac{dB_x}{d\theta} \langle I_x \rangle, \quad (7.42)$$

$$I_f \frac{d^2}{dt^2} \langle I_x \rangle + \frac{2I_f}{T_2} \frac{d}{dt} \langle I_x \rangle + I_f \left( \omega_h^2 + \frac{1}{T_2^2} \right) \langle I_x \rangle = \gamma \hbar \frac{dB_x}{d\theta} \langle \theta \rangle. \quad (7.43)$$

The coupling between the two formal oscillators is associated with the potential function

$$V_1 = -\gamma \hbar \frac{dB_x}{d\theta} \langle I_x \rangle \langle \theta \rangle. \quad (7.44)$$

Note that a potential function of the same form is obtained when two linear harmonic oscillators are coupled by a spring. For instance, let  $x_1$  and  $x_2$  represent the coordinates of two linear oscillators, and suppose that they are coupled by a spring whose potential energy is

$$A(x_1 - x_2)^2 = Ax_1^2 + Ax_2^2 - 2Ax_1x_2. \quad (7.45)$$

In (7.45), the terms  $Ax_1^2$  and  $Ax_2^2$  can be considered to modify the potential wells of the individual oscillators, while the term  $-2Ax_1x_2$  couples the two oscillators. We can therefore visualize the spin-resonator system as consisting of two oscillators coupled by a spring.

In order to obtain tractable solutions for the evolution of the system, we must replace (7.35) through (7.38) with equations obtained under the rotating-wave approximation. The master equation (7.9), in combination with the approximations

$$\begin{aligned} \langle I_z a \rangle &\approx \langle I_z \rangle \langle a \rangle, \\ \langle I_z \rangle &\approx \text{constant} \\ &\equiv \langle I_z \rangle_\infty, \end{aligned}$$

yields a linear equation in the two variables  $\langle a \rangle$ ,  $\langle I_+ \rangle$ :

$$\frac{d}{dt} \langle a \rangle = - \left( i\omega_h + \frac{1}{\tau_h} \right) \langle a \rangle - ig \langle I_+ \rangle, \quad (7.46)$$

$$\frac{d}{dt} \langle I_+ \rangle = - \left( i\omega_h + \frac{1}{T_2} \right) \langle I_+ \rangle - 2ig \langle I_z \rangle_\infty \langle a \rangle. \quad (7.47)$$

We look for a steady-state solution to equations (7.46) and (7.47) of the form

$$\langle a \rangle (t) = e^{-(i\omega' + 1/\tau')t} \langle a \rangle (0), \quad (7.48)$$

$$\langle I_+ \rangle (t) = e^{-(i\omega' + 1/\tau')t} \langle I_+ \rangle (0), \quad (7.49)$$

$$\langle I_+ \rangle (0) = \eta \langle a \rangle (0). \quad (7.50)$$

A motivation for this ansatz is the fact that steady motion of the oscillator creates a sinusoidal transverse field; in the limit of weak spin-oscillator coupling, we expect the response of the spins to be similar to the linear response described by the steady-state solutions to the Bloch equations. Substituting (7.48) through (7.50) into (7.46) and (7.47) yields a solution for  $\eta$ ,  $\omega'$ ,  $\tau'$ . We obtain

$$\eta = \frac{1 \pm \sqrt{1 - 8 \langle I_z \rangle_\infty (gb)^2}}{2gb} i, \quad (7.51)$$

$$\frac{1}{b} \equiv \left( \frac{1}{\tau_h} - \frac{1}{T_2} \right), \quad (7.52)$$

and

$$\omega' = \omega_h + g \operatorname{Re}(\eta), \quad (7.53)$$

$$1/\tau' = 1/\tau_h - g \operatorname{Im}(\eta). \quad (7.54)$$

The physical content of these equations can be clarified by writing (7.53) and (7.54) in a more explicit form. Define

$$s \equiv 8 \langle I_z \rangle_\infty (gb)^2$$

and consider two cases. For  $s \leq 1$ , we have

$$\omega' = \omega_h, \quad (7.55)$$

$$\frac{1}{\tau'} = \frac{1}{2} \left( \frac{1}{\tau_h} + \frac{1}{T_2} \right) \pm \frac{\sqrt{1-s}}{2} \left( \frac{1}{\tau_h} - \frac{1}{T_2} \right), \quad (7.56)$$

while for  $s > 1$ , we have

$$\omega' = \omega_h \pm \frac{\sqrt{s-1}}{2} \left( \frac{1}{\tau_h} - \frac{1}{T_2} \right), \quad (7.57)$$

$$\frac{1}{\tau'} = \frac{1}{2} \left( \frac{1}{\tau_h} + \frac{1}{T_2} \right). \quad (7.58)$$

Equations (7.55) through (7.58) can be understood as natural results for a system of two coupled oscillators. In the limit of strong coupling between the oscillators (that is, large  $g$  or large  $\langle I_z \rangle_\infty$ ) or similar dissipation rates for the two oscillators (that is, large  $|b|$ ), energy can be exchanged between the oscillators quickly enough that the net dissipation rate is just the average of  $1/\tau_h$  and  $1/T_2$ . The ratio  $|\langle a \rangle / \langle I_+ \rangle|$  that characterizes the relative excitation of the spins and the resonator is equal for the two modes, so neither mode can be specifically considered to be the mechanical mode. In the limit of weak coupling or dissimilar dissipation rates, equation (7.56) shows that the ringdown times for the two modes approach  $\tau_h$  and  $T_2$  as  $g \rightarrow 0$ . The solution with ringdown time  $\sim \tau_h$  has larger excitation in the mechanical oscillator than the solution with ringdown time  $\sim T_2$ .

In section 4, we presented numerical examples in which resonators were cooled by hyperpolarized spins from the ambient temperature of 300 K to temperatures of 100 K or less. The results obtained in the current discussion imply that for these numerical examples, the spins and resonator are so strongly coupled that it is not possible to distinguish a mechanical mode or a spin mode. Indeed, we will now show that the value  $s = 1$ , which corresponds to the disappearance of distinct spin and mechanical modes, occurs when

$$T_\infty \approx \frac{4}{5} T_h.$$

Note first that when one of the decay times  $\tau_h$ ,  $T_2$  is much longer than the other, the term  $s$  which determines the form of the modes can be written in a simpler way, since in this case

$$b \approx \min \{ \tau_h, T_2 \}.$$

We find that

$$s \approx \frac{4\tau_1}{\tau_c},$$

where the rate constant  $2/\tau_c$  for cooling of the resonator by the spins is given by (7.29), and  $\tau_1$  is defined by (7.20). When  $\tau_h \ll T_2$ , as in the numerical examples of cooling that we considered, the transition to the strong-coupling regime occurs when

$$\frac{4\tau_h}{\tau_c} \approx 1. \quad (7.59)$$

Equation (7.59) implies that

$$\begin{aligned} n_\infty &= \frac{\tau_h n_c + \tau_c n_h}{\tau_h + \tau_c} \\ &\approx \frac{4}{5} n_h, \end{aligned}$$

where we have assumed that  $4n_h \gg n_c$ . If

$$n_\infty \gg 1,$$

it follows that

$$T_\infty \approx \frac{4}{5} T_h, \quad (7.60)$$

since

$$\begin{aligned} \frac{T_\infty}{T_h} &= \frac{\ln(1 + 1/n_h)}{\ln(1 + 1/n_\infty)} \\ &\approx \frac{n_\infty}{n_h}. \end{aligned}$$

Substantial cooling of the resonator by cold spins therefore requires that the coupling

be strong enough to transform the mechanical mode into a mode which includes significant contributions from both mechanical motion and spin precession. Consistent with this observation is the fact that for the numerical example in which  $T_h = 300$  K to and  $T_\infty = \sim 100$  K,

$$s \approx 8.$$

In section 1 we analyzed the spin-resonator system using a simple model in which the cold spins were represented by a cold bath whose properties were not affected by the warm bath. This model is incorrect in the general case, for two reasons. First, the theory supporting the use of a linear, time-independent superoperator to describe relaxation due to coupling with a reservoir [7] is valid only in the limit of weak coupling with the reservoir. As a result, it is only in the limit of weak-spin resonator coupling ( $s \ll 1$ ) that the cold spins might be expected to behave as a cold reservoir. Second, the rate constant  $2/\tau_c$ , which characterizes the resonator's relaxation toward equilibrium with the spins, depends on  $\tau_h$ , that is, on the coupling between the resonator and the warm bath. Except in the limiting case where  $2/\tau_c$  is independent of the resonator's coupling to the warm bath, it is incorrect to represent the spins as a reservoir which acts independently of the warm bath. This limit corresponds to the condition  $T_2 \ll \tau_h$ , since this condition guarantees that it is spin relaxation rather than the ringdown time  $\tau_h$  that limits the lifetime of spin-resonator correlations. In the regime defined by

$$s \ll 1, \tag{7.61}$$

$$T_2 \ll \tau_h, \tag{7.62}$$

however, we might expect to recover the results obtained from equation (7.1) to be valid. Indeed, replacing  $\sqrt{1-s}$  by  $1-s/2$  in (7.56) and using condition (7.62) to simplify the resulting expression shows that the decay time of the mechanical mode

is

$$\begin{aligned} \frac{1}{\tau_h} + 2g^2 T_2 \langle I_z \rangle_\infty &= \frac{1}{\tau_h} + \frac{1}{\tau_c} \\ &\equiv \frac{1}{\tau_\infty}, \end{aligned}$$

which agrees with equation (7.3), the result obtained by treating the cold spins as an independent thermal bath.

## 6 Response of the system to a torque acting on the resonator

In order to determine how the coupling to the hyperpolarized spins modifies the resonator's sensitivity as a detector of an external torque, we will calculate the system's response to a torque acting on the resonator. An external torque  $f(t)$  corresponds to a term  $-f(t)\theta$  added to the oscillator's Hamiltonian  $H_{\text{osc}}$  in (7.9), so that the equations governing  $\langle \theta \rangle$  and  $\langle I_+ \rangle$  become

$$\frac{d}{dt} \langle a \rangle = - \left( i\omega_h + \frac{1}{\tau_h} \right) \langle a \rangle - ig \langle I_+ \rangle + i \sqrt{\frac{1}{2I_h \hbar \omega_h}} f(t), \quad (7.63)$$

$$\frac{d}{dt} \langle I_+ \rangle = - \left( i\omega_h + \frac{1}{T_2} \right) \langle I_+ \rangle - 2ig \langle I_z \rangle_\infty \langle a \rangle. \quad (7.64)$$

We consider the case where

$$f(t) = F e^{-i\omega t} \quad (7.65)$$

and we look for a steady-state solution of the form

$$\langle a \rangle(t) = A_\omega e^{-i\omega t}, \quad (7.66)$$

$$\langle I_+ \rangle(t) = \eta_\omega \langle a \rangle(t) = \eta_\omega A_\omega e^{-i\omega t}. \quad (7.67)$$

The solution for  $A_\omega$  and  $\eta_\omega$  can be expressed as

$$\left\{ (\omega - \omega_h) f(\omega) + \frac{i}{\tau_d(\omega)} \right\} A_\omega = -\sqrt{\frac{1}{2I_h \hbar \omega_h}} F, \quad (7.68)$$

$$\eta_\omega = \frac{2g \langle I_z \rangle_\infty}{(\omega - \omega_h) + i/T_2}, \quad (7.69)$$

where

$$f(\omega) \equiv 1 - \frac{1}{\tau_c \tau_1 \{(\omega - \omega_h)^2 + 1/T_2^2\}}, \quad (7.70)$$

$$1/\tau_d(\omega) \equiv \frac{1}{\tau_h} + \frac{1}{T_2 \tau_c \tau_1 \{(\omega - \omega_h)^2 + 1/T_2^2\}}. \quad (7.71)$$

The content of (7.68) becomes clearer if we compare it to the formula obtained in the case where the coupling constant  $g$  is zero:

$$\left\{ (\omega - \omega_h) + \frac{i}{\tau_h} \right\} A_\omega = -\sqrt{\frac{1}{2I_h \hbar \omega_h}} F. \quad (7.72)$$

Although (7.72) is an unusual way to describe the steady-state response of the oscillator, it is straightforward to verify that in the limit of weak coupling to the reservoir, it yields the familiar steady-state expression for  $\langle \theta \rangle(t)$ . We may calculate the mechanical response to a torque at frequency  $\omega_h$  as if the ringdown time were

$$\frac{1}{\tau_d} = \frac{1}{\tau_h} + 2g^2 T_2 \langle I_z \rangle_\infty. \quad (7.73)$$

At frequencies  $\omega \neq \omega_h$ , the resonator responds as if its ringdown time were  $\tau_d(\omega)$  and the driving torque were off resonance by  $(\omega - \omega_h) f(\omega)$ .

In the case where (7.62) holds, we recover the expression  $\tau_\infty$  obtained by treating the spins as a cold bath:

$$\begin{aligned} \frac{1}{\tau_d} &= \frac{1}{\tau_h} + 2g^2 \tau_1 \langle I_z \rangle_\infty \\ &= \frac{1}{\tau_\infty}. \end{aligned}$$

For the numerical examples we considered in section 4, however, the resonator's linear response will be considerably weaker at resonance than it would be for a mechanical oscillator with ringdown time  $\tau_\infty$ , since

$$\begin{aligned} \frac{1}{\tau_d} &= \frac{1}{\tau_h} + 2g^2 T_2 \langle I_z \rangle_\infty \\ &\gg \frac{1}{\tau_h} + 2g^2 \tau_h \langle I_z \rangle_\infty \\ &\approx \frac{1}{\tau_\infty}. \end{aligned}$$

A physical interpretation of this conclusion is that in the presence of the cold spins with long relaxation time, energy initially donating to the resonator by the driving torque is efficiently transferred onward to the cold spins, since the long relaxation time of the spins allows for a strong resonant response to the driving of the spins by the mechanical resonator. The transverse spin magnetization then exerts a torque on the resonator which counteracts the external torque and prevents a large mechanical response from developing.

The correctness of this interpretation can be demonstrated formally by considering the steady-state form of equation (7.63):

$$-i\omega A_\omega = -\left(i\omega_h + \frac{1}{\tau_h}\right) A_\omega - ig\eta_\omega A_\omega + i\sqrt{\frac{1}{2I_h\hbar\omega_h}} F. \quad (7.74)$$

The four terms in (7.74) represent distinct physical contributions which must cancel in the steady state. The last term on the right side of the equation represents the external torque, while the term  $-(i\omega_h + 1/\tau_h) A_\omega$  represents the torques associated with the potential well and the damping by the warm bath. The term  $-i\omega A_\omega$  can be interpreted as an "inertial torque." The remaining term,  $-ig\eta_\omega A_\omega$ , characterizes the torque exerted on the resonator by the spins. The torque associated with the imaginary part of  $-ig\eta_\omega$  may be interpreted as modifying the resonator's potential energy, since it oscillates in phase with the torque exerted by the potential well, and it is responsible for replacing the term  $(\omega - \omega_h)$  in (7.72) by  $(\omega - \omega_h) f(\omega)$  in (7.68). The torque associated with the real part of  $-ig\eta_\omega$  acts in phase with the damping

torque exerted by the warm bath, and it can be considered to damp the mechanical motion, causing  $\tau_h$  to be replaced by  $\tau_d(\omega)$ . Equation (7.69) shows that the value of  $\eta_\omega$  is peaked around  $\omega = \omega_h$ , and in the case where  $T_2$  is long, the peak value of  $\eta_\omega$  will be large. This peak value will be associated with a large transverse magnetization which exerts a damping torque on the resonator. Even in the case where the condition

$$\begin{aligned} \frac{1}{\tau_c} &= 2g^2\tau_h \langle I_z \rangle_\infty \\ &\ll \frac{1}{\tau_h} \end{aligned}$$

implies that cooling will be negligible, a sufficiently large value of  $T_2$  will guarantee that during steady-state driving, most of the energy donated to the spin-resonator system by an external torque acting on the resonator will take the form of spin excitation. In the regime where  $T_2 \gg \tau_h$ , the mechanical resonator could be considered a device for transferring an external torque at frequency  $\omega_h$  into excitation of hyperpolarized spins.

Although the mechanical response to a driving torque at  $\omega_h$  becomes weak when  $T_2 \gg \tau_h$ , equations (7.70) and (7.71) allow for the possibility of a resonant mechanical response at frequencies which are out of resonance with the spins. This occurs at frequencies  $\omega$  sufficiently far from  $\omega_h$  that the damping torque exerted by the spins is negligible, but close enough to  $\omega_h$  that the resonator's potential function is modified by the spins, yielding

$$(\omega - \omega_h) f(\omega) = 0.$$

Under these conditions, the mechanical response has the same amplitude that it would if the spins were absent and the driving torque were at frequency  $\omega_h$ . To demonstrate this formally, note that when

$$(\omega - \omega_h)^2 \gg \frac{1}{T_2^2}, \quad (7.75)$$

the resonator responds as if its ringdown time were

$$\frac{1}{\tau_d} = \frac{1}{\tau_h} \left( 1 + \frac{1}{T_2\tau_c(\omega - \omega_h)^2} \right), \quad (7.76)$$

and the driving torque were off resonance by

$$(\omega - \omega_h) f(\omega) = (\omega - \omega_h) \left( 1 - \frac{1}{\tau_c \tau_h (\omega - \omega_h)^2} \right). \quad (7.77)$$

When  $\omega$  satisfies

$$(\omega - \omega_h)^2 \gg \frac{1}{\tau_c T_2} \quad (7.78)$$

in addition to (7.75), then

$$\tau_d \approx \tau_h. \quad (7.79)$$

If

$$\tau_c \leq T_2, \quad (7.80)$$

then condition (7.75) automatically holds when (7.78) does, and we assume that this is the case, since  $\tau_c \geq T_2 \gg \tau_h$  would otherwise imply that cooling is negligible. The condition  $T_2 \gg \tau_h$  then allows us to choose  $\omega$  such that (7.75) and

$$\frac{1}{\tau_c \tau_h (\omega - \omega_h)^2} \approx 1 \quad (7.81)$$

are both satisfied. Equation (7.77), (7.79), and (7.81) then imply that the resonator responds as if the spins were absent and  $\omega$  were resonant with the mechanical frequency. Note that in the limit of strong-coupling, defined by  $s \gg 1$ , equation (7.81) is satisfied at the frequencies of the two modes of the system.

As an illustration, we consider the example resonator of table 7.1 which is cooled from  $T_h = 300$  K to  $T_\infty = 104$  K. The rate at which quanta are donated to the spins is such that  $\langle I_z \rangle$  changes by 0.1% during a time period of length  $\tau_h$ , and so we may choose the flow rate such that the interaction time between spins and resonator is  $T_2 = 50\tau_h$ , without invalidating the assumption that the spins are only weakly perturbed from the hyperpolarized state during their interaction with the resonator. Since

$$\tau_h \approx 2\tau_c,$$

conditions (7.78) can be expressed as

$$(\omega - \omega_h)^2 \gg \frac{1}{25\tau_h^2},$$

and the zero of  $f(\omega)$  occurs at

$$(\omega - \omega_h)^2 \approx \frac{2}{\tau_h^2}. \quad (7.82)$$

When  $\omega$  satisfies (7.82), the mechanical response has the same magnitude that it would have if the spins were absent and  $\omega$  were resonant with the mechanical frequency.

## 7 The cooled mode as a sensitive detector?

Equation (7.5), obtained by modelling the spins as a cold bath, predicts that the noisy thermal torque which acts on the resonator will not be diminished by the presence of the cold spins. To investigate the validity of this result, we use the symmetric correlation function

$$C(t_2 - t_1) = \frac{1}{2} \langle \theta(t_2)\theta(t_1) - \theta(t_1)\theta(t_2) \rangle$$

to evaluate the thermal fluctuations of a system. We assume that the mechanical fluctuations during driving by an external torque can be estimated using the steady-state correlation function during cooling in the absence of an external torque. As support for this approach, we note that our model of the spin-resonator system has yielded a linear system, and that the motion of such a system under the influence of a driving force or torque is the sum of the steady-state driven motion plus motion identical with that of the undriven system.

The details of the derivation, as well as the general formula for  $C(t)$ , are presented in Appendix N. In the limit where (7.61) and (7.62) hold, we recover the results obtained by treating the cold spins as a thermal bath: the correlation function reduces to that of an oscillator which has ringdown time  $\tau_\infty$  and is at temperature

$T_\infty$ . The examples we considered in which cooling was substantial had  $T_2 \gg \tau_h$  and  $s \gg 1$ , and in this regime,  $C(t)$  can be expressed as

$$C(t) \approx \exp(-t/2\tau_h) \cos(\omega_h t) \{ \langle \theta^2 \rangle_\infty \cos(dt) - c_2 \langle I_y \theta \rangle_\infty \sin(dt) \}, \quad t > 0 \quad (7.83)$$

$$\approx \frac{\hbar}{I_h \omega_h} n_\infty \exp(-t/2\tau_h) \cos(\omega_h t) \left\{ \cos(dt) - \sqrt{\tau_h/\tau_c} \sin(dt) \right\}, \quad t > 0 \quad (7.84)$$

$$\begin{aligned} &\approx \frac{\hbar}{I_h \omega_h} n_\infty \left( 1 + \frac{\tau_h}{\tau_c} \right) \exp(-t/2\tau_h) \times \\ &\quad \frac{\cos((\omega_h + d)t + \phi) + \cos((\omega_h - d)t - \phi)}{2}, \quad t > 0, \end{aligned} \quad (7.85)$$

where

$$\begin{aligned} d &\approx 1/\sqrt{\tau_h \tau_c}, \\ c_2 &= -\sqrt{\frac{2\hbar}{I_h \omega_h}} \frac{2g\tau_h}{\sqrt{4\tau_h/\tau_c - 1}}, \end{aligned}$$

with  $\phi$  a phase constant that can be evaluated using equation (N.23). (In making this simplification, we have also assumed  $n_\infty \gg 1/2$  and  $n_\infty \gg n_c$ .)

In the absence of the spin-resonator coupling, the correlation function would be

$$C_1(t) = \frac{\hbar}{I_h \omega_h} n_h \exp(-t/\tau_h) \cos(\omega_h t), \quad t > 0. \quad (7.86)$$

By comparing (7.83) through (7.85) with (7.86), we can give a physical interpretation of the spins' effect on the mechanical fluctuations in this regime. From (7.84), we see that in cooling the resonator, the spins reduce the instantaneous correlation  $C(0) = \langle \theta^2 \rangle$  from  $(\hbar/I_h \omega_h) n_h$  to  $(\hbar/I_h \omega_h) n_\infty$ , the same value it would have for an oscillator at temperature  $T_\infty$ . The coupling to the spins also slows down the decay of the correlations, since the time constant in the exponential term increases from  $\tau_h$  to  $\tau' = 2\tau_h$ , the decay constant for each of the spin-resonator modes. Since the modes of the system have frequencies  $\omega_h \pm d$ , the correlations oscillate at these two frequencies rather than at frequency  $\omega_h$ , as shown by equation (7.85). Note that the resonant mechanical response will be observed at these frequencies, since they

satisfy equation (7.81). Finally, we see from (7.83) and (7.84) that although the spin-resonator correlations characterized by  $\langle I_y \theta \rangle_\infty$  do not contribute to  $C(0)$ , they are converted to correlations in  $\theta$  within a time  $t = \pi\sqrt{\tau_h \tau_c}/2$ . The contribution made by the correlation  $\langle I_y \theta \rangle_\infty$  increases the amplitude of  $C(t)$  by a factor of  $1 + \tau_h/\tau_c$ , as can be seen from equation (7.85).

The significance of the term  $\langle I_y \theta \rangle_\infty$  can be understood by noting from (7.39) that in the absence of the rotating-wave approximation, the rate  $K$  at which quanta are transferred from spins to oscillator is given by

$$K = -\gamma \frac{dB_x}{d\theta} \langle I_y \theta \rangle.$$

The energy exchange characterized by  $K$  is mediated by fluctuating fields which induce correlations  $I_y(t_1)\theta(t_1)$ . The instantaneous value of these correlations can be viewed as a fluctuating random variable, and the conversion of this fluctuating variable into fluctuating values of  $\theta(t_1)\theta(t_2)$  and  $\theta(t_2)\theta(t_1)$  can make a significant contribution to the mechanical fluctuations. Since the term  $n_\infty(1 + \tau_h/\tau_c)$  appearing in (7.85) can be written as

$$n_\infty \left( 1 + \frac{\tau_h}{\tau_c} \right) = n_h + \frac{\tau_h}{\tau_c} n_c,$$

we can consider the effective number of quanta in the resonator to be greater than  $n_h$  for purposes of estimating the mechanical fluctuations. Although the instantaneous correlation  $\langle \theta^2 \rangle_\infty$  has the value characteristic of a cooled oscillator, the amplitude of  $C_1(t)$  is not decreased by the cooling process.

The conditions  $T_2 \gg \tau_h$  and  $s \gg 1$  guarantee that the mechanical response to torques at the frequencies  $\omega_h \pm d$  is that of a resonant mechanical oscillator with ringdown time  $\tau_h$ . At these frequencies, the spectral density of the thermal torque can therefore be written as

$$S_N = \left( \frac{4I_h^2 \omega_h^2}{\tau_h^2} \right) S_\theta,$$

where the spectral density  $S_\theta$  for position is found by taking the Fourier transform

of  $C(t)$ , and where the difference between  $\omega_h^2$  and  $(\omega_h \pm d)^2$  has been neglected. We can obtain  $S_\theta$  by noting that the spectral density obtained from a correlation function of the form

$$A \exp(-t/\tau) \cos(\omega_a t)$$

yields a spectral density which can be approximated as

$$A \frac{\tau}{1 + \tau^2 (\omega - \omega_a)^2}$$

provided that  $\tau\omega_a \gg 1$  and  $|\omega - \omega_a| \ll \omega_a$ . Since the phase factors  $\phi$  in (7.85) have negligible effect on the spectral density,  $S_\theta$  can be written as the sum of two terms, each having the form

$$\frac{\hbar}{2I_h\omega_h} n_\infty \left(1 + \frac{\tau_h}{\tau_c}\right) \frac{2\tau_h}{1 + 4\tau_h^2 (\omega - \omega_i)^2},$$

where  $\omega_i = \omega_h \pm d$  is a frequency of one of the modes of the spin-resonator system. We find that at each of these frequencies

$$\begin{aligned} S_\theta &\approx \frac{\tau_h \hbar}{I_h \omega_h} \left( n_h + \frac{\tau_h}{\tau_c} n_c \right), \\ S_N &\approx \frac{4I_h \hbar \omega_h}{\tau_h} \left( n_h + \frac{\tau_h}{\tau_c} n_c \right). \end{aligned} \quad (7.87)$$

The spectral density of the mechanical fluctuations and the thermal torque at frequencies  $\omega_h \pm d$  are thus larger than they would be at  $\omega_h$  in the absence of the hyperpolarized spins.

In conclusion, the use of hyperpolarized spins to cool a mechanical resonator does not improve its sensitivity as a detector of an applied torque, since the mechanical thermal noise, characterized by equation (7.87), is not decreased by the coupling to the hyperpolarized spins; indeed, we have found that when  $n_\infty \gg 1/2$  and  $n_\infty \gg n_c$ , the thermal torque at the eigenfrequencies  $\omega_h \pm d$  becomes larger than it would be at  $\omega_h$  in the absence of the hyperpolarized spins. In this regime, as well as in the regime where the spins behave as a cold bath, the noisy thermal torque acting on the

resonator is not decreased by the presence of the cold spins.

## Appendix A

# Derivation of the spin-relaxation equations from the full master equation

In this appendix we illustrate the method we have used in deriving equations of motion for spin operators using the interaction-frame master equation for the spin-resonator system:

$$\frac{d}{dt}\rho = \frac{1}{i\hbar} [H_s + V, \rho] + \Lambda\rho. \quad (\text{A.1})$$

We assume that the resonator's ringdown time  $\tau_h$  is so short that the resonator functions as a reservoir, remaining near thermal equilibrium during its interaction with the spins, and we derive a coarse-grained derivative  $\Delta \langle I_z \rangle / \Delta t$ , where

$$\Delta t \gg \tau_h. \quad (\text{A.2})$$

In addition to satisfying (A.2), the time step  $\Delta t$  must be short compared to the time required for relaxation of  $\langle I_z \rangle$ .

We use time-dependent perturbation theory to evaluate the coarse-grained derivative to lowest order in the coupling constant  $g$ . To motivate the approach, we first recall that a master equation of the form

$$\frac{d}{dt}\rho(t) = \mathcal{L}\rho(t)$$

can be transformed into an integral equation:

$$\rho(t) = \rho(0) + \int_0^t \mathcal{L}\rho(t_1) dt_1.$$

Replacing the density matrix  $\rho(t_1)$  appearing in the integrand by an integral equation for  $\rho(t_1)$  yields

$$\rho(t) = \rho(0) + \int_0^t \mathcal{L}\rho(0) dt_1 + \int_0^t \int_0^{t_1} \mathcal{L}(\mathcal{L}\rho(t_2)) dt_2 dt_1.$$

Repeating the process of substituting an integral equation for the time-dependent integrand yields a series expansion in which successive terms depend on higher powers of the superoperator  $\mathcal{L}$ .

An analogous process can be used to obtain a series expansion of  $\Delta \langle I_z \rangle / \Delta t$ . We use (A.1) to find the instantaneous derivative  $d \langle I_z \rangle / dt$ , and this derivative is transformed to an integral equation for  $\langle I_z \rangle$ . Time-dependent quantities appearing in the integrand are themselves replaced by integral equations, and the process is repeated to yield a series expansion for  $\langle I_z \rangle$ . Terms of high-order in the coupling constant  $g$  are discarded, and the remaining integrals are evaluated to yield an explicit formula for  $\Delta \langle I_z \rangle / \Delta t$ .

In carrying out this procedure, we will use the following equations:

$$\langle I_z \rangle(t) = \langle I_z \rangle(0) + \int_0^t (-ig) \langle I_+ a^\dagger - I_- a \rangle(t_1) dt_1, \quad (\text{A.3})$$

$$\langle I_+ a^\dagger - I_- a \rangle(t) = e^{-t/\tau_h} \langle I_+ a^\dagger - I_- a \rangle(0) \quad (\text{A.4})$$

$$+ e^{-t/\tau_h} \int_0^t e^{t_1/\tau_h} (-4ig) \langle I_z a^\dagger a \rangle(t_1) dt_1$$

$$+ e^{-t/\tau_h} \int_0^t e^{t_1/\tau_h} 2ig \langle I_- I_+ \rangle(t_1) dt_1,$$

$$\langle I_z a^\dagger a \rangle(t) = e^{-2t/\tau_h} \langle I_z a^\dagger a \rangle(0) \quad (\text{A.5})$$

$$+ e^{-2t/\tau_h} \int_0^t e^{2t_1/\tau_h} \left( \frac{2n_{\text{th}}}{\tau_h} \right) \langle I_z \rangle(t_1) dt_1 + O(g),$$

$$\langle I_- I_+ \rangle(t) = \langle I_- I_+ \rangle(0) + O(g). \quad (\text{A.6})$$

These are derived by transforming derivatives obtained from (A.1) into integral equations. Replacing  $t$  in (A.3) by  $\Delta t$  gives

$$\begin{aligned} \frac{\Delta \langle I_z \rangle}{\Delta t} &= \frac{\langle I_z \rangle(t) - \langle I_z \rangle(0)}{\Delta t} \\ &= \frac{-ig}{\Delta t} \int_0^{\Delta t} \langle I_+ a^\dagger - I_- a \rangle(t_1) dt_1. \end{aligned} \quad (\text{A.7})$$

From (A.4), we obtain an integral equation for  $\langle I_+ a^\dagger - I_- a \rangle(t_1)$  which is substituted into the integrand of (A.7):

$$\begin{aligned} \frac{\Delta \langle I_z \rangle}{\Delta t} &= \frac{-ig}{\Delta t} \langle I_+ a^\dagger - I_- a \rangle(0) \int_0^{\Delta t} e^{-t_1/\tau_h} dt_1 \\ &+ \frac{-ig}{\Delta t} (-4ig) \int_0^{\Delta t} e^{-t_1/\tau_h} \int_0^{t_1} e^{t_2/\tau_h} \langle I_z a^\dagger a \rangle(t_2) dt_2 dt_1 \\ &+ \frac{-ig}{\Delta t} (2ig) \int_0^{\Delta t} e^{-t_1/\tau_h} \int_0^{t_1} e^{t_2/\tau_h} \langle I_- I_+ \rangle(t_2) dt_2 dt_1. \end{aligned}$$

Continuing in this way, we obtain

$$\begin{aligned} \frac{\Delta \langle I_z \rangle}{\Delta t} &= \frac{-ig}{\Delta t} \langle I_+ a^\dagger - I_- a \rangle(0) \int_0^{\Delta t} e^{-t_1/\tau_h} dt_1 \\ &+ \frac{-ig}{\Delta t} (-4ig) \langle I_z a^\dagger a \rangle(0) \int_0^{\Delta t} e^{-t_1/\tau_h} \int_0^{t_1} e^{t_2/\tau_h} e^{-2t_2/\tau_h} dt_2 dt_1 \\ &+ \frac{-ig}{\Delta t} (-4ig) n_{\text{th}} \langle I_z \rangle(0) \int_0^{\Delta t} e^{-t_1/\tau_h} \int_0^{t_1} e^{t_2/\tau_h} (1 - e^{-2t_2/\tau_h}) dt_2 dt_1 \\ &+ \frac{-ig}{\Delta t} (2ig) \langle I_- I_+ \rangle(0) \int_0^{\Delta t} e^{-t_1/\tau_h} \int_0^{t_1} e^{t_2/\tau_h} dt_2 dt_1 + O(g^3), \end{aligned}$$

which is evaluated as

$$\begin{aligned} \frac{\Delta \langle I_z \rangle}{\Delta t} &= \frac{\tau_h}{\Delta t} (1 - e^{-\Delta t/\tau_h}) (-ig) \langle I_+ a^\dagger - I_- a \rangle(0) \\ &+ \frac{1}{\Delta t} \left[ \tau_h^2 \left( \frac{1}{2} - e^{-\Delta t/\tau_h} + \frac{1}{2} e^{-2\Delta t/\tau_h} \right) \right] (-4g^2) \langle I_z a^\dagger a \rangle(0) \\ &+ \frac{1}{\Delta t} \left[ \tau_h \Delta t + \tau_h^2 \left( -\frac{3}{2} + 2e^{-\Delta t/\tau_h} - \frac{1}{2} e^{-2\Delta t/\tau_h} \right) \right] (-4g^2) n_{\text{th}} \langle I_z \rangle(0) \\ &+ \frac{1}{\Delta t} \left[ \tau_h \Delta t - \tau_h^2 (1 - e^{-\Delta t/\tau_h}) \right] (2g^2) \langle I_- I_+ \rangle(0) + O(g^3). \end{aligned} \quad (\text{A.8})$$

Equation (A.8) is correct to second order in the coupling constant, regardless of the relative sizes of  $\tau_h$  and  $\Delta t$ . In the case where  $\tau_h \ll \Delta t$ , negligible error is introduced by considering the resonator to be uncorrelated with the spins and in a thermal state at the beginning of the time step. A similar approximation is made in the general derivation of the master equation given in reference [7], where it is shown that correlations present at the beginning of the time step make a contribution to the motion only during a time period of order  $\tau_h$ . Since the initial spin-resonator correlations decay almost immediately on the scale of the time step  $\Delta t$ , these correlations do not make a significant contribution to the motion of  $\langle I_z \rangle$  during  $\Delta t$ . Relaxation of  $\langle I_z \rangle$  depends on the new correlations which develop continually during  $\Delta t$ , and the contribution of these correlations is not affected by the approximation of treating the resonator and spins as initially uncorrelated. This approximation yields

$$\begin{aligned} \langle I_+ a^\dagger - I_- a \rangle (0) &= \langle I_+ \rangle (0) \langle a^\dagger \rangle_{\text{th}} - \langle I_- \rangle (0) \langle a \rangle_{\text{th}} \\ &= 0, \\ \langle I_z a^\dagger a \rangle (0) &= \langle I_z \rangle (0) \langle a^\dagger a \rangle_{\text{th}} \\ &= \langle I_z \rangle (0) n_{\text{th}}, \end{aligned}$$

from which it follows that

$$\begin{aligned} \frac{\Delta \langle I_z \rangle}{\Delta t} &= \frac{1}{\Delta t} \left[ \tau_h^2 \left( \frac{1}{2} - e^{-\Delta t/\tau_h} + \frac{1}{2} e^{-2\Delta t/\tau_h} \right) \right] (-4g^2) n_{\text{th}} \langle I_z \rangle \\ &+ \frac{1}{\Delta t} \left[ \tau_h \Delta t + \tau_h^2 \left( -\frac{3}{2} + 2e^{-\Delta t/\tau_h} - \frac{1}{2} e^{-2\Delta t/\tau_h} \right) \right] (-4g^2) n_{\text{th}} \langle I_z \rangle \\ &+ \frac{1}{\Delta t} \left[ \tau_h \Delta t - \tau_h^2 (1 - e^{-\Delta t/\tau_h}) \right] (2g^2) \langle I_- I_+ \rangle. \end{aligned} \quad (\text{A.9})$$

Since  $\tau_h^2$  is negligible compared to  $\tau_h \Delta t$ , we can discard terms in (A.9) proportional to  $\tau_h^2$  and obtain an equation of motion for  $\langle I_z \rangle$ :

$$\begin{aligned} \frac{\Delta \langle I_z \rangle}{\Delta t} &= -4g^2 \tau_h n_{\text{th}} \langle I_z \rangle + 2g^2 \tau_h \langle I_- I_+ \rangle \\ &= R_0 (n_{\text{th}} + 1) \langle I_- I_+ \rangle - R_0 n_{\text{th}} \langle I_+ I_- \rangle. \end{aligned} \quad (\text{A.10})$$

## Appendix B

# Relative magnitudes of the rate constants for lifetime and secular broadening

Section 2 of chapter 2 presents the interaction-frame equations for resonator-induced transverse relaxation. In the case where the magnetic field  $\mathbf{B}(\theta)$  is approximated to second order in  $\theta$ , the equations can be expressed in the form

$$\begin{aligned}\frac{d}{dt} \langle I_x \rangle &= - (R_{\text{lifetime}} + R_{\text{secular}}) \langle I_x \rangle - R_0 \left\langle \frac{1}{2} (I_x I_z + I_z I_x) \right\rangle, \\ \frac{d}{dt} \langle I_y \rangle &= - (R_{\text{lifetime}} + R_{\text{secular}}) \langle I_y \rangle - R_0 \left\langle \frac{1}{2} (I_y I_z + I_z I_y) \right\rangle,\end{aligned}$$

where

$$\begin{aligned}R_{\text{lifetime}} &= g^2 \tau_h (2n_{\text{th}} + 1) \\ &= \left( \frac{\gamma}{2} \frac{dB_x}{d\theta} \right)^2 \frac{\hbar}{2I_h \omega_h} \tau_h (2n_{\text{th}} + 1)\end{aligned}$$

and

$$\begin{aligned}R_{\text{secular}} &= \frac{1}{2} f^2 \tau_h n_{\text{th}} (n_{\text{th}} + 1) \\ &= \frac{1}{2} \left( \gamma \frac{d^2 B_z}{d\theta^2} \frac{\hbar}{2I_h \omega_h} \right)^2 \tau_h n_{\text{th}} (n_{\text{th}} + 1).\end{aligned}$$

We estimate the relative magnitude of  $R_{\text{lifetime}}$  and  $R_{\text{secular}}$  for the example resonator described by table 5.3. Section 5.1 of chapter 5 shows that the field can be expressed as

$$\mathbf{B}(\theta) = \mathbf{B}_a + B_h \left( \frac{3}{2}\theta, 0, 1 - 3\theta^2 \right), \quad (\text{B.1})$$

where  $B_h$  is the magnitude of the resonator's field at the spins. Equation (B.1) implies that

$$\begin{aligned} \frac{dB_x}{d\theta} &= \frac{3}{2}B_h, \\ \frac{d^2B_z}{d\theta^2} &= -3B_h, \end{aligned}$$

which yields

$$\frac{R_{\text{secular}}}{R_{\text{lifetime}}} = \frac{4n_{\text{th}}(n_{\text{th}} + 1)}{(2n_{\text{th}} + 1)} \frac{\hbar}{I_h\omega_h}.$$

For the example resonator, we have

$$I_h = 6.3 \times 10^{-33} \text{ kg m}^2,$$

$$\omega_h = (2\pi) 628 \text{ MHz},$$

$$n_{\text{th}} = 0.052,$$

and

$$\frac{R_{\text{secular}}}{R_{\text{lifetime}}} \approx 10^{-14}.$$

Note that the rate constant  $R_{\text{secular}}$  becomes comparable to  $R_{\text{lifetime}}$  at temperatures high enough that

$$\frac{R_{\text{secular}}}{R_{\text{lifetime}}} \approx 2n_{\text{th}} \frac{\hbar}{I_h\omega_h}$$

is of order unity or greater. Using the high-temperature approximation

$$n_{\text{th}} \approx \frac{k_B T}{\hbar\omega},$$

we find that this occurs when

$$T \gtrsim \frac{I_h \omega_h^2}{2k_B},$$

which is of order  $10^9$  K for the example resonator.

## Appendix C

# Longitudinal relaxation when the resonator's field is inhomogeneous

In this appendix, we remove the constraint that the resonator's field is uniform across the sample. The method used in Appendix A to obtain a series expansion for  $\Delta \langle I_z \rangle / \Delta t$  can be extended to this more general problem in a natural way. We first consider a problem in which the spins all experience the same field but are not perfectly resonant with the mechanical oscillator. We define the frequency offset  $\beta$  by

$$\omega_0 = -\omega_h + \beta.$$

As in Appendix A, a series expansion for  $\Delta \langle I_z \rangle / \Delta t$  is obtained by repeatedly replacing time-dependent integrands with integral equations. The expansion is in powers of the coupling constant  $g$  as well as the offset  $\beta$ . Term of order  $g^3$  or higher are discarded, but the series in  $\beta$  is not truncated, since we wish to allow for the possibility that  $\beta \gg g$ .

Including the frequency offset in the spin Hamiltonian introduces an additional term into the integral equation (A.4), while leaving (A.3), (A.5), and (A.6) unchanged.

The full set of integral equations needed for the derivation is

$$\langle I_z \rangle (t) = \langle I_z \rangle (0) + \int_0^t (-ig) \langle I_+ a^\dagger - I_- a \rangle (t_1) dt_1 \quad (\text{C.1})$$

$$\begin{aligned} \langle I_+ a^\dagger - I_- a \rangle (t) &= e^{-t/\tau_h} \int_0^t e^{t_1/\tau_h} (i\beta) \langle I_+ a^\dagger + I_- a \rangle (t_1) dt_1 \\ &+ e^{-t/\tau_h} \int_0^t e^{t_1/\tau_h} (-4ig) \langle I_z a^\dagger a \rangle (t_1) dt_1 \\ &+ e^{-t/\tau_h} \int_0^t e^{t_1/\tau_h} (2ig) \langle I_- I_+ \rangle (t_1) dt_1 \end{aligned} \quad (\text{C.2})$$

$$\langle I_+ a^\dagger + I_- a \rangle (t) = e^{-t/\tau_h} \int_0^t e^{t_1/\tau_h} (i\beta) \langle I_+ a^\dagger - I_- a \rangle (t_1) dt_1 \quad (\text{C.3})$$

$$\langle I_z a^\dagger a \rangle (t) = n_{\text{th}} \langle I_z \rangle (0) + O(g) \quad (\text{C.4})$$

$$\langle I_- I_+ \rangle (t) = \langle I_- I_+ \rangle (0) + O(g). \quad (\text{C.5})$$

Note that the we have used the approximations

$$\langle I_z a^\dagger a \rangle (0) = n_{\text{th}} \langle I_z \rangle (0)$$

and

$$\begin{aligned} \langle I_+ a^\dagger - I_- a \rangle (0) &= \langle I_+ \rangle (0) \langle a^\dagger \rangle_{\text{th}} - \langle I_- \rangle (0) \langle a \rangle_{\text{th}} \\ &= 0, \end{aligned}$$

which introduce negligible error provided  $\tau_h \ll \Delta t$ . After two iterations of replacing time-dependent integrands by integral equations, we obtain

$$\begin{aligned} \langle I_z \rangle (t) &= \langle I_z \rangle (0) + [-4g^2 n_{\text{th}} \langle I_z \rangle (0) + 2g^2 \langle I_- I_+ \rangle (0)] \times \\ &\int_0^t e^{-t_1/\tau_h} \int_0^{t_1} e^{t_2/\tau_h} dt_2 dt_1 \\ &+ (-ig) (i\beta)^2 \int_0^t e^{-t_1/\tau_h} \int_0^{t_1} \int_0^{t_2} e^{t_3/\tau_h} \langle I_+ a^\dagger - I_- a \rangle (t_3) dt_3 dt_2 dt_1, \end{aligned}$$

where terms of order  $g^3$  or higher have been discarded. Repeating this process yields

a series expansion for  $\langle I_z \rangle (t)$ :

$$\langle I_z \rangle (t) = \langle I_z \rangle (0) + [-4g^2 n_{\text{th}} \langle I_z \rangle (0) + 2g^2 \langle I_- I_+ \rangle (0)] \times C, \quad (\text{C.6})$$

with

$$\begin{aligned} C = & \int_0^t e^{-t_1/\tau_h} \int_0^{t_1} e^{t_2/\tau_h} dt_2 dt_1 + \\ & (i\beta)^2 \int_0^t e^{-t_1/\tau_h} \int_0^{t_1} \int_0^{t_2} \int_0^{t_3} e^{t_4/\tau_h} dt_4 \dots dt_1 + \\ & (i\beta)^4 \int_0^t e^{-t_1/\tau_h} \int_0^{t_1} \int_0^{t_2} \int_0^{t_3} \int_0^{t_4} \int_0^{t_5} e^{t_6/\tau_h} dt_6 \dots dt_1 + \dots \end{aligned} \quad (\text{C.7})$$

Note that the expansion given by equations (C.6) and (C.7) includes arbitrarily high powers of the offset  $\beta$ . To estimate  $C$ , we replace  $t$  in (C.7) by  $\Delta t \gg \tau_h$  and evaluate the integral:

$$\begin{aligned} C \approx & (\tau_h \Delta t - \tau_h^2) - (\beta \tau_h)^2 (\tau_h \Delta t - 3\tau_h^2) \\ & + (\beta \tau_h)^4 (\tau_h \Delta t - 5\tau_h^2) + \dots \end{aligned} \quad (\text{C.8})$$

Although the factors  $(\tau_h \Delta t - 3\tau_h^2)$  and  $(\tau_h \Delta t - 5\tau_h^2)$  are each close to  $\tau_h \Delta t$ , the approximation of replacing  $(\tau_h \Delta t - j\tau_h^2)$  by  $\tau_h \Delta t$  will be invalid for high-order terms in the series (C.8). Provided that  $|\beta \tau_h|$  is sufficiently small that  $C$  is well approximated by a sum of the initial terms for which

$$\tau_h \Delta t - j\tau_h^2 \approx \tau_h \Delta t,$$

we obtain

$$\begin{aligned} C \approx & \tau_h \Delta t [1 - (\beta \tau_h)^2 + (\beta \tau_h)^4 - \dots] \\ \approx & \tau_h \Delta t \frac{1}{1 + (\beta \tau_h)^2}. \end{aligned} \quad (\text{C.9})$$

Equations (C.6) and (C.9) yield

$$\frac{\Delta \langle I_z \rangle}{\Delta t} = [R_0 (n_{\text{th}} + 1) \langle I_- I_+ \rangle - R_0 n_{\text{th}} \langle I_+ I_- \rangle] \frac{1}{1 + (\beta \tau_h)^2}. \quad (\text{C.10})$$

In the case where the resonator's field varies across the sample, we define at spin  $k$  a local coordinate frame such that the static field is directed along the  $z$ -axis and the resonator's field is confined to the  $xz$ -plane. The spin operators  $I_{z,k}$ ,  $I_{+,k}$ , and  $I_{-,k}$  are defined relative to the local frame. Under the rotating wave approximation, the two terms of the Hamiltonian which act on the  $k^{\text{th}}$  spin are  $\hbar(-\omega_h + \beta_k) I_{k,z}$  and  $\hbar g_k (I_{+,k} a^\dagger + I_{-,k} a)$ , where  $(-\omega_h + \beta_k)$  and  $g_k$  are the respective Larmor frequency and coupling constant for the  $k^{\text{th}}$  spin. We define the lab-frame operator  $I'_z$  by

$$I'_z = \sum_k I_{z,k}.$$

The derivation of equation (C.10) can be adapted to the problem of finding an expression for  $\Delta \langle I'_z \rangle / \Delta t$  in this more general case, and we find that

$$\frac{\Delta \langle I'_z \rangle}{\Delta t} = - \sum_k \frac{4g_k^2 \tau_h n_{\text{th}}}{1 + (\beta_k \tau_h)^2} \langle I_{z,k} \rangle + \sum_k \sum_j \frac{2g_j g_k \tau_h}{1 + (\beta_k \tau_h)^2} \langle I_{-,j} I_{+,k} \rangle,$$

which reduces to (C.10) if all spins experience the same frequency offset and the same coupling to the resonator.

## Appendix D

# Derivation of the semiclassical equation for longitudinal relaxation

In deriving a semiclassical equation for longitudinal relaxation, we note first that the steps used in Appendix A to obtain the equation (A.10) from the set of integral equations (A.3) through (A.6) are purely mathematical; given a similar set of integral equations for the semiclassical system, the same steps could be performed to yield an equation analogous to (A.10). We therefore proceed by defining semiclassical variables analogous to those appearing in the quantum mechanical integral equations of Appendix A, and we will use standard rules of calculus, in combination with some physical reasoning, to obtain integral equations for the semiclassical system. In order to simplify notation, we drop the superscript  $c$  used to distinguish semiclassical variables from analogous quantum operators.

The equation of motion of a semiclassical spin  $\mathbf{I}$  is

$$\frac{d}{dt}\mathbf{I} = \gamma\mathbf{I} \times \mathbf{B}, \quad (\text{D.1})$$

while the motion of a driven torsional resonator with coordinate  $\theta$  and momentum  $p_\theta$  is governed by the equations

$$\frac{d}{dt}\theta = \frac{1}{I_h}p_\theta - \frac{1}{\tau_h}\theta, \quad (\text{D.2})$$

$$\frac{d}{dt}p_\theta = -I_h\omega_h^2\theta - \frac{1}{\tau_h}p_\theta + f(t), \quad (\text{D.3})$$

where  $f(t)$  is the driving torque. The interaction energy between spins and resonator is

$$W = -\boldsymbol{\mu} \cdot \mathbf{B}(\theta),$$

where

$$\boldsymbol{\mu} = \gamma \hbar \mathbf{I}$$

is the magnetic dipole associated with the spins. The driving torque exerted by the spins is

$$-\frac{\partial W}{\partial \theta} = \frac{dB_x}{d\theta} \mu_x.$$

and the total torque  $f(t)$  acting on the resonator is

$$f(t) = \frac{dB_x}{d\theta} \gamma \hbar I_x(t) + N(t),$$

where  $N(t)$  is the thermal torque.

Semiclassical analogs of the raising and lowering operators for the spin and the resonator are defined in the same way as the quantum operators:

$$a = \frac{1}{\sqrt{2}} \left( \sqrt{\frac{I_h \omega_h}{\hbar}} \theta + i \sqrt{\frac{1}{I_h \omega_h \hbar}} p_\theta \right),$$

$$a^\dagger = \frac{1}{\sqrt{2}} \left( \sqrt{\frac{I_h \omega_h}{\hbar}} \theta - i \sqrt{\frac{1}{I_h \omega_h \hbar}} p_\theta \right),$$

$$I_+ = I_x + iI_y,$$

$$I_- = I_x - iI_y,$$

and we move to the "semiclassical interaction frame" by multiplying these variables by exponentials which cancel the time-dependence associated with the fast, unperturbed

motion:

$$\begin{aligned}
\tilde{a} &= e^{i\omega_h t} a, \\
\tilde{a}^\dagger &= e^{-i\omega_h t} a^\dagger, \\
\tilde{I}_+ &= e^{i\omega_h t} I_+, \\
\tilde{I}_- &= e^{-i\omega_h t} I_-.
\end{aligned}
\tag{D.4}$$

The right side of equation (D.1) is expressed in terms of these interaction frame variables, and the quickly oscillating terms are discarded, as in the rotating-wave approximation. Simplification of the resulting equations yields

$$\frac{d}{dt} I_z = -ig \left( \tilde{I}_+ \tilde{a}^\dagger - \tilde{I}_- \tilde{a} \right)
\tag{D.5}$$

and

$$\frac{d}{dt} \tilde{I}_+ = -2ig I_z \tilde{a}.
\tag{D.6}$$

The first-order approximation to  $\mathbf{B}(\theta)$  is used in calculating these derivatives:

$$\mathbf{B}(\theta) = \left( \frac{dB_x}{d\theta} \theta, 0, B_z \right).$$

The derivative of  $\tilde{a}$  is found by differentiating (D.4), substituting (D.2) and (D.3) into the derivative, expressing the resulting equation in the interaction frame, and using the rotating-wave approximation:

$$\frac{d}{dt} \tilde{a} = -\frac{1}{\tau_h} \tilde{a} - ig \tilde{I}_+ + \frac{i}{\sqrt{2I_h \omega_h \hbar}} e^{i\omega_h t} N.
\tag{D.7}$$

The product rule of elementary calculus, in combination with equations (D.5), (D.6), and (D.7) is used to obtain integral equations similar to equations (A.3) through (A.6) of Appendix A. In order to obtain equations which do not include the thermal torque  $N$ , an average is taken over the statistical ensemble, and correlations between spin variables and the thermal torque acting on the resonator are neglected. The

quickly fluctuating thermal torque  $N$  can be considered an impulse which acts on the resonator during the short correlation time of the torque, and the impulse response of the resonator appears as a weak correlation between the resonator motion and the torque. The thermal motion of the resonator is thus a sum of decaying responses to many uncorrelated impulses, with each impulse response contributing only weakly to the motion. Correlation between the instantaneous thermal torque  $N(t)$  and the spin motion depends on the spins' response to the small fraction of the resonator motion which results from the impulse occurring at time  $t$ , and can thus be neglected.

We obtain in this way the differential equations

$$\frac{d}{dt} \langle I_z \rangle = -ig \langle \tilde{I}_+ \tilde{a}^\dagger - \tilde{I}_- \tilde{a} \rangle, \quad (\text{D.8})$$

$$\frac{d}{dt} \langle \tilde{I}_+ \tilde{a}^\dagger - \tilde{I}_- \tilde{a} \rangle = \frac{1}{\tau_h} \langle \tilde{I}_+ \tilde{a}^\dagger - \tilde{I}_- \tilde{a} \rangle - 4ig \langle I_z \tilde{a}^\dagger \tilde{a} \rangle + 2ig \langle \tilde{I}_- \tilde{I}_+ \rangle, \quad (\text{D.9})$$

$$\frac{d}{dt} \langle \tilde{I}_- \tilde{I}_+ \rangle = O(g), \quad (\text{D.10})$$

which yield integral equations analogous to (A.3), (A.4), and (A.6). Note that these equations are unchanged if they are transformed from the interaction frame to the lab frame, since

$$\begin{aligned} \tilde{I}_+ \tilde{a}^\dagger &= I_+ a^\dagger, \\ \tilde{I}_- \tilde{a} &= I_- a, \\ I_z \tilde{a}^\dagger \tilde{a} &= I_z a^\dagger a, \\ \tilde{I}_- \tilde{I}_+ &= I_- I_+. \end{aligned}$$

Since the integral equations being derived are valid in both frames, we simplify notation by dropping tildes from the variables.

The semiclassical analog of (A.5) is

$$\frac{d}{dt} \langle I_z a^\dagger a \rangle = -\frac{2}{\tau_h} \langle I_z a^\dagger a \rangle + \frac{1}{I_h \omega_h \hbar} \langle I_z p_\theta N \rangle + O(\Omega). \quad (\text{D.11})$$

In evaluating  $\langle I_z p_\theta N \rangle$ , we note that the resonator evolves under the influence of

distinct torques which are associated with the spins and the reservoir fluctuations, so we may write  $p_\theta$  as a sum of the two terms:

$$p_\theta = p_\theta^{(S)} + p_\theta^{(R)}.$$

Here  $p_\theta^{(S)}$  and  $p_\theta^{(R)}$  give the resonator's response to the respective torques associated with the spins and the reservoir. Since the spins and the damping torque  $N$  are considered uncorrelated, both  $I$  and  $p_\theta^{(S)}$  are statistically independent of the thermal torque  $N$ , and we can write

$$\begin{aligned} \langle I_z p_\theta N \rangle &\approx \langle I_z p_\theta^{(S)} \rangle \langle N \rangle + \langle I_z p_\theta^{(R)} N \rangle \\ &= \langle I_z p_\theta^{(R)} N \rangle. \end{aligned}$$

Similarly, we may neglect correlations between  $I_z$  and the thermal function  $p_\theta^{(R)} N$ :

$$\langle I_z p_\theta N \rangle \approx \langle I_z \rangle \langle p_\theta^{(R)} N \rangle.$$

In order to obtain an explicit expression for the thermal average  $\langle p_\theta^{(R)} N \rangle$ , we consider a resonator which interacts only with a reservoir, simplifying notation by dropping the superscript 'R' from the resonator momentum. The correlation between the momentum and the thermal torque can be found by considering the derivative  $dE_h/dt$ , where

$$E_h = \frac{1}{2I_h} p_\theta^2 + \frac{I_h \omega_h^2}{2} \theta^2$$

is the resonator energy. Substituting the equations of motion (D.2) and (D.3) into the expression

$$\frac{d}{dt} E_h = \frac{1}{I_h} p_\theta \frac{d}{dt} p_\theta + I_h \omega_h^2 \theta \frac{d}{dt} \theta$$

gives

$$\frac{d}{dt} E_h = \frac{-2}{\tau_h} E_h + \frac{1}{I_h} p_\theta N,$$

where  $N(t)$  is the thermal torque acting on the resonator. Taking the mean value of

both sides yields

$$\frac{d}{dt} \langle E_h \rangle = \frac{-2}{\tau_h} \langle E_h \rangle + \frac{1}{I_h} \langle p_\theta N \rangle.$$

Since

$$\langle E_h \rangle = k_B T,$$

we have  $d \langle E_h \rangle / dt = 0$  and

$$\langle p_\theta N \rangle = \frac{2I_h}{\tau_h} \langle E_h \rangle.$$

Defining

$$n_c = \frac{\langle E_h \rangle}{\hbar \omega_h},$$

we may express (D.11) as

$$\frac{d}{dt} \langle I_z a^\dagger a \rangle = -\frac{2}{\tau_h} \langle I_z a^\dagger a \rangle + \frac{2}{\tau_h} n_c \langle I_z \rangle + O(g). \quad (\text{D.12})$$

Converting (D.8), (D.9), (D.10), and (D.12) to integral equations and using these to derive a coarse-grained derivative equation yields the semiclassical relaxation equation

$$\frac{d \langle I_z \rangle}{dt} = -2R_0 n_c \langle I_z \rangle + R_0 \langle I_- I_+ \rangle.$$

## Appendix E

# Longitudinal relaxation due to coupling between product-state populations

Section 4 of chapter 3 presents a heuristic argument for the idea that if product states can be chosen as eigenstates, and if the spin-resonator interaction does not induce couplings between populations and coherences, then spin-spin correlations make no contribution to the relaxation of  $\langle I_z \rangle$ . To formalize this argument, we note first that the spin-resonator interaction Hamiltonian (2.11) couples product-state populations  $\rho_{aa}$  and  $\rho_{cc}$  only if eigenstates  $|a\rangle, |c\rangle$  differ by exactly one spin flip. The rate constants  $\Gamma_{c \rightarrow a}, \Gamma_{a \rightarrow c}$  for population transfer have the same value as they do for transfer between the two states of a single spin interacting with the resonator.

Consider the changes in populations which occur during a time step  $\Delta t$ . All such changes can be accounted for by summing the population transfers associated with the set of transition probabilities  $\Gamma_{n \rightarrow m}$ . These population transfers may be considered to occur in any order we choose, and each  $\Gamma_{n \rightarrow m}$  couples two states which differ by exactly one spin flip. We initially focus attention on spin 1, and we take  $Z_1$  to be the set of all  $\Gamma_{n \rightarrow m}$  which couple eigenstates differing by a flip of this spin. We will show that if all population transfers associated with  $Z_1$  occur, and if these are the only transfers that occur, then  $\langle I_{z,1} \rangle$  relaxes exactly as if spin 1 were an isolated spin interacting with its own resonator, while  $\langle I_{z,j} \rangle$  is unchanged, for  $j \neq 1$ . By defining  $Z_j$  to be the set of all  $\Gamma_{n \rightarrow m}$  which couple eigenstates differing by a flip of spin  $j$ , and

then sequentially applying all population transfers associated with  $Z_2$ ,  $Z_3$ , and so on, we find that during  $\Delta t$  each spin has relaxed toward its thermal population as if it were interacting with its own resonator.

To establish this argument, we must show that if all population transfers associated with  $\Gamma_{n \rightarrow m} \in Z_k$  occur, and if these are the only transfers that occur, then  $\langle I_{z,k} \rangle$  relaxes as if spin  $k$  were an isolated spin interacting with a resonator, while  $\langle I_{z,j} \rangle$  is unchanged, for  $j \neq k$ . Group the product eigenstates into pairs, with the eigenstates of each pair differing by a flip of spin  $k$ , and let  $|+\beta\rangle$ ,  $|-\beta\rangle$  denote the respective eigenstates of pair  $\beta$  for which spin  $k$  is oriented parallel and antiparallel to  $B_z$ . In addition, let  $\rho_{(+\beta)}$ ,  $\rho_{(-\beta)}$  denote the respective populations of states  $|+\beta\rangle$ ,  $|-\beta\rangle$ , and define

$$\rho_+ = \sum_{\beta} \rho_{(+\beta)},$$

$$\rho_- = \sum_{\beta} \rho_{(-\beta)}.$$

Population transfers associated with  $Z_k$  cause  $\rho_{(+\beta)}$  and  $\rho_{(-\beta)}$  to evolve during the time step  $\Delta t$  exactly as if they were the populations of an isolated spin interacting with the resonator. Indeed, arguments similar to those used in deriving equation (2.29) show that population is transferred from  $\rho_{(+\beta)}$  to  $\rho_{(-\beta)}$  at rate  $R_0 n_{\text{th}} \rho_{(+\beta)}$  and from  $\rho_{(-\beta)}$  to  $\rho_{(+\beta)}$  at rate  $R_0 (n_{\text{th}} + 1) \rho_{(-\beta)}$ . It follows that  $\rho_+$  and  $\rho_-$  evolve under the same differential equations as the populations of an isolated spin relaxing due to its interactions with a resonator:

$$\frac{d}{dt} \rho_+ = -R_0 n_{\text{th}} \rho_+ + R_0 (n_{\text{th}} + 1) \rho_-,$$

$$\frac{d}{dt} \rho_- = -R_0 (n_{\text{th}} + 1) \rho_- + R_0 n_{\text{th}} \rho_+,$$

and since  $\langle I_{z,k} \rangle$  can be expressed as

$$\langle I_{z,k} \rangle = \frac{1}{2} \rho_+ - \frac{1}{2} \rho_-,$$

these transitions cause  $\langle I_{z,k} \rangle$  to relax as if it were an isolated spin.

Note that for each pair  $\beta$ , the sum

$$\rho_\beta \equiv \rho_{(+\beta)} + \rho_{(-\beta)}$$

does not change during these transitions, and that for  $j \neq k$ , we have

$$\langle I_{z,j} \rangle = \sum_{\beta} \lambda_{z,j} \rho_\beta,$$

where  $\lambda_{z,j}$  is the eigenvalue of  $I_{z,j}$  for the two states in pair  $\beta$ . Since  $\rho_\beta$  does not change during these transitions,  $\langle I_{z,j} \rangle$  remains constant. This establishes our claim that direct coupling between populations, in the absence of any coupling between populations and coherences, causes  $\langle I_z \rangle$  to relax exponentially with rate constant  $R_h$  to thermal equilibrium with the resonator.

## Appendix F

# Transverse relaxation due to coupling between product-state coherences

Although section 5 of chapter 3 shows that the damping constant for a coherence between product states increases with the size of the sample, transfer between product-state coherences can yield exponential transverse relaxation with rate constant  $R_h/2$ , regardless of the size of the sample. In particular, suppose that the single-quantum coherences are grouped into sets  $Z_k$ , where the coherences in set  $Z_k$  are between states which differ by a flip of spin  $k$ . Recall that in section 3 of chapter 3, we argued that the transfer between coherences  $\rho_{cd}$  and  $\rho_{ab}$  that is characterized by  $\mathcal{R}_{abcd}$  will be suppressed if the frequency difference  $|\omega_{ab} - \omega_{cd}|$  is perturbed to a value larger than  $2\pi\mathcal{R}_{abcd}$ . We show here that if the frequency differences between coherences within each set  $Z_k$  are small enough that transfers within  $Z_k$  are preserved, while transfers between coherences belonging to  $Z_k$  and other coherences are suppressed by frequency differences, then the transverse relaxation induced by the resonator is exponential with rate constant  $R_h/2$ .

In demonstrating this result, we first define  $s_k$  to be the sum of all coherences within  $Z_k$ :

$$s_k = \sum_{\rho_{ab} \in Z_k} \rho_{ab},$$

and we claim that

$$\langle I_{x,k} \rangle = \frac{1}{2} s_k. \quad (\text{F.1})$$

Equation (F.1) can be established by expanding the density matrix as

$$\rho = \sum \rho_{ab} |a\rangle \langle b|,$$

and writing  $I_{x,k}$  as

$$I_{x,k} = \frac{1}{2} (I_{+,k} + I_{-,k}).$$

For coherences  $\rho_{ab}$  belonging to  $Z_k$ , we have one of two possibilities:

$$\begin{aligned} \text{Tr} \{ \rho_{ab} I_{+,k} |a\rangle \langle b| \} &= \rho_{ab}, \\ \text{Tr} \{ \rho_{ab} I_{-,k} |a\rangle \langle b| \} &= 0, \end{aligned}$$

or

$$\begin{aligned} \text{Tr} \{ \rho_{ab} I_{+,k} |a\rangle \langle b| \} &= 0, \\ \text{Tr} \{ \rho_{ab} I_{-,k} |a\rangle \langle b| \} &= \rho_{ab}, \end{aligned}$$

while for coherences  $\rho_{cd}$  not belonging to  $Z_k$ , we have

$$\text{Tr} \{ \rho_{cd} I_{+,k} |c\rangle \langle d| \} = \text{Tr} \{ \rho_{cd} I_{-,k} |c\rangle \langle d| \} = 0.$$

Summing over the coherences belonging to  $Z_k$ , we obtain equation (F.1).

Since

$$\langle I_x \rangle = \sum_k \langle I_{x,k} \rangle,$$

it suffices to show that

$$\frac{d}{dt} s_k = -\frac{1}{2} R_h s_k \quad (\text{F.2})$$

if transfers within  $Z_k$  are preserved while transfers between coherences belonging to  $Z_k$  and other coherences are suppressed. Two types of couplings contribute to  $(d/dt) s_k$ .

First, coupling constants  $\mathcal{R}_{abab}$  contribute terms of the form

$$\mathcal{R}_{abab}\rho_{ab} = -\frac{1}{2} \left( \sum_{n \neq a} \Gamma_{a \rightarrow n} + \sum_{n \neq b} \Gamma_{b \rightarrow n} \right) \rho_{ab}. \quad (\text{F.3})$$

Equation (F.3) can be written as

$$\mathcal{R}_{abab}\rho_{ab} = -\frac{1}{2} (\Gamma_{a \rightarrow b} + \Gamma_{b \rightarrow a}) \rho_{ab} - \frac{1}{2} \left( \sum_{n \neq a, b} \Gamma_{a \rightarrow n} + \sum_{n \neq b, a} \Gamma_{b \rightarrow n} \right) \rho_{ab} \quad (\text{F.4})$$

$$= -\frac{1}{2} R_h \rho_{ab} - \frac{1}{2} \left( \sum_{n \neq a, b} \Gamma_{a \rightarrow n} + \sum_{n \neq b, a} \Gamma_{b \rightarrow n} \right) \rho_{ab}. \quad (\text{F.5})$$

In going from (F.4) to (F.5), we used the fact that the rate constants  $\Gamma_{m \rightarrow n}$  for transfer of population between product states which differ by a single spin flip are the same as for the two states of a single-spin system.

Assume that coherences in  $Z_k$  are coupled only to other coherences belonging to the same set. These couplings are associated with processes in which two transitions  $|a\rangle \rightarrow |c\rangle$  and  $|b\rangle \rightarrow |d\rangle$  occur, with both transitions involving a flip of spin  $j \neq k$  in the same direction. Without loss of generality, we assume that both transitions involve a flip up of spin  $j$ :

$$I_{+,j} |a\rangle = |c\rangle,$$

$$I_{+,j} |b\rangle = |d\rangle.$$

The product of matrix elements which contributes to  $\mathcal{R}_{cdab}$  is  $\langle \mu, b | V | \nu, d \rangle \langle \nu, c | V | \mu, a \rangle$ . We first demonstrate that the matrix elements  $\langle \nu, d | V | \mu, b \rangle$  and  $\langle \nu, c | V | \mu, a \rangle$  have

the value  $\langle \nu | a^\dagger | \mu \rangle$ :

$$\begin{aligned}
\langle \nu, d | V | \mu, b \rangle &= \langle \nu, d | I_+ a^\dagger | \mu, b \rangle \\
&= \langle d | I_+ | b \rangle \langle \nu | a^\dagger | \mu \rangle \\
&= \langle d | I_{+,j} | b \rangle \langle \nu | a^\dagger | \mu \rangle \\
&= \langle d | d \rangle \langle \nu | a^\dagger | \mu \rangle \\
&= \langle \nu | a^\dagger | \mu \rangle.
\end{aligned}$$

Since similar steps can be used to obtain  $\langle \nu, c | V | \mu, a \rangle = \langle \nu | a^\dagger | \mu \rangle$ , we have

$$\langle \nu, c | V | \mu, a \rangle = \langle \nu, d | V | \mu, b \rangle$$

and

$$\begin{aligned}
\langle \mu, b | V | \nu, d \rangle \langle \nu, c | V | \mu, a \rangle &= |\langle \nu, c | V | \mu, a \rangle|^2 \\
&= |\langle \nu, d | V | \mu, b \rangle|^2.
\end{aligned}$$

It follows from (3.6) and (3.9) that

$$\begin{aligned}
\mathcal{R}_{cdab} &= \Gamma_{a \rightarrow c} = \Gamma_{b \rightarrow d} \\
&= \frac{1}{2} (\Gamma_{a \rightarrow c} + \Gamma_{b \rightarrow d}).
\end{aligned}$$

We can thus write (F.5) as

$$\mathcal{R}_{abab} \rho_{ab} = -\frac{1}{2} R_h \rho_{ab} + \sum_{Z_k} -\mathcal{R}_{cdab} \rho_{ab}, \quad (\text{F.6})$$

where the sum is over all coherences in  $Z_k$  except  $\rho_{ab}$ . Equation (F.6) can be interpreted to mean that the evolution governed by the coefficient  $\mathcal{R}_{abab}$  of the master equation includes a contribution associated with the "intrinsic decay" of  $\rho_{ab}$ , for which

the rate constant is  $R_h/2$ , and a contribution associated with transfers from  $\rho_{ab}$  to other coherences belonging to the set  $Z_k$ . If we sum the derivatives of all coherences in  $Z_k$ , all contributions of the form  $\pm\mathcal{R}_{cdab}\rho_{ab}$  and  $\pm\mathcal{R}_{abcd}\rho_{cd}$  cancel, and the only remaining terms have the form  $-(R_h/2)\rho_{ab}$  or  $-(R_h/2)\rho_{cd}$ . It follows that equation (F.2) holds, i.e., transverse relaxation induced by the resonator is exponential and has rate constant  $R_h/2$ .

## Appendix G

# Comparison between the use of an optimal filter and least-squares fitting

Unknown parameters in a measured signal are often estimated by least-squares fitting, rather than by applying an optimal filter. In this section, we compare the two methods of data analysis for signals of the form  $Gm_0(t)$ , with  $m_0(t)$  a known function. The signal and the noise are assumed to be continuous functions of time, and errors arising from digitization of the signal are neglected. We show that if the noise is white, least-squares fitting yields the same value of  $G$  as that obtained from an optimal filter. If the noise is not white, however, the two methods in general yield different values of  $G$ , and the least-squares fit corresponds to an estimate made using a non-optimal filter.

Given a function  $f(t) = m(t) + n(t)$ , the least-squares fit is the function  $Gm_0(t)$  that minimizes the integral

$$\|f - Gm_0\|^2 = \int_{-\infty}^{\infty} [f(t) - Gm_0(t)]^2 dt. \quad (\text{G.1})$$

If the functions  $f(t)$  and  $m_0(t)$  belong to a Hilbert space such as  $L_2$ , the problem of finding  $G$  can be cast in geometric language. The set of scalar multiples of  $m_0(t)$  constitutes a one-dimensional subspace, and the least-squares fit  $Gm_0(t)$  is

the projection of  $f(t)$  onto this subspace. Indeed,  $Gm_0(t)$  will be given by

$$Gm_0(t) = m_0(t) \frac{\langle m_0, f \rangle}{\|m_0\|^2},$$

where

$$\langle m_0, f \rangle = \int_{-\infty}^{\infty} m_0(t) f(t) dt$$

and

$$\|m_0\|^2 = \int_{-\infty}^{\infty} m_0^2(t) dt.$$

We see that least-squares fitting produces the amplitude estimate

$$G = \frac{\int_{-\infty}^{\infty} m_0(t) f(t) dt}{\int_{-\infty}^{\infty} m_0^2(t) dt}. \quad (\text{G.2})$$

(Note that under the standard convention, which has  $n(t) \not\rightarrow 0$  as  $t \rightarrow \pm\infty$ , it is not true that  $f(t)$  belongs to  $L_2(\mathbb{R})$ . This is merely a matter of convention, however. If we limit the domain of integration for equation G.1 to a finite interval  $[a, b]$  that includes all times  $t$  for which  $m_0(t)$  is non-negligible, then  $f(t)$  and  $m_0(t)$  can be assumed to belong to  $L_2[a, b]$ .)

We compare equation G.2 to the estimate that would be obtained using an optimal filter. The signal  $f(t)$  is passed through the filter  $\mathcal{K}$  having transfer function

$$K(\omega) = c \frac{M_0^*(\omega)}{S_n(\omega)}.$$

The amplitude estimate  $X$  is given by

$$X = \frac{\phi}{\mu_0},$$

where

$$\begin{aligned}\phi &= \frac{1}{2\pi} \int_{-\infty}^{\infty} K(\omega) F(\omega) d\omega \\ &= c \frac{1}{2\pi} \int_{-\infty}^{\infty} \frac{M_0^*(\omega)}{S_n(\omega)} F(\omega) d\omega\end{aligned}\tag{G.3}$$

and

$$\mu_0 = c \frac{1}{2\pi} \int_{-\infty}^{\infty} \frac{M_0^*(\omega)}{S_n(\omega)} M_0(\omega) d\omega.\tag{G.4}$$

If the noise is white, then the constant term  $S_n$  can be taken outside the integrals of equations G.3 and G.4, and we find that

$$\phi = \int_{-\infty}^{\infty} m_0(t) f(t) dt$$

and

$$\mu_0 = \int_{-\infty}^{\infty} m_0^2(t) dt.$$

The amplitude estimate obtained in this way is

$$X = \frac{\int_{-\infty}^{\infty} m_0(t) f(t) dt}{\int_{-\infty}^{\infty} m_0^2(t) dt},$$

which is identical to the value obtained with a least-squares fit. We conclude that using a least-square fit is equivalent to using a filter which is optimal for extracting the signal from white noise. In the case where  $S_n(\omega)$  varies over the spectral width of  $m_0(t)$ , the least-squares fit does not take account of the structure of  $S_n(\omega)$ , whereas the optimal filter does.

## Appendix H

# Spectral density in signal-to-noise ratio estimates

In this appendix, we introduce the spectral density as a tool to be used in SNR calculations. Recall that in analyzing the variance of a measured amplitude due to noise superimposed on the signal, we considered a noisy signal

$$f(t) = m(t) + n(t),$$

where  $m(t)$  is the useful signal and  $n(t)$  is the noise. When  $f(t)$  is passed into filter  $\mathcal{K}$ , the output function is

$$\phi(t) = \mu(t) + \nu(t),$$

where  $\mu(t)$  and  $\nu(t)$  would be the respective outputs if  $m(t)$  and  $n(t)$  were passed through  $\mathcal{K}$  individually. The amplitude estimate, denoted by  $X$  and given by equation (4.2), differs from the actual amplitude by a term proportional to  $\nu(t_0)$ , where  $t_0$  is a time determined by the filter's transfer function. (If we do not care about whether the filter is causal, then  $t_0$  can be chosen arbitrarily. In section 1 of chapter 4, for instance, we set  $t_0 = 0$ .) To calculate SNR, we divide the mean value  $\langle X \rangle$  by the standard deviation of  $X$ , which can be calculated if the variance  $\nu(t_0)$  is known. In the context of calculating SNR, the spectral density is used only as a tool for calculating this variance.

Since  $\nu(t_0)$  is obtained by passing the noise  $n(t)$  through a filter, one natural

approach might be to calculate the frequency components of  $n(t)$  and then use the filter's transfer function to determine the frequency components of  $\nu(t)$ . This approach presents a technical difficulty, however, since the function  $n(t)$  is conventionally assumed not to approach zero as  $t \rightarrow \pm\infty$ . As a result, the Fourier transform of  $n(t)$  is not defined. Fortunately, we merely need the variance of  $\nu(t_0)$ , not the frequency components of  $\nu(t)$ . An alternate approach to obtaining this variance can be used if we assume that  $n(t)$  is stationary and has zero mean, with  $\mathcal{K}$  linear and time-invariant. An outline of this approach introduces the spectral density in a simple way.

The assumptions on  $n(t)$  and  $\mathcal{K}$  guarantee that  $\nu(t)$  is also stationary and has zero mean [19]. The variance of  $\nu(t_0)$  is represented by the notation  $\langle \nu^2 \rangle$ , and it is given by  $C_\nu(0)$ , where

$$C_\nu(t) = \langle \nu(t) \nu(0) \rangle.$$

Our strategy will be to calculate  $C_\nu(0)$  in terms of the correlation function  $C_n(t)$ , which is defined similarly to  $C_\nu(t)$ :

$$C_n(t) = \langle n(t) n(0) \rangle.$$

We define the spectral densities  $S_n(\omega)$ ,  $S_\nu(\omega)$  to be the respective Fourier transforms of  $C_n(t)$  and  $C_\nu(t)$ :

$$\begin{aligned} S_n(\omega) &= \int_{-\infty}^{\infty} e^{-i\omega t} C_n(t) dt, \\ S_\nu(\omega) &= \int_{-\infty}^{\infty} e^{-i\omega t} C_\nu(t) dt. \end{aligned}$$

Reference [19] shows that

$$S_\nu(\omega) = |K(\omega)|^2 S_n(\omega), \tag{H.1}$$

where the transfer function of  $\mathcal{K}$  is denoted by  $K(\omega)$ . If the correlation function

$C_n(t)$  has been previously derived, then equation H.1 can be used to calculate  $\langle \nu^2 \rangle$ :

$$\begin{aligned} \langle \nu^2 \rangle &= C_\nu(0) \\ &= \frac{1}{2\pi} \int_{-\infty}^{\infty} S_\nu(\omega) d\omega \\ &= \frac{1}{2\pi} \int_{-\infty}^{\infty} |K(\omega)|^2 S_n(\omega) d\omega. \end{aligned}$$

This integral can in principle be evaluated, since the transfer function  $|K(\omega)|$  is assumed to be known, while the spectral density  $S_n(\omega)$  can be calculated from knowledge of  $C_n(t)$ .

This short introduction to the spectral density includes the ideas needed to understand its use as a tool in calculating SNR. The mean-square magnitude of the unfiltered noise is expressed as a sum over Fourier components of the noise's correlation function. Filtering the noise modifies these Fourier components, and the mean-square magnitude of the filtered noise is calculated as a sum over the modified Fourier components.

# Appendix I

## Statistics of a classical resonator

In this appendix we derive an expression for the spectral density of the thermal torque exerted on a classical torsional oscillator in equilibrium with a reservoir. The first section provides a shortened derivation of the correlation function of a classical oscillator, adapted from a derivation originally given by McCombie [47], as well as formal justification for an assumption made by McCombie. The second section derives the spectral density of the thermal torque.

### 1 Correlation function of the oscillator's coordinate

McCombie shows that the correlation function for a classical torsional resonator is [47]

$$\begin{aligned} C_\theta(t) &\equiv \langle \theta(t) \theta(0) \rangle \\ &= \langle \theta^2 \rangle e^{-|t|/\tau_h} \left( \cos \omega_d t + \frac{1}{\tau_h \omega_d} \sin \omega_d |t| \right), \end{aligned} \quad (\text{I.1})$$

where

$$I_h \ddot{\theta}(t) + \frac{2I_h}{\tau_h} \dot{\theta}(t) + k\theta = N'(t) \quad (\text{I.2})$$

is the Langevin equation of motion that governs the resonator,

$$\langle \theta^2 \rangle = \frac{k_B T}{k}$$

is the mean-square thermal displacement, and

$$\omega_d = \sqrt{\frac{k}{I_h} - \frac{1}{\tau_h^2}}$$

is the frequency of the freely-running damped resonator. From (I.1) it follows that the spectral density  $S_\theta(\omega)$  of the thermal fluctuations is

$$S_\theta(\omega) = \frac{4k_B T}{\tau_h I_h} \left( \frac{1}{(\omega^2 - \omega_\theta^2)^2 + 4\omega^2/\tau_h^2} \right). \quad (\text{I.3})$$

A significant assumption behind McCombie's derivation of (I.1) is that "subsequent to any given instant the history of the random couple is quite independent of the fluctuation in the deflection at that instant" [47]. Stated in mathematical notation, McCombie's assumption is

$$\langle N'(t') \theta(t) \rangle = 0, \quad t < t'.$$

In investigating this assumption, we note first that the resonator's equation of motion (I.2) can be integrated [48] to give a formal expression for  $\theta(t)$ :

$$\theta(t) = \frac{1}{I_h} \int_{-\infty}^t e^{-(t-t')/\tau_h} \frac{\sin \omega_d (t-t')}{\omega_d} N'(t') dt'. \quad (\text{I.4})$$

Inspection of this equation shows that  $\theta(t)$  retains a memory of the fluctuating torque  $N'(t')$  for a period on the order of the ringdown time  $\tau_h$ , since  $N'(t')$  in general contributes to the integral when  $(t-t')/\tau_h$  is on the order of unity. Torques exerted after time  $t$  do not directly contribute to  $\theta(t)$ , so we do not expect them to be correlated with  $\theta(t)$ . These statements can be demonstrated formally by calculating  $\langle N'(t') \theta(t) \rangle$ . If we consider the torque to vary so quickly that its correlation function

is approximated as

$$\langle N'(t) N'(t') \rangle = \sigma_{N'}^2 \delta(t - t'),$$

with  $\sigma_{N'}^2$  the variance of  $N'$ , and  $\delta$  the Dirac delta function, then we can use equation (I.4) to find  $\langle N'(t') \theta(t) \rangle$ . Changing the variable of integration in (I.4) to  $t''$ , multiplying by  $N'(t')$ , and taking the mean of each side gives

$$\langle N'(t') \theta(t) \rangle = \begin{cases} \frac{\sigma_{N'}^2}{I_h} \frac{\sin \omega_d(t-t')}{\omega_d} e^{-(t-t')/\tau_h}, & t' < t \\ 0 & t < t' \end{cases} \quad (\text{I.5})$$

Equation (I.5) shows that the resonator coordinate  $\theta(t)$  is correlated with  $N'(t')$  when  $t'$  precedes  $t$  by a time on the order of  $\tau_h$ . Intuitively, we can say that the resonator retains a memory of the torques exerted on it in the past during a period whose length is on the order of  $\tau_h$ , but it has no knowledge of the torques that will be exerted on it in the future, since the reservoir itself has no memory.

It is now simple to derive the correlation function  $C_\theta(t)$ . We multiply the Langevin equation

$$I_h \frac{d^2}{dt^2} \theta(t) + \frac{2I_h}{\tau_h} \frac{d}{dt} \theta(t) + k\theta(t) = N'(t)$$

by  $\theta(t')$ , with  $t' < t$ , and take the mean value of each side. Since  $\langle \theta(t') N'(t) \rangle = 0$ , we find that

$$I_h \frac{d^2}{dt^2} \langle \theta(t') \theta(t) \rangle + \frac{2I_h}{\tau_h} \frac{d}{dt} \langle \theta(t') \theta(t) \rangle + k \langle \theta(t') \theta(t) \rangle = 0.$$

The solution to this differential equation in  $t$  is

$$\langle \theta(t') \theta(t) \rangle = \langle \theta^2(t') \rangle e^{-(t-t')/\tau_h} \left[ \cos(\omega_d(t-t')) + \frac{1}{\tau_h \omega_d} \sin(\omega_d(t-t')) \right], \quad t > t'. \quad (\text{I.6})$$

Since  $\theta(t)$  is a stationary random process, equation (I.6) depends only on the differ-

ence between  $t'$  and  $t$ . We can thus consider  $t' = 0$  and write

$$\langle \theta(0) \theta(t) \rangle = \langle \theta^2 \rangle e^{-t/\tau_h} \left( \cos \omega_d t + \frac{1}{\tau_h \omega_d} \sin \omega_d t \right), \quad t > 0. \quad (\text{I.7})$$

Alternatively, we can choose  $t = 0$  to obtain

$$\langle \theta(t') \theta(0) \rangle = \langle \theta^2 \rangle e^{-|t'|/\tau_h} \left( \cos \omega_d |t'| + \frac{1}{\tau_h \omega_d} \sin \omega_d |t'| \right), \quad 0 > t'. \quad (\text{I.8})$$

Equations (I.7) and (I.8) can be combined in the form

$$C_\theta(t) = \langle \theta(t) \theta(0) \rangle = \langle \theta^2 \rangle e^{-|t|/\tau_h} \left( \cos \omega_d t + \frac{1}{\tau_h \omega_d} \sin \omega_d t \right),$$

which is the desired result.

## 2 Spectral density of the thermal torque

The thermal torque  $N'$  and the angular displacement  $\theta$  are considered to be ergodic, stationary random processes with zero mean. For each sample function  $N'(t)$ , there is an associated sample function  $\theta(t)$  giving the displacement of the resonator driven by  $N'(t)$ . For a given pair  $N'(t)$ ,  $\theta(t)$ , we define truncated functions  $N'_T(t)$  and  $\theta_T(t)$  which have as their domain some large interval  $[-T, T]$  and which coincide respectively with  $N'(t)$ ,  $\theta(t)$  on this interval. The spectral density of  $N'_T(t)$  and  $\theta_T(t)$  will be denoted by  $S_{N',T}(\omega)$  and  $S_{\theta,T}(\omega)$ , respectively. In addition,  $C_{N'}(t)$ , and  $S_{N'}(\omega)$  denote the respective correlation function and the spectral density of  $N'$ , while  $C_\theta(t)$  and  $S_\theta(\omega)$  are defined analogously for  $\theta$ . Our goal in this section is to find an expression for  $S_{N'}(\omega)$ , the spectral density of the thermal torque.

If  $N'_T(t)$  is given by

$$N'_T(t) = \sum_{n=1}^{\infty} N'_n \cos(\omega_n t + \phi_n),$$

with  $\omega_n = \pi n/T$ , then

$$\theta_T(t) = \theta_{\text{ini}}(t) + \sum_{n=1}^{\infty} \theta_n \cos(\omega_n t + \psi_n),$$

where

$$\theta_n = \frac{N'_n}{I_h} \frac{1}{\sqrt{(\omega_n^2 - \omega_\theta^2)^2 + 4\omega_n^2/\tau_h^2}}. \quad (\text{I.9})$$

Here  $I_h$ ,  $\omega_\theta$ , and  $\tau_h$  are the resonator's moment of inertia, frequency, and ringdown time, respectively. The function  $\theta_{\text{ini}}(t)$  is included because the resonator's response to the driving torque during the interval  $[-T, T]$  depends on the initial state of the resonator at time  $t = -T$ ; that is,  $\theta_{\text{ini}}(t)$  corresponds to the ringing down of an undriven resonator. If the time interval is sufficiently large compared to the ringdown time  $\tau_h$ , then  $\theta_{\text{ini}}(t)$  will make a negligible contribution to the Fourier components of  $\theta_T(t)$ , which we may consider to be given by  $\theta_n$ . From equation I.9, we conclude that

$$\begin{aligned} S_{\theta,T}(\omega_n) &= \frac{|\theta_n|^2}{2T} \\ &= \frac{|N'_n|^2}{2T} \frac{1}{I_h^2 \left( (\omega_n^2 - \omega_\theta^2)^2 + 4\omega_n^2/\tau_h^2 \right)} \\ &= S_{N',T}(\omega_n) \frac{1}{I_h^2 \left( (\omega_n^2 - \omega_\theta^2)^2 + 4\omega_n^2/\tau_h^2 \right)}. \end{aligned}$$

In general, the spectral density of a random process can be obtained by calculating the spectral density of truncated functions such as  $N'_T(t)$  and  $\theta_T(t)$ , averaging over the ensemble, and then taking the limit as  $T \rightarrow \infty$  [19]:

$$\begin{aligned} S_\theta(\omega) &= \lim_{T \rightarrow \infty} \langle S_{\theta,T}(\omega) \rangle, \\ S_{N'}(\omega) &= \lim_{T \rightarrow \infty} \langle S_{N',T}(\omega) \rangle. \end{aligned}$$

We find that

$$\begin{aligned}
 S_\theta(\omega) &= \frac{1}{I_h^2 \left( (\omega^2 - \omega_\theta^2)^2 + 4\omega^2/\tau_h^2 \right)} \lim_{T \rightarrow \infty} \langle S_{N',T}(\omega) \rangle \\
 &= \frac{S_{N'}(\omega)}{I_h^2 \left( (\omega^2 - \omega_\theta^2)^2 + 4\omega^2/\tau_h^2 \right)}.
 \end{aligned} \tag{I.10}$$

It follows from (I.10) and (I.3) that

$$S_{N'}(\omega) = \frac{4I_h k_B T}{\tau_h}.$$

The single-sided spectral density  $S_{N'}^s$  of the fluctuating torque is

$$\begin{aligned}
 S_{N'}^s &= 2S_{N'}(\omega) \\
 &= \frac{8I_h k_B T}{\tau_h}.
 \end{aligned} \tag{I.11}$$

## Appendix J

# Contribution of the induced electric field to the resonator's kinetic energy

Movement of the magnetic mechanical resonator will cause the magnetic field in the space surrounding the resonator to vary with time, and the oscillating magnetic field will induce an electric field. The energy of the induced electric field is proportional to the square of the magnet's angular velocity, and may thus be considered to contribute to the resonator's kinetic energy. A simple argument suggests that this contribution is negligible for a radio-frequency nanoscale resonator. Note first that the resonator's magnetic field  $\mathbf{B}_h(\mathbf{x}, t)$  can be estimated using the quasistatic approximation, since the wavelength of light at a typical resonator frequency of 500 MHz is many orders of magnitude larger than the dimensions of the resonator [49, 50]. A quasistatic estimate of  $\mathbf{B}_h(\mathbf{x}, t)$  is obtained by dropping the displacement current from the Maxwell equation

$$\nabla \times \mathbf{B} = \mu_0 \mathbf{J} + \mu_0 \varepsilon_0 \frac{\partial \mathbf{E}}{\partial t} \quad (\text{J.1})$$

and calculating  $\mathbf{B}$  as if it were generated by a static current distribution

$$\nabla \times \mathbf{B} = \mu_0 \mathbf{J}.$$

Note, however, that if the displacement current is removed from equation (J.1), then the magnetic field cannot exchange energy with the electric field unless  $\mathbf{J}$  is changed

by the induced electric field. In the case where  $\mathbf{B}$  is generated by the bound current of magnetic material, then there is no mechanism for energy exchange between the magnetic and electric fields. Conservation of energy therefore implies that if the quasistatic approximation is valid, the energy of the induced electric field is negligible compared to the energy of  $\mathbf{B}_h(\mathbf{x}, t)$ .

We used a simple example resonator model to make a numerical estimate of the ratio

$$r = \frac{T_{\text{elec}}}{T_{\text{mech}}},$$

where  $T_{\text{elec}}$  is the energy of the induced electric field, and  $T_{\text{mech}}$  is the mechanical kinetic energy. A Halbach cylinder [43] is a circular tube of magnetic material for which the arrangement of magnetization produces a nominally uniform magnetic field within the tube and zero field outside of the tube. The simplicity of this magnetic field facilitates an estimate of the electric field induced by the rotation of the cylinder around its axis. For this estimate, we used an equation similar in form to the Biot-Savart law:

$$\mathbf{E}(\mathbf{x}, t) = \frac{-1}{4\pi} \int \frac{\frac{\partial \mathbf{B}}{\partial t}(\mathbf{x}', t) \times (\mathbf{x} - \mathbf{x}')}{|\mathbf{x} - \mathbf{x}'|^3} d^3x', \quad (\text{J.2})$$

where  $\mathbf{B}_h(\mathbf{x}, t)$  is calculated using the quasistatic approximation. We assumed

$$\frac{R_o}{R_i} = 3,$$

where  $R_i$ ,  $R_o$  are the respective inner radius and outer radius of the Halbach cylinder, as well as a remanent magnetization of

$$\mu_0 M = 1.5 \text{ T},$$

and a magnetic density equal to that of iron. For the ratio  $r$  we obtained a scale-invariant expression with the approximate value

$$r \sim 10^{-15}.$$

The contribution of the energy of the induced electric field to the kinetic energy of a nanoscale magnetic mechanical oscillator is therefore negligible.

## Appendix K

# General formula for the magnetic spring constant

For a magnetic mechanical oscillator whose magnetization remains constant in a reference frame fixed in the oscillator, a simple formula for the magnetic spring constant can be obtained. A magnetic dipole  $\mu$  in a static applied field  $B_a$  has energy

$$U = -B_a\mu \cos \theta, \quad (\text{K.1})$$

where  $\theta$  is the angle between  $\mu$  and  $B_a$ . For small  $\theta$ , (K.1) can be approximated as

$$U = -B_a\mu + \frac{1}{2}B_a\mu\theta^2,$$

which is the potential energy of a harmonic oscillator with magnetic spring constant

$$k_{\text{mag}} = B_a\mu. \quad (\text{K.2})$$

In the case where a soft magnetic oscillator moves in a large applied field, the magnetization can be considered to remain continuously aligned with the applied field, so that

$$\theta \approx 0$$

throughout the motion. Naive use of equation (K.1) would suggest that in this case, magnetic energy makes no contribution to the oscillator's spring constant. This

conclusion is incorrect, however, since (K.1) only takes account of the interaction between the magnetization and the applied field, without including the magnetostatic energy associated with the interaction between dipoles at different points within the magnetic material.

In this appendix, we derive a formula for the magnetic spring constant in the general case where magnetization can change as the oscillator moves. We begin by considering the Hamiltonian for a nonrelativistic system of particles evolving in an external electromagnetic field [51]. The vector and scalar potentials for the electromagnetic field are each expressed as the sum of a dynamical variable and an externally-determined function associated with the applied field. The particles evolve under the action of the total electromagnetic fields  $\mathbf{E}$ ,  $\mathbf{B}$ , and act as sources for the fields  $\mathbf{E}'$ ,  $\mathbf{B}'$  associated with the dynamical variables. In the case where the applied field is purely magnetic, the Hamiltonian for the system is [51]

$$H = \sum_{\alpha} \frac{1}{2m_{\alpha}} (\dot{\mathbf{r}}_{\alpha})^2 - \sum_{\alpha} \mu_{\alpha} \cdot \mathbf{B}(\mathbf{r}_{\alpha}) + V_{\text{Coul}} + H_R. \quad (\text{K.3})$$

Here  $\mathbf{r}_{\alpha}$  and  $\mu_{\alpha}$  are the respective position and magnetic moment of particle  $\alpha$ , and the Coulomb energy  $V_{\text{Coul}}$  is given by

$$V_{\text{Coul}} = \varepsilon_{\text{Coul}}^{\alpha} + \sum_{\alpha > \beta} \frac{q_{\alpha} q_{\beta}}{4\pi\varepsilon_0 |\mathbf{r}_{\alpha} - \mathbf{r}_{\beta}|},$$

with  $q_{\alpha}$  the charge on particle  $\alpha$ , and  $\varepsilon_{\text{Coul}}^{\alpha}$  the "self-energy" of its Coulomb field. The Hamiltonian  $H_R$  governs the dynamical fields  $\mathbf{E}'$  and  $\mathbf{B}'$ :

$$H_R = \frac{1}{2} \int \varepsilon_0 (E'_{\perp})^2 + \frac{1}{\mu_0} (B')^2 d^3x. \quad (\text{K.4})$$

In equation (K.4),  $E'_{\perp}$  denotes the transverse electric field. Excitation of the transverse electric field can be interpreted as quanta in electromagnetic modes.

If the system can be characterized with sufficient accuracy by a single pair of conjugate dynamical variables  $\theta$  and  $p_{\theta}$ , and if the terms in (K.3) can be separated

into two distinct expressions  $U$  and  $T$ , with  $U$  depending only on  $\theta$ , and  $T$  depending only on  $p_\theta$ , then an "effective potential energy"  $U$  and an "effective kinetic energy"  $T$  can be defined. Note that if the system is considered to be semiclassical, with dynamical variables represented by functions rather than operators, then  $H = U + T$  is a constant of the motion. Since a change  $\Delta T$  will be accompanied by a corresponding change  $-\Delta U$ , we see that  $U$  and  $T$  conform to our expectations for kinetic and potential energy. In particular, if  $\theta$  is an angular coordinate, and if  $U$  and  $T$  can be approximated as

$$U = \frac{1}{2}k_h\theta^2,$$

$$T = \frac{1}{2}I_h\dot{\theta}^2$$

for some constants  $k_h, I_h$ , then we can consider the system to be a torsional harmonic oscillator with spring constant  $k_h$  and moment of inertia  $I_h$ .

In the case where the system of particles governed by (K.3) is a magnetic mechanical oscillator, we define

$$U = -\sum_{\alpha} \mu_{\alpha} \cdot \mathbf{B}(\mathbf{r}_{\alpha}) + V_{\text{Coul}} + \frac{1}{2\mu_0} \int (B')^2 d^3x,$$

$$T = \sum_{\alpha} \frac{1}{2m_{\alpha}} (\dot{\mathbf{r}}_{\alpha})^2 + \frac{1}{2} \int \epsilon_0 (E'_{\perp})^2 d^3x.$$

We argued in Appendix J that the contribution of the electric field to the kinetic energy of a nanoscale magnetic oscillator is negligible, and so we assume that  $T$  can be approximated as

$$\sum_{\alpha} \frac{1}{2m_{\alpha}} (\dot{\mathbf{r}}_{\alpha})^2 = \frac{1}{2}I_h\dot{\theta}^2.$$

We seek a formula for the contribution made to  $U$  by the magnetic energy  $U_{\text{mag}}$ . Note first that  $V_{\text{Coul}}$  is responsible for magneto-crystalline anisotropy, as well as exchange interactions, and can therefore affect  $U_{\text{mag}}$ . To simplify the discussion, we assume that these forms of energy do not contribute significantly to the oscillator's potential. The field  $\mathbf{B}'$  generated by the oscillator's magnetization can be expressed

as the sum of an averaged field  $\mathbf{B}_h$  and an internal field  $\mathbf{B}_i$ :

$$\mathbf{B}' = \mathbf{B}_h + \mathbf{B}_i.$$

The field  $\mathbf{B}_h(\mathbf{r})$  is calculated by treating the ferromagnetic material as a continuum described by the magnetization  $\mathbf{M}$ , while  $\mathbf{B}_i(\mathbf{r})$  corrects  $\mathbf{B}_h(\mathbf{r})$  by subtracting the contribution made by the continuum in the immediate vicinity of  $\mathbf{r}$  and by adding the actual contribution of the sources in this region. These approximations allow us to write  $U_{\text{mag}}$  as

$$\begin{aligned} U_{\text{mag}} &= -\sum_{\alpha} \mu_{\alpha} \cdot (\mathbf{B}_a + \mathbf{B}_h + \mathbf{B}_i) + \frac{1}{2\mu_0} \int (\mathbf{B}_h + \mathbf{B}_i)^2 d^3x \\ &= -\mu \cdot \mathbf{B}_a - \sum_{\alpha} \mu_{\alpha} \cdot \mathbf{B}_h + \frac{1}{2\mu_0} \int B_h^2 d^3x \\ &\quad - \sum_{\alpha} \mu_{\alpha} \cdot \mathbf{B}_i + \frac{1}{\mu_0} \int \mathbf{B}_i \cdot \mathbf{B}_h d^3x + \frac{1}{2\mu_0} \int B_i^2 d^3x, \end{aligned} \quad (\text{K.5})$$

where  $\mu$  is the oscillator's net dipole moment.

We next observe that the integral of  $B_h^2$  can be simplified using the vector identity

$$\int_V \mathbf{P} \cdot (\nabla \times \mathbf{Q}) d^3x = \int_V \mathbf{Q} \cdot (\nabla \times \mathbf{P}) d^3x + \int_S (\mathbf{Q} \times \mathbf{P}) \cdot d\mathbf{a}, \quad (\text{K.6})$$

where  $\mathbf{P}$  and  $\mathbf{Q}$  are vector functions,  $V$  is a volume of integration, and  $S$  is the surface of  $V$ . We let  $\mathbf{A}_h$  denote the vector potential of the bound current density  $\mathbf{J}_h = \nabla \times \mathbf{M}$ , and we apply (K.6) repeatedly, noting that in each case the surface

integral vanishes:

$$\begin{aligned}
\frac{1}{2\mu_0} \int B_h^2 d^3x &= \frac{1}{2\mu_0} \int \mathbf{B}_h \cdot (\nabla \times \mathbf{A}_h) d^3x \\
&= \frac{1}{2\mu_0} \int \mathbf{A}_h \cdot (\nabla \times \mathbf{B}_h) d^3x \\
&= \frac{1}{2\mu_0} \int \mathbf{A}_h \cdot \mu_0 \mathbf{J}_h d^3x \\
&= \frac{1}{2} \int \mathbf{A}_h \cdot (\nabla \times \mathbf{M}) d^3x \\
&= \frac{1}{2} \int \mathbf{M} \cdot (\nabla \times \mathbf{A}_h) d^3x \\
&= \frac{1}{2} \int \mathbf{M} \cdot \mathbf{B}_h d^3x.
\end{aligned} \tag{K.7}$$

If we replace the sum

$$-\sum_{\alpha} \mu_{\alpha} \cdot \mathbf{B}_h$$

appearing in (K.5) by an integral over the volume of magnetic material, the sum of the second and third terms in (K.5) can be expressed as

$$\begin{aligned}
-\sum_{\alpha} \mu_{\alpha} \cdot \mathbf{B}_h + \frac{1}{2\mu_0} \int B_h^2 d^3x &= - \int \mathbf{M} \cdot \mathbf{B}_h d^3x + \frac{1}{2\mu_0} \int B_h^2 d^3x \\
&= - \int \mathbf{M} \cdot \mathbf{B}_h d^3x + \frac{1}{2} \int \mathbf{M} \cdot \mathbf{B}_h d^3x \\
&= -\frac{1}{2} \int \mathbf{M} \cdot \mathbf{B}_h d^3x,
\end{aligned}$$

and we obtain

$$\begin{aligned}
U_{\text{mag}} &= -\mu \cdot \mathbf{B}_a - \frac{1}{2} \int \mathbf{M} \cdot \mathbf{B}_h d^3x \\
&\quad - \sum_{\alpha} \mu_{\alpha} \cdot \mathbf{B}_i + \frac{1}{\mu_0} \int \mathbf{B}_i \cdot \mathbf{B}_h d^3x + \frac{1}{2\mu_0} \int B_i^2 d^3x.
\end{aligned} \tag{K.8}$$

An alternative form which may be more convenient for some purposes is found by

using (K.7) to replace the second term of (K.8) by an integral over  $B_h^2$ :

$$U_{\text{mag}} = -\boldsymbol{\mu} \cdot \mathbf{B}_a - \frac{1}{2\mu_0} \int B_h^2 d^3x \quad (\text{K.9})$$

$$- \sum_{\alpha} \mu_{\alpha} \cdot \mathbf{B}_i(\mathbf{r}_{\alpha}) + \frac{1}{\mu_0} \int \mathbf{B}_i \cdot \mathbf{B}_h d^3x + \frac{1}{2\mu_0} \int B_i^2 d^3x.$$

In using equations (K.8) or (K.9) to analyze a device, it is natural to make the simplification of assuming that terms which depend on the internal field  $\mathbf{B}_i$  do not vary during the motion. We can show that this assumption is consistent with a simple classical model by expressing  $\mathbf{B}_i(\mathbf{r})$  as

$$\mathbf{B}_i(\mathbf{r}) = \mathbf{B}_{\text{near}}(\mathbf{r}) - \mathbf{B}_{\text{avg}}(\mathbf{r}),$$

where  $\mathbf{B}_{\text{near}}(\mathbf{r})$  is the contribution to the magnetic field at  $\mathbf{r}$  made by particles in the immediate vicinity of  $\mathbf{r}$ , and  $\mathbf{B}_{\text{avg}}(\mathbf{r})$  is the contribution made by treating these particles as a continuum. In order to estimate  $\mathbf{B}_{\text{near}}$ , we consider a model in which  $\mathbf{B}_{\text{near}}$  is generated by a distribution of classical magnetic dipoles. Reference [49] points out that for most materials, the total electric field acting on a particle due to contributions from nearby electric dipoles distributed either randomly or at lattice sites throughout the material can be considered to be approximately zero. Since magnetic and electric dipole fields have the same functional form, we assume that a similar result holds for  $\mathbf{B}_{\text{near}}$ , so that the only nonzero contribution to  $\mathbf{B}_{\text{near}}$  comes from magnetic fields within each magnetic dipole.

For a current distribution localized in a sphere of radius  $R$  centered at the origin, we have

$$\int_{r < R} \mathbf{B} d^3x = \frac{2\mu_0}{3} \boldsymbol{\mu}, \quad (\text{K.10})$$

where  $\mathbf{B}$  is the field generated by the current distribution, and  $\boldsymbol{\mu}$  is its dipole moment [49]. Since this result holds for an arbitrarily small sphere surrounding a magnetic dipole, we can consider the field of the dipole to have a delta function contribution

at the dipole, so that

$$\mathbf{B}_{\text{near}}(\mathbf{r}) \approx \frac{2\mu_0}{3} \sum_{\alpha} \mu_{\alpha} \delta(\mathbf{r}_{\alpha}). \quad (\text{K.11})$$

Averaging the near field given by (K.11) yields

$$\mathbf{B}_{\text{avg}}(\mathbf{r}) = \frac{2\mu_0}{3} \mathbf{M}. \quad (\text{K.12})$$

From (K.11) and (K.12), we obtain

$$\mathbf{B}_i(\mathbf{r}) \approx \frac{2\mu_0}{3} \sum_{\alpha} \mu_{\alpha} \delta(\mathbf{r}_{\alpha}) - \frac{2\mu_0}{3} \mathbf{M}(\mathbf{r}). \quad (\text{K.13})$$

We can use (K.13) to simplify (K.8). It follows from (K.13) that

$$\frac{1}{\mu_0} \int \mathbf{B}_i \cdot \mathbf{B}_h d^3x = 0.$$

If we assume that for a ferromagnetic dipole  $\mu_{\alpha}$  located at  $\mathbf{r}_{\alpha}$ , both  $\mu_{\alpha} \cdot \mathbf{M}(\mathbf{r}_{\alpha})$  and  $|\mathbf{M}(\mathbf{r}_{\alpha})|$  remain constant as the oscillator moves, then the remaining terms

$$-\sum_{\alpha} \mu_{\alpha} \cdot \mathbf{B}_i(\mathbf{r}_{\alpha})$$

and

$$\frac{1}{2\mu_0} \int B_i^2 d^3x$$

appearing in (K.8) are constant and can be discarded. The oscillator's potential energy can therefore be expressed as

$$U_{\text{mag}} = -\mu \cdot \mathbf{B}_a - \frac{1}{2} \int \mathbf{M} \cdot \mathbf{B}_h d^3x, \quad (\text{K.14})$$

or, equivalently, as

$$U_{\text{mag}} = -\mu \cdot \mathbf{B}_a - \frac{1}{2\mu_0} \int B_h^2 d^3x.$$

The magnetic spring constant  $k_{\text{mag}}$  is given by

$$k_{\text{mag}} = \frac{d^2 U_{\text{mag}}}{d\theta^2}.$$

As a check on (K.14), we note that it is closely related to the expression

$$E = -\mathbf{M} \cdot \mathbf{H} \quad (\text{K.15})$$

which is frequently used in the literature of magnetic materials for the energy of a magnetization  $\mathbf{M}$  in a averaged field  $\mathbf{H}$ . In the case of ferromagnetic materials,  $|\mathbf{M}|$  can be considered constant on a microscopic scale (since to a first approximation the direction but not the magnitude of  $\mathbf{M}$  varies between domains and within domain walls), and (K.15) can be written as

$$\begin{aligned} E &= -\frac{1}{\mu_0} \mathbf{M} \cdot \mathbf{B} + \mathbf{M} \cdot \mathbf{M} \\ &= -\frac{1}{\mu_0} \mathbf{M} \cdot \mathbf{B} + \text{constant}, \end{aligned}$$

which differs only by an additive constant and a proportionality constant from the energy expression

$$E = -\mathbf{M} \cdot \mathbf{B}. \quad (\text{K.16})$$

If we had naively used (K.16) to obtain a potential energy expression for the oscillator, taking care to avoid double counting of spin-spin interactions, we would have obtained the same expression derived more carefully in this discussion.

## Appendix L

# Spring constant and moment of inertia of a torsion beam

The spring constant and moment of inertia of a torsion beam can be most naturally obtained from the Lagrangian for the fundamental mode, which can be derived from the Lagrangian that governs arbitrary motions of the beam. For this analysis, we consider a simple rectangular beam, and we suppose that the  $z$ -axis lies along the central axis of the beam. Let  $\phi(z, t')$  be the angular displacement of the beam at position  $z$  and time  $t'$ . (The time is denoted by  $t'$  to distinguish it from the thickness  $t$  of the beam.)

Note first that the elastic potential energy  $U$  of the beam is [52, 53]

$$U = \frac{1}{2}C \int_0^l \left( \frac{\partial \phi}{\partial z} \right)^2 dz. \quad (\text{L.1})$$

The constant  $C$  is known as the torsional rigidity of the beam. The explicit definition of  $C$  depends on the assumption that the displacement  $u_z(x, y, z)$  in the direction of the  $z$ -axis is proportional to  $\partial \phi / \partial z$ , that is, there is a function  $\psi(x, y)$  such that  $u_z = \psi \partial \phi / \partial z$ . The integral

$$\int \int \left( x^2 + y^2 + x \frac{\partial \psi}{\partial y} - y \frac{\partial \psi}{\partial x} \right) dx dy,$$

taken over the cross section of the beam, is called the torsional constant of the beam. (Formulas for torsional constants are available in reference [54].) If we denote the

torsional constant by  $J$ , then  $C$  is given by

$$C = GJ,$$

where  $G$  is the beam's modulus of rigidity.

The kinetic energy  $T$  of the beam is [52, 53]

$$T = \frac{1}{2} \rho_b I_p \int_0^l \left( \frac{\partial \phi}{\partial t'} \right)^2 dz. \quad (\text{L.2})$$

Here  $I_p$  is the polar moment of inertia of the cross section:

$$I_p = \int \int (x^2 + y^2) dx dy.$$

Note that equation (L.2) neglects the kinetic energy due to motion along the beam's axis, and that both (L.1) and (L.2) depend on the condition  $R \frac{\partial \phi}{\partial z} \ll 1$ , where  $R$  is the maximum transverse dimension of the rod. This condition is necessary in order to achieve consistency between the assumption that strains are infinitesimal and the assumption that  $u_x = -yz \frac{\partial \phi}{\partial z}$  and  $u_y = zx \frac{\partial \phi}{\partial z}$ , where  $u_x$  and  $u_y$  are the displacements along the  $x$ -axis and  $y$ -axis, respectively. These assumptions on  $u_x$  and  $u_y$  lead to strains which depend on the products  $x \frac{\partial \phi}{\partial z}$  and  $y \frac{\partial \phi}{\partial z}$ .

The Lagrangian  $\mathfrak{L} = T - U$  can be used to derive a wave equation:

$$\rho_b I_p \frac{\partial^2 \phi}{\partial (t')^2} + \frac{1}{2} C \frac{\partial^2 \phi}{\partial z^2} = 0.$$

For a rod of length  $l$  fixed at both ends, the (non-normalized) modes are [55]

$$\sin \left( \frac{n\pi}{l} z \right) \cos (\omega_n t'), \quad (\text{L.3})$$

where

$$\rho_b I_p \omega_n^2 = C \left( \frac{n\pi}{l} \right)^2,$$

or

$$\omega_n = \frac{n\pi}{l} \sqrt{\frac{C}{\rho_b I_p}}. \quad (\text{L.4})$$

We write  $\phi$  in the form

$$\phi(z, t') = \sum_n q_n(t') \sin\left(\frac{n\pi}{l} z\right),$$

and observe that the Lagrangian can be written as a sum of Lagrangians governing independent modes, with mode  $n$  characterized by discrete variables  $q_n$  and  $\dot{q}_n$ . Focusing our attention on the fundamental mode, we define  $q \equiv q_n$ . The Lagrangian  $\mathfrak{L}$  governing this mode is

$$\mathfrak{L} = \frac{1}{2} \left[ \rho_b I_p \int_0^l \sin^2\left(\frac{\pi}{l} z\right) dz \right] (\dot{q})^2 - \frac{1}{2} \left[ C \int_0^l \left(\frac{\pi}{l}\right)^2 \cos^2\left(\frac{\pi}{l} z\right) dz \right] q^2,$$

which simplifies to

$$\mathfrak{L} = \frac{1}{2} \left( \frac{\rho_b I_p l}{2} \right) (\dot{q})^2 - \frac{1}{2} \left( \frac{C \pi^2}{2l} \right) q^2. \quad (\text{L.5})$$

Equation (L.5) describes a harmonic resonator with spring constant

$$K_{\text{beam}} = \frac{C \pi^2}{2l}$$

and moment of inertia

$$I_{\text{beam}} = \frac{\rho_b I_p l}{2}.$$

Note that if the only excited mode is the fundamental, then the variable  $q$  gives the angular displacement at the center of the beam. For a rectangular beam, the torsional rigidity  $C$  and polar moment of inertia  $I_p$  are [54]

$$C = G w t^3 \left[ \frac{1}{3} - 0.21 \frac{t}{w} \left( 1 - \frac{t^4}{12 w^4} \right) \right],$$

$$I_p = \frac{1}{12} t w (t^2 + w^2).$$

We can express the beam's spring constant and moment of inertia as

$$K_{\text{beam}} = \frac{\pi^2 G w t^3}{2l} \left[ \frac{1}{3} - 0.21 \frac{t}{w} \left( 1 - \frac{t^4}{12w^4} \right) \right] \quad (\text{L.6})$$

and

$$I_{\text{beam}} = \frac{\rho_b t w l}{24} (t^2 + w^2). \quad (\text{L.7})$$

Equations (L.6) and (L.7) were derived under the assumption that the elastic material is isotropic. If the material is a cubic crystal and the beam axis is perpendicular to one of the faces of the cubic cell, similar equations can be derived, with the modulus of rigidity  $G$  replaced by the stiffness constant  $C_{44}$ . Reference [14] tabulates adiabatic stiffness constants for several cubic crystals. The magnitude of  $C_{44}$  typically decreases by 10% or less as the crystal is cooled from room temperature to  $\sim 0$  K. For numerical examples, we used the room temperature adiabatic stiffness constant for Si as a characteristic value of  $C_{44}$  [14]:

$$C_{44} = 7.96 \times 10^{10} \text{ N/m}^2.$$

## Appendix M

# Eddy-current heating of metallic cylinders

In this appendix, we present a rough estimate of the temperature increase  $\Delta T_h$  caused by eddy-current heating. Since experimental information regarding the heat conductivity of nanoscale beams at mK temperatures is not available in the literature, and since the dimensions of the ferromagnetic cylinders are small enough that the low-temperature conductivity of the cylinders may be nonlocal, an accurate estimate cannot be made using results available in the literature. The simplified analysis we present here illustrates the way in which  $\Delta T_h$  is determined by physical parameters which depend strongly on the dimensions and temperature of the resonator. Estimates of the order of magnitude of these parameters based on the limited information available in the literature leave open the possibility that detection sensitivity would be decreased by the temperature change  $\Delta T_h$  if the magnetic cylinders are metallic. The possibility of eliminating eddy-current heating by the use of semiconducting ferromagnets is discussed in section 7 of chapter 5.

We first consider eddy currents in a nonmagnetic conducting particle placed in a uniform alternating magnetic field, and we assume that the mean free path of the conduction electrons is short enough that Ohm's law holds. If the dimensions of the particle are small compared to the skin depth of the conducting material, then we can expect the fields generated within the particle by the eddy currents themselves to be negligible compared to the alternating applied field and the Faraday electric

field induced by it. If the particle is a sphere, the electric field driving eddy currents within it will consist of circular loops, and surface charges will in general develop on the surface of the particle. Altering the geometry of the particle does not perturb the Faraday electric field but leads to an altered configuration of surface charges, with the result that the circular electric field loops within the particle are perturbed. If a fixed magnetization is added to the particle and a static magnetic field is present, we may in general expect additional modifications to the configuration of surface charges (as in the Hall effect) and the configuration of eddy currents. Provided that the particle bears some resemblance to a sphere, however, a rough estimate of the power dissipation associated with the eddy currents can be made by treating the particle as a nonmagnetic spherical conductor.

If the mean free path of the electrons is at least as large as the dimensions of the particle, the conductivity becomes nonlocal, since most electron trajectories would sample a variety of different electric fields. An electron in a trajectory that crosses a loop of the electric field lines, for instance, would be accelerated in different directions during different portions of the trajectory, and the current at each point in the particle would depend on an integral over all points of all trajectories. We might guess that eddy currents within the particle would be weakened by the nonlocal nature of the conductivity, since many of the trajectories would have an electron experiencing accelerations during different portions of the trajectory which do not add constructively. Note, however, that when the conductivity becomes nonlocal, heating of the particle by the Faraday electric field may not be correlated in a simple way with the size of the eddy currents. It is the kinetic energy donated to individual electrons during their trajectories which contributes to heating, not the kinetic energy associated with the net current at a given point. Even if the net current is negligible because the contributions from different trajectories do not add constructively, the acceleration of electrons by the induced electric field as they move along trajectories might lead to a temperature increase in the metal.

For the example resonator presented in table 5.3, each of the magnetic cylinders has a length of 40 nm and a diameter of 55 nm. In a reasonably pure conductor at

a temperature of a few Kelvin or below, the mean free path of an electron in the bulk metal would be significantly larger than the dimensions of the cylinder. The mean free path of an electron in room-temperature bulk iron is about 5 nm [56], for instance, and this can increase by orders of magnitude at low temperatures, when the scattering of electrons by phonons is "frozen out." At temperatures below a few Kelvin, the conductivity of a normal conductor does not depend on temperature; its value depends instead on the extent to which electrons are scattered by surfaces, lattice defects, impurities, and the like. A high concentration of scattering centers would be needed within the ferromagnetic material to yield a mean free path which is small on the scale of the curving electric field lines within the magnetic particles of the resonator.

If the resistivity of the cylinders is high enough that the mean free path of the electrons is smaller than the dimensions of the cylinders by a factor of  $\sim 10$  or more, an analysis of eddy currents based on Ohm's law is relevant. In order to illustrate the eddy-current heating which could occur in this case, we assume a mean free path of 4 nm for the electrons. Note that if the mean free path is reduced below this value, both the conductivity and eddy-current power dissipation will decrease, and so we may consider this heating estimate to be a "worst-case" estimate for the regime in which Ohm's law holds. In converting the mean free path into a resistivity, we assume that conductivity is proportional to mean free path, and we note that the mean free path and resistivity for Fe at room-temperature are 4.75 nm and  $9 \times 10^{-8} \Omega \text{ m}$ , respectively [56]. The resistivity  $\rho$  corresponding to a mean free path of 4 nm in Fe is therefore

$$\rho = 9 \times 10^{-8} \Omega \text{ m} \frac{4.75}{4.0} = 10.7 \times 10^{-8} \Omega \text{ m}.$$

The skin depth [49] associated with this resistivity at frequency 630 MHz is

$$\delta = 6.6 \mu\text{m},$$

which is much larger than the dimensions of the magnetic particle.

Smythe has derived a general expression for eddy currents induced in a conducting sphere by a uniform alternating magnetic field in the quasi-static regime [57]. For a nonmagnetic particle whose radius  $r$  is small compared to the skin depth, Smythe's expression for the power dissipation in the particle reduces to [58, 59]

$$P_{\text{diss}} = \frac{\pi r^5 \omega_0^2 B_1^2}{15\rho},$$

where  $B_1$  and  $\omega_0$  are the magnitude and frequency of the alternating field,  $\rho$  is the resistivity of the particle, and  $r$  is its radius. We model each ferromagnetic particle as a sphere of radius  $r = 25$  nm, and we assume continuous irradiation by a resonant field (frequency  $\omega_0/2\pi = 630$  MHz) strong enough to give protons a Rabi frequency of 20 kHz:

$$\begin{aligned} B_1 &= 2(2\pi) 20 \text{ kHz} / \left( \frac{267.5 \times 10^6}{\text{s T}} \right) \\ &= 9.3954 \times 10^{-4} \text{ T}. \end{aligned}$$

We find that the power deposited in each particle is

$$P_{\text{diss}} = 2.6271 \times 10^{-19} \text{ W}. \quad (\text{M.1})$$

For a long, thin beam with rough surfaces but no scattering centers within the crystal, the predicted thermal conductance is [60, 61]

$$K = \frac{2\pi^2 k_B^4 l A}{15\hbar^3 v_s L} T^3, \quad (\text{M.2})$$

where  $L$  and  $A$  are the length cross-sectional area of the beam,  $v_s = 4500$  m/s is the speed of sound in silicon,  $T$  is the temperature, and  $l$  is the phonon mean free path length. A recent experimental test of the low-temperature thermal conductance of nanoscale Si beams of cross section  $130 \text{ nm} \times 200 \text{ nm}$  found that although the conductance varied as  $T^3$  above  $T = 1.4$  K, the temperature dependence was less strong below this temperature and appeared to flatten out at the lowest temperature

( $\sim 0.5$  K) at which a measurement was taken [60]. Temperature dependence weaker than  $T^3$  was also observed at temperatures between 20 K and 60 K for beams of width 37 nm and 22 nm [62].

Although these departures from the predicted  $T^3$  dependence are promising for our purposes, they are not well understood, and there is no experimental information on the temperature dependence of thermal conductivity below  $\sim 0.5$  K. In estimating the thermal conductance of the resonator's beam, we therefore start from the expression which was found to be valid above 1.4 K [60]:

$$K_{\text{cond}} = 2.6 \times 10^{-11} T^3 \frac{\text{W}}{\text{K}}. \quad (\text{M.3})$$

From equation M.2, we see that if the mean free path did not depend on the dimensions of the beam or the temperature, then at 10 mK the value of thermal conductance for a section of the resonator beam stretching from the sample to the bulk substrate is

$$\begin{aligned} K_{\text{cond}} &= 2.6 \times 10^{-11} T^3 \frac{\text{W}}{\text{K}} \left( \frac{2.5 \mu\text{m}}{3.5 \mu\text{m} / 2} \right) \left( \frac{50 \text{ nm} \times 50 \text{ nm}}{130 \text{ nm} \times 200 \text{ nm}} \right) \\ &= 3.5714 \times 10^{-18} \frac{\text{W}}{\text{K}}. \end{aligned} \quad (\text{M.4})$$

The mean free path obtained by comparing (M.3) to (M.2) was  $\sim 600$  nm [60]. In a simplified model which assumes that phonon scattering occurs only at the surface of the beam, and that a fraction  $p$  of the phonons incident upon a surface is reflected specularly, while the remainder are scattered diffusely, the mean free path can be written as [61]

$$l = \frac{1+p}{1-p} l_0,$$

where  $l_0$  is the mean free path in the case where no specular reflection occurs. For a circular cross-section of diameter  $d$  or a square cross-section of side  $d$ , we have  $l_0 = d$  and  $l_0 = 1.12d$ , respectively. We might therefore guess that if the cross-

section corresponding to equation (M.3) were scaled down from  $130 \text{ nm} \times 200 \text{ nm}$  to  $50 \text{ nm} \times 50 \text{ nm}$ , the mean free path would decrease by a factor between 2 and 4. Due to lack of experimental information regarding either the size dependence or the temperature dependence of the phonon mean free path for nanowires  $\leq 1.4 \text{ K}$ , however, we will use equation (M.4) for our estimate of eddy-current heating rather than attempting to incorporate this guess into the estimate. Combining equations (M.1) and (M.4) yields a temperature difference of

$$\begin{aligned} \Delta T_{\text{beam}} &= \frac{P_{\text{diss}}}{K_{\text{cond}}} \\ &= 75 \text{ mK} \end{aligned} \tag{M.5}$$

between the center of the resonator beam and each of its ends.

An estimate of the temperature gradient across the magnet-silicon interface can also be made. For interfaces between bulk solids, simplified theories of thermal boundary resistance have been shown to agree with experiment at low temperatures down to  $\sim 100 \text{ mK}$  [63]. The acoustic mismatch theory and the diffuse mismatch theory estimate the probability of phonon transmission across the boundary in the respective limits of specular reflection and diffuse scattering at the boundary. These theories are found to yield similar values for the thermal resistance  $R_{Bd}$ , and in the case of interfaces between Si and transition metals,  $R_{Bd}T^3$  is typically found to lie in the range  $10$  to  $20 \text{ K}^4 / (\text{W} / \text{cm}^2)$  [63]. Setting

$$\begin{aligned} R_{Bd} &= \frac{15 \text{ K}^4}{T^3 \text{ W} / \text{cm}^2}, \\ T &= 10 \text{ mK} \end{aligned}$$

we obtain

$$\Delta T_{\text{boundary}} = P_{\text{diss}} R_{Bd} / A \tag{M.6}$$

$$= 0.166 \text{ K}. \tag{M.7}$$

In (M.6),  $A$  represents the area of the flat surface of each ferromagnetic cylinder.

Equations (M.5) and (M.7) depend on the assumption that the temperature differences  $\Delta T$  are small enough that a single value of  $T \approx 10$  mK can be used to characterize the beam and the magnetic particle. Since the temperature differences we obtained are roughly an order of magnitude greater than 10 mK, this assumption is clearly invalid. A simple correction can be made by assuming that the  $T \approx 25$  mK, which yields

$$\Delta T_{\text{beam}} = 4.7 \text{ mK},$$

$$\Delta T_{\text{boundary}} = 11 \text{ mK}.$$

Since increasing the temperature from 10 mK to 25 mK decreases the polarization from 0.91 to 0.54, and increases the thermal noise in the resonator, the estimates we have made of thermal and electric conductivity suggest that sensitivity could be decreased by the temperature change  $\Delta T_h$ . The use of semiconducting ferromagnetic material such as EuO may therefore be preferred, since the resistivity of the cylinders would be orders of magnitude larger than the values we used for this estimate [38].

## Appendix N

# Correlation function of the mechanical coordinate during cooling by hyperpolarized spins

This appendix derives the symmetric autocorrelation function  $C(t)$  of the resonator's mechanical coordinate during cooling by hyperpolarized spins, required for the analysis in section 7 of chapter 7. In deriving a formula for  $C(t)$ , we will need a general expression for  $\langle \theta \rangle(t)$ . We define

$$\eta_\alpha = \frac{1 + \sqrt{1 - 8 \langle I_z \rangle_\infty (gb)^2}}{2gb} i, \quad (\text{N.1})$$

$$\eta_\beta = \frac{1 - \sqrt{1 - 8 \langle I_z \rangle_\infty (gb)^2}}{2gb} i, \quad (\text{N.2})$$

and

$$\omega'_k = \omega_h + g \operatorname{Re}(\eta_k), \quad (\text{N.3})$$

$$1/\tau'_k = 1/\tau_h - g \operatorname{Im}(\eta_k), \quad (\text{N.4})$$

for  $k = \alpha, \beta$ . The general solution to the system of differential equations given by (7.46) and (7.47) is

$$\langle a \rangle (t) = p \exp [-(i\omega'_a + 1/\tau'_a) t] + q \exp [-(i\omega'_\beta + 1/\tau'_\beta) t], \quad (\text{N.5})$$

$$\langle I_+ \rangle (t) = p\eta_\alpha \exp [-(i\omega'_a + 1/\tau'_a) t] + q\eta_\beta \exp [-(i\omega'_\beta + 1/\tau'_\beta) t], \quad (\text{N.6})$$

$$p = \frac{\eta_\beta \langle a \rangle (0) - \langle I_+ \rangle (0)}{\eta_\beta - \eta_\alpha}, \quad (\text{N.7})$$

$$q = \frac{-\eta_\alpha \langle a \rangle (0) + \langle I_+ \rangle (0)}{\eta_\beta - \eta_\alpha}. \quad (\text{N.8})$$

Given the general expression for  $\langle a \rangle (t)$ , we can write  $\langle \theta \rangle (t)$  as

$$\langle \theta \rangle (t) = \sqrt{\frac{2\hbar}{I_h \omega_h}} \operatorname{Re} \{ \langle a \rangle (t) \}. \quad (\text{N.9})$$

The method presented in reference [8] can be used to express the correlation function  $C(t)$  as

$$C(t) = \langle \theta(t) \rangle,$$

where the initial conditions which determine  $\langle \theta(t) \rangle$  are calculated as if the density matrix at time  $t = 0$  were

$$\rho(0) = \frac{1}{2} (\rho_\infty \theta + \theta \rho_\infty),$$

with  $\rho_\infty$  the steady state density matrix of the spin-resonator system. From equations (N.5) through (N.9), it follows that it is sufficient to find formulas for

$$p = \frac{1}{2(\eta_\beta - \eta_\alpha)} \{ \eta_\beta \langle a\theta + \theta a \rangle_\infty - \langle I_+\theta + \theta I_+ \rangle_\infty \},$$

$$q = \frac{1}{2(\eta_\beta - \eta_\alpha)} \{ -\eta_\alpha \langle a\theta + \theta a \rangle_\infty + \langle I_+\theta + \theta I_+ \rangle_\infty \}.$$

We show below that the steady-state expectation values  $\langle \theta^2 \rangle_\infty$ ,  $\langle p_\theta \theta + \theta p_\theta \rangle_\infty$ ,  $\langle I_x \theta \rangle_\infty$ ,

and  $\langle I_y \theta \rangle_\infty$  can be approximated as

$$\langle \theta^2 \rangle_\infty = \frac{\hbar}{I_h \omega_h} \left( n_\infty + \frac{1}{2} \right), \quad (\text{N.10})$$

$$\langle p_\theta \theta + \theta p_\theta \rangle_\infty = 0, \quad (\text{N.11})$$

$$\langle I_x \theta \rangle_\infty = 0, \quad (\text{N.12})$$

$$\langle I_y \theta \rangle_\infty = -K_\infty / (\gamma dB_x / d\theta), \quad (\text{N.13})$$

where  $n_\infty$  is given by (7.28) and  $K_\infty$  by equation (7.24).

The formula for  $\langle I_y \theta \rangle_\infty$  can be estimated by noting from (7.39) that in the absence of the rotating-wave approximation, the rate  $K$  at which quanta are transferred from spins to oscillator is given by

$$K = -\gamma \frac{dB_x}{d\theta} \langle I_y \theta \rangle. \quad (\text{N.14})$$

Equations (N.10) through (N.12) can be obtained by deriving the equations of motion for selected operators using the master equation (7.9), setting derivatives to zero, and solving the resulting set of equations. The equations of motion which are needed are

$$\begin{aligned} \frac{d}{dt} \langle \theta^2 \rangle &= -\frac{2}{\tau_h} \left\{ \langle \theta^2 \rangle - \frac{\hbar}{I_h \omega_h} \left( n + \frac{1}{2} \right) \right\} \\ &\quad + \frac{1}{I_h} \langle p_\theta \theta + \theta p_\theta \rangle - \frac{dB_x}{d\theta} \frac{\hbar \gamma}{I_h \omega_h} \langle I_y \theta \rangle, \end{aligned} \quad (\text{N.15})$$

$$\begin{aligned} \frac{d}{dt} \langle p_\theta \theta + \theta p_\theta \rangle &= -\frac{2}{\tau_h} \langle p_\theta \theta + \theta p_\theta \rangle - 4I_h \omega_h^2 \langle \theta^2 \rangle + 4\hbar \omega_h \left( \langle a^\dagger a \rangle + \frac{1}{2} \right) \\ &\quad + \hbar \gamma \frac{dB_x}{d\theta} \left( \langle I_x \theta \rangle - \frac{1}{I_h \omega_h} \langle I_y p_\theta \rangle \right), \end{aligned} \quad (\text{N.16})$$

$$\begin{aligned} \frac{d}{dt} \langle I_y \theta \rangle &= -\frac{1}{\tau_1} \langle I_y \theta \rangle - \omega_h \langle I_x \theta \rangle + \frac{1}{I_h} \langle I_y p_\theta \rangle \\ &\quad - \frac{dB_x}{d\theta} \frac{\hbar \gamma}{2I_h \omega_h} \langle I_y^2 \rangle + \frac{dB_x}{d\theta} \frac{\gamma}{2} \langle \theta^2 I_z \rangle, \end{aligned} \quad (\text{N.17})$$

$$\frac{d}{dt} \langle I_+ a^\dagger + I_- a \rangle = -\frac{1}{\tau_1} \langle I_+ a^\dagger + I_- a \rangle. \quad (\text{N.18})$$

From (N.18), we obtain

$$\begin{aligned} 0 &= \langle I_+ a^\dagger + I_- a \rangle_\infty \\ &= \sqrt{\frac{2I_h \omega_h}{\hbar}} \langle I_x \theta \rangle_\infty + \sqrt{\frac{2}{\hbar I_h \omega_h}} \langle I_y p_\theta \rangle_\infty, \end{aligned}$$

from which it follows that

$$\langle I_y p_\theta \rangle_\infty = -I_h \omega_h \langle I_x \theta \rangle_\infty. \quad (\text{N.19})$$

Setting the left sides of (N.16) through (N.15) to zero and making the assumption that

$$\langle \theta^2 I_z \rangle_\infty \approx \langle \theta^2 \rangle_\infty \langle I_z \rangle_\infty$$

yields the following solution for  $\langle \theta^2 \rangle_\infty$ :

$$\begin{aligned} \frac{I_h \omega_h}{\hbar} \left( 1 + \frac{1}{\omega_h^2 \tau_h^2} + \frac{1}{2\omega_h^2 \tau_c \tau_1} \right) \langle \theta^2 \rangle_\infty &= n_\infty \left( 1 + \frac{1}{\omega_h^2 \tau_h \tau_\infty} - \frac{1}{\omega_h^2 \tau_h \tau_c} + \frac{1}{2\omega_h^2 \tau_c \tau_1} \right) \\ &+ \frac{1}{2} \left( 1 + \frac{1}{\omega_h^2 \tau_h^2} + \frac{1}{2\omega_h^2 \tau_c \tau_1} \right) \\ &+ \frac{1}{\langle I_z \rangle_\infty} \left( \langle I_y^2 \rangle_\infty - \frac{N}{4} \right) \frac{1}{2\omega_h^2 \tau_c \tau_1}. \end{aligned}$$

Each of the decay times  $\tau_h$ ,  $\tau_c$ ,  $\tau_1$ , and  $\tau_\infty$  can be assumed to be much longer than the period of the resonator; if we assume in addition that

$$\langle I_y^2 \rangle_\infty \approx N/4,$$

then we obtain the solution (N.10) through (N.12).

In the regime where  $\tau_h$  is short and the coupling is strong ( $4\tau_h/\tau_c > 1$ ), the

correlation function  $C(t)$  can be written as

$$\begin{aligned}
C(t) &= \exp(-t/2\tau_h) \cos(\omega_h t) \times & (\text{N.20}) \\
&\quad \left\{ \langle \theta^2 \rangle_\infty \cos(dt) - (c_1 \langle \theta^2 \rangle_\infty + c_2 \langle I_y \theta \rangle_\infty) \sin(dt) \right\}, \quad t > 0, \\
d &= \left( \sqrt{4\tau_h/\tau_c - 1} \right) / 2\tau_h, \\
c_1 &= 1/\sqrt{4\tau_h/\tau_c - 1}, \\
c_2 &= -\sqrt{\frac{2\hbar}{I_h \omega_h}} \frac{2g\tau_h}{\sqrt{4\tau_h/\tau_c - 1}},
\end{aligned}$$

and in the limit of strong coupling ( $4\tau_h/\tau_c \gg 1$ ), this reduces to

$$C(t) \approx \exp(-t/2\tau_h) \cos(\omega_h t) \left\{ \langle \theta^2 \rangle_\infty \cos(dt) - c_2 \langle I_y \theta \rangle_\infty \sin(dt) \right\}, \quad t > 0 \quad (\text{N.21})$$

$$\approx \frac{\hbar}{I_h \omega_h} n_\infty \exp(-t/2\tau_h) \cos(\omega_h t) \left\{ \cos(dt) - \sqrt{\tau_h/\tau_c} \sin(dt) \right\}, \quad t > 0 \quad (\text{N.22})$$

$$d \approx 1/\sqrt{\tau_h \tau_c}.$$

(In making this simplification we have also assumed  $n_\infty \gg 1/2$  and  $n_\infty \gg n_c$ .) The expression in curly brackets is a sinusoidal function which can be written as

$$\cos(dt) - \sqrt{\tau_h/\tau_c} \sin(dt) = (1 + \tau_h/\tau_c) \cos(dt + \phi). \quad (\text{N.23})$$

We obtain

$$C(t) = \frac{\hbar}{I_h \omega_h} n_\infty \left( 1 + \frac{\tau_h}{\tau_c} \right) \exp(-t/2\tau_h) \cos(\omega_h t) \cos(dt + \phi), \quad t > 0 \quad (\text{N.24})$$

$$\begin{aligned}
&= \frac{\hbar}{I_h \omega_h} n_\infty \left( 1 + \frac{\tau_h}{\tau_c} \right) \exp(-t/2\tau_h) \times & (\text{N.25}) \\
&\quad \frac{\cos((\omega_h + d)t + \phi) + \cos((\omega_h - d)t - \phi)}{2}, \quad t > 0.
\end{aligned}$$

# Bibliography

- [1] J. A. Sidles, *et al.*, *Reviews of Modern Physics* **67**, 249 (1995).
- [2] L. A. Madsen, G. M. Leskowitz, D. P. Weitekamp, *Proceedings of the National Academy of Sciences of the United States of America* **101**, 12804 (2004).
- [3] D. Rugar, R. Budakian, H. J. Mamin, B. W. Chui, *Nature* **430**, 329 (2004).
- [4] B. W. Shore, P. L. Knight, *Journal of Modern Optics* **40**, 1195 (1993).
- [5] S. Haroche, *Les Houches, Session XXXVIII, 1982 – New Trends in Atomic Physics*, G. Grynberg, R. Stora, eds. (Elsevier Science Publishers, Amsterdam, 1984), pp. 195–309.
- [6] R. Bonifacio, P. Schwendiman, F. Haake, *Physical Review A* **4**, 302 (1971).
- [7] C. Cohen-Tannoudji, J. Dupont-Roc, G. Grynberg, *Atom-Photon Interactions: Basic Process and Applications* (John Wiley, New York, 1992).
- [8] G. W. Ford, R. F. O’Connell, *Optics Communications* **179**, 451 (2000).
- [9] U. Haeberlen, *High Resolution NMR in Solids: Selective Averaging*, vol. 1 of *Advances in Magnetic Resonance Supplement* (Academic Press, New York, 1976).
- [10] G. S. Agarwal, *Quantum Statistical Theories of Spontaneous Emission and their Relation to other Approaches*, vol. 70 of *Springer Tracts in Modern Physics* (Springer-Verlag, Berlin, 1974).
- [11] C. M. Caves, *Physical Review D* **26**, 1817 (1982).
- [12] A. Abragam, *Principles of Nuclear Magnetism* (Clarendon Press, Oxford, 1961).

- [13] G. M. Leskowitz, Force-detected magnetic resonance independent of field gradients, Ph.D. thesis, California Institute of Technology (2003).
- [14] C. Kittel, *Introduction to Solid State Physics* (John Wiley, New York, 1996), 7th edn.
- [15] V. A. Norton, D. P. Weitekamp, personal communication.
- [16] R. H. Dicke, *Physical Review* **93**, 99 (1954).
- [17] M. Gross, S. Haroche, *Physics Reports-Review Section of Physics Letters* **93**, 301 (1982).
- [18] L. A. Wainstein, V. D. Zubakov, *Extraction of Signals from Noise* (Dover, New York, 1962).
- [19] W. Davenport, W. Root, *An Introduction to the Theory of Random Signals and Noise* (McGraw-Hill, New York, 1958).
- [20] R. R. Ernst, *Advances in Magnetic Resonance* **2**, 1 (1966).
- [21] G. M. Leskowitz, L. A. Madsen, D. P. Weitekamp, *Solid State Nuclear Magnetic Resonance* **11**, 73 (1998).
- [22] L. A. Madsen, Force-detected NMR in a homogeneous field: Experiment design, apparatus, and observations, Ph.D. thesis, California Institute of Technology (2002).
- [23] G. W. Ford, J. T. Lewis, R. F. O'Connell, *Physical Review A* **37**, 4419 (1988).
- [24] A. A. Clerk, *Physical Review B* **70**, Art. No. 245306 (2004).
- [25] M. D. LaHaye, O. Buu, B. Camarota, K. C. Schwab, *Science* **304**, 74 (2004).
- [26] W. K. Rhim, D. P. Burum, D. D. Elleman, *Physical Review Letters* **37**, 1764 (1976).

- [27] B. D. Cullity, *Introduction to Magnetic Materials* (Addison-Wesley Publishing Company, Reading, Massachusetts, 1972).
- [28] C. Kittel, *Reviews of Modern Physics* **21**, 541 (1949).
- [29] J. L. Dormann, D. Fiorani, E. Tronc, *Advances in Chemical Physics* **98**, 283 (1997).
- [30] D. L. Mills, S. M. Rezende, *Topics in Applied Physics* **87**, 27 (2003).
- [31] H. Chang, *British Journal of Applied Physics* **12**, 160 (1961).
- [32] D. P. Weitekamp, *Advances in Magnetic Resonance* **11**, 111 (1983).
- [33] B. T. Matthias, R. M. Bozorth, *Physical Review Letters* **7**, 160 (1961).
- [34] J. Lettieri, *et al.*, *Applied Physics Letters* **83**, 975 (2003).
- [35] S. Thongchant, Y. Hasegawa, Y. Wada, S. Yanagida, *Chemistry Letters* **30**, 1274 (2001).
- [36] Y. Hasegawa, *et al.*, *Angewandte Chemie-International Edition* **41**, 2073 (2002).
- [37] M. R. Oliver, McWhorte.Al, J. O. Dimmock, T. B. Reed, *Physical Review B* **5**, 1078 (1972).
- [38] Y. Shapira, S. Foner, T. B. Reed, *Physical Review B* **8**, 2299 (1973).
- [39] S. A. Smith, T. O. Levante, B. H. Meier, R. R. Ernst, *Journal of Magnetic Resonance Series A* **106**, 75 (1994).
- [40] X. J. Zhou, Q. Li, Z. H. He, X. Yang, K. T. Leung, *Surface Science* **543**, L668 (2003).
- [41] T. Koerner, R. S. Brown, J. L. Gainsforth, M. Klobukowski, *Journal of the American Chemical Society* **120**, 5628 (1998).
- [42] M. Poggio, C. L. Degen, H. J. Mamin, D. Rugar, *Physical Review Letters* **99** (2007).

- [43] K. Halbach, *Nuclear Instruments & Methods* **169**, 1 (1980).
- [44] U. Ruth, T. Hof, J. Schmidt, D. Fick, H. J. Jansch, *Applied Physics B-Lasers and Optics* **68**, 93 (1999).
- [45] R. T. Jacobsen, S. G. Penoncello, E. W. Lemmon, *Thermodynamic Properties of Cryogenic Fluids* (Plenum Press, 1997).
- [46] M. V. Romalis, M. P. Ledbetter, *Physical Review Letters* **8706** (2001).
- [47] C. W. McCombie, *Reports on Progress in Physics* **16**, 266 (1953).
- [48] G. W. Ford, R. F. O'Connell, *Physical Review Letters* **77**, 798 (1996).
- [49] J. D. Jackson, *Classical Electrodynamics* (Wiley, New York, 1999), third edn.
- [50] D. J. Griffiths, *Introduction to Electrodynamics* (Prentice Hall, Upper Saddle River, New Jersey, 1999), third edn.
- [51] C. Cohen-Tannoudji, J. Dupont-Roc, G. Grynberg, *Photons and Atoms: Introduction to Quantum Electrodynamics* (John Wiley, New York, 1989).
- [52] L. D. Landau, E. M. Lifshitz, A. M. Kosevich, L. P. Pitaevskii, *Theory of Elasticity*, vol. 7 of *Theoretical Physics* (Pergamon Press, Oxford, 1986), third edn.
- [53] A. E. H. Love, *A Treatise on the Mathematical Theory of Elasticity* (Dover Publications, New York, 1944), fourth edn.
- [54] R. J. Roark, W. C. Young, *Roark's Formulas for Stress and Strain* (McGraw-Hill, New York, 1989), 6th edn.
- [55] W. D. Pilkey, *Formulas for Stress, Strain, and Structural Matrices* (John Wiley and Sons, New York, 1994).
- [56] N. W. Ashcroft, N. D. Mermin, *Solid State Physics* (Saunders College, Philadelphia, 1976).

- [57] W. R. Smythe, *Static and Dynamic Electricity*, International Series in Pure and Applied Physics (McGraw-Hill, New York, 1967), third edn.
- [58] P. Keblinski, D. G. Cahill, A. Bodapati, C. R. Sullivan, T. A. Taton, *Journal of Applied Physics* **100**, Art. No. 054305 (2006).
- [59] D. I. Hoult, P. C. Lauterbur, *Journal of Magnetic Resonance* **34**, 425 (1979).
- [60] O. Bourgeois, T. Fournier, J. Chaussy, *Journal of Applied Physics* **101**, Art. No. 016104 (2007).
- [61] J. M. Ziman, *Electrons and Phonons* (Clarendon, Oxford, 2001).
- [62] D. Y. Li, *et al.*, *Applied Physics Letters* **83**, 2934 (2003).
- [63] E. T. Swartz, R. O. Pohl, *Reviews of Modern Physics* **61**, 605 (1989).